ISSN 1831-9424

European Commission

JRC TECHNICAL REPORT

INFORM Climate Change Risk Index

Concept and Methodology

Poljanšek, K.

Marzi, S.

Galimberti, L.

Dalla Valle, D.

Pal, J.S.

Essenfelder, A.H.

Mysiak, J.

Corbane, C.

2022

INFORMCLIMATECHANGE

Joint Research Centre

EUR 31138 EN

Contact information
Name: Karmen Poljanšek
Address: European Commission, Joint Research Centre, Via Fermi, 2479, Ispra (VA), Italy
Email: karmen.poljansek@ec.europa.eu

For more information see https://drmkc.jrc.ec.europa.eu/inform-index

EU Science Hub
https://ec.europa.eu/jrc

JRC129896

EUR 31138 EN

PDF	ISBN 978-92-76-54411-1	ISSN 1831-9424	doi:10.2760/822072	KJ-NA-31138-EN-N
Print	ISBN 978-92-76-54410-4	ISSN 1018-5593	doi:10.2760/732121	KJ-NA-31138-EN-C

Luxembourg: Publications Office of the European Union, 2022

How to cite this report:
Poljansek, K., Marzi, S., Galimberti, L., Dalla Valle, D., Pal, J., Essenfelder, A.H., Mysiak, J., Corbane, C., 2022. INFORM Climate Change Risk Index: Concept and Methodology, Publications Office of the European Union, Luxembourg, doi:10.2760/822072, JRC129896.

Contents

Acknowledgements

The authors would like to acknowledge the contributions of all INFORM partners provided through the dedicated sessions.

Special thanks to Euro-Mediterranean Center on Climate Change (CMCC) for their advice on the conceptualization and significant inputs to the project as well as Matthias Garschagen who has been following us closely trough many important steps of the development and implementation of INFORM Climate Change model.

In particular, the authors would like to thank Luca Vernaccini who helped to create a vision of the model and tool, therefore, made an essential and precious contributions to the development of the conceptual framework and methodology.

Role of Authors

Karmen Poljanšek, as the scientific coordinator of INFORM at JRC, coordinated the work, was responsible for the preparation of the report and wrote parts of the report.

Sepehr Marzi as external consultant and front-end (Application Architect), designed the methodology, coordinated data implementation into the system and website and wrote major part of the report.

Daniele Dalla Valle as external consultant and back-end IT developer of the database, system and website, executed the data implementation into the system and website.

Luca Galimberti, as Visiting Scientist and data analyst developed and implemented the tool into the website.

Jeremy S. Pal, as external contributor provided the SPEI data used for drought exposure and advice on the methodology.

Arthur H. Essenfelder, as external contributor contributed to the preparation of the codes for exposure and uncertainty analysis.

Jaroslav Mysiak, as external reviewer from CMCC, contributed to many aspects of the report.

Christina Corbane, as the team leader of the DRMKC, overviewed the whole process and contributed to many aspects of the report.

Abstract

Climate change has already shown diverse adverse impacts on human systems. Higher levels of humanitarian aid will be essential to alleviate the future extreme weather-related human suffering, fatalities, injuries and displacement. Having in place a risk assessment tool that includes climate change projections and future adaptation measures would be an important contribution for humanitarian and development sector in terms of horizon scanning and global humanitarian risk monitoring.

INFORM Climate Change Risk Index is a new INFORM product based on the INFORM Risk Index. It incorporates climate and socioeconomic projections to analyse how risk will evolve as a result of climate change under different emission and population scenarios. INFORM Climate Change is a result of collaboration between the Euro-Mediterranean Center on Climate Change and Joint Research Centre of European Commission.

The objective of INFORM Climate Change Risk Index is to inform decision-making around the risk of climate-amplified hazards, as well as how increased risks could be offset by improved vulnerability and coping capacity. Specifically, it is intended to lead to a shared and objective understanding of the impact of climate change on the risk of humanitarian crises, and to support decisions on the allocation of DRR and climate adaptation resources that is consistent with SDG and Sendai targets.

This report describes the concept and methodology of INFORM Climate Change Risk Index as well as instructions on how to use the online interactive tool. INFORM Climate Change tool provides insight into the results of the climate change risk analysis. It helps the users to easily navigate within different scenario combinations and different points in time, exploring the potential changes in risk and Hazard&Exposure variables.

1 Introduction and background

1.1 Rationale

The Increasing concentration levels of greenhouse gases caused by human activity are recognized as a main driver of climate change resulting in more frequent and intense climate related disaster events. According to EM-DAT (CRED, 2020), between 2000 and 2019 there were 6,681 climate related disasters resulting in 3.9 billion people affected , and in 510,837 people death. This compares with 3,656 climate related events resulting in 3.2 billion affected and 995,330 people death in the period 1980-1999. Additionally, all disasters inflicted 2.97 trillion USD (2.64 trillion €)[1] of economic losses in 2000-2019 compared to 1.63 trillion USD (1.45 trillion €) in 1980-1999, each time almost 80% due to floods and storms. The number of people affected by disasters and the associated economic losses are increasing in contrast to decreasing number of fatalities.

As many of these events are happening successively and leaving less and less time in between for recovery they undermine sustainable development. Therefore, they are more likely to cause humanitarian crisis and conflicts or exacerbate the existing ones. Humanitarian needs are becoming more profound, complex and protracted. The impacts of climate change are putting the countries most at risk of humanitarian crisis or already in crisis in devastating situation. For instance, an estimated 45.1 million people in the Horn of Africa and 62 million people in eastern and southern Africa needed humanitarian assistance due to climate-related food emergencies between 2015 and 2019 (IPCC, 2022) often compounded with conflict situations, political instabilities, migrations and increased risk of diseases. Climate-related emergencies are not happening only in low-income countries but also medium and high-income countries, especially related to heatwaves and wildfires (Bose-O'Reilly et al., 2021; Walton and van Aalst, 2020).

It is observed that despite more coordinated funding mechanism and more efficient delivery of humanitarian aid, the global humanitarian aid funding system cannot keep up with the increasing requirements (HNO, 2021). Only humanitarian program aid support cannot get the people in need out of the grip of on-going crisis. It is important, more than ever, to step together with international development and peace-making organizations as well as governments and align development investment to achieve common risk-management, resilience and adaptation objectives that would address root causes of humanitarian crisis and conflicts. Ultimately, the goal is not only to reduce humanitarian needs but also bring societies back on track of the development growth.

INFORM is a collaboration of the Inter-Agency Standing Committee and the European Commission that brings together 28 organizations from across the multilateral system, including the humanitarian and development sector, donors, and technical partners. In 2014, INFORM initiative developed INFORM Risk Index (De Groeve et al., 2014), a common framework based on composite indicator methodology, and a product for assessing risk of humanitarian crisis and disaster concerned with structural risk factors. Since then, INFORM Risk has not only become a global reference for the multihazard risk assessment but INFORM initiative is developing common evidence-based tools for risk-informed decision-making relevant to humanitarian crises and disasters and to be used in different phases of disaster risk management.

In 2019, Euro-Mediterranean Centre on Climate Change (CMCC) and Joint Research centre (JRC) started research on introducing climate hazard and demographic projections into existing model of INFORM Risk Index[2]. In 2021 the first outcomes were published in the journal of Global Environmental Change (Marzi et al, 2021). The paper presented an upgrade of INFORM risk Index model with climate change impacts projections based on a few future scenarios defined as a combination of Representative Concentration Pathway (RCP) and Shared Socio-economic Pathways (SSP). It allowed to calculate risk in 2050 and respective vulnerability gap, i.e., a level of vulnerability reduction and capacity increase for each country needed to preserve the risk at the current level.

Such a risk assessment tool that includes climate change projections and future adaptation measures would be an important contribution for INFORM partners (e.g. FCDO[3], UNDCO[4] and IOM[5]) in terms of horizon scanning and global humanitarian risk monitoring (Messina et al., 2019). Capturing the projections of climate, exposure and vulnerability in INFORM is key to invest in appropriate preparedness measures, according to FCDO. For UNDCO, climate change enhanced risk indices are able to explore long-term drivers of social inequalities. IOM's

[1] Euro foreign exchange reference rate in 31 December 2019 extracted from European Central Bank available at: https://www.ecb.europa.eu/stats/exchange/eurofxref/shared/pdf/2019/12/20191231.pdf

[2] This piece of research was supported by the project - RECEIPT - Remote Climate Effects and their Impact on European sustainability, Policy and Trade (https://climatestorylines.eu/) - funded from the European Union's Horizon 2020 Research and Innovation Programme under Grant Agreement No. 820712

[3] https://www.gov.uk/government/organisations/foreign-commonwealth-development-office

[4] https://www.un.org/internal-displacement-panel/news/united-nations-development-coordination-office-undco

[5] https://www.iom.int/

global preparedness effort benefits from INFORM's integration of climate and demographic projections as it provides an additional layer of information on the needs of individual mobile populations.

Therefore, JRC decided in collaboration with CMCC to further develop a robust methodology for the new tool, so called "INFORM Climate Change Risk Index". INFORM Climate change Risk Index is an upgrade of INFORM Risk Index. It will be considered as the first version of the methodology because it is expected to be upgraded with the experiences gained through further usage and confronting new situations, feedbacks from the partners and the availability of better data. In the initial phase, INFORM Climate Change Risk Index includes climate and demographic projections. The modification affects only Hazard & Exposure dimension. Indices related to Vulnerability and Lack of coping capacity do not change to account for future socioeconomic expansion and climate-related impacts. That phase will be concluded with the implementation of the INFORM Climate Change tool. Second phase will be dedicated to the research on how to include vulnerability and coping capacity future projections into risk assessment.

The overall objective of the INFORM Climate Change Risk Index would be:

- to develop a common evidence-based tool for risk-informed decision-making that can help unify disaster risk reduction and climate change adaptation strategies,
- a shared and objective understanding of the impact of climate change on the risk of humanitarian crisis and associated vulnerability and coping capacity

This report provides a detailed description of methodology of INFORM Climate Change Risk Index. In its first chapters the report presents the objectives of INFORM Climate Change Risk Index, the phenomena portrayed by the INFORM Climate Change Risk index and its development process. Then it presents the overall logic behind the modelling of the phenomena and existing concepts, i.e. future risk and vulnerability gap. It is followed by the conceptual framework of the climate change and demographic projections and related future scenarios adopted in the INFORM Climate Change Risk Index, the Hazard & Exposure calculation as well as scale and scope of the product. The report provides information on the indicators' selection and their combination through a sound weighting and aggregation schema. Furthermore, it addresses other relevant methodological issues, strengths, limits, opportunities and risks of the current information product generated by the INFORM Climate Change Risk Index model, interpretation of its results and which considerations need to be made when processing the outputs of the model. Last but not least it presents INFORM Climate Change Risk tool, the implementation challenges and how to be used.

1.2 Relevant background information

Scientific community has identified the integration and coherence of disaster risk reduction (DRR), climate change adaptation (CCA) and mitigation strategies as well as sustainable development goals (SDGs) as one of the key components required to strengthen and implement the global response to growing impacts of climate and humanitarian priorities (de Coninck et al., 2018; Lindley et al., 2019). Several major studies and reports have addressed the importance of CCA and DRR integration (EC, 2020; EEA, 2020, 2017; IFRC, 2013; Ilan, 2017; OECD, 2020; Poljansek et al., 2021, 2017; UNDRR, 2019; Wijenayake, 2019).

Global political agenda has followed. Agenda for Humanity calls for disaster risk reduction on a global scale to address and reduce humanitarian needs, risk and vulnerability through risk informed investments in sustainable development (UNDRR, 2019). The Sendai Framework on DRR (SFDRR) calls for more dedicated action to address climate change and variability as one of the underlying disaster risk drivers (UNISDR, 2015a). Global Assessment Report 2019 (UNDRR, 2019) emphasizes the full integration of sustainable development plans and DRR and CCA strategies to achieve the Sendai targets. It also updates progress made in implementing DRR, climate change and sustainable development targets and priorities. The Organisation for Economic Co-operation and Development (OECD)'s report on Common Ground between the Paris Agreement and the Sendai Framework (OECD, 2020) highlights the benefits of increased coherence between CCA and DRR through comprehensive and coordinated action across public administrations.

Also the Intergovernmental Panel on Climate Change (IPCC, 2022) recognizes the disaster risk reduction as a central component of adaptation and mitigation for meeting SDGs and for climate-resilient future. Accordingly, there can be no sustainable development without disaster risk reduction and climate change adaptation. Sustainable Development Goal (SDG) 13 is dedicated to combatting climate change and its impacts, calling for the widest possible international cooperation to accelerate the efforts on climate change mitigation and adaptation policies and practices (UN, 2015). Synergies between CCA and DRR can aid progress in SDGs poverty reduction, economic growth, social inclusion and environmental protection (UN, 2015). In October 2020, the

United Nations Framework Convention on Climate Change (UNFCCC) and United Nations Office for Disaster Risk Reduction (UNDRR) signed a Memorandum of Understanding to enhance and promote CCA and DRR collaboration in National Adaptation Plans and National Strategies for Disaster Risk Reduction (UNFCCC, 2020).

The European Union together with its Member States is the world's leading humanitarian donor, accounting for some 36% of global humanitarian assistance. The European Union recognizes climate change as one the main challenges ahead of humanitarian assistance (EC, 2021a). To step up with recognized challenges Commission proposed within the frameworks of The European Consensus on Humanitarian Aid (EU, 2008) a new strategic vision to strengthen the EU's humanitarian impact globally (EC, 2021a). One of the objectives was to mainstream climate change impacts into humanitarian programming and strengthen coordination with development, security and climate/environment actors to build resilience of vulnerable communities. Furthermore, European Civil Protection and Humanitarian Aid Operations (DG ECHO) renewed its work on disaster preparedness and promote a risk-informed approach to humanitarian action (EC, 2021a). In their mandate, climate change has been considered as a risk multiplier exacerbating the risk of humanitarian crisis and further humanitarian interventions (EC, 2021b). Mainstreaming preparedness and climate change concerns has been also embedded into the European Green Deal to guide the external action of the EU to increase resilience among recipients of EU humanitarian aid (EC, 2019a). The interface between climate change adaptation and disaster risk reduction is also central to the EU Adaptation Strategy (EC, 2021c).

1.3 Identified research gap

Developing common evidence-based tools for risk-informed decision-making and monitoring, reporting and evaluation (MRE) purposes can help unify DRR and CCA strategies and sustainable development plans (UNISDR, 2015a; Wijenayake, 2019). These include common monitoring, evaluation and learning processes, risk and vulnerability assessments, and indicators for target measuring (Wijenayake, 2019). MRE systems for adaptation and risk reduction strategies have to be designed in a way to address not only climate change and/or specific climate hazards, but also human vulnerability and existing adaptation gaps and thereby the different starting points that societies or different groups have towards climate resilience. Such MRE systems are most effective when supported by capacities and resources and embedded in governance systems (Birkmann et al., 2021; IPCC, 2022).

There have been several attempts to design disaster risk reduction and adaptation MRE frameworks across the multilateral system including disaster risk management, climate change adaptation, development and humanitarian communities. For example, the International Institute for Environment and Development (IIED) developed the Tracking Adaptation and Measuring Development (TAMD) tool to track adaptation and measure its impact on development by means of vulnerability and development indicators (IIED, 2014; Kabesiime et al., 2015). In addition, the UN High Level Committee on Programmes Senior Managers Group on Disaster Risk Reduction for Resilience (HLCP/SMG) developed a benchmark indicator-based tool to support and align with SGD progress monitoring by countries, the post-2015 framework for DRR and any future CCA goals and targets (UNISDR, 2015b). This is based on the Sendai framework call for development of coherent global and regional follow-up and indicators in coordination with relevant mechanisms for disaster risk management, sustainable development and climate change (UNISDR, 2015a). The Sendai Framework Monitor provides a set of standards and 38 indicators for countries to track progress towards the targets of the Framework. This can provide valuable information in monitoring disaster risk-related indicators of the SDGs and in measuring CCA progress.

Disaster risk assessment and MRE approaches include quantitative, indicator-based assessments and qualitative, community participatory measures (Birkmann et al., 2020; EEA, 2020, 2015; Poljansek et al., 2017; UNDRR, 2019). Indicator-based assessments are widely used both for analysing risks and assessing progress made by combining hazard, exposure and vulnerability (Bakkensen et al., 2017; Birkmann et al., 2013; EC, 2018; EEA, 2015; ESPON, 2011; Poljanšek et al., 2019a; RESIN, 2018; UNDRR, 2019). The Global Climate Risk Index (Eckstein et al., 2021), the World Risk Index (Welle and Birkmann, 2015), the Notre Dame Global Adaptation Initiative (ND-GAIN) Country Index (University of Notre Dame, 2018), the EU Global Climate Change Alliance plus Flagship Initiative (GCCA+) Index (Miola et al., 2015), and the INFORM Risk Index (De Groeve et al., 2015) are examples of indicator-based multi-hazard disaster risk assessments at the global scale.

2 INFORM initiative

INFORM is a multi-stakeholder forum that develops shared, quantitative analysis relevant to humanitarian crises and disasters. It includes organizations from across the multilateral system, including the humanitarian and development sector, donors, and technical partners.

INFORM partners believe that the availability of shared analysis of crises and disasters can lead to better coordination of actors and better outcomes for at-risk and crisis-affected people. INFORM creates a space and process for shared analysis that can support joint strategy development, planning and action to prevent, prepare for, respond to and recover from crises. This can bring together development, humanitarian and other actors to manage risk and respond better when crises do occur.

INFORM is developing a suite of quantitative, analytical products to support decision-making on humanitarian crises and disasters, mostly at a country-level resolution (**Figure 1**). These tools aid in decision-making at different stages of the disaster risk management cycle, specifically prevention, preparedness and response.

As a result of the recent developments on INFORM Climate Change Risk Index, a new product has been added to the INFORM Suite called INFORM Climate Change. With this new addition, the INFORM Suite can inform also decision-making processes on climate change adaptation.

The purpose of INFORM products is to make information about crises and disasters more accessible for decision-makers. INFORM products are intended to aggregate and present existing information in a way that can create a common evidence base and be easily incorporated into decision-making systems. INFORM methodologies are flexible and open and can therefore be adapted to the needs of different organizations.

Figure 1. INFORM products

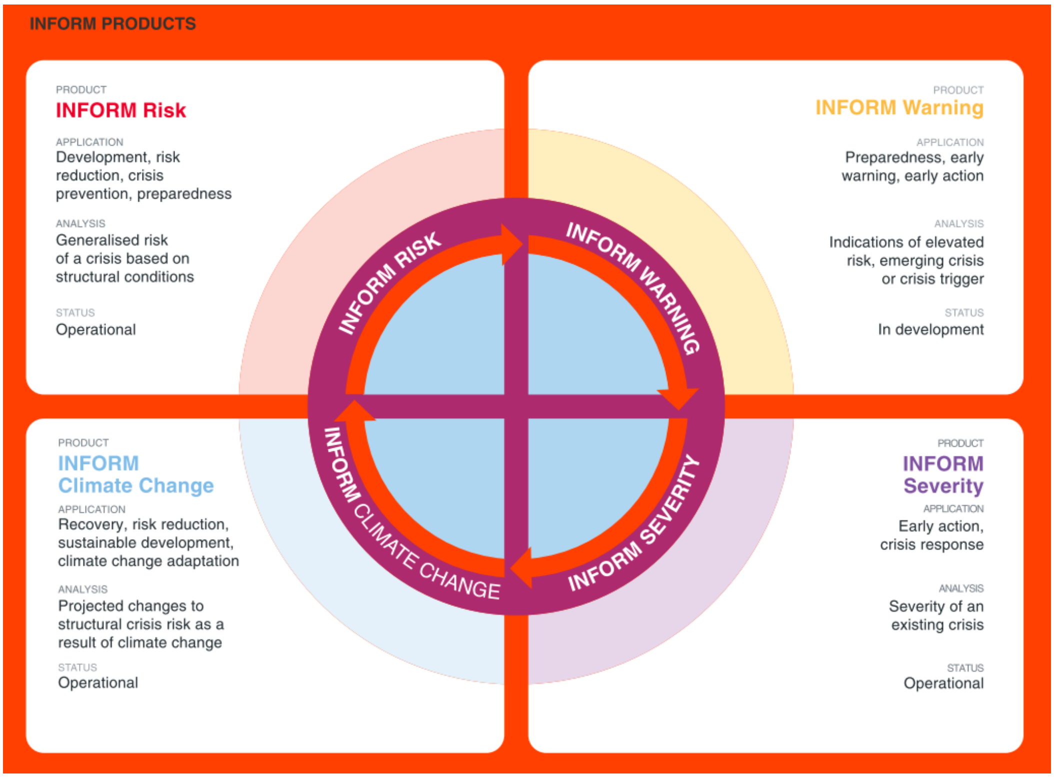

Source: Inter-Agency Standing Committee and the European Commission (2022)

2.1 INFORM Risk

INFORM Risk is an open, composite index that identifies: “countries at risk from humanitarian emergencies that could overwhelm current national response capacity, and therefore lead to a need for international assistance”. It was developed in response to recommendations by numerous organizations (e.g. the World Bank, 2013 and OCHA, 2014) to improve the common evidence basis for risk analysis. Although the index quantifies the risk of humanitarian crisis, it is equally relevant for development and DRR actors, and for high income countries.

INFORM Risk facilitates access to a wealth of information about risk and considers two facets: hazards and human exposure to them; and societal vulnerability to those hazards and their capacity to cope with them. The index is defined by combining approximately 50 different indicators that measure these dimensions and their underlying categories, components and indicators (**Figure 2**). Each of the indicators is normalized for each country to a value that varies from 0 and 10, essentially creating a risk profile that is comparable across countries, then combined into an overall index that also varies from 0 to 10. All levels of the index, including the source data, are open.

Figure 2. INFORM Risk Index model

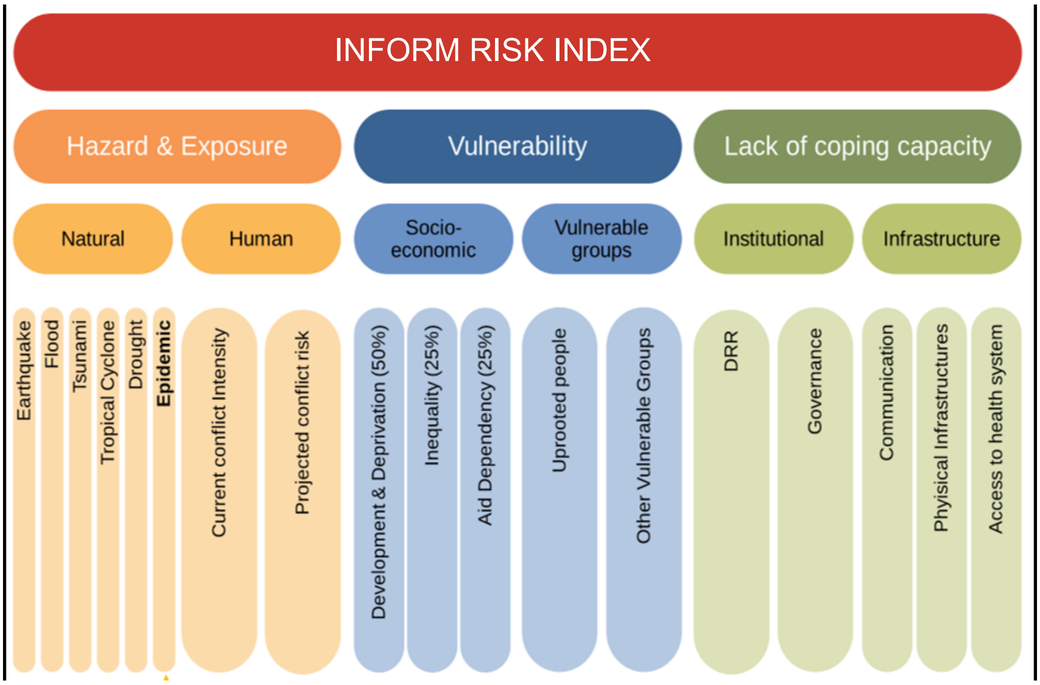

Source: Poljanšek et al. (2018)

INFORM Risk Index can be used to help develop priorities for risk management and building resilience; to support decisions about resource allocation; and to monitor risk trends over time. A shared understanding of risk can lead to programmes and investments that are more commensurate with the risks people face.

The index, in the current framework, considers people's exposure to all main type of natural and human hazards. There are six "natural" hazards: earthquakes, tsunamis, floods, tropical cyclones, droughts and epidemics. The coverage of weather and climate related hazards, namely flood, tropical cyclone wind, storm surge and drought, is based on Global Risk Assessment (UNISDR, 2015c), FAO Agricultural Stress Index (ASI) (Rojas, 2018) and Emergency Events Database (EM-DAT) (CRED, 2019) data for different hazard intensities.

Besides hazard and exposure, vulnerability and lack of coping capacity are the two other dimensions of the INFORM Risk Index, and key factors in the analysis of risk. Vulnerability is the susceptibility of communities to potential hazards, while (lack of) coping capacity measures the (lack of) resources that can alleviate the impact of those hazards. Functionally, vulnerability and coping capacity are inversely related. The vulnerability dimension encompasses socioeconomic vulnerability and vulnerable groups. The socioeconomic category is composed of development and deprivation, inequality and aid dependency, and the vulnerable groups category includes uprooted people, refugees and displaced populations, and other vulnerable groups as a result of recent shocks or different health, age and food security conditions. Lack of coping capacity indicators relate to infrastructure and institutional measures The institutional category evaluates government efficacy in carrying out DRR activities. The infrastructure category combines communication, physical infrastructures, and access to health systems (Marin-Ferrer et al., 2017).

3 About INFORM Climate Change

The INFORM Climate Change Risk Index is an upgrade of the INFORM Risk Index as it includes climate and demographic projections. It offers:

- Snapshots of current and future risk resulting from climate change under different emission and population scenarios in different points in time.
- Change in risk, Hazard&Exposure dimension as well as Natural and Human hazard categories
- And so called "Vulnerability gap" which is the level of vulnerability reduction or coping capacity increase required for a country to preserve its current level of risk.

The Vulnerability gap is intended to inform decision-making processes on the threats imposed by climate-related amplified hazards and the extent the increasing risk could be offset by improved vulnerability and adaptive capacity.

Furthermore, the Vulnerability gap estimates how future climate change risks may alter the need of humanitarian assistance across the globe.

Therefore, it can be used as a proxy to measure the extent of the required adaptation efforts as well as potential humanitarian aid increase.

The INFORM Climate Change Risk Index can benefit humanitarian crisis management planning as well as designing effective disaster risk reduction and climate change adaptation strategies.

3.1 Objective of the INFORM Climate Change Risk Index

The overall objective of the INFORM Climate Change Risk is to develop a common evidence-based tool for risk-informed decision-making that can help unify disaster risk reduction and climate change adaptation strategies. It seeks to communicate the potential impacts of climate change and associated vulnerability gap under various climate change and development pathways in a systematic, objective and understandable way. In its use - in combination with other sources of information - the INFORM Climate Change Risk Index is intended to:

- Lead to a shared and objective understanding of the impact of climate change on the risk of humanitarian crisis and associated vulnerability and coping capacity
- Guide Climate Change Adaptation to further address discrimination by identifying inequalities in terms of the climate impact on marginalized groups such as people on the move and including risks to youth and future generations not accounted for in typical short-term policymaking.
- Support economic policymaking in direction of more resilient to the adverse impacts of climate change
- Provide operational recommendations on where to allocate disaster risk reduction and adaptation resources consistent with SDG and Sendai targets.

Policy implications and uses of the INFORM Climate Change Risk Index have been identified by its partners (Box 1), namely the United Kingdom's Foreign, Commonwealth & Development Office (FCDO), the United Nations Development Cooperation Office (UNDCO), the International Organization for Migration (IOM), and the International Federation of Red Cross and Red Crescent Societies (IFRC) [6].

Box 1: Possible uses of INFORM Climate Change Risk Index identified by some partners

FCDO: INFORM data feed into the FCDO's global risk monitoring and early warning systems which guides FCDO's humanitarian work. The FCDO early warning system provides a centralized, independently assesses humanitarian need, flags overlooked risks, and informs senior decision makers about new crises or ongoing emergencies that may require intervention on a monthly and on-demand basis. In the context of a changing climate, many factors that underpin the INFORM Risk Index values will also change (both natural hazards and likely exposed populations). By capturing the projected effects of climate change, the extended INFORM Risk Index enables the FCDO and its partners to assess future likely humanitarian need and invest in appropriate preparedness measures in risk-prone countries.

[6] https://www.undrr.org/publication/projecting-effects-climate-change-framework-inform-risk-index

UNDCO: The UNDCO recognises the benefit of the INFORM Risk tool in its work such as supporting the UN's activities for sustainable development, which inform policy, program and operations on the ground. The UNDCO highlights several thematic areas in which climate informed risk data could strengthen the annual United Nations Common Country Analysis (UN-CCA) and Sustainable Development Cooperation Framework (SDCF). CCA is a strategic planning and implementation instrument which prioritizes development activities at country level and is ultimately translated into an agreement with the government through the SDCF. All CCAs include a section summarizing the country's climate and environmental challenges. This typically covers SDG progress, obligations under international environmental law and climate agreements, implementation challenges, capacity gaps and opportunities. With climate informed risk data, this analysis could additionally include a forward-looking analysis with predictions or scenarios on future climatic conditions and their environmental, development, humanitarian or peace implications. Climate informed risk data could also guide CCA to further address discrimination by identifying inequalities in terms of the climate impact on marginalized groups such as people on the move and including risks to youth and future generations not accounted for in typical short-term policymaking. Furthermore, the economic transformation analysis in CCA can benefit from INFORM Risk climate change data which support economic policymaking that is more resilient to the adverse impacts of climate change. Since climate does not exist in a vacuum but interacts with multidimensional risks, exacerbating socio-economic vulnerabilities climate-informed risk data can breakdown the siloes around related disciplines, such as CCA and DRR, for a more comprehensive analysis of present and emerging risks. The UNDCO also identifies disaggregating climate-informed risk data at sub-national level and by gender as a possible development of the INFORM instrument.

IOM: IOM's approach in managing and preventing migration and forced displacement is implemented through DRR, CCA and environmental sustainability measures. IOM uses INFORM Risk data as a key indicator for its global preparedness efforts, including to identify gaps in available capacities for response and priorities for capacity building. Moreover, risk profiles based on available assessments of different hazards support the development or update country-specific contingency plans and preparedness measures in IOM Country Offices. INFORM Climate Change offers an additional layer of information, which can contribute to develop a stronger analytical capacity that can link the IOM's current data collection capacities to operational preparedness and offer Member States the possibility to ensure the needs of individual mobile populations are anticipated and met at all stages of their journey.

IFRC: Understanding the potential impacts of climate and population change is important for the IFRC. Information about future risks is essential for the prevention and alleviation of human suffering in order to address underlying risk drivers, take anticipatory action and respond to crises in a timely manner. The IFRC uses INFORM's climate change impacts data to inform DRR and CCA interventions, ensuring these efforts are based on sound science and facilitating the engagement of communities in the process. In the near term, this information is also useful for IFRC's annual programming, knowing what kind of assistance is likely to be needed, when and where, during the course of a year and in support of forecast-based action. Early results from the INFORM Climate Change tool have been included in the IFRC's World Disaster Report (WDR) (IFRC, 2020) "Come Heat or High Water".

3.2 Climate change impacts, adaptation, and vulnerability in the context of humanitarian assistance

Climate change contributes to worsening humanitarian crises where climate hazards interact with high vulnerability and low coping capacity. Countries in Africa, Central and South America have experienced increasing trends in **flood, drought-related acute food insecurity and malnutrition**. Extreme weather events, particularly droughts, can result in poverty traps and widening inequalities within and across countries. According to estimates from the Famine Early Warning Systems Network (FEWS, 2018), more than 83 million people experienced crisis conditions requiring food assistance in 2018—75% more than in 2015. Future climate warming will likely have a severe impact on agriculture and food security in Africa where 85% of Africa's poor live in rural areas and mostly depend on agriculture for their livelihoods (Adams, 2018; Mahmood et al., 2019). The majority of countries in Central America are exposed to 2 or more risks derived from natural extreme events (drought, intense rains, cyclones and El Niño–Southern Oscillation), affecting between 57% to 96% of the GDP of the countries (ECLAC, 2015). With continued increase in the frequency and intensity of extreme events, there will be increased demand for international efforts, including disaster aid and humanitarian efforts.

Climate and weather extremes are increasingly driving **displacement of the people** in all regions of the globe, with small island states disproportionately affected. Climate extremes are already causing an average of more than 20 million people internally displaced each year (UNHCR, 2021). Climate change has also exacerbated the degradation of **human security and conflicts** causing additional migration and displacement in vulnerable areas. Reducing the future risk of large-scale population displacements, including those requiring active humanitarian interventions and organized relocations, requires the international community to take further action to control future warming (IPCC, 2022).

Climate change has adversely affected physical **health of people** globally. The impacts on physical health include increased human mortality and morbidity from heatwaves, higher occurrence of climate-related food-borne and water-borne diseases, and higher incidence of vector-borne diseases from range expansion and/or increased reproduction of disease vectors (IPCC, 2022; Norwegian Red Cross, 2019). A highly conservative projections show additional 250 000 deaths each year due to climate change between 2030 and 2050; of these, 38 000 will result from exposure of the elderly to heat, 48 000 from diarrhoea, 60 000 from malaria and 95 000 from childhood undernutrition (WHO, 2018). The World Health Organization developed a Global Action Plan for Healthy Lives and Wellbeing for All to bring together multilateral health, development, and humanitarian agencies to urgently support countries to accelerate health and humanitarian services in fragile and vulnerable settings (WHO, 2021a).

Climate change has already shown diverse adverse impacts on human systems. Higher degrees of humanitarian interventions would be essential to alleviate the future extreme weather-related human suffering, fatalities, injuries and displacement. Humanitarian funding appeals has almost tripled from EUR 6.8 billion in 2008 to EUR 23.8 billion in 2017 triggered by multiple complex crisis, as well as increased frequency of natural disasters caused by climate change (UN, 2016). In 2018, around 108 million people required international humanitarian assistance as a result of weather and climate extreme events including storms, floods, droughts and wildfire. Projections show that over 200 million people could need humanitarian assistance every year as a result of climate-related disasters and the socioeconomic impact of climate change by mid-century (EC, 2021a).Despite the growing humanitarian impact of climate change, far too little global climate finance has been provided to support the most vulnerable countries (IFRC, 2020). Continued efforts through partnerships, blending adaptation and disaster risk reduction, and long-term international financing from public and private sources are needed to bridge humanitarian and sustainable development priorities (Lindley et al., 2019). Such efforts should address vulnerability and its root causes (including poverty, inequality, environmental degradation, social injustice, environmental mismanagement, and failed governance) as the critical part of adaptation to climate-related disasters. **Climate change adaptation strategies** should integrate poverty reduction, disaster risk reduction and humanitarian development in order to **reduce vulnerabilities and strengthen people's adaptive capacity**. Otherwise, humanitarian crisis will be aggravated even with moderate climate change, as a result of further erosion of livelihood security in vulnerable regions (IFRC, 2020; IPCC, 2022).

3.3 Climate models, projections and scenarios

The projections of future climate can be made using climate models. Climate models study how different factors interact to influence a climate and help us to design the most plausible future scenarios. This chapter provides detailed information on climate models, available projections and IPCC-led climate and socioeconomic scenarios to analyse future climate change impacts.

3.3.1 Climate models and projections

Climate models simulate the key components of the earth system that affect weather and climate based on the physical equations for the conservation of momentum, energy and mass. Climate models can make short term predictions (seasons to years) and long-term projections of the climate (decades to centuries) system. Short term predictions consider natural factors (e.g., changes in ocean state, solar irradiance and volcanic aerosol). Seasonal forecasts attempt to provide information about the "climate" that can be expected in the coming months. The seasonal forecast is not a weather forecast as it considered the statistical summary of the weather events in a given season. Long term projections introduce also anthropogenic impacts on the climate system, such as greenhouse gas (GHG) emissions and land-use changes. Changes in GHGs become important in climate change modelling as GHG emission concentrations accumulate in the atmosphere. Short term and long-term climate models also differ in the initialization period. Short term prediction models start the simulations from the current observed state of the climate system. Long term projections are based on (1) historical runs including observed greenhouse gas emissions due to industrialization started in 1850 and (2) projections including scenarios of GHG emissions (**Figure 3**) (DWD, 2021; IPCC, 2021; Met Office, 2021; NOAA, 2022).

Figure 3. Schematic representation of a climate projection. Modified from DWD (2021)

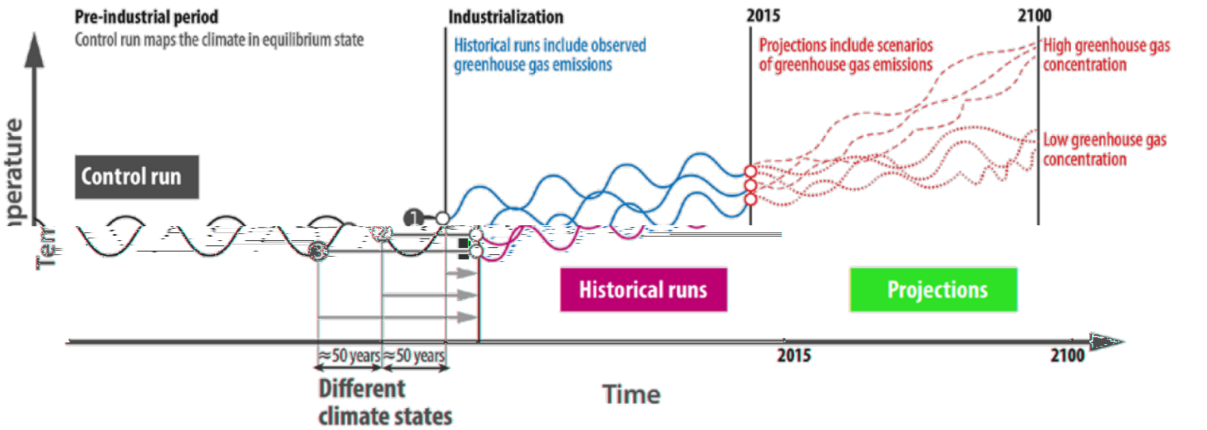

Source: Modified from DWD (2021)

Both, short-term and long-term predictions and projections have to deal with uncertainties. They originate from the chaotic behaviour of climate system and the imperfect description or understanding of climate processes. Using various initial values or modified model parameters modellers calculate several climate simulations. They provide a spectrum of possible future changes in the climate system to provide a range of uncertainty. The final statements are the outcome of the analysis of the ensemble of all climate simulations. For example, the 2050 projections are the average of the ensemble mean of climate simulations within the 30-year time window. According to WMO, it is common practice to use 30-year periods to record the climate and climate changes in order to reduce the influence of natural variability in statistical analyses.

We can only describe the climate with statistical properties (such as averages, extreme values, frequencies, etc.) of the climate elements over a sufficiently long period of time. The WMO uses reference period 1981–2010 for assessing climate change and for comparisons with recent measurement data (WMO, 2021).

3.3.2 IPCC-led climate change scenarios

Looking into future requires agreement on scenarios of possible development. Over the past decade, the climate change research community has developed a scenario framework combining alternative projections of future climate and society to support science-policy interface (O'Neill et al., 2020). Such scenario framework includes:

- the Representative Concentration Pathway (RCPs) describing the evolution of future atmospheric greenhouse gas concentrations and other radiative forcings[7] (**Box 2**) and
- Shared Socioeconomic Pathways (SSPs) that portray how socioeconomic factors may change over the next century (Ebi et al., 2014; Kriegler et al., 2014; O'Neill et al., 2014; van Vuuren et al., 2014) (**Box 3**).

The primary goals of the RCP-SSP frameworks are:

- To harmonize climate change-related research across different research communities;
- To integrate climate and societal futures to facilitate impacts, adaptation and mitigation studies;
- To introduce uncertainty in future climate and societal conditions using a wide range of plausible future climate and development pathways;
- To support science-policy interface and joint construction of knowledge with the aim of enriching disaster risk and adaptation decision-making.

[7] amount of downward-directed radiant energy impinging upon Earth's surface

Box 2. The Representative Concentration Pathways (RCPs)

RCPs include time series of emissions and concentrations of the full suite of greenhouse gases and aerosols and chemically active gases, as well as land use/land cover that would lead to the specific radiative forcing characteristics (IPCC, 2014). RCPs are used as an input for climate model simulations carried out under the framework of the Coupled Model Intercomparison Project Phase (CMIP5 and CMIP6) of the World Climate Research Programme. RCPs usually refer to the concentration pathway and corresponding emission scenarios up to 2100 produced by Integrated Assessment Models. IPCC 5th Assessment Report considers four RCPs (2.6, 4.5, 6 and 8.5) produced from Integrated Assessment Model as a basis for the climate predictions and projections (Mach et al., 2014):

RCP2.6: A stringent mitigation scenario for which the surface temperature by the end of the 21st century (2081–2100) relative to 1986–2005 is likely to be 0.3°C to 1.7°C.

RCP4.5 and RCP6.0: Two intermediate stabilization pathways where the surface temperature by the end of the 21st century (2081–2100) relative to 1986–2005 is likely to be 1.1°C to 2.6°C, and 1.4°C to 3.1°C under RCP6.0 respectively.

RCP8.5: One high pathway for which the surface temperature by the end of the 21st century (2081–2100) relative to 1986–2005 is likely to be 2.6°C to 4.8°C.

The latest IPCC sixth assessment report (IPCC, 2021) has developed five pathways, spanning a broad range of forcing in 2100 (1.9, 2.6, 4.5, 7, and 8.5 watts per meter squared) carried out under the CMIP6 models. Unlike AR5, the RCPs in AR6 are coupled with socio-economic assumptions based on feasibility or likelihood of individual scenario. Accordingly, the increase of global mean surface temperature by the end of the 21st century relative to 1850–1900 is likely to be 1°C to 1.8°C under SSP1-1.9, 1.3°C to 2.4°C under SSP1-2.6, 2.1°C to 3.5°C under SSP2-4.5, 2.8°C to 4.6°C under SSP3-7.0.and 3.3°C to 5.7°C under SSP5-8.5 (Figure B1).

Figure B1: Global surface temperature change relative to 1850–1900

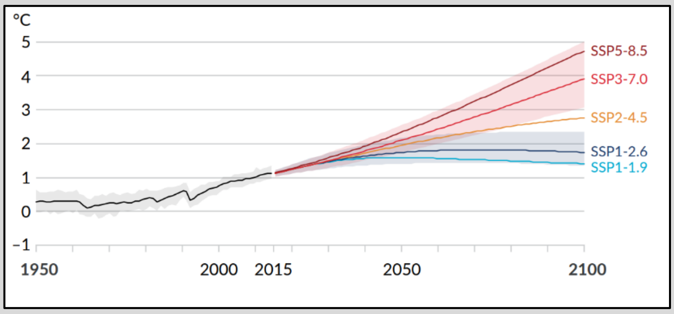

Source: IPCC (2021)

Box 3. The Shared Socioeconomic Pathways (SSPs)

SSPs include societal factors such as demographics, human development, economic growth, inequality, governance, technological change and policy orientations (O'Neill et al., 2017; Riahi et al., 2017; van Vuuren et al., 2017). Socioeconomic projections with consistent 21st Century narratives are available for the SSPs for population (KC and Lutz, 2017), urbanization (Jiang and O'Neill, 2017), gross domestic product (Dellink et al., 2017), educational attainment and age structure dynamics (Crespo Cuaresma, 2017). Five SSPs are developed to span a range of potential outcomes for the challenges associated with both climate change mitigation and adaptation. The SSPs do not include neither mitigation and adaptation responses, nor the impacts of climate change. This allows the SSPs to be used as a reference case for assessing a variety of policies and projected risks. Five SSP narratives (O'Neill et al., 2017, 2014) are:

SSP1 (sustainability): considers low challenges to mitigation and adaptation, global population peak in mid-century, reasonably high pace in sustainable development, lessened inequalities, rapid technological growth based on low carbon energy sources and high productivity of land.

SSP2 (middle of the road): considers moderate challenges to mitigation and adaptation, population growth stabilized toward the end of the century, an intermediate case between SSP1 and SSP3.

SSP3 (regional rivalry): considers high challenges to mitigation and adaptation, high population growth in developing countries, moderate economic growth, slow technological change in the energy sector, low investments in human capital, high inequality, unfavourable institutional development with low adaptive capacity.

SSP4 (inequality): considers low challenges to mitigation and high challenges to adaptation, population growth stabilizes toward the end of the century, relatively rapid low carbon technological development and large mitigative capacity in major emitting regions. Other regions experience slow technological development, high inequality and relatively isolated economies, leading to high vulnerability and limited adaptive capacity.

SSP5 (fossil-fuel development): considers high challenges to mitigation and low challenges to adaptation, global population peak in mid-century, high energy demand mostly met with carbon-based fuels, low investments in alternative energy technologies, rapid economic development driven by high investments in human capital leading to a more equitable distribution of resources, stronger institutions, and slower population growth.

Figure B2: SSPs presented as different futures with uncertainties spanned among mitigation vs adaptation to climate change challenges

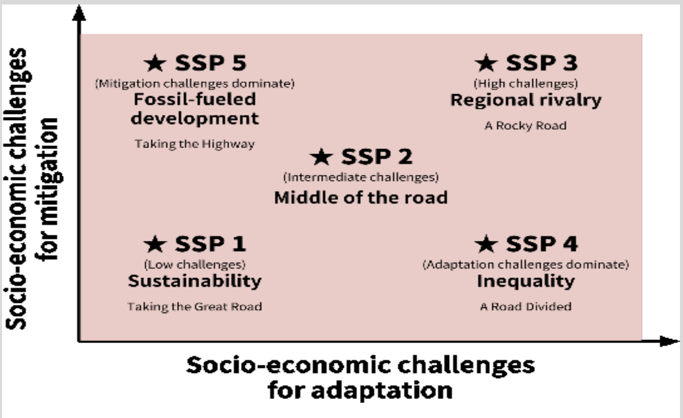

Source: O'Neill et al. (2012)

Figure B3: Total world population size by the end of 21st Century under SSPs

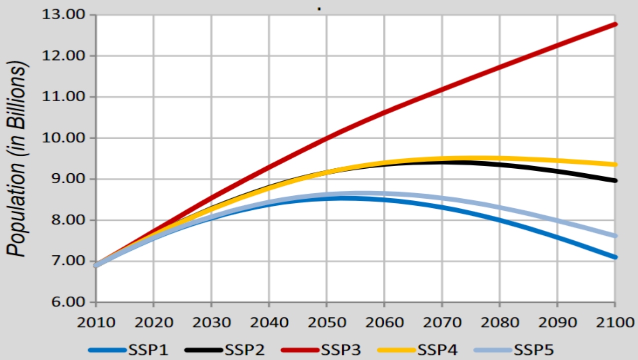

Source: KC and Lutz (2017)

The two set of scenarios, RCPs and SSPs, complement each other. The RCPs set pathways for greenhouse concentration and, so, the amount of warming that could occur by the end of century regardless of any specific societal pathways (Figure B1). Whereas the SSPs set the alternative future societal pathways in which no climate change impacts occur, nor climate policy responses implemented (O'Neill et al., 2020; Riahi et al., 2017).

Since 2014, different combinations of RCP-SSP scenarios have been applied to assess the future climate change impacts. O'Neill et al. (2020) explores the applications of RCP-SSP combinations in 715 total studies applying integrated scenarios, published over the period 2014–2019. Accordingly, RCP8.5-SSP2, RCP8.5-SSP2 and RCP8.5-SSP5 are the most applied combinations followed by RCP8.5-SSP3, RCP2.6-SSP1 and RCP2.6-SSP2. In total, SSP2 is the most applied SSP scenario followed by SSP1 and SSP3, and, in the same terms, RCP4.5 and

RCP8.5 among RCPs. Van Vuuren *et al.* (2014) developed a scenario matrix to address the effectiveness of various RCP-SSP combinations in year 2100 using different integrated assessment modelling (IAM) teams. They conclude that the plausible combinations are: RCP4.5 with SSP1, RCP6 with SS2, SSP3 and SSP4, and RCP8.5 with SSP3 and SSP5. The IPCC sixth assessment report recognizes RCP4.5-SSP2 and RCP8.5-SSP5 as the most plausible combinations based on the new generation of the RCPs (IPCC, 2021).

3.4 Development process of INFORM Climate Change Risk Index model and the tool

The development of the INFORM Climate Change Risk Index was initiated in 2019 in a joint effort between JRC and CMCC. The development process included:

- Visiting scientist exchange in 2019 – conceptualization and data collection
- INFORM annual meeting 2019 – presenting conceptual framework and preliminary exposure analysis
- September 2020 – submission of an abstract to UNDRR Global Assessment Report 2022 call for contributing papers (chapter 3-6, Unpacking and revealing characteristics of vulnerability, exposure and managing systemic risks)
- January 2021 - submission of the scientific article (journal of Global Environmental Change[8])
- January 2021 – special webinar dedicated to present the first results to INFORM partners
- February 2021 - submission of the policy report for UNDRR Global Assessment Report 2022
- August 2021 – Receiving the acceptance from UNDRR
- November 2021 – publication of the scientific article November 2021 – publication of the scientific article (Marzi et al., 2021)
- November 2021 – conceptualization and review process for the INFORM Climate Change tool
- February 2022 – finalizing the data collection and analysis
- May 2022 – publication of the policy report for UNDRR Global Assessment Report 2022[9]
- May 2022 – INFORM annual meeting 2022 – presenting beta version of the Climate Change Tool and sharing the draft of this report with partners for review

The technical development of the INFORM Climate Change Risk Index has been continuously presented to and consulted with the INFORM partners in several stages. The partners were also involved in the preparation of the UNDRR policy report expressing their interest in the tool and further policy implications and use cases.

The development of the INFORM Climate Change Risk Index has taken a set of steps to identify the conceptual framework, data sources, workflow and analytical tool design:

- Understand the concept of climate change risk and define the model:
    - identify alternatives to expand the original INFORM Risk model with climate and socioeconomic projections including scenario combinations and time frame.
    - Identify the expected outcomes of the model that can be further used as a policy measure (e.g vulnerability gap)
- Identify open-source datasets that could be potentially used to develop the model. Our criteria were to have consistent dataset covering at least two different concentration pathways (RCP4.5 and RCP8.5), and two different points in time (2050 and 2080)
- Importing the data and calculate risk variables using INFORM Risk workflow developed to foster the calculation process.
- Design INFORM Climate Change tool, the analytical dashboard which provides insight into the results of the climate change risk analysis.

[8] https://www.sciencedirect.com/science/article/pii/S0959378021001722
[9] https://www.undrr.org/publication/projecting-effects-climate-change-framework-inform-risk-index

Future developments will focus on extending the index with available projections of various drivers of vulnerability and coping capacity such as social characteristics, migration, governance, urbanization, infrastructure, and health status under the SSPs.

4 Conceptual framework

4.1 Existing concepts

The concept of risk has been interpreted in different ways, reflecting the evolution of a variety of scientific disciplines in the fields of disaster risk reduction (DRR) and climate change adaptation (CCA) (Mysiak et al., 2018). The DRR community defines risk as the potential loss of life, injury, or destroyed or damaged assets which could occur to a system, society, or a community in a specific period of time, determined probabilistically as a function of hazard, exposure, vulnerability and capacity[10]. The CCA community under the IPCC guidance has traditionally put more emphasis on vulnerability (ESPON, 2011; IPCC, 2007, 1996; McCarthy, 2001), denoted as a function of exposure, sensitivity and adaptive capacity (Bizikova et al., 2009; Brooks, 2003; KC et al., 2015; Smit and Wandel, 2006; Turner et al., 2003).

Since 2012, with IPCC Special Report on Managing the Risks of Extreme Events and Disasters to Advance Climate Change (SREX) (IPCC, 2012) and the Fifth Assessment Report (IPCC, 2014a), the community focus has shifted towards a risk-centred framework. IPCC Fifth Assessment Report defines risk in the context of climate change impacts as a result from dynamic interactions between climate-related hazards with the exposure and vulnerability of human and natural systems (IPCC, 2014a; Reisinger et al., 2020). Vulnerability comprises “sensitivity or susceptibility to harm” and “lack of capacity to cope and adapt” (IPCC, 2014a). The susceptibility is a function of hazard intensity and the properties of the exposed elements (Poljansek et al., 2017). The adaptive capacity refers to capabilities, resources and institutions driving adoption of adaptation strategies and implementation of effective action (IPCC, 2014a; Marzi et al., 2018).

IPCC defines adaptive capacity as ‘the ability of systems, institutions, humans, and other organisms to adjust to potential damage, to take advantage of opportunities, or to respond to consequences’ (IPCC, 2014). These aspects are partly covered in the INFORM Risk Index’ coping capacity and mostly related to the outcome sound disaster risk governance system. The latter acknowledges also the changes in risk landscape due to climate change as well as climate change adaptation strategies and integrates adaptation measures in DRM planning.

The concept of risk in the latest IPPC report refers not only to the climate change impacts, but also climate change responses. Accordingly, risk can be a result of “failures in achieving the intended targets (e.g. Paris Agreement, Sendai framework, etc.), or from potential trade-offs with, or negative side effects on, other societal objectives, such as the Sustainable Development Goals” (Reisinger et al., 2020).

4.2 Concept of the INFORM Climate Change Risk model

INFORM Climate Change Risk is the upgrade of the INFORM Risk model (**Figure 2**). INFORM Risk model is a composite of three dimensions: the hazard and exposure (events that could occur and exposure to them), vulnerability (the susceptibility of communities to those hazards) and lack of coping capacity ((lack of resources available that can alleviate the impact) conceptualized based on pressure and release model (PAR model) and Cardona’s holistic perspective of vulnerability and risk (De Groeve et al., 2014). The INFORM Risk model balances two major forces: hazard and exposure dimension on one side, and the vulnerability and the lack of coping capacity dimensions on the other side. Hazard-dependent factors are treated in the hazard & exposure dimension, while hazard-independent factors are divided among two dimensions: the vulnerability dimension that considers the strength of the individuals and households relative to a crisis situation, and the lack of coping capacity dimension that considers factors of institutional strength.

In initial phase of this exploratory study the modification affects only Hazard&Exposure dimension. Indices related to Vulnerability and Lack of coping capacity will not change to account for future socioeconomic expansion and climate-related impacts. INFORM Risk hazard and exposure data are based on historical probabilistic hazards combined with the latest population estimates. Six natural hazards are included: earthquakes, tsunamis, floods, tropical cyclones, droughts and epidemics. In this study, the INFORM Climate Change Risk’s Hazard&Exposure dimension will be upgraded with hazard and exposure projections based on plausible RCP-SSP combinations for different points in time (baseline, 2050 and 2080). It also considers other – not climate related natural and human hazards. Natural hazards components are adjusted to available data for projections, that is earthquakes, tsunamis, river flood, coastal flood, tropical cyclone winds and epidemics. The upgraded (**Figure 4**) and original (**Figure 2**) frameworks differ only in the case of “Tropical cyclone”

[10] https://www.undrr.org/terminology/disaster-risk

component which has been split to “Tropical cyclone wind” and “Coastal flood” to better describe the amplified climate-related hazards and risk.

Figure 4. INFORM Climate Change Risk Index model

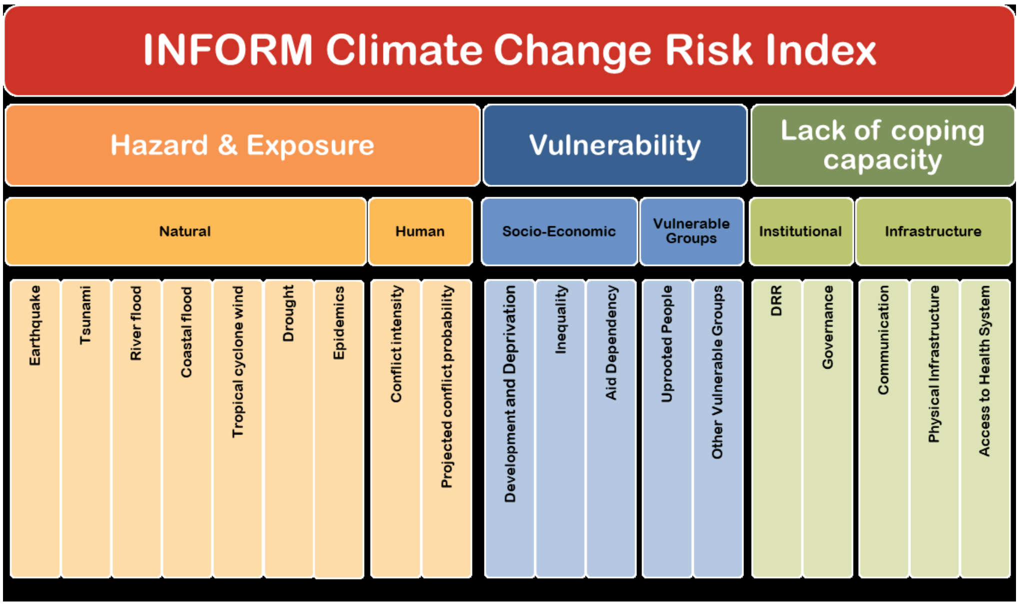

Source: Authors

Calculation will follow moderate (RCP4.5) and high (RCP8.5) concentration pathways combined with sustainability (SSP1), middle of the road (SSP2), regional rivalry (SSP3) and fossil fuel development (SSP5) socioeconomic pathways for river and coastal flood, drought and epidemics together with SSP-based projections of civil conflict. The population projections derived from SSPs are also applied to non-climate natural hazards and climate hazards for which projection data are not available (earthquake, Tsunami and tropical cyclone wind). This provides snapshots of possible future risk changes resulting from different greenhouse gas concentrations, population, and other socioeconomic scenarios. The narratives might change in the updates based on data availability and methodological issues. **Figure 5** illustrates the conceptual workflow used to develop the INFORM Climate Change Risk index.

In order to investigate the interactions between climate change hazard and population growth, the risk has been calculated also using only RCPs with the population estimates fixed at 2015 values using the Global Human Settlement Layer (GHSL, Pesaresi et al., 2016). This isolates the climate change risk without accounting for projected changes in population.

Figure 5. INFORM Climate Change Risk Index conceptual framework

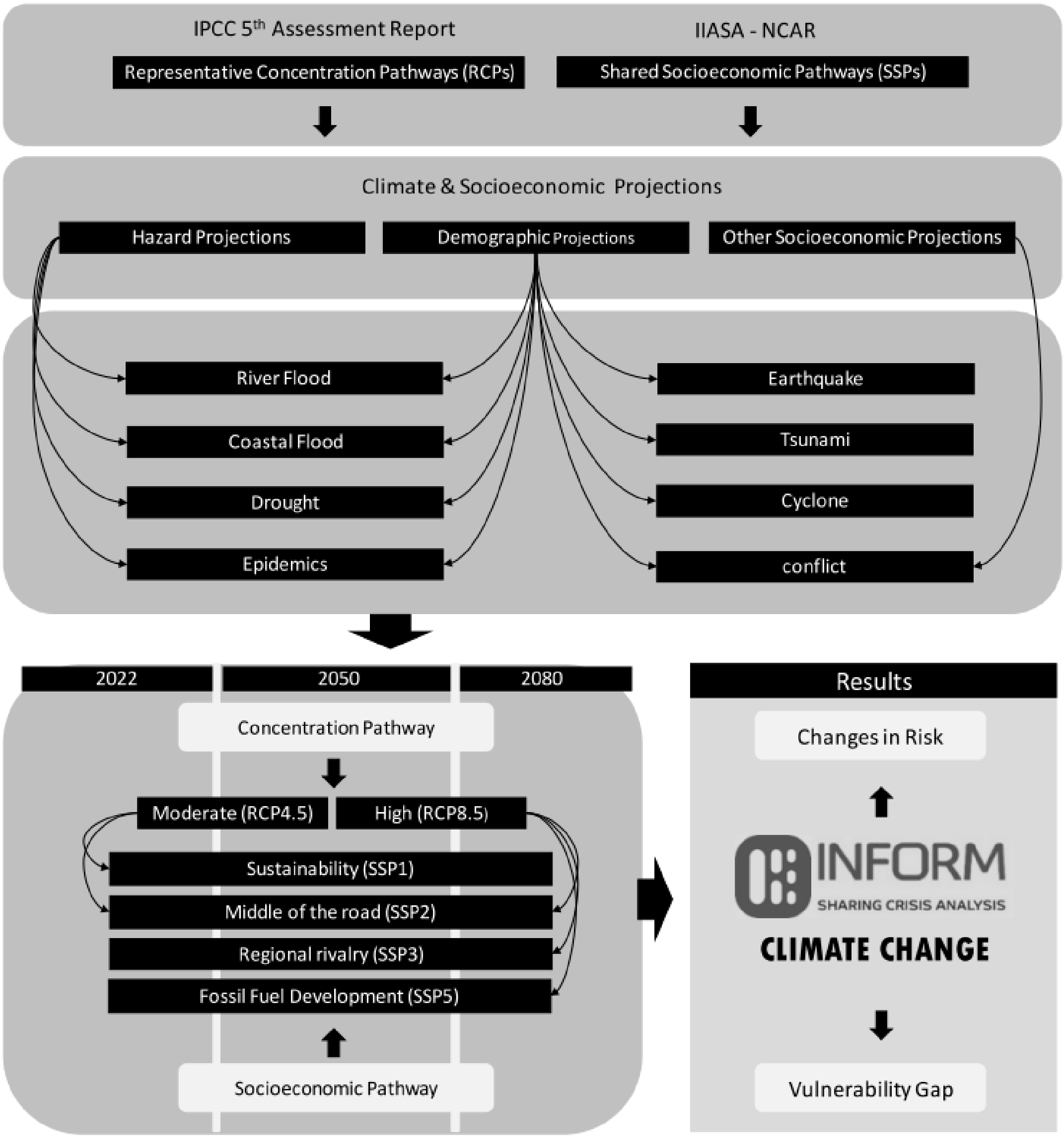

Source: Authors

4.3 Calculating risk in the future

The INFORM Climate Change risk is calculated with the same multiplicative equation as INFORM Risk (De Groeve et al., 2014), where each of the dimensions are equally weighted (33% each). In this form also INFORM Climate Change Risk score is more susceptible to Vulnerability and Lack of coping capacity, the internal forces of risk that can be most influenced by the DRR activities (**Figure 6**, **Equation 1**).

Figure 6. The risk concept behind INFORM Risk and INFORM Climate Change Risk indices

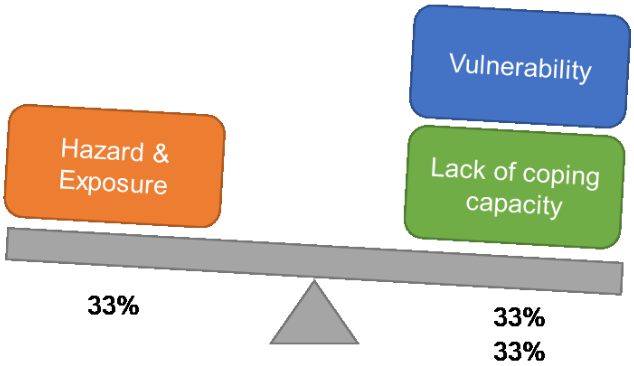

Source: De Groeve et al., 2014

$$Risk = Hazard\&Exposure^{\frac{1}{3}} \times Vulnerability^{\frac{1}{3}} \times Lack\ of\ coping\ capacity^{\frac{1}{3}} \qquad \textbf{Equation 1}$$

Although both INFORM and IPCC consider analogous dimensions to assess the risk, the importance and order of the dimensions are different. IPCC considers vulnerability as a result of sensitivity, lack of coping and adaptive capacity while INFORM vulnerability reflects the susceptibility of the population to hazards and has been combined with INFORM lack of coping capacity related to the effort of the governments. Therefore, IPCC vulnerability components are equivalent to the combined INFORM's Vulnerability and Lack of coping capacity.

4.4 Calculating vulnerability gap

Vulnerability gap is the level of vulnerability reduction and coping capacity increase for each country which is needed to at least preserve the risk at the current level. It is assumed that this is the only mechanism to counteract the amplified hazards. To compute the vulnerability gap, we keep the risk constant at the current level (INFORM Climate Change Risk Index baseline - Hazard & Exposure analysis based on 2015 population), alter the hazard and exposure (H&E) using the projections, and compute the required vulnerability (VU) – lack of coping capacity (LCC) component to balance the equation (**Equation 2**). Afterwards, we calculate the difference between the required vulnerability - lack of coping capacity and the one from the INFORM Climate Change Risk Index baseline (**Equation 3** and **Equation 4**).

$$Risk_{Current} = H\&E_{Future}{}^{\frac{1}{3}} \times (VU \times LCC)_{Required}{}^{\frac{1}{3}} \qquad \textbf{Equation 2}$$

$$Risk_{Current} = H\&E_{Current}{}^{\frac{1}{3}} \times (VU \times LCC)_{Current}{}^{\frac{1}{3}} \qquad \textbf{Equation 3}$$

$$VU\ gap = (VU \times LCC)_{Current} - (VU \times LCC)_{required} \qquad \textbf{Equation 4}$$

$$= Risk_{Current}{}^{3} \times \left(\frac{1}{H\&E_{Current}} - \frac{1}{H\&E_{Future}}\right)$$

4.5 Scope and Scale – spatial and temporal

The scope and scale of the composite indicator define requirements for data. When selecting the indicators, the possible scalability in geographical and temporal scale is always considered as an important property.

The spatial scope of INFORM Climate Change Risk Index is global, the scale is country level. The hazard and exposure data are primarily assessed at pixel level with various resolution based on the input data, and then aggregated at country level to fit the INFORM scope.

Box 4. Incorporating climate change into INFORM subnational model

INFORM subnational model uses the same risk assessment methodology and development process but is adapted to regional or national level. Since the Hazard&Exposure data are analysed at very fine scale, it is also possible to incorporate analogous modifications into INFORM subnational models, based on the interest of the stakeholders. This does not apply to small island states where the resolution of the global and regional climate models exceeds the size of those countries, especially in the case of drought.

Regarding the temporal scale and scope, INFORM Climate Change Risk Index covers the projections up to the end of 21st century. The baseline Hazard&Exposure index covers the historical climate and population fixed at 2015 estimates. The projections are calculated for 2050 and 2080, which are the average of the ensemble mean of climate simulations within the 30-year time window, (e.g. 2036 to 2065, and 2070 to 2099 for drought exposure projections), and SSP-based population projection for 2050 and 2080.

4.6 Frequency of update

The baseline data for INFORM Climate Change risk Index will be updated annually with the latest official INFORM Risk Index release especially for vulnerability and lack of coping capacity indicators.

The climate projections used for the INFORM Climate Change Risk Index are based on Coupled Model Intercomparison Project Phase 5 (CMIP5) of the World Climate Research Programme. The recently published IPCC sixth assessment report is based on new generation of climate models (CMIP6) with a wider range of climate sensitivity compared to CMIP5 climate models. The hazard projections based on the CMIP6 climate models will be incorporated in the INFORM Climate Change Risk Index as soon as the bias-corrected simulations' data are available.

4.7 The combination of RCP-SSP scenarios used

In this study, we consider a large suite of five plausible scenario combinations (**Figure 7**) namely RCP4.5-SSP1, RCP4.5-SSP2, RCP8.5-SSP2, RCP8.5-SSP3 and RCP8.5-SSP5 suggested by climate change community (O'Neill et al., 2020; Riahi et al., 2017; van Vuuren et al., 2014). In this way, we are able to expand the uncertainty in future climate changes and provide a challenging yet plausible scenario context to inform the climate change adaptation and disaster risk management. In addition, we also consider two "constant population" scenarios where the exposure has been calculated using only RCPs with the population estimates fixed at 2015 values. The projected conflict risk is fixed at baseline levels as well to help identifying distinct impacts of climate-related amplified hazards on future exposure and risk.

Figure 7. Scenario combinations used to assess the risk

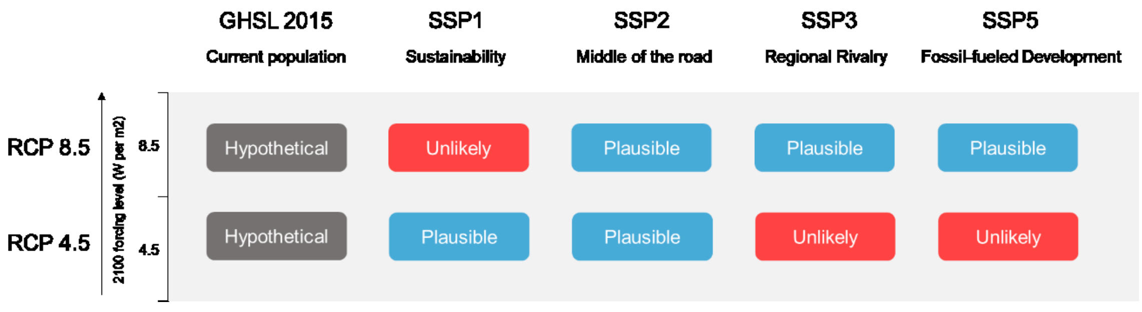

Source: Authors

5 Building the INFORM Climate Change Risk Index model

INFORM Risk's Hazard&Exposure dimension is modified using the projections of climate-related hazards, population projections and probability of civil conflicts by the end of 21st century (Chapter 5.1 and 5.2). At this stage the Vulnerability and Lack of coping capacity dimension do not account for future socioeconomic expansion and climate-related impacts. They are taken from INFORM Risk Index 2022 release (Figure 2). Since there have been a few changes introduced in methodology since the last available report (Marin-Ferrer et al, 2017) their short description is provided in Chapter 5.3 and 5.4.

5.1 Incorporating projections into INFORM Risk Index model

Climate-related hazards projections are available for intermediate (RCP4.5) and high (RCP8.5) concentration scenarios for:

- river floods,
- coastal floods,
- droughts and
- epidemics.

The influence of climate change on the tropical cyclone wind risk has not been considered at this stage due to lack of data.

To quantify the population exposure, the hazard layers for the historical and future periods are overlayed with Global Human Settlement Layer (GHSL, Pesaresi et al., 2016) and SSP1,SSP2, SSP3 and SSP5 population density layers (see chapter 4.5.2).

The following chapter presents the projections of population, climate-related hazards and conflict used to develop INFORM Climate Change Risk Index model.

5.1.1 Population projections

The projected size and spatial distribution of future population are the key drivers of exposure and vulnerability to hazards. Spatial demographic projections are widely used for the integrated analyses of climate change impacts. To compute the projected exposure to climate-related hazards, spatially explicit population scenarios consistent with the Shared Socioeconomic Pathways (SSPs) are considered.

Data source: The data set has been produced by NCAR's IAM group and the City University of New York Institute for Demographic Research (Gao, 2017; Jones and O'Neill, 2016). It covers the period 2010-2100 in ten-year time steps at 1-km spatial resolution for each SSP scenario. The changes in population density relative to GHSL 2015 for SSPs in mid and late 21st century are shown in Annex 20.

Technical explanation: The projections are based on assumptions on future fertility, mortality, migration, educational transitions and urbanization under shared socioeconomic pathways (SSP) storylines (Jiang and O'Neill, 2017; Jones and O'Neill, 2016; KC and Lutz, 2017). **Table 1** shows chosen SSP narratives regarding future trends in spatial development patterns.

SSP1 (sustainability) and SSP5 (fossil-fuel development) consider a development pathway with relatively high income growth, increased investment in education and health, leading to low population growth in the high fertility countries, and medium (SSP1) or high levels (SSP5) in currently low fertility countries. High migration and rapid urbanization is expected in both pathways. For SSP2 (middle of the road), demographic outcomes are consistent with middle of the road expectations (medium and central) for population growth, urbanization, and other spatial patterns of development. SSP3 (regional rivalry) considers low income growth and relatively low investments in human capital, results in relatively high population growth in the currently high fertility countries, and relatively low population growth (or decline) in the currently low fertility countries. Migration is relatively low, and urbanization proceeds slowly.

Table 1. SSP narratives for future trends of fertility, mortality, migration, education and urbanization level.

	SSP1 Sustainability	SSP2 Middle of the road	SSP3 Regional rivalry	SSP5 Fossil-fuelled development
Fertility				
High fertility*	Low	Medium	High	Low
Other low fertility**	Low	Medium	High	Low
Rich-OECD low fertility***	Medium	Medium	Low	High
Mortality				
High fertility	Low	Medium	High	Low
Other low fertility	Low	Medium	High	Low
Rich-OECD low fertility	Low	Medium	High	Low
Migration				
High fertility	Medium	Medium	Low	High
Other low fertility	Medium	Medium	Low	High
Rich-OECD low fertility	Medium	Medium	Low	High
Education				
High fertility	High	Medium	Low	High
Other low fertility	High	Medium	Low	High
Rich-OECD low fertility	High	Medium	Low	High
Urbanization				
High income****	Fast	Central	Slow	Fast
Medium income	Fast	Central	Slow	Fast
Low income	Fast	Central	Slow	Fast

* total fertility rate of more than 2.9 in 2005–2010

** all countries with a total fertility rate of 2.9 and below that are not "Rich-OECD countries"

*** OECD members defined as World Bank high income country

**** groupings for current income are from Jiang and O'Neill (2017)

Source: Jones and O'Neill (2016); KC and Lutz (2017)

5.1.2 River Flood

Floods are often predictable natural hazards, which can encompass incredibly large areas, causing a very large impact on population. Floods have affected 1.6 billion people globally, accounting for 44% of all disaster events from 2000 to 2019 (CRED, 2020). Climate change is intensifying the water cycle leading to increased extreme rainfall and associated flooding in the future (IPCC, 2021).

Global flood models (GFMs) have developed rapidly over the last decade as a result of increased computational power and global data availability, on account of increased contribution from remotely sensed products. GFMs are based on a cascade of meteorological-hydrological-hydraulic models. They are particularly suitable for estimating potential inundation areas under different flood probabilities, hence, to project potential future flood hazard. A non-exhaustive list of non-commercial GFMs belonging to this category includes CaMa-UT from the University of Tokyo (Yamazaki et al., 2011), CIMA-UNEP developed for the UNISDR Global Assessment Report 2015 (GAR) (Rudari et al., 2015), the ECMWF model (Pappenberger et al., 2012), GLOFRIS by Deltares (Winsemius et al., 2013), and the European Commission - Joint Research Centre (JRC) model (Dottori et al., 2016) which benefits from continuous research efforts and operational improvements of the Copernicus Emergency Management Service (EMS) – Global Flood Awareness System (GloFAS, Alfieri et al., 2020b, 2013).

Data source: Flood hazard in the current INFORM Risk Index are based on the CIMA-UNEP GFM developed for the UNISDR Global Assessment Report 2015 (GAR) (Rudari et al., 2015). The flood component is assessed using flood inundation levels for 25-, 50-, 100-, 200-, 500- and 1,000-year return periods (RPs) developed at a 1-km grid spacing (Marin-Ferrer et al., 2017). For the INFORM Climate Change Risk Index, we use publicly available projections from the Aqueduct Global Flood Maps ([11]) which are based on the Glofris ([12]) model developed by Deltares (Winsemius et al., 2013). It includes flood inundations maps for RCP4.5 and RCP8.5 by the end of 21st century for nine return periods, from 2-year flood to 1 000-year flood for current and future projection.

Technical explanation: The hazard layers for the individual return periods are produced using global hydrological model PCRaster Global Water Balance (PCR-GLOBWB) (Sutanudjaja et al., 2018). PCR-GLOBWB allows to make long-term simulations of discharge and flood levels for several climate conditions. The model has been forced over various time periods, between 1950 and 2099 using the meteorological datasets of the European Union Water and Global Change (EUWATCH) program (Weedon et al., 2014, 2011) and the Inter-sectoral Impact Model Inter-comparison Project (ISI-MIP) (Hempel et al., 2013). Future simulations are carried for using data from five different global climate models (GCMs) forced under RCP4.5 and RCP8.5 scenarios. The outputs are then used to derive the flood extension and water depths for 2, 5, 10, 25, 50, 100-, 250-, 500-, and 1,000-year return periods for the historical (1960–99), and future climate - 2050 (2030–69) and 2080 (2060–99). The inundations were downscaled to 1-km resolution using spreading flood model developed by Winsemius et al. (2013). The potential exposed population (PEP) is computed for each of the return periods using GHSL2015, SSP1, SSP2, SSP3 and SSP5 population density layers assuming exposure for any positive flood depth. The expected annual exposed population (EAEP) - annual average exposed population (AAEP) in INFORM- is estimated as the integral sum of the PEP for all flood frequencies for each ensemble member, and averaged over the models.

5.1.3 Coastal Flood

Coastal flooding is a major global concern that can negatively impact a wide-range of social, economic, and environmental processes. Although the most intensive coastal flood events usually occur when the peak storm surge coincides with high spring tide (in an event defined as storm tide), other factors such as sea level rise, wind-waves, currents, freshwater input, and vertical land movement also play a role in characterising coastal flood hazard. Long-term risks of coastal flooding and impacts on populations, infrastructure and assets are projected to increase with higher levels of warming (IPCC, 2022). Tropical regions and small islands are the most sensitive areas, and are expected to experience the largest increases in coastal flooding frequency in the future. Analysis suggests that due to temperature rise from 1.5°C to 2°C, impacts could be increasingly widespread by the 2070s, even with adaptation measures in place (Hoegh-Guldberg et al., 2018).

A non-exhaustive list of flood models that have been applied in a context of estimating global coastal flooding hazard includes GLOFRIS (Ward et al., 2013) and Aqueduct global flood analyser (Ward et al., 2020), DIVA (Brown et al., 2016; Vafeidis et al., 2008), Global Tide and Surge Reanalysis (GTSR) (Muis et al., 2016), and LISFLOOD-FP (Dottori et al., 2016; Vousdoukas et al., 2020).

[11] http://www.wri.org/resources/data-sets/aqueduct-global-flood-risk-maps
[12] Global Flood Risk with IMAGE Scenarios.

Data source: In the original INFORM Risk Index, the coastal flooding component is represented by storm surge levels obtained from GAR 2015 at a 1-km spacing for the 10-, 25-, 50-, 100- and 250-year RPs (Marin-Ferrer et al., 2017). For INFORM Climate Change Risk Index, we use publicly available projections for coastal floods from the Aqueduct Global Flood Maps [13]. It includes coastal flood inundations maps for RCP4.5 and RCP8.5 by the end of 21st century for nine return periods, from 2-year flood to 1 000-year coastal flood for current and future projection.

Technical explanation:

Aqueduct estimates of coastal hazard are based on:

- Extreme water levels data from Global Tide and Surge Reanalysis (GTSR) dataset (Muis et al., 2016) including global daily sea levels (due to tide and storm surge) for 1979–2014, based on the hydrodynamic Global Tide and Surge Model (GTSM).
- Surge simulations using wind and pressure fields from the European Centre for Medium-Range Weather Forecasts (ECMWF) Re-analysis-Interim (ERA-Interim) dataset (Dee et al., 2011).
- Tide simulations using the Finite Element Solution 2012 (FES 2012) model (Carrère and Lyard, 2003).

Gumbel distribution is fitted and applied to produce extreme tide and surge levels for 2, 5, 10, 25, 50, 100, 250, 500, and 1,000-year return periods. Inundation maps at 1-km resolution are produced using geographic information system (GIS)-based inundation routine (Vafeidis et al., 2019). To estimate the future extreme sea levels and subsidence under RCPs in 2050 and 2080, gridded sea level changes from the Responses to Coastal Climate Change: Innovative Strategies for High-End Scenarios—Adaptation and Mitigation (RISES-AM) project (Jevrejeva et al., 2014) are employed. The simulation of subsidence—the lowering of the land level— is based on three models—namely, the hydrological model PCR-GLOBWB integrated with the global Modular Finite-Difference Flow (MODFLOW) groundwater model (de Graaf et al., 2017; Sutanudjaja et al., 2018), and a land subsidence model (Erkens and Sutanudjaja, 2015). Consistent with river floods, the expected annual exposed population is the integral of the potentially exposed population to coastal flood inundation at each flood probability.

5.1.4 Drought

Drought is also one of the major weather-related natural hazards worldwide, causing severe economic losses, environmental damage and human suffering. EM-DAT historical observations show that more than one billion people were affected by droughts in the period 2000-2019 which was more than a quarter of all people affected by all types of weather related disasters worldwide (CRED, 2020). Climate change has already increased the frequency and magnitude of drought in many regions, and the trend is projected to continue, causing severe disturbances in water and food security around the globe (IPCC, 2022).

Measuring drought impacts is more complex than for other natural hazard impacts that cause immediate and structural damages such as floods and storms (UNDRR, 2019). A wide variety of drought indices are used to characterize the severity and frequency and typically depend on one or more components of the hydrological cycle such as precipitation, soil moisture, snowpack, reservoir levels, river flow, and groundwater levels and can also depend on water demands (EC, 2017; Svoboda and Fuchs, 2016). The standardized precipitation index (SPI) and the standardized precipitation evapotranspiration index (SPEI) are widely used to assess the meteorological droughts (Beguería et al., 2014; Spinoni et al., 2019; Vicente-Serrano et al., 2010). Drought indices such as European Drought Observatory (EDO)'s Soil Moisture Anomaly (SMA), the Drought Severity Index (DSI), or the Palmer Drought Severity Index (PDSI) characterize plant water stress based on soil water content (EC, 2019b, 2017). Hydrological droughts are mainly assessed through indicators that measure water deficit in rivers and reservoirs such as EDO's Low Flow Index (LFI) (EC, 2017; Svoboda and Fuchs, 2016).

Data source: Drought component in the original INFORM Risk Index is considered as a combination of the probability of agricultural drought and population affected by drought. In recent years, agricultural drought, measured with the ASI, is defined as a dry period in a region over the cropping season in which at least 30% of the crop area is under stress for a duration exceeding 10 days. The average annual population affected by drought is based on historical events in the EM-DAT database for the last 25 years (Marin-Ferrer et al., 2017). To upgrade the INFORM Risk Index for climate change, we use a 12-month standardized precipitation evapotranspiration index (SPEI) data computed using surface temperature and precipitation from NASA Earth

[13] http://www.wri.org/resources/data-sets/aqueduct-global-flood-risk-maps

Exchange Global Daily Downscaled Projections (NEX-GDDP) dataset (NCCS, 2020). The SPEI data has been taken from a multi-hazard assessment research conducted by Marzi et al. (2021).

Technical explanation: SPEI is a multi-scalar drought index based on climatic data, namely precipitation and potential evapotranspiration (PET). It measures drought severity according to its intensity and duration and can be used to identify the onset and end of drought episodes (Beguería et al., 2014; Vicente-Serrano et al., 2010). For this study, the SPEI is computed using temperature and precipitation from 21 Atmosphere-Ocean General Circulation Models (AOGCMs) from NASA Earth Exchange Global Daily Downscaled Projections (NEX-GDDP) dataset (NCCS, 2020). NEX-GDDP is comprised of daily precipitation and minimum and maximum temperature statistically downscaled CMIP5 AOGCM simulations for RCP4.5 and RCP 8.5 to 0.25° grid. PET is estimated from the NEX-GDDP surface temperatures according to the Hargreaves (1994) formulation modified by Droogers and Allen (2002). For the scope of INFORM Climate Change analysis, 12-month SPEI has been considered which captures medium term water deficits and hydrological droughts likely to affect agriculture, river discharge and groundwater recharge (Farinosi et al., 2020; Liu and Chen, 2021; Naumann et al., 2018). Drought occurs when SPEI is less than −1.5, which is defined as the threshold for severe drought (Smirnov et al., 2016; Törnros and Menzel, 2014; UK Centre for Ecology and Hydrology, 2020). Exposure is based on the multi-model ensemble mean of the population exposed (GHSL 2015, SSP1, SSP2, SSP3 and SSP5 density layers) to severe or greater drought for historical period (1976 to 2005) and the future period - 2050 (2036 to 2065) and 2080 (2070-2099) - averaged over 30 years.

5.1.5 Epidemics

Climate change is expected to affect the risk of vector-borne and other environmentally-transmitted diseases (IPCC, 2022). Vector-borne diseases are human illnesses caused by parasites, viruses and bacteria that are transmitted by mosquitoes, fleas and ticks. They account for more than 17% of all infectious diseases, causing more than 700,000 deaths annually [14]. Transmission is likely to increase in the regions where the temperature is shifted toward the thermal optima of vector-borne disease transmission. In contrast, it is likely to decrease where the temperature is shifted above optima and toward upper thermal limits for other vectors and pathogens (Mordecai et al., 2020, 2019). Malaria and dengue are the most important mosquito borne diseases. According to WHO (WHO, 2021b), malaria caused an estimated 241 million cases globally (14 million more cases in 2020 compared to 2019), with more than 627,000 deaths in 2020 (69 000 more deaths compared to 2019). In addition, more than 3.9 billion people are at risk of contracting dengue, with an estimated annual 96 million symptomatic cases and 40,000 deaths. Research suggests that malaria and dengue transmission is likely to increase due to increased spatial range and length of the transmission season, placing a greater proportion of the global population at risk (Colón-González et al., 2021; Ryan et al., 2020, 2019).

Malaria is a life-threatening disease caused by Plasmodium falciparum and Plasmodium vivax, with the former being responsible for about 97% of all global cases (WHO, 2019). Several models have been developed to assess the changes in the malaria transmission dynamics in human population and climate variability, with varying amounts of complexity:

- The Threshold-based Lancet Countdown malaria indicator (LCMI) which tracks global changes in the climatic suitability for malaria (coincidence of precipitation accumulation greater than 80 mm, an average temperature of 18–32°C, and relative humidity greater than 60% as an indication of the lower limit for P falciparum transmission) (Watts et al., 2019)
- The Liverpool Malaria Model which is a weather-driven, mathematical–biological model of the parasite dynamics, comprising both the weather-dependent within-vector stages and the weather-independent within-host stages (Hoshen and Morse, 2004)
- VECTRI model developed by Tompkins and Ermert (2013) which is a mathematical malaria model that accounts for the effects the temperature and rainfall influences on the parasite and vector life, as well as population density in the calculation of daily biting rates.

Dengue is the fastest-growing mosquito-borne viral disease in the world, transmitted by Aedes aegypti and to a lesser extent Aedes albopictus vectors. Several models have been developed to assess the changes in the dengue transmission dynamics in human population and climate variability, with varying amounts of complexity:

[14] https://www.who.int/en/news-room/fact-sheets/detail/vector-borne-diseases

- The statistical dengue model (DGM) which is a generalised additive mixed model which simulates dengue incidence as a function of temperature, precipitation, relative humidity, and population density. Delayed effects and non-linear relationships are assumed for the climatic effects (Colón-González et al., 2018).
- UMEÅ mechanistic models coupling vectorial capacity models including basic vector to human interactions, and stage-structured data driven dynamic models to describe the population dynamics of dengue vectors. These models simulates dengue incidence as a function of temperature, precipitation, daylight length in the ecological processes and the spatiotemporal dynamics of mosquito populations (DiSera et al., 2020; Liu-Helmersson et al., 2019, 2016).

Data source: Vector borne hazard & exposure in the original INFORM Risk Index is considered as a combination of population at risk of malaria (Plasmodium falciparum and Plasmodium vivax), Zika, Aedes and Dengue. For INFORM Climate Change Risk Index, we use the projections of population at risk of malaria and dengue from Colón-González et al. (2021). The study uses a multi-model multi-scenario framework (six mosquito-borne disease models, driven by four GCMs, using four RCPs, and three SSPs) to estimate the changes in the length of the transmission season and global population at risk of malaria and dengue for different altitudes and population densities for the historical period 1970–1999 and future period 2050 (2040-2069) and 2080 (2070-2099).

Technical explanation: Colón-González et al. (2021) uses bias-corrected global daily mean surface temperature, total precipitation, and relative humidity data from the ISI-MIP database for four CMIP5 GCMs (HadGem2-ES, IPSLCM5A-LR, MIROC-ESM-CHEM, and GFDL-ESM2M) across four RCPs (RCP2·6, RCP4·5, RCP6·0, and RCP8·5) on a 0·5 × 0·5 degree latitude–longitude grid. For population input, global gridded population counts on a 0·5×0·5 degree grid were retrieved from SSP population projections (SP1, SSP2 and SSP5) for historical and future period. The climatic and population data are then used as an input for six above-mentioned malaria and dengue models to assess the changes in the length of the transmission season and the additional population at risk. For the sake of comparability with original INFORM Risk malaria and dengue components, we only use malaria outputs from VECTRI model and dengue outputs from UMEÅ-aegypti model retrieved from Centre for Open Science ([15]). Population at risk under SSP3 is here considered as country-based multipliers (the ratio between SSP2 and SSP3 projected population). In the same manner, the baseline values are corrected using country-based multipliers for 2015 (ratio between SSP baseline (2000) and GHSL 2015 population density layers).

5.1.6 Conflict

Although climate hazards have affected armed conflict within countries, the direct influence of climate on conflict is assessed as relatively weak compared to other socioeconomic factors (IPCC, 2022). There is emerging evidence with medium confidence that positive temperature anomalies can indirectly increase the risks of violent conflicts though the hydrological changes and droughts, affecting food and water insecurity in vulnerable regions with large populations, weather-sensitive economy, weak institutions and high levels of poverty and inequality (Brzoska, 2018; Heslin, 2020; Koren et al., 2021). However, IPCC (2022) concludes by high confidence that future violent conflict risk is largely mediated by socio-economic development trajectories.

Several attempts have been made to predict long-run probabilities of armed conflict using dynamic models and projections for key independent variables (Chenoweth and Ulfelder, 2015; Gleditsch, 2016; Goldstone et al., 2010; Hegre et al., 2016, 2013; Ryan-Mosley, 2019). Hegre et al. (2013) predicted variations in global and regional incidences of armed conflict for the 2010–2050 period. Their predictions are based on a dynamic multinomial logit model using exogenous predictors such as population size, infant mortality rates, demographic composition, education levels, oil dependence, ethnic cleavages, and neighbourhood characteristics. In 2016, they updated their forecasts for the period 2014–2100 consistent with five SSPs (Hegre et al., 2016).

Data Source: INFORM Risk's Human hazards include conflict intensity from the Heidelberg Institute for International Conflict Research conflict barometer (HIIK, 2019) and the projected conflict risk within the next four years from the Global Conflict Risk Index (GCRI) (JRC, 2017), For INFORM Climate Change Risk index, we replace the projected conflict risk with SSP-based civil conflict forecasts for the period 2014–2100 from Hegre et al. (2016). Since there is still scepticism about the performance of long-term forecasting models due to complexity, heterogeneity and idiosyncratic nature of conflicts (Bowlsby et al., 2020; Cederman and Weidmann, 2017; Hegre et al., 2021), we keep the current intensities from HIIK and combine them with the SSP-based

[15] https://osf.io/hpaey/

projected conflict data. In this way, we are able to diminish the substantial uncertainty underlying future projections of such complex social phenomena.

Technical explanation: Hegre et al. (2016) approach includes three main steps:

1. Developing a joint global dataset of historical and projected variables including economic output, educational attainment, population size, conflict history, time since independence, and conflict involvement among neighbouring countries for all years, 1960–2100.
2. Developing a random-effects multinomial logit statistical model of civil conflict onset, duration, and termination for the period 1960–2013 based on temporally and spatially lagged indicators from the joint dataset
3. Using the statistical model and a simulation procedure to generate annual projections of armed conflict for each country over all SSPs, for 2014–2100.

In order to build our baseline model, we use SSP5 probabilities in 2020 due to considerable correlation with projected violent conflict projections from GCRI used to form INFORM Risk's projected conflict component.

5.2 Dimension: Hazard & Exposure

5.2.1 Overview

The Hazard & exposure dimension reflects the probability of physical exposure associated with specific hazards. There is no risk if there is no physical exposure, no matter how severe the hazardous event is. Therefore, the hazard and exposure dimensions are merged into Hazard & exposure dimension. As such it represents the load that the community has to deal with when exposed to a hazardous event.

5.2.1.1 Hazard & exposure: Categories

The dimension comprises two categories: Natural hazards and Human hazards, aggregated with the geometric mean, where both indexes carry equal weight within the dimension (**Figure 8**).

Figure 8. Graphical presentation of the Hazard & exposure dimension

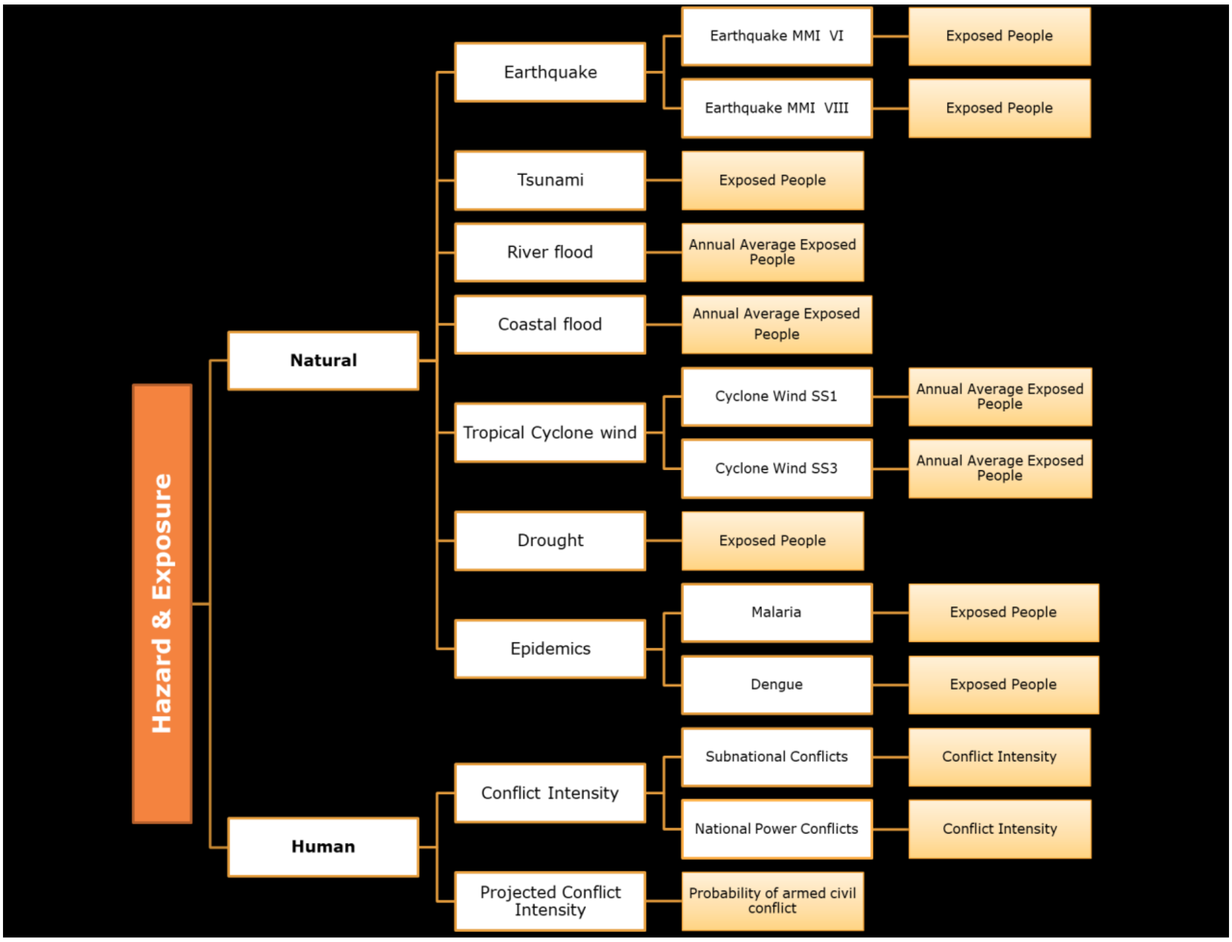

Source: Authors

5.2.2 Category: Natural hazard

5.2.2.1 Definition

According to the CRED EM-DAT database (CRED, 2020), 7,348 natural disasters events were recorded, affecting more than 4.03 billion people (approximately 200 million per year) and claimed 1.2 million lives (approximately 60,000 deaths per year) during 2000 and 2019.. All the figures have been increased relative to the period 1980 - 1999 where 4,212 natural disasters events were recorded, 3.25 million people were affected, and 1.19 million lost their lives. In the past two decades, floods, droughts and storms were accounted for 41%, 35% and 18% of total affected population respectively. Earthquakes and tsunamis were the deadliest form of disasters accounting for 58% of total deaths, followed by storms (16%), extreme temperature (13%) and floods (9%).

Moreover, the vector borne diseases (accounting for more than 17% of all infectious diseases) such as Malaria and Dengue caused more than 700 000 deaths every year. According to WHO (WHO, 2021b), malaria caused an estimated 241 million cases globally (14 million more cases in 2020 compared to 2019), with more than 627,000 deaths in 2020 (69 000 more deaths compared to 2019). In addition, more than 3.9 billion people are at risk of contracting dengue, with an estimated annual 96 million symptomatic cases and 40,000 deaths. Global warming and demographic changes are estimated to increase the frequency and severity of potentially high impact natural hazard events and epidemics across the world.

In the original INFORM Risk Index, rapid-onset hazards, i.e., earthquakes, tsunamis, tropical cyclones and floods, are dealt with differently than slow-onset hazards, i.e., droughts. For INFORM Climate Change Risk Index, the drought component is analysed in the same manner as for the rapid-onset hazards due to data limitation. Indicators for each component of rapid-onset hazards are based on the physical exposure to the hazard.

The **metric for the natural hazard** components used in INFORM Climate Change Risk Index is the **annual average exposed population (AAEP)** or, when hazard maps for different return periods are not available, **exposed population.**

Different studies have employed different terminologies for exposure to probabilistic hazards. The climate change community uses **Expected Annual Exposed Population (EAEP)**, for the integral sum of the population exposed for all frequencies (Alfieri et al., 2020a). For the sake of comparability, we keep the terminology as it was introduced in the original INFORM Risk Index (Marin-Ferrer et al., 2017).

The hazard zone does not contain information on internal variability of intensity. The population is either in the hazard zone or outside, the people are either exposed or not, respectively. The exposure of the population is thus a binary value, rather than a degree of exposure.

Furthermore, in the case of earthquakes and cyclone winds, the available hazard maps provide information on different intensity level zones. The hazard zones where minimum intensity is set to low intensities inherit also the hazard zones with high intensities, but their more detrimental impact is not visible with a simple overlay of the population map. It would be high intensity events that would more likely cause humanitarian crises.

To overcome this shortcoming of the hazard zone definition the areas of high intensities within the hazard zone of low intensities were extracted. Their presence was introduced into the model as a parallel indicator at the sub-component level where AAEP was based on the hazard zone with the higher minimum intensity level. We took the advantage of the composite indicator methodology and considered the areas of high intensities as another type of event with the same probability of occurrence. Such indicator pushes up the countries exposed to extreme events as well as pull down those countries where high intensity events are not very likely to happen and/or are spatially very limited. The final hazard component indicator is a geometric average of the normalised AAEP gained from two hazard zones of two distinct levels of minimum intensity, i.e., a low as well as extreme one. A high hazard component indicator is the result of high values in both levels of intensities. While low values of the indicator for high intensities will decrease high values of the indicator for low intensities and indirectly suggest that despite the high number of people exposed the share of affected people is expected to be comparatively smaller.

There are different intensity scales for different hazard types, e.g., Modified Mercalli Intensity (MMI) scale for earthquakes and Saffir-Simpson (SS) hurricane scale for cyclone wind. For each hazard type we chose intensity levels equivalent to two distinct damage levels:

- Light/moderate potential damage for resistant/vulnerable buildings, respectively; and
- Moderate/heavy potential damage for resistant/vulnerable buildings, respectively.

In the case of the earthquakes MMI VI and VIII, while in the case of the cyclone winds SS 1 and 3 fit the chosen damage levels description (**Table 3**).

Table 2. Minimum intensity/magnitude levels used for different type of hazards and data source

Hazard type	Intensity levels	Source
Earthquake	Modified Mercalli Intensity scale VI and VIII	GEM-JRC Seismic hazard intensity map (475-year return period - 10 % probability of exceedance in 50-year of exposure)
Tsunami	Inundated area	Tsunami Hazard (Run up) RP 500 years (GAR 2015)
River flood	Inundated area	Flood hazard map for 2, 5, 10, 25, 50, 100-, 250-, 500-, and 1,000-year return periods for baseline, RCP4.5 and RCP8.5 scenarios (WRI Aqueduct)
Cyclone wind	Saffir-Simpson category 1 and 3	Cyclone wind hazard map 50, 100, 250, 500, 1 000 years RP (GAR 2015)
Coastal flood	Inundated area	Coastal flood hazard map for 2, 5, 10, 25, 50, 100, 250, 500, and 1,000-year return periods for baseline, RCP4.5 and RCP8.5 scenarios (WRI Aqueduct)
Drought	Masked sever and extreme levels (below -1.5)	12-months SPEI for baseline, RCP4.5 and RCP8.5 scenarios (Marzi et al., 2021)
Epidemics	Impact (exposed people)	Projections of vector borne diseases for baseline, RCP4.5 and RCP8.5 scenarios from LANCET (Colón-González et al., 2021)

Source: Authors

Table 3. Intensity scale levels vs. damage level

Hazard type	Intensity levels	Damage level	Reference
Earthquake	Modified Mercalli scale VI	Perceived shaking: **strong** Resistant structures: **light damage** Vulnerable structures: **moderate damage**	USGS(PAGER) [16]
	Modified Mercalli scale VIII	Perceived shaking: **severe** Resistant structures: **moderate/heavy damage** Vulnerable structures: **heavy damage**	USGS(PAGER)
Cyclone wind	Saffir-Simpson category 1	Wind speed: 119-153 km/h **Very dangerous winds will produce some damage**: Well-constructed frame homes could have damage to roof, shingles, vinyl siding and gutters. Large branches of trees will snap and shallowly rooted trees may be toppled. Extensive damage to power lines and poles likely will result in power outages that could last a few to several days.	NOAA [17]
	Saffir-Simpson category 3	Wind speed: 178-208 km/h **Devastating damage will occur**: Well-built framed homes may incur major damage or removal of roof decking and gable ends. Many trees will be snapped or uprooted, blocking numerous roads. Electricity and water will be unavailable for several days to weeks after the storm passes	NOAA

Source: Marin-Ferrer et al., 2017

[16] http://pubs.usgs.gov/fs/2010/3036/pdf/FS10-3036.pdf
[17] http://www.nhc.noaa.gov/aboutsshws.php

Box 5. Absolute vs. relative physical exposure — correction in favour of small countries

There are two ways to consider population exposed to natural hazards. The absolute value of people exposed will favour more populated countries while the value of population exposed relative to the total population will reverse the problem and favour less populated hazard-prone countries, especially small islands where the entire population may be affected by a single cyclone. To enable a proper comparison between countries, also in INFORM Climate Change Risk the subcomponent indicator is calculated both ways and then aggregated using an arithmetic average.

At the level of core indicators (**Table 5**) the datasets are rescaled into a range of 0 to 10 in combination with a min–max normalisation. Since distribution of the absolute value of exposed people is extremely skewed, the log transformation is applied.

5.2.2.2 Natural hazards: components

The Natural hazard category of INFORM Climate Change Risk Index is slightly changed compared to INFORM Risk Index to introduce the costal flood projection independently of Tropical cyclone wind. It includes 7 components aggregated with a geometric average (**Table 4** - **Table 5**):

- Earthquake,
- Tsunami,
- River flood,
- Coastal flood,
- Tropical cyclone wind,
- Drought,
- Epidemics

Table 4. Indicators of the Natural hazard category

Component	Indicator	Source	MIN–MAX	No of missing values
Earthquake	Physical exposure to MMI VI earthquake (absolute)	GEM-JRC	Log(10)-Log(10E5)	-
	Physical exposure to MMI VI earthquake (relative)	GEM-JRC; GHSL-POP, SSPs	0 %-0.2 %	-
	Physical exposure to MMI VIII earthquake (absolute)	GEM-JRC	Log(10)-Log(10E5)	-
	Physical exposure to MMI VIII earthquake (relative)	GEM-JRC; GHSL-POP,SSPs	0 %-0.2 %	-
Tsunami	Physical exposure to tsunamis (absolute)	UNISDR GAR 2015	Log(10E-1)-Log(10E3.5)	-
	Physical exposure to tsunamis (relative)	UNISDR GAR 2015; GHSL-POP, SSPs	Log(10E-7.5)-Log(10E-3.5)	-
River flood	Physical exposure to river flood (absolute)	WRI Aqueduct	Log(10E2.5)-Log(10E7)	14/191
	Physical exposure to river flood (relative)	WRI Aqueduct; GHSL-POP,SSPs	0 %-6 %	14/191
Coastal flood	Physical exposure to coastal flood (absolute)	WRI Aqueduct	Log(10)-Log(10E6)	14/191
	Physical exposure to coastal flood (relative)	WRI Aqueduct; GHSL-POP,SSPs	Log(10E-5)-Log(10E-0.5)	14/191

Tropical cyclone wind	Physical exposure to SS-1 tropical cyclone (absolute)	UNISDR GAR 2015	Log(100)-Log(10E6)	-
	Physical exposure to SS-1 tropical cyclone (relative)	UNISDR GAR 2015; GHSL-POP	0 %-1.8 %	-
	Physical exposure to SS-3 tropical cyclone (absolute)	UNISDR GAR 2015	Log(-1)-Log(10E5)	-
	Physical exposure to SS-3 tropical cyclone (relative)	UNISDR GAR 2015; GHSL-POP	0 %-0.8 %	-
Drought	Physical exposure to droughts (absolute)	SPEI-12 (Marzi et al., 2021)	Log(10E3)-Log(10E7.5)	21/191
	Physical exposure to droughts (relative)	SPEI-12 (Marzi et al., 2021); GHSL-POP, SSPs	Log(10E-2)-Log(10E-0.5)	21/191
Epidemics	Physical exposure to malaria (absolute)	LANCET (Colón-González et al., 2021)	Log(10E2)-Log(10E8)	10/191
	Physical exposure to malaria (relative)	LANCET (Colón-González et al., 2021); GHSL-POP, SSPs	0 %-100 %	10/191
	Physical exposure to dengue (absolute)	LANCET (Colón-González et al., 2021)	Log(10E2)-Log(10E8)	10/191
	Physical exposure to dengue (relative)	LANCET (Colón-González et al., 2021); GHSL-POP, SSPs	0 %-100 %	10/191

Source: Authors

Table 5. Aggregation of the Natural hazards category

<table>
<tr><td>Category</td><td colspan="20">Natural hazard</td></tr>
<tr><td rowspan="2">Component</td><td colspan="20">GEOMETRIC AVERAGE</td></tr>
<tr><td colspan="4">Earthquake</td><td colspan="2">Tsunami</td><td colspan="2">River Flood</td><td colspan="2">Coastal flood</td><td colspan="4">Tropical cyclone wind</td><td colspan="2">Drought</td><td colspan="4">Epidemics</td></tr>
<tr><td rowspan="2">Aggregation</td><td colspan="4">GEOMETRIC AVERAGE</td><td colspan="2">GEOMETRIC AVERAGE</td><td colspan="2">GEOMETRIC AVERAGE</td><td colspan="2">GEOMETRIC AVERAGE</td><td colspan="4">GEOMETRIC AVERAGE</td><td colspan="2">GEOMETRIC AVERAGE</td><td colspan="4">GEOMETRIC AVERAGE</td></tr>
<tr><td colspan="2">EQ Abs</td><td colspan="2">EQ Rel</td><td colspan="6"></td><td colspan="2">CW Abs</td><td colspan="2">CW rel</td><td colspan="2"></td><td colspan="2">MAL</td><td colspan="2">DENG</td></tr>
<tr><td rowspan="2">Core indicator</td><td colspan="2">GEOMETRIC AVERAGE</td><td colspan="2">GEOMETRIC AVERAGE</td><td colspan="6"></td><td colspan="2">GEOMETRIC AVERAGE</td><td colspan="2">GEOMETRIC AVERAGE</td><td colspan="2"></td><td colspan="2">GEOMETRIC AVERAGE</td><td colspan="2">GEOMETRIC AVERAGE</td></tr>
<tr><td>EQ MMI VI Log(abs)</td><td>EQ MMI VIII Log(abs)</td><td>EQ MMI VI Relative</td><td>EQ MMI VIII Relative</td><td>Log(absolute)</td><td>Log(relative)</td><td>Log(absolute)</td><td>Relative</td><td>Log(absolute)</td><td>Log(relative)</td><td>CW SS1 Log (abs)</td><td>CW SS3 Log (abs)</td><td>CW SS1 Relative</td><td>CW SS3 Relative</td><td>Log(absolute)</td><td>Log(relative)</td><td>Log(absolute)</td><td>Relative</td><td>Log(absolute)</td><td>Relative</td></tr>
</table>

Absolute: Absolute value of physical exposure
Relative: Relative value of physical exposure. Absolute exposure is normalised with country's total population.

Source: Authors

Normalization: In order to identify the outliers and setting min and max values for each hazard component, we use distributions from a joint dataset of historical and projected raw values. In this way, we end up with lower normalized values for the baseline compared to projected hazards, which allows tracking changes across time and scenario combination. Nevertheless, the comparability between original and upgraded baselines will be lower due to changes in the min and max values.

Scalability: Approach used enables geographical and temporal scalability of physical exposure. Hazard zones and population distribution maps are analysed at pixel level which allows extraction of indicators at lower level administrative units (e.g., subnational models).

5.2.2.3 Component: Earthquake

Earthquakes can be one of the most destructive natural hazards. The unpredictability of the seismic event can cause several fatalities in areas with high physical vulnerability of the buildings (2010 Haiti, 2015 Nepal). The future risk of earthquake can be quantified in terms of fatalities and capital loss using SSP-based projections of population and GDP (Murnane et al., 2017).

Data source: Global Seismic Hazard Map (version 2018.1) from the Global Earthquake Model (GEM) [18] are used to derive the exposed population.

Technical explanation to derive hazard zone: The Global Earthquake Model (GEM) depicts the geographic distribution of the Peak Ground Acceleration (PGA) with a 10% probability of being exceeded in 50 years, computed for reference rock conditions (shear wave velocity, VS30, of 760-800 m/s). In INFORM a derived product based on Global Seismic Hazard Map dataset was used, converted to Modified Mercalli Intensity (MMI) using the methodology developed by Wald et al. (1999).

Two hazard zones for each country were extracted using two different minimum intensity levels, i.e. MMI VI and MMI VIII (**Table 3**). The choice of the minimum intensities is simply based on two distinct damage levels. This is a way to overcome the hazard zone definition that ignores the internal variability of the hazard intensity and it takes advantage of the composite indicator methodology. We consider a hazard zone with a higher minimum intensity as another event and aggregate the metric derived with the geometric average into earthquake component (**Table 5**). The population projections derived from SSPs are applied to provides snapshots of possible future risk changes resulting from different population scenarios. Population at risk under SSP1, SSP2, SSP3 and SSP5 in 2050 and 2080 is here considered as country-based multipliers (the ratio between GHSL 2015 and SSPs projected population). The score of the Earthquake component is based on “exposed population” metric.

5.2.2.4 Component: Tsunami

As earthquakes, **tsunamis** can be very destructive. Even if the frequency of the events is very low, the humanitarian impact of the most intensive tsunamis is huge (2004 Indian Ocean, 2011 Japan). The future exposure to Tsunamis can be modelled using demographic variables such as SSP-based projections of population (Saito and Kubota, 2020).

Data source: GAR 2015 (UNISDR, 2015c) provides tsunami hazard map for only one return period, i.e. 500-year RP. The score of the Tsunami component is based on the exposed population for 500-year RP only.

Technical explanation to derive hazard zone: The GAR Tsunami hazard map displays binary information on the probable inundated areas. Those areas represent the hazard zones. To estimate the current exposure, the hazardous areas are overlayed with GHSL 2015 population density layers. Population at risk under SSP1, SSP2, SSP3 and SSP5 in 2050 and 2080 is here considered as country-based multipliers (the ratio between GHSL 2015 and SSPs projected population). The score of the Tsunami component is based on “exposed population” metrics.

5.2.2.5 Component: Cyclone wind

Tropical cyclones winds are some of the most damaging events. They occur in yearly cycles and affect coastal population through high **wind speeds**, destroying dwellings and infrastructure. They originate over tropical or subtropical waters and rotate clockwise in the southern hemisphere and counter-clockwise in the northern hemisphere. Assessments of future changes in extreme winds are dealt with large uncertainty due to both the rare nature of extreme wind events and the fact that most models are unable to properly represent them (Outten and Sobolowski, 2021). For the current upgrade of INFORM Risk, we only consider the population projections derived from SSPs to provide future risk of cyclone winds. The component will be updated with RCP-based projections in the future releases.

[18] https://maps.openquake.org/map/global-seismic-hazard-map/#3/32.00/-2.00

Data source: GAR 2015 (UNISDR, 2015c) provides cyclone wind intensity maps for 50, 100, 250, 500, 1 000 years RP.

Technical explanation to derive hazard zone: GAR 2015 cyclone wind hazard maps display different intensity levels of cyclone wind presented in terms of Saffir-Simpson Hurricane Scale (Category 1-5). Therefore two hazard zones for each country were extracted for the same return period using two different minimum intensity levels, i.e. SS1 and SS3 (Table 3). Population at risk in the future under SSP1, SSP2, SSP3 and SSP5 in 2050 and 2080 is here considered as country-based multipliers (the ratio between GHSL 2015 and SSPs projected population). The score of the Cyclone wind component is based on AAEP risk metrics.

5.2.2.6 Component: River Flood

Floods are often predictable natural hazards, which can encompass incredibly large areas, causing a very large impact on population. Climate change is intensifying the water cycle leading to increased rainfall and associated flooding in the future (IPCC, 2021).

Data source: Publicly available flood inundations maps from the Aqueduct Global Flood Maps [19] for RCP4.5 and RCP8.5 by the end of 21st century for 2, 5, 10, 25, 50, 100-, 250-, 500-, and 1,000-year return periods for current and future projection (ensembles).

Technical explanation: The 1-km resolution inundation maps are masked considering any positive flood depth (larger than 5 cm). The binary hazard zones are then overlayed with GHSL2015, SSP1, SSP2, SSP3 and SSP5 population density layers to compute the potential exposure, and expected annual exposed population (EAEP) – here is referred as “annual average exposed people”. For detailed explanation please refer to Section 5.1.2.

5.2.2.7 Component: Coastal Flood

EM-DAT defines coastal flooding as “higher-than-normal water levels along the coast caused by tidal changes or thunderstorms that result in flooding, which can last from days to weeks” [20]. Coastal flooding is responsible for some of the worst human and economic losses worldwide (Tavares et al., 2021). About 680 million people currently live in the low-lying coastal zone with high risk of sea-level rise and associated coastal flooding (IPCC, 2019; McMichael et al., 2020). Climate change is expected to amplify extreme sea levels and the frequency of coastal flooding (IPCC, 2022).

Data source: Publicly available coastal flood inundations maps from the Aqueduct Global Flood Maps [21] for RCP4.5 and RCP8.5 by the end of 21st century for 2, 5, 10, 25, 50, 100-, 250-, 500-, and 1,000-year return periods for current and future projection.

Technical explanation: The 1-km resolution inundation maps are masked considering any positive coastal flood depth (larger than 5 cm). The binary hazard zones are then overlayed with GHSL2015, SSP1, SSP2, SSP3 and SSP5 population density layers to compute the potential exposure, and expected annual exposed population (EAEP) – here is referred as “annual average exposed people”. For detailed explanation please refer to Section 5.1.3.

5.2.2.8 Component: Drought

According to the FAO, droughts are ‘the world’s most destructive natural hazard’ with ‘devastating impacts on food security and food production’. EM-DAT has recorded 338 drought events in the period 2000-2019, caused 1.43 billion affected population around the globe (CRED, 2020). The frequency as well as intensity of droughts has increased in the past 20 years due to climate change and it is expected that this trend will intensify in the future.

Data source: severe and extreme drought hazard maps based on projections of 12-month standardized precipitation evapotranspiration index (SPEI) data for RCP4.5 and RCP8.5, taken from Marzi et al. (2021).

Technical explanation: SPEI-12 hazard maps are masked considering drought occurrence when SPEI is less than −1.5. The binary hazard zones are then overlayed with GHSL2015, SSP1, SSP2, SSP3 and SSP5 population density layers to compute the potential exposure across different scenarios. The score of the Drought component is based on “exposed population” metric. For detailed explanation please refer to Section 5.1.4.

[19] http://www.wri.org/resources/data-sets/aqueduct-global-flood-risk-maps
[20] https://www.emdat.be/Glossary
[21] http://www.wri.org/resources/data-sets/aqueduct-global-flood-risk-maps

5.2.2.9 Component: Epidemics

Epidemics of infectious diseases like recent outbreaks of COVID-19, Ebola, Middle East Respiratory Syndrome (MERS – CoV), Zika and other emerging and re-emerging diseases have shown the capacity to disrupt many dimensions of human existence. Moreover, they can affect anywhere in the world and severely test the global community's resilience (Marin-Ferrer et al., 2017). Vector borne diseases account for more than 17% of all infectious diseases, causing more than 700,000 deaths annually [22]. Malaria and dengue are the most important vector borne diseases. Climate change is expected to affect the risk of vector-borne diseases (IPCC, 2022).

Data source: projections of population at risk of malaria and dengue for different RCP-SSP scenarios, taken from Colón-González et al. (2021).

Technical explanation: malaria outputs from VECTRI model and dengue outputs from UMEÅ-aegypti model are retrieved from Centre for Open Science[23]. Population at risk under SSP3 is considered as country-based multipliers (the ratio between SSP2 and SSP3 projected population). In the same manner, the baseline values are corrected using country-based multipliers for 2015 (ratio between SSP baseline (2000) and GHSL 2015 population density layers). The score of the Epidemics component is based on “exposed population” metric. For detailed explanation please refer to Section 5.1.5.

5.2.3 Category: Human hazard

5.2.3.1 Definition

Human-made hazards are either technological (e.g. industrial accidents with environmental impact) or sociological in nature. The latter encompass such divergent phenomena as civil wars, high-intensity crime, civil unrest as well as terrorism. Especially armed internal conflict yields catastrophic results for populations and economies and is almost always accompanied by humanitarian risk on a larger scale, caused by the breakdown of supply lines, absent harvests, refugee flows as well as an overall deterioration of health services (Marin-Ferrer et al., 2017). The future violent conflict risk will be largely mediated by socio-economic development trajectories (IPCC, 2022).

5.2.3.2 Human hazard: Components

INFORM Climate Change includes two quantitative variables on man-made disaster that complement the Hazard & exposure section with the dimension of violent conflict and the consequences generated by it, such as large refugee flows and overall destruction of infrastructure.

Table 6. Indicators of the Human hazard category

Component	Indicator	Source	MIN–MAX	No of missing values
Conflict intensity	National power conflicts	Conflict Barometer, HIIK	4-5	-
	Subnational power conflicts	Conflict Barometer, HIIK	4-5	-
Projected risk of conflict	Probability for civil conflict	Hegre et al. (2016)	0-0.8	164-191

Source: Authors

Scalability: data has been produced based on national estimates of socioeconomic variable. Therefore, disaggregated data at finer scales is not yet available.

[22] https://www.who.int/en/news-room/fact-sheets/detail/vector-borne-diseases
[23] https://osf.io/hpaey/

Table 7. Aggregation of Human hazard category

Category	Human hazard		
	MAXIMUM		
Component	Current conflict intensity		Projected conflict intensity
Aggregation	MAXIMUM		
Core indicator	Conflict Barometer (Subnational)	Conflict Barometer (National Power)	Projected conflict risk (Probability of civil conflict)

Source: Authors

5.2.3.3 Component: Conflict intensity

INFORM takes into account the current intensity of conflict in a country or — in case there is currently no conflict — an estimate of future conflict probability. To determine the **current intensity** of a conflict, we use data by the annual **Conflict Barometer** (HIIK, 2019) of the Heidelberg Institute for International Conflict Research (HIIK)[24].

Table 8. Adaption of conflict intensity

Type of conflict	HIIK intensity	INFORM conflict intensity
Non-violent conflict	1 (dispute) 2 (non-violent crisis)	0-5
Violent conflict	3 (violent crisis)	5-8
Highly violent conflict	4 (limited war) 5 (war)	9-10

urce: Marin-Ferrer et al., 2017

The HIIK defines conflict as a dynamic process made up of a sequence of interlocking conflict episodes. The conflict intensity is determined by two criteria: Instruments on the use of force (use of weapons and use of personnel) and the consequences of the use of force (casualties, refugees, and demolition). Its values (**Table 8**) range from 1 (dispute) to 5 (war).

For our purpose, we cluster the conflicts observed by the HIIK into three different groups:

- Conflicts over national power in a country (National power);
- Over intrastate items apart from national power such as secession (Subnational);
- Interstate conflicts [25].

[24] The HIIK approach distinguishes a total of five intensity levels, subdivided into non-violent conflicts (Disputes and Non-violent Crises) and violent conflicts (Violent Crises, Limited Wars, and Wars). The overall intensity is determined by the number of casualties and refugees caused by conflict, as well as by the number of personnel involved, the weapons that were used, and the destruction that was caused. The basic data is provided by the HIIK's annual Conflict Barometer which includes information about more than 400 political conflicts in the world (see http://hiik.de/en/konfliktbarometer/).

[25] In our model, we only take into consideration the two intrastate dimensions of conflict. This has several reasons: First of all, scientific evidence shows that interstate conflict has become a rather rare phenomenon since the end of the Cold War. Besides, if military

We clearly distinguish conflicts over national power from those over subnational items, as they have different causes and drivers that attributes to onset, duration, and escalation of violence.

Table 9. Conflict items, groups, and intensity

HIIK conflict item	INFORM conflict groups	HIIK intensity level	INFORM conflict intensity
National power	National power	5 (war)	10
		4 (limited war)	8
Secession Autonomy Subnational predominance	Subnational	5 (war)	9
		4 (limited war)	7
Any	Violent conflict with lower intensity	3 (violent crisis)	Not considered
International power Territory	Interstate	-	Not considered

Source: Marin-Ferrer et al., 2017

In INFORM Risk Index we consider conflicts over national power to have a graver impact on population, supplies, and long-term development than those over subnational items. First of all, they constrain the overall national production and supply lines and are mostly fought with heavier weapons and more personnel and turn more people into refugees than conflicts over e.g., secession. Second, wars over government usually affect large parts of national territory and often have the tendency of involving foreign powers. Subnational conflicts are mostly restricted to certain regions of a country and only affect regional production and security. We therefore transfer the HIIK data on conflict intensity into a modified intensity scale: Conflicts with HIIK intensity 5 receive an INFORM intensity of 10 if the object is National power, and 9 if the object is Subnational. Analogously, conflicts with HIIK intensity 4 (limited wars) are attributed values of 8 (National power) and 7 (Subnational).

5.2.3.4 Component: Projected risk of conflict

For INFORM Climate Change Risk index, we use the projected conflict risk with SSP-based civil conflict forecasts from Hegre et al. (2016). The data set includes annual projections of armed conflict for each country over the SSPs, for 2014–2100 estimated based on variables such as economic output, educational attainment, population size, conflict history, time since independence, and conflict involvement among neighbouring. For detailed explanation please refer to Section 5.1.6.

For the sake of comparability between current and projected values, the probabilities are transformed to 0-7 HIIK intensity range. A probability of 95% is thereby equivalent to a risk level of 7, countries with a risk score lower than 5 are considered to have no risk of conflict.

The total risk score for the Human hazard category is then calculated by using the maximum score of either the actual conflict intensity or the projected intensity. As both models are purely data-driven and composed of broadly accepted quantitative factors that add up to a comprehensive reflection of risk for and consequences of armed conflict, it allows us to complement our risk assessment with a man-made variable and contributes adequately to the overall predictive abilities of the model.

Note: In order to smoothen the effect of the actual conflict in the future, the HIIK data can be scale down linearly in the future (e.g., 50 % in 2050 and 10% in 2080). In this way, there will be more focus on the projections derived from SSPs in the future, and subsequently improved consistency among population and conflict projections. The factors will be determined through expert elicitation and incorporated in the future release of the index.

5.3 Dimension: Vulnerability

5.3.1 Overview

The Vulnerability dimension addresses the intrinsic predispositions of an exposed population to be affected, or to be susceptible to the damaging effects of a hazard, even though the assessment is made through hazard-independent indicators. So, the Vulnerability dimension represents economic, political and social characteristics

confrontations between states occur, they are mostly restricted to remote border regions and tend not to last longer than several weeks or even days, whereby they do not affect the civilian population as much as intrastate conflicts.

of the community that can be destabilised in case of a hazardous event. Physical vulnerability, which is a hazard dependent characteristic, is dealt with separately in the Hazard & exposure dimension. For the initial phase of INFORM Climate Change Risk study, modifications are considered only for Hazard & Exposure. The Vulnerability component do not change to account for future socioeconomic expansion and climate-related impacts. The modifications for vulnerability will be included in the next releases. To make it more comprehensive for the users, here we summarise the description of the vulnerability component from Marin-Ferrer et al. (2017). The indicators and corresponding min-max and missing values are consistent with INFORM Risk Index 2022 release.

5.3.2 Vulnerability: Categories

Figure 9. Graphical presentation of the vulnerability dimension

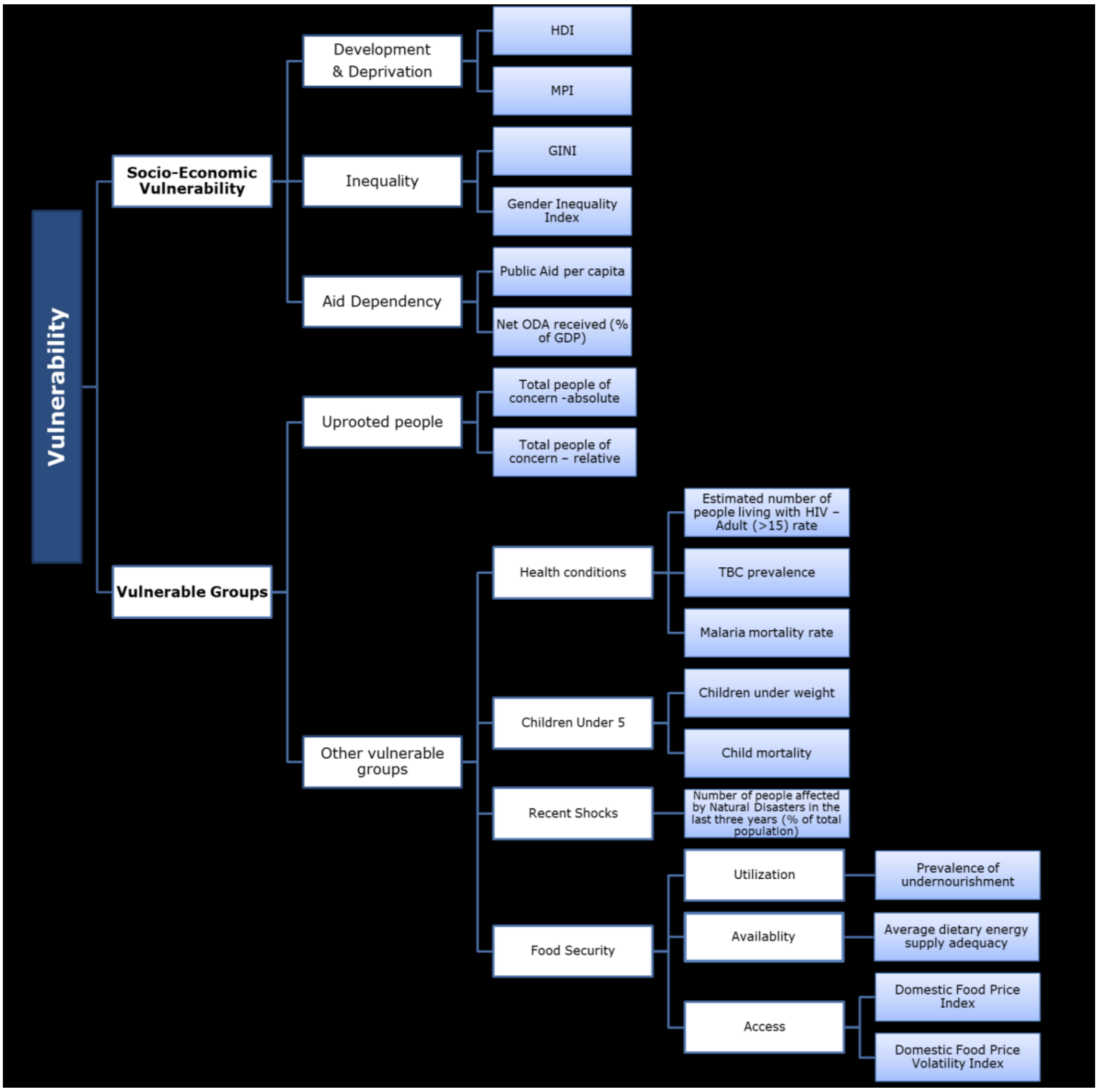

Source: Authors

There are two categories aggregated through the geometric average: Socio-economic vulnerability and Vulnerable groups. The indicators used in each category are different in time variability and the social groups considered in each category are the target of different humanitarian organisations. If the Socio-economic vulnerability category refers more to the demography of a country in general, the Vulnerable group category captures social groups with limited access to social and health care systems.

5.3.3 Category: Socio-economic vulnerability

5.3.3.1 Definition

The Socio-economic vulnerability category measures the (in)ability of individuals or households to afford safe and resilient livelihood conditions and well-being. These in turn dictate whether people can live in safe houses and locations as well as maintain an adequate health in terms of nutrition and preventive medicine to be resistant to increased health risk and reduced food intake in the case of disasters. Socio-economic vulnerability depends only in part on adequate income. Other deficiencies can be corrected with adequate development level that strengthens those cultural processes, which raise level of awareness and knowledge.

5.3.3.2 Socio-economic vulnerability: Components

INFORM Risk Index describes population performance with the weighted arithmetic average of three components (**Table 11**).

Table 10. Indicators of the socio-economic vulnerability category

<table>
<tr><th>Component</th><th>Indicator</th><th>Source</th><th>MIN– MAX</th><th>No of missing values</th></tr>
<tr><td rowspan="2">Development & deprivation</td><td>Human Development Index</td><td>Human Development Report, UNDP</td><td>0.4-0.9</td><td>4/191</td></tr>
<tr><td>Multidimensional Poverty Index</td><td>Human Development Report, UNDP</td><td>0-2.7</td><td>84/191</td></tr>
<tr><td rowspan="2">Inequality</td><td>GINI index</td><td>World Bank</td><td>25-65</td><td>36/191</td></tr>
<tr><td>Gender Inequality Distribution</td><td>Human Development Report, UNDP</td><td>0-0.75</td><td>29/191</td></tr>
<tr><td rowspan="4">Aid dependency</td><td>Total ODA in the last 2 years per capita</td><td>OECD</td><td rowspan="2">0-500</td><td>-</td></tr>
<tr><td>Global Humanitarian Funding per capita</td><td>Financial Tracking System, UNOCHA</td><td>-</td></tr>
<tr><td>Net ODA Received in percentage of GDP</td><td>World Bank</td><td>0 %-15 %</td><td>-</td></tr>
<tr><td>Volume of remittances (in USD) as a proportion of total GDP (%)</td><td>World Bank</td><td>0 %-30 %</td><td>10/191</td></tr>
</table>

Source: Authors

Scalability: All core indicators (Table 10) of Socio-economic vulnerability are published annually. The data for indicators of Development & deprivation, and Inequality component are available on subnational level, while the unit of analysis for the indicators of the aid dependency component is country.

Table 11. Aggregation of the Socio-Economic vulnerability category

Category	Socio-Economic vulnerability							
Aggregation	ARITHMETIC AVERAGE 50/25/25							
	50 %		25 %		25 %			
Component	Development & deprivation		Inequality		Aid dependency			
Core indicator	GEOMETRIC AVERAGE		ARITHMETIC AVERAGE		ARITHMETIC AVERAGE			
					Public Aid per capita		Net ODA Received (% of GNI)	Volume of remittances
					SUM			
	Human Development Index	Multidimensional Poverty Index	GINI index	Gender Inequality Distribution	Total ODA in the last 2 years per capita	Total Humanitarian Funding in the last 2 years per capita		

Source: Authors

5.3.3.3 Component: Development & deprivation

The **Development & deprivation** component describes how a population is doing on average. It comprises two well recognised composite indices by UNDP: the Human Development Index (HDI) and the Multidimensional Poverty Index (MPI). The Human Development Index covers both social and economic development and combines factors of life expectancy, educational attainment, and income. While the Multidimensional Poverty Index identifies overlapping deprivations at the household level across the same three dimensions as the Human Development Index (living standards, health, and education), it also includes the average number of poor people and deprivations, with which poor households contend. This component is weighted 50 % to fairly convey the contribution of both aspects, development as well as deprivation.

5.3.3.4 Component: Inequality

The **Inequality** component introduces the dispersion of conditions within population presented in Development & deprivation component as an arithmetic average of two proxy measures: the Gini index by the World Bank and Gender Inequality Index by UNDP. The Gini index measures how evenly distributed resident's income is among a country's population while the Gender Inequality Index exposes differences in the distribution of achievements between men and women. This component is weighted 25 % based on expert opinion.

5.3.3.5 Component: Aid dependency

With the **Aid dependency** component, the methodology points out the countries that lack sustainability in development growth due to economic instability and humanitarian crisis. It is comprised of three indicators: Public aid per capita, net official development assistance (ODA) received in percentage of gross national income (GNI), and the Volume of remittances as a proportion of total GDP. Public aid per capita is obtained as a sum of total official development assistance in the last 2 years per capita published by OECD and Global Humanitarian Funding per capita published by UN OCHA. The Aid dependency score is the arithmetic average of the three abovementioned indicators, and is weighted 25 % based on expert opinion.

5.3.4 Category: Vulnerable groups

5.3.4.1 Definition

The Vulnerable group category refers to the population within a country that has specific characteristics that make it at a higher risk of needing humanitarian assistance than others or being excluded from financial and social services. In a crisis situation such groups would need extra assistance, which appeals for additional measures, i.e. extra capacity, as a part of the emergency phase of disaster management.

5.3.4.2 Vulnerable groups: Components

The Vulnerable group category (**Table 13**) is split in two: **Uprooted people** and **Other vulnerable groups**. Uprooted people are effectively weighted more because they are not a part of the society or the social system, are only partially supported by the community and often trigger the humanitarian intervention.

Table 12. Indicators of the Vulnerable groups category

Component/ Sub-component	Indicator	Source	MIN–MAX	No of Missing values
Uprooted people	Number of refugees, returned refugees, internally displaced persons (absolute)	UNHCR, IDMC	Log(1,000)-Log(1 000 000)	-
	Number of refugees, returned refugees, internally displaced persons (relative)	UNCHR, IDMC, World Bank	0.005 %-10 %	-
Other Vulnerable groups/Health conditions	Prevalence of HIV-AIDS above 15 years	WHO	0 %-5 %	69/191
	Tuberculosis prevalence	WHO	0-550	1/191
	Malaria incidence per 1,000 population at risk	WHO	0-400	106/191
	People requiring interventions against neglected tropical diseases relative to total population	WHO	0 – 0.9	1/191
Other Vulnerable groups/ Children under 5	Children underweight	Unicef, WHO	0 %-45 %	64/191
	Child mortality	Unicef, WHO	0-130	1/191
Other Vulnerable groups/Recent shocks	Relative number of affected population by natural disasters in the last three years	EM-DAT, CRED	0 %-10 %	-
Other Vulnerable groups/Food security	Prevalence of undernourishment	FAO	5 %-35 %	-
	Average dietary energy supply adequacy	FAO	75 %-150 %	-

Source: Authors

Table 13. Aggregation of the Vulnerable groups category

Category	Vulnerable groups											
Component	GEOMETRIC AVERAGE											
	Uprooted people			Other vulnerable groups								
Aggregation	ARITHMETIC AVERAGE			GEOMETRIC AVERAGE								
	Log(absolute)	Relative		Health conditions				Children under 5		Recent shocks	Food security	
				ARITHMETIC AVERAGE				ARITHMETIC AVERAGE			ARITHMETIC AVERAGE	
	SUM										Utilisation	Availability
Core Indicator	Number of refugees	Number of returned refugees	Number of IDPs	Prevalence of HIV-AIDS (> 15 years)	Tuberculosis prevalence	Malaria mortality rate	People requiring interventions against neglected tropical diseases relative to total population	Children underweight	Child mortality	Relative number of affected population by natural disasters in the last 3 years	Prevalence of undernourishment	Average dietary energy supply adequacy

Absolute: Absolute value of physical exposure (AAEP)
Relative: Relative value of physical exposure (AAEP per capita). AAEP is normalised with country's total population.

Source: Authors

Scalability: The indicators for the Uprooted people component are foreseen to be updated as soon as data are available on subnational scale. The indicators of the Health Conditions and the Children under-5 sub-component are updated annually and could be potentially provided sub-nationally if the data would exist. The data for the Recent shock sub-component are limited to national scale and provided every 3 months. In case of Food Security indicators the data are available annually on national scale but other options considered in **Box 4**, not available at the moment globally, would allow geographical and temporal disaggregation.

5.3.4.3 Component: Uprooted people

The total number of uprooted people is the sum of the highest figures from the selected sources for each uprooted group. The **Uprooted people** component is the arithmetic average of the absolute and relative value of uprooted people. The absolute value is presented using the log transformation while the uprooted people relative to the total population are transformed into indicator using the GNA[26]. criteria and then normalised into range from 0 to 10 (**Table 14**).

Table 14. Transformation criteria for the relative value of uprooted people

% of total population	Level of vulnerability	Uprooted people (relative subcomponent)
> 10 %	High	10.0
> 3 % AND < 10 %		8.3
> 1 % AND < 3 %	Medium	6.7
> 0.5 % AND < 1 %		5.0
> 0.1 % AND < 0.5 %	Low	3.3
> 0.005 % AND < 0.1 %		1.7
< 0.005 %	No vulnerability	0.0

Source: Marin-Ferrer et al., 2017

5.3.4.4 Component: Other vulnerability groups/Health condition

A **Health condition** subcomponent refers to people in a weak health conditions. It is calculated as the arithmetic average of the AIDS, tuberculosis, malaria and other neglected tropical diseases which are considered as pandemics of low- and middle-income countries. The combat against these diseases is one of the 2015 Millennium Development Goals (MDG) [27] and the Sustainable Development Goals (SDG) [28].

5.3.4.5 Component: Other vulnerability groups/Children under 5

A **Children under-5** subcomponent captures the health condition of children. It is referred to with two indicators, malnutrition and mortality of children under 5. Children Underweight extracts the group of children that are in a weak health condition mainly due to hunger. Child mortality shows general health condition of the children and is closely linked to maternal health since more than one third of children deaths occur within the first month of life and to how well the country tackles major childhood diseases (e.g. proper nutrition, vaccinations, monitoring system, family care practice, health system access, sanitation and water resources). Therefore, decrease of underweight children and the child deaths are one of the MDG by 2015 as well.

5.3.4.6 Component: Other vulnerability groups/Recent shocks

Recent shocks subcomponent accounts for increased vulnerability during the recovery period after a disaster and considers people affected by natural disasters in the past 3 years. The affected people from the most recent year are considered fully while affected people from the previous years are scaled down with the factor 0.5 and 0.25 for the second and third year, respectively, assuming that recovery decreases vulnerability progressively. This way the smoothness of the INFORM Risk Index in time series is assured.

5.3.4.7 Component: Other vulnerability groups/Food security

The FAO definition of **food security** is: 'A situation that exists when all people, at all times, have physical, social and economic access to sufficient, safe and nutritious food that meets their dietary needs and food preferences for an active and healthy life' [29]. For our model, we therefore suggest that the Food security subcomponent is dependent on Food availability and Food utilisation. This concept serves as a set of proxy measures for the number of people lacking secure access to food. Leaning on definitions provided by the Integrated Phased Food Security Classification (IPC), we determine **Food availability** on whether food is actually or potentially physically present regarding production, wild foods, food reserves, markets, and transportation. **Food utilisation** covers the question as to whether or not households are sufficiently utilising food in terms of food preferences, preparation, feeding practices, storage and access to improved water sources.

[26] In our model, Global Needs Assessment methodology that was used by European Commission Humanitarian Aid for the identification of priority countries used until 2013.
[27] https://mdgs.un.org/unsd/mdg/Default.aspx
[28] https://sustainabledevelopment.un.org/sdgs
[29] http://www.fao.org/3/a-i4030e.pdf

The combination of lack of food, lack of means to actually make it available, and lacking quality of food may lead to famine and hunger for poor populations. Therefore, the three components are aggregated with an arithmetic average.

5.4 Dimension: Lack of coping capacity

5.4.1 Overview

For the Lack of coping capacity dimension, the question is, which issues the government has addressed to increase the resilience of the society and how successful their implementation is. The Lack of coping capacity dimension measures the ability of a country to cope with disasters in terms of formal, organised activities and the effort of the country's government as well as the existing infrastructure, which contribute to the reduction of disaster risk. For the initial phase of INFORM Climate Change Risk study, modifications are considered only for Hazard & Exposure. The lack of coping capacity component do not change to account for future socioeconomic expansion and climate-related impacts. The modifications for lack of coping capacity will be included in the next releases. To make it more comprehensive for the users, here we summarise the description of the lack of coping capacity component from Marin-Ferrer et al. (2017). The indicators and corresponding min-max and missing values are consistent with last INFORM Risk update (2022).

5.4.2 Lack of coping capacity: categories

Figure 10. Graphical presentation of the lack of coping capacity dimension

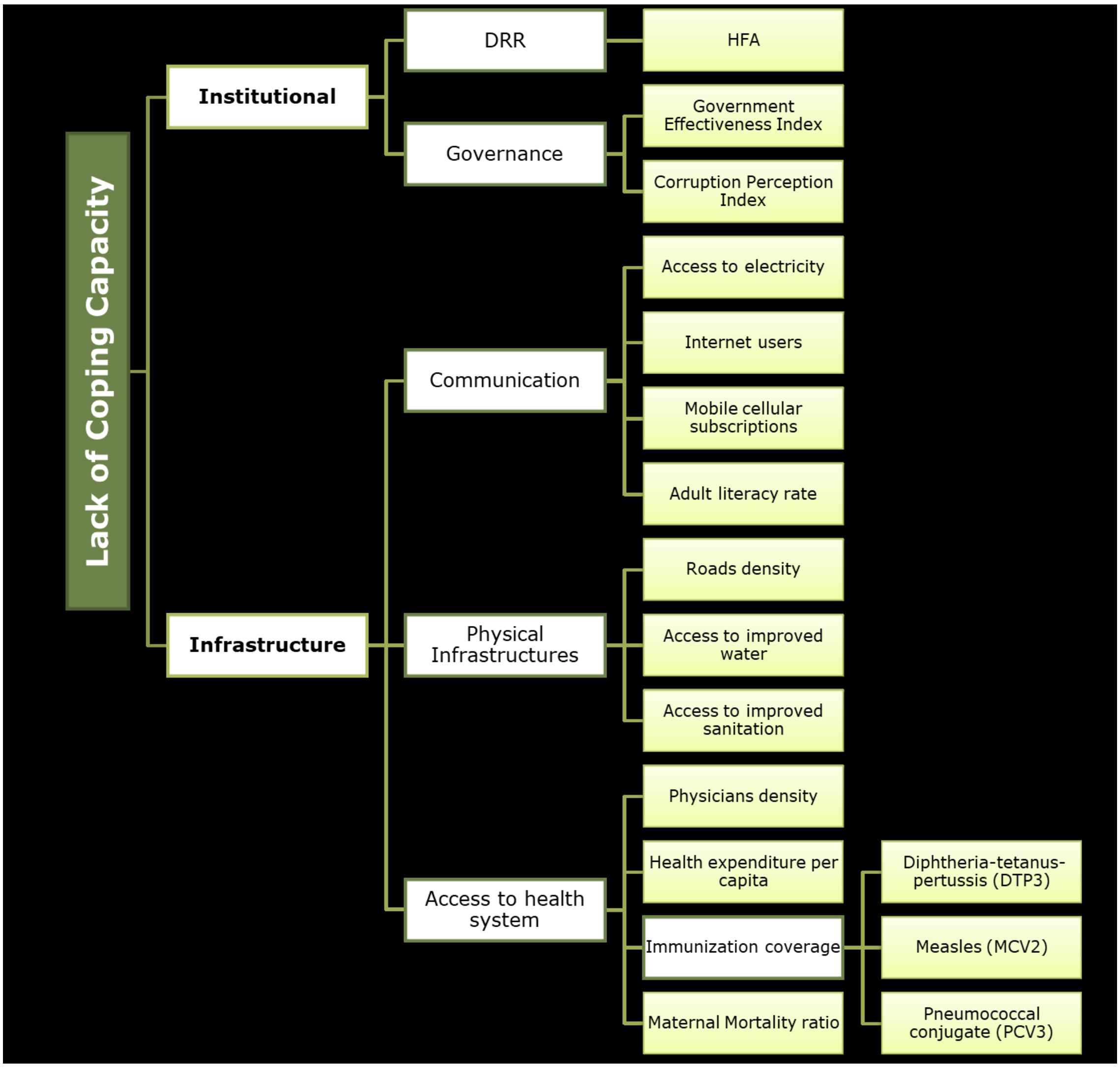

Source: Authors

It is aggregated by a geometric mean of two categories: Institutional and Infrastructure. The difference between the categories is in the stages of the disaster management cycle that they are focusing on. If the Institutional category covers the existence of DRR programmes, which address mostly mitigation and preparedness/early warning phase, then the Infrastructure category measures the capacity for emergency response and recovery.

5.4.3 Category: Institutional

5.4.3.1 Definition

The Institutional category quantifies the government's priorities and institutional basis for the implementation of DRR activities. It is calculated as an arithmetic average of two components, **Disaster risk reduction** and **Governance** (**Table 16**), in order to incorporate the effectiveness of the governments' effort for building resilience across all sectors of society.

Table 15. Indicators of the Institutional category

Component	Indicator	Source	MIN–MAX	No of missing values
Disaster risk reduction	Hyogo Framework for Action self-assessment reports	UNISDR	1-5	40/191
Governance	Government effectiveness	World Bank	– 2.5-2.5	-
	Corruption Perception Index	Transparency International	0-100	14/191

Source: Authors

Table 16. Aggregation of Institutional category

Category	Institutional		
	ARITHMETIC AVERAGE		
Component	Disaster risk reduction	Governance	
		ARITHMETIC AVERAGE	
Core indicator	Hyogo Framework for Action Scores	Government effectiveness	Corruption Perception Index

Source: Authors

Scalability: For all indicators of the Institutional category only annual updates on a national scale are possible.

5.4.3.2 Component: Disaster Risk Reduction

The indicator for the **Disaster Risk Reduction** *activity* in the country comes from the score of Hyogo Framework for Action self-assessment reports of the countries. The Hyogo Framework for Action (UNISDR, 2007) covers the following topics:

1. Ensure that disaster risk reduction is a national and a local priority with a strong institutional basis for implementation.

2. Identify, assess and monitor disaster risks and enhance early warning.
3. Use knowledge, innovation and education to build a culture of safety and resilience at all levels.
4. Reduce the underlying risk factors.
5. Strengthen disaster preparedness for effective response at all levels.

Self-evaluation has a risk of being perceived as a process of presenting inflated grades and being unreliable.

5.4.3.3 Component: Governance

The subjectivity of HFA Scores is counterweighted by arithmetical average with external indicators of **Governance component**, i.e. the Government Effectiveness and Corruption Perception Index.

The Government Effectiveness [30] captures perceptions of the quality of public services, the quality of the civil service and the degree of its independence from political pressures, the quality of policy formulation and implementation, and the credibility of the government's commitment to such policies while the **Corruption Perception Index** adds another perspective, that is the level of misuse of political power for private benefit, which is not directly considered in the construction of the Government Effectiveness even though interrelated.

5.4.4 Category: Infrastructure

5.4.4.1 Definition

Communication networks, physical infrastructure and accessible health systems are treated as essential parts of the infrastructure needed during emergency response, focusing on the early warning phase, and carrying through response and recovery. Since all parts of the infrastructure should be operational to a certain level, the aggregation process uses the arithmetic average of indicators describing accessibility as well as the redundancy of the concerned system that are two crucial characteristics in a crisis situation.

Table 17. Indicators of the Infrastructure category

Component	Indicator	Source	MIN–MAX	No of missing values
Communication	Access to electricity	World Bank	0 %-100 %	-
	Internet users	World Bank	0 %-100 %	2/191
	Mobile cellular subscriptions	World Bank	5-200	1/191
	Adult literacy rate	Unesco	0 %-100 %	40/191
Physical infrastructure	Roads density	OpenStreetMap	1-100	-
	Access to improved water source	WHO/Unicef	50 %-100 %	-
	Access to improved sanitation facilities	WHO/Unicef	10 %-100 %	-
Access to health system	Physicians density	WHO	0-40	12/191
	Health expenditure per capita	WHO	50-3 000	6/191
	Proportion of the target population with access to 3 doses of diphtheria-tetanus-pertussis (DTP3) (%)	WHO	40-99	1/191
	Proportion of the target population with access to measles-containing-vaccine second-dose (MCV2) (%)	WHO	40-99	19/191
	Proportion of the target population with access to pneumococcal conjugate 3rd dose (PCV3) (%)	WHO	40-99	51/191
	Maternal Mortality ratio	WHO, UNICEF, UNFPA, World Bank	0-900	7/191

Source: Authors

[30] http://info.worldbank.org/governance/wgi/index.aspx#doc

Table 18. Aggregation of the Infrastructure category

Category	Infrastructure												
	ARITHMETIC AVERAGE												
Component	Communication				Physical infrastructure			Access to health system					
	ARITHMETIC AVERAGE				ARITHMETIC AVERAGE			ARITHMETIC AVERAGE					
										Immunization coverage			
										ARITHMETIC AVERAGE			
Core indicator	Access to electricity	Internet users	Mobile cellular subscriptions	Adult literacy rate	Roads density	Access to improved water source	Access to improved sanitation facilities	Physicians density	Health expenditure per capita	Access to diphtheria-tetanus-pertussis (DTP3)	Access to measles-containing-vaccine (MCV2)	Access to pneumococcal conjugate (PCV3)	Maternal mortality rate

Source: Authors

Scalability: Health expenditure per capita has a unit of analysis locked to country while all the other indicators could be potentially developed on subnational scale if the data would exist. Regarding the temporal scalability only annual updates are expected.

5.4.4.2 Component: Communication

The **Communication** component aims at measuring the efficiency of dissemination of early warnings through a communication network as well as coordination of preparedness and emergency activities. It is dependent on the dispersion of the communication infrastructure as well as the literacy and education level of the recipients.

5.4.4.3 Component: Physical infrastructure

Physical infrastructure component is the arithmetic average of different proxy measures. We mainly try to assess the accessibility as well as the redundancy of the lifeline systems, which are crucial in a crisis situation, i.e. roads, water and sanitation systems.

5.4.4.4 Component: Access to health system

Access to health system component is the arithmetic average of different proxy measures. We mainly try to assess the accessibility as well as the redundancy of the different assets of the existing health systems.

6 Statistical analysis

6.1 Correlation analysis

6.1.1 Raw data comparability

As a first step, we compare the raw data for the modified components (river flood, cyclone surge, coastal flood, drought-affected people, vector borne diseases and conflict probability) of INFORM Climate Change Risk Index for the historical climate (baseline) to those from the original index (INFORM Risk Index 2022) using the Pearson correlation coefficient (De Groeve et al., 2015; OECD, 2008). The Pearson's correlation coefficient has been widely used to measure the linear association between normally distributed continuous variables. Nevertheless, it can offer an effective description of linear association even in the case of bivariate non-normal distributions (Puth et al., 2015). The correlation coefficients can help us to investigate to what extent the raw variables used for INFORM Climate Change Risk Index and INFORM Risk Index are statistically comparable (Marzi et al., 2021). Before calculating the Pearson correlation coefficients, the variables (except conflict probability) are log-transformed and left-censored to avoid disturbances from outliers and zero-clusters.

Figure 11. Correlogram for raw data used for upgraded and original variables (scatter plots, distribution and Pearson correlation. The abbreviations are RF = River Flood, CS = Cyclone Surge, CS = Coastal Flood, DR = Drought, MAL = Malaria, DNG = Dengue, CON= Conflict probability, OR = Original INFORM, and UPG = Upgraded INFORM, ** =significance level p < 0.01, *** = significance level p < 0.001.

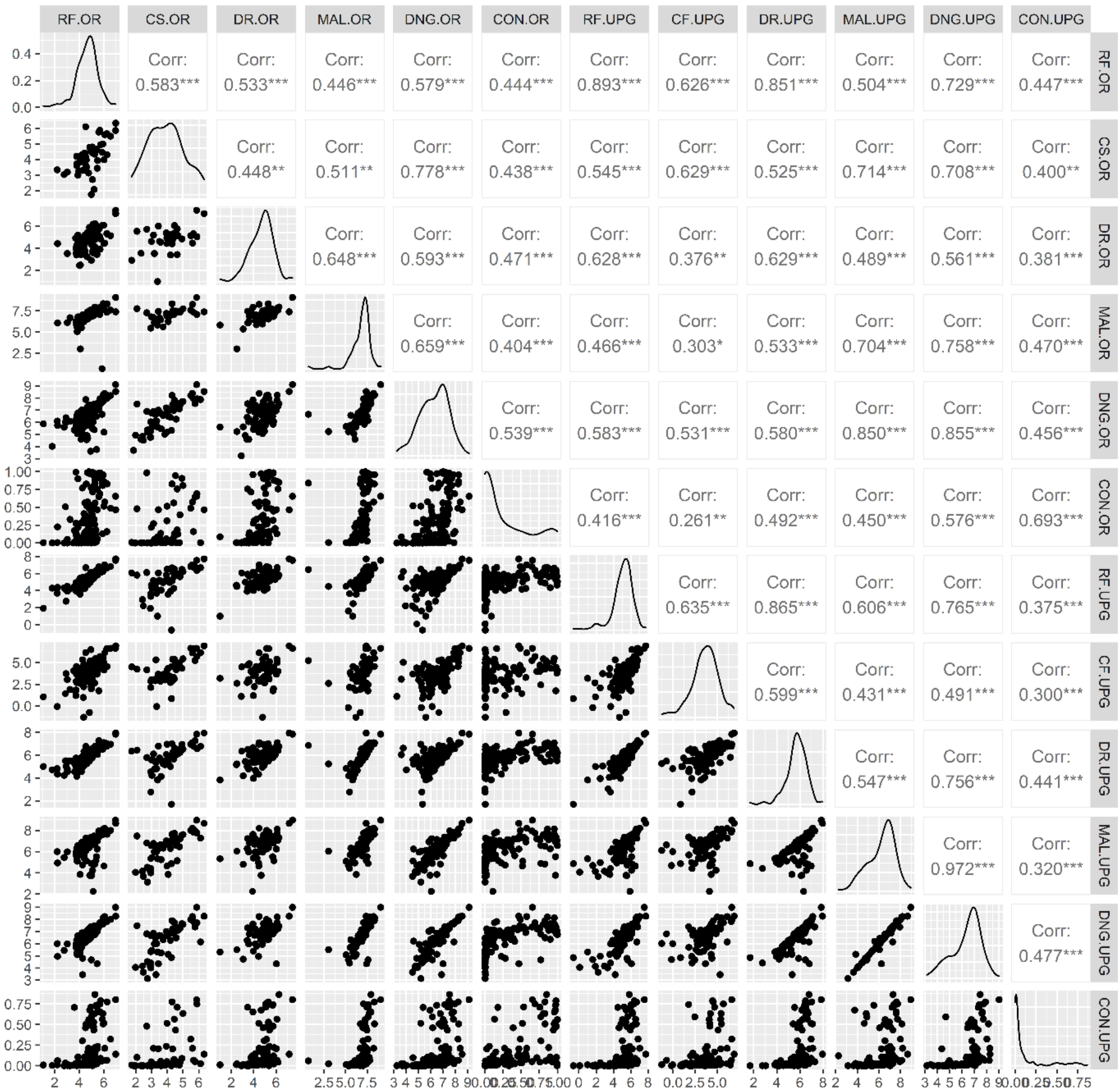

Source: Authors

The correlations range from 0.893 for river flood to 0.629 for coastal flood and drought, and are all statistically significant ($p < 0.001$). These correspond to correlation strengths in the range “moderate” to “strong” according to the classes defined by (Akoglu, 2018; Bendanillo et al., 2016) suggesting that the INFORM Climate Change Risk Index and INFORM Risk Index variables are statistically compatible.

6.1.2 Hazard & Exposure components

In the second step, we investigate the linear correlation between the normalized indices at different levels of Hazard & Exposure dimension. It is not possible to perform a pairwise correlation test due to modifications in the natural hazard and exposure component (tropical cyclone break down to cyclone wind and coastal flood). In order to have a pairwise correlation test, we consider only the comparable modified sub-indices namely river flood, drought, epidemics and projected conflict risk. The influence of the modified components on the aggregate Natural and Hazard&Exposure indices will be thoroughly investigated through sensitivity analysis. **Figure 12** illustrates the Pearson correlation coefficient among Hazard&Exposure components and final aggregate.

Figure 12. Correlation of Hazard&Exposure components of INFORM Risk Index and INFORM Climate Change Risk Index

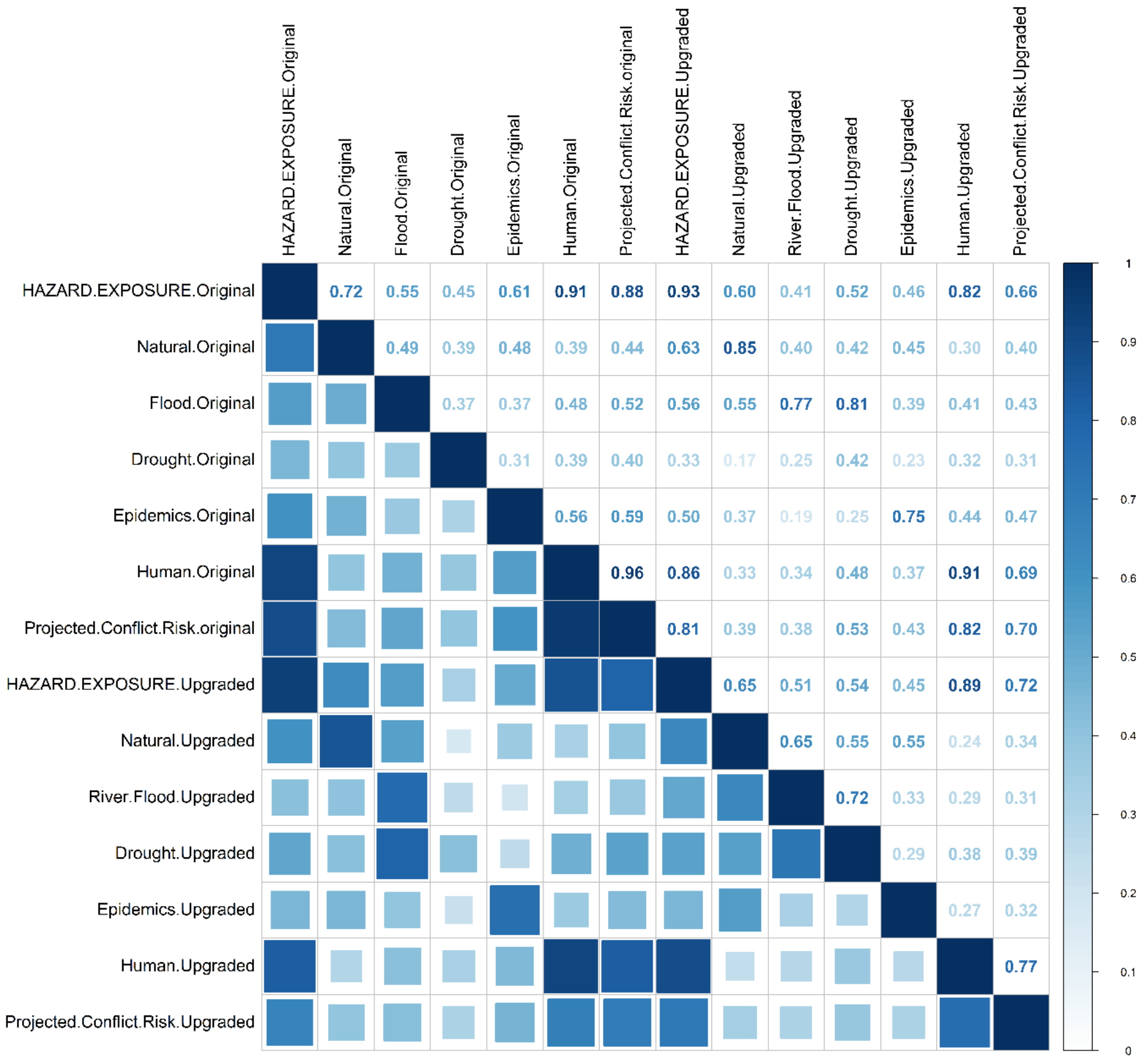

INFORM Risk Index = original
INFORM Climate Change Risk Index = upgraded

Source: Authors

The analysis shows very strong correlation (0.93) between original and upgraded Hazard&Eposure indices suggesting that the modified dimensions are statistically compatible. The same applies to Natural and Human components with 0.85 and 0.91 correlation coefficients, respectively. At component level, the largest correlation is found for river flood (0.77), followed by epidemics (0.75), projected conflict risk (0.7) and drought (0.42) – the lowest. The low correlations for drought are caused by differences in the sub indicators used to evaluate this phenomenon. The INFORM Risk Index (original) drought component is a combination of affected people by drought, frequency of drought events and agricultural drought probability, while the INFORM Climate Change Risk Index (upgraded) includes exposed (affected) people to drought. Hence, only one component can be conceptually compared, and this leads to low correlation between aggregated drought components. The frequency of drought events and agricultural drought probability based on SPEI will be computed and added to the analysis in the future releases. The full correlation matrix for INFORM Climate Change Risk Index baseline is available in Annex 1.

6.1.3 INFORM Risk scores

In the last step, we compare statistical and spatial correlations between the original and upgraded risk indices (**Table 19**). To have a broader class of association, we consider also Spearman's and Kendall rank order correlation coefficients (OECD, 2008; Puth et al., 2015). These two measure the degree of monotonic (but not necessarily linear) correspondence between two rankings.

Table 19. Correlation analysis of the original and upgraded risk indices

Index	Pearson	Spearman	Kendall
INFORM Risk Index (2022) INFORM Climate Change Risk Index (baseline)	0.98	0.97	0.89

Source: Authors

The high values of correlation coefficients suggest a very strong monotonic association between the Risk indices. Hence, the INFORM Climate Change Risk Index baseline is statistically comparable to the original INFORM Risk Index.

In order to assess the spatial correlation between indices, we compare the top 30 countries with largest risk scores (**Table 20**). Accordingly, 50 percent of the countries have identical rankings. The rest experience shifts in rankings but still placed as top 30, and only 6 do not match. Among not matched observations, three of them have very close rankings (Liberia with 29, Burundi with 33 and Philippines with 34). The rankings for other three vary significantly with largest changes for Eritrea. The comparison suggests moderate spatial comparability among the top 30 very high and high risk countries despite considerable variations in input data and methodology.

In the final step, we investigate the shifts in risk classes between the INFORM Risk Index 2022 and INFORM Climate Change Risk Index baseline (Annex 2). More than 78 percent (150) of the countries have identical risk classes. The rest of the countries experience one-class shifts, six from Very Low to Low (e.g., Germany and UK), six from Low to Very Low (e.g., Turkmenistan), one from Low to Medium (Suriname), 15 from Medium to Low (e.g., Namibia and Tajikistan), two from Medium to High (Brazil and Mexico), and 11 from High to Medium (e.g., Tanzania and Mauritania). The major source of the positive shifts (Medium to Low, High to Medium, and Low to Very Low) are the changes in human hazard category, while the negative shifts (Very Low to Low, Low to Medium and Medium to High) are mainly caused by changes in Natural hazard category. No shift was found from Very high to High classes and vice versa, suggesting that the Very High risk class is robust, and not influenced by the variations in data sources and methodology.

Table 20. Top 30 countries with highest risk scores for INFORM Risk Index 2022 and INFORM Climate Change Risk Index baseline. Green colour stands for identical rankings, Orange for shifts in the rankings in the top 30 range, and red for not matched countries

NFORM Risk Index 2022					INFORM Climate Change Risk Index Baseline				
COUNTRY	ISO 3	INFORM RISK	RISK CLASS	Rank	**COUNTRY**	ISO 3	INFORM RISK	RISK CLASS	Rank
Somalia	SOM	8.8	Very High	1	**Somalia**	SOM	8.8	Very High	1
South Sudan	SSD	8.4	Very High	2	**South Sudan**	SSD	8.5	Very High	2
Afghanistan	AFG	8.2	Very High	3	**Yemen**	YEM	8.1	Very High	3
Yemen	YEM	8.2	Very High	3	**Afghanistan**	AFG	8	Very High	4
Chad	TCD	7.9	Very High	5	**Chad**	TCD	7.8	Very High	5
Central African Republic	CAF	7.8	Very High	6	**Central African Republic**	CAF	7.7	Very High	6
Congo DR	COD	7.6	Very High	7	**Congo DR**	COD	7.6	Very High	7
Niger	NER	7.4	Very High	8	**Niger**	NER	7.3	Very High	8
Mozambique	MOZ	7.2	Very High	9	**Mozambique**	MOZ	7.2	Very High	9
Syria	SYR	7.1	Very High	10	**Syria**	SYR	7	Very High	10
Mali	MLI	7	Very High	11	**Mali**	MLI	6.9	Very High	11
Ethiopia	ETH	6.8	Very High	12	**Ethiopia**	ETH	6.8	Very High	12
Iraq	IRQ	6.6	Very High	13	**Iraq**	IRQ	6.6	Very High	13
Nigeria	NGA	6.5	Very High	14	**Nigeria**	NGA	6.6	Very High	13
Burkina Faso	BFA	6.4	High	15	**Burkina Faso**	BFA	6.4	High	15
Sudan	SDN	6.4	High	15	**Sudan**	SDN	6.4	High	15
Myanmar	MMR	6.3	High	17	**Cameroon**	CMR	6.2	High	17
Haiti	HTI	6.2	High	18	**Libya**	LBY	6.2	High	17
Libya	LBY	6.2	High	18	**Myanmar**	MMR	6.2	High	17
Cameroon	CMR	6.1	High	20	**Uganda**	UGA	6.2	High	17
Uganda	UGA	6	High	21	**Pakistan**	PAK	6	High	21
Azerbaijan	AZE	5.9	High	22	**Azerbaijan**	AZE	5.8	High	22
Burundi	BDI	5.9	High	22	**Bangladesh**	BGD	5.5	High	23
Pakistan	PAK	5.9	High	22	**Haiti**	HTI	5.5	High	23
Papua New Guinea	PNG	5.9	High	22	**India**	IND	5.5	High	23
Eritrea	ERI	5.8	High	26	**Colombia**	COL	5.4	High	26
Bangladesh	BGD	5.7	High	27	**Papua New Guinea**	PNG	5.4	High	26
Kenya	KEN	5.7	High	27	**Armenia**	ARM	5.3	High	28
Armenia	ARM	5.4	High	29	**Liberia**	LBR	5.3	High	28
Colombia	COL	5.4	High	29	**Philippines**	PHL	5.3	High	28

Source: Authors

6.2 Sensitivity analysis

The literature suggests (Paruolo et al., 2012; Wang and Stanley, 1970) that the influence of the i-th indicator on a composite index y is expressed as the squared correlation between the two (correlation ratio):

$$Influence_{x_i,y} = cor^2(x_i, y) \qquad \textbf{Equation 5}$$

Correlation ratio can be applied when relationships between the index and its components are linear or non-linear. Non-linearities may arise from the aggregation (in the case of geometric mean used in INFORM) and/or non-linear relationships between the single variables. It can be used regardless of the degree of correlation between variables. Unlike the Pearson or Spearman correlation coefficients, it is not constrained by assumptions of linearity or monotonicity (Paruolo et al., 2012). To explore to what extent the Hazard&Exposure component is sensitive to variations in the sub-indices and the balance of the whole dimension, we compare the correlation ratio for each sub-indicator both in original and upgraded indices (**Table 21**).

Table 21. Statistical influence of the INFORM categories and sub-indices within dimensions for original and upgraded models

INFORM product	**INFORM Risk Index 2022**				**INFORM Climate Change Risk Index Baseline**			
Components vs Categories vs Dimension	**Natural**		**Hazard& Exposure**		**Natural**		**Hazard& Exposure**	
	CR	**NORM**	**CR**	**NORM**	**CR**	**NORM**	**CR**	**NORM**
Natural	-	-	0.853	0.480	-	-	0.894	0.483
Human	-	-	0.924	0.519	-	-	0.955	0.516
Earthquake	0.593	0.185	-	-	0.562	0.138	-	-
Flood	0.520	0.162	-	-	0.633	0.155	-	-
Tsunami	0.553	0.173	-	-	0.566	0.139	-	-
Tropical cyclone	0.554	0.173	-	-	-	-	-	-
Cyclone wind	-	-	-	-	0.649	0.159	-	-
Coastal flood	-	-	-	-	0.636	0.156	-	-
Drought	0.469	0.146	-	-	0.581	0.143	-	-
Epidemics	0.503	0.157	-	-	0.433	0.106	-	-

CR = Correlation ratio
NORM = Normalized Coefficient

Source: Authors

The correlation ratios and normalized coefficients show that the categories within the Hazard&Exposure dimension (Natural and Human) maintain the equal importance across original and upgraded models. This suggest that the structure of the Hazard&Exposure dimension is robust and not sensitive to the variations in the Natural and Human components. For the lower levels (Natural Hazard & Exposure components), the results show that the correlation ratios of the original and upgraded variables in the composite index are all in the range of 0.4 to 0.6. The largest variations are found for river flood, coastal flood, cyclone wind and drought. The normalized importance coefficients are lower for upgraded index' components due to difference in the number of variables (6 instead of 5 in the upgraded model). Coastal flood and cyclone wind in the upgraded index hold similar correlation ratios. This suggests that the importance would be equally distributed between these two if they were aggregated into a higher-level index as the original model. Therefore, the split of the tropical cyclone into two components would not have major influence on the aggregated index.

As the last step of the sensitivity analysis, we compare the correlation ratios within upper-level dimensions to explore the influence of each dimension at final risk score (**Table 22**).

Table 22. Statistical influence of the INFORM dimensions on the final Risk score for original and upgraded models

INFORM product	INFORM Risk Index 2022		INFORM Climate Change Risk Index (baseline)	
Dimension	**CR**	**NORM**	**CR**	**NORM**
Hazard & Exposure	0.798	0.329	0.798	0.329
Vulnerability	0.863	0.355	0.863	0.355
Lack of coping capacity	0.763	0.314	0.763	0.314

The comparison suggests that the influence of the three core dimensions on the aggregated risk scores will not change between two models. Therefore, both models are comparable, well-structured and balanced.

6.3 Uncertainty analysis

Uncertainty analyses can help determine whether the main results change substantially when the methodological choices vary over a reasonable range of possibilities (Nardo et al., 2005; OECD, 2008; Tate, 2012). Uncertainty in the weighting and aggregation process for **Natural Hazard&Exposure** category is introduced by varying the weights based on the extent to which the indicators compensate each other. We consider the worst scenario combination RCP8.5 - SSP3 to maximize the sampling of uncertainty in future climate changes and provide a challenging yet plausible scenario context. The degree of "compensation" denotes trade-offs between higher performance in some indicators and lower performance in others. Using additive aggregators with a high degree of compensation implies that one or more of the indicators may not be receiving the adequate attention (Marzi et al., 2018). For instance, combining Natural and Human hazard components using additive approach (high degree of compensation) implies that, to have a high hazard and exposure score for a country, both components should be high simultaneously. Instead, the use of a geometric average (low degree of compensation) implies that it is sufficient for a country to have a high score either in the Natural Hazard or the Human hazard category to have an overall high Hazard&Exposure score.

To explore the uncertainty in the weighting and aggregation process, we apply the ordered weighted average (OWA) operator introduced by Yager (1988) which provides a circumstance in which the degree of compensation can be adjusted and modified. The OWA operator is defined as follows:

$$OWA(x_1, \ldots, x_n) = \sum_{i=1}^{n} w_i . x_{\sigma(i)}$$ **Equation 6**

where σ is a permutation ordering the elements as $x_{\sigma(1)} \leq \cdots \leq x_{\sigma(n)}$, with associated non-negative weights in the range of [0,1] summing up to one ($\sum_{i=1}^{n} w_i = 1$) (Jin et al., 2017; R. Yager, 1988; Zabeo, 2011). The OWA operator provides a family of operators, including a maximum (1,0, 0,...,0), minimum (0,0,...,1), k-order statistics (kth weight equal to 1 and the rest zero), the arithmetic mean ($\frac{1}{n}, \frac{1}{n} \ldots \frac{1}{n}$) and a window type OWA, which takes the average of m components in the center (Fullér, 1996; Zabeo, 2011). The weights can be ordered in different ways and distributed by using either linear or uniform patterns (Jin et al., 2017; Mysiak et al., 2018).

In order to examine the trade-offs, Yager (1988) introduced the degree of ORNESS determining the proximity to the maximum operator for a particular set of weights (Chaji et al., 2018; Zabeo, 2011). The ORNESS index is given by:

$$ORNESS(w_1, \ldots, w_n) = \frac{1}{n-1}\sum_{i=1}^{n} w_i.(n-i) \qquad \textbf{Equation 7}$$

The ORNESS index evaluates the extent to which the indicators compensate each other. ORNESS equal to unity shows the highest proximity to a maximum operator indicating full compensative trade-offs (optimistic approach). Contrarily, ORNESS equal to zero indicates the highest propensity to a minimum operator reflecting perfect complementary behaviour (pessimistic approach). The special case of ORNESS equal to 0.5 determines the highest proximity to an arithmetic mean operator (additive approach) (Pinar et al., 2014). The ANDNESS index is a complement of the ORNESS ($ANDNESS + ORNESS = 1$), measuring the level of complementarity among the indicators (Belles-Sampera et al., 2014; Dujmović and Cordeliers, 2006; Pinar et al., 2014). The OWA operator controls the level of compensation by using a different order of weights. The order of weights corresponding to higher ORNESS levels indicates a higher degree of compensation and proximity to a maximum operator and vice versa. Since we are dealing with hazards, employing non-compensatory approaches (e.g. geometric mean used in original INFORM) are more plausible. Hence, we only consider the ANDNESS in the range of 0.5 to 1.

In order to evaluate how different weights distributions can affect OWA, different combinations of weights have been simulated following a linear distribution. To populate the weight configurations, we followed a quasi Monte Carlo approach (Marzi et al., 2019). The number of Monte Carlo simulation can be computed using $N = 2B(k + 1)$ where N is the number of runs in the Monte Carlo simulation, B stands for sample size (191 countries), and k is the number of parameters (7 natural hazard & exposure components) (Tate, 2012). Using the equation, 3056 runs are required to produce reliable measures. We simulated 3100 OWA weight configuration ordered by ORNESS measure.

In order to interpret the uncertainty analysis results for various OWA simulations, we follow the approach proposed by Poljansek et al. (2020) and Saisana and Saltelli (2008). To do so, we calculate the percentage of the OWA simulations that fall in the five different classes (very low to very high) of Natural category score of INFORM Risk Index. We then calculate the percentage of the match with the different classes (very low to very high) of Natural category score of INFORM Climate Change Risk Index (**Table 23** and **Table 24**). The numbers represent the frequency a country remains in the same class of Natural hazard category. The 5th and 95th percentiles of the simulations are considered to eliminate the extreme cases of compensation (full and non-compensatory trade-offs) (Lafortune et al., 2018; Saisana and Saltelli, 2008). The results show that there are more than 70 percent of correct matching countries for both cases suggesting that the index in these countries is robust and not strongly influenced by the final aggregation and weighting choice. The index in the remaining 30% of the countries fluctuates between risk classes (e.g., Netherlands and Eswatini) and any conclusion on the performance of these countries should be drawn with some caution.

The dominant source of the deviations arises from the degree of compensation among the indicators. Moving toward lower degrees of compensation (higher ANDNESS), the results tend towards the maximum risk. In contrary, having higher degrees of compensation (lower ANDNESS) shifts the results toward the average. For high-exposure countries (e.g., Philippines), underperformance among the indicators leads to higher scores with a low degree of compensation. Contrarily, the underperformance is relaxed when shifting toward the higher level of compensation and yields lower scores. For the countries exposed to few hazards (e.g. land locked countries with no coastal flooding), moving toward high compensation (average) will result in far lower values in compare to countries which face all types of hazard. The results depend also on the theoretical framework and data used but are for the majority of simulations independent of the methodological choices (weighting and aggregation).

Table 23. Probabilities of Natural hazard category scores under all tested combinations of weights – RCP8.5-SSP3 scenario in 2050, ordered from highest to lowest score.

INFORM Climate Change Risk Index Natural hazard category – RCP8.5-SSP3 2050															
	Natural	Class	Very Low	Low	Medium	High	Very High		Natural	Class	Very Low	Low	Medium	High	Very High
Bangladesh	8.9	Very high	0%	0%	0%	0%	100%	Niger	4.8	High	0%	0%	84%	13%	3%
Japan	8.9	Very high	0%	0%	0%	0%	100%	South Sudan	4.8	High	0%	0%	78%	18%	4%
Philippines	8.9	Very high	0%	0%	0%	0%	100%	United Arab Emirates	4.8	High	0%	0%	78%	19%	3%
India	8.7	Very high	0%	0%	0%	0%	100%	Burkina Faso	4.7	High	0%	0%	86%	11%	3%
Indonesia	8.6	Very high	0%	0%	0%	0%	100%	Chad	4.7	High	0%	0%	83%	13%	3%
China	8.4	Very high	0%	0%	0%	0%	100%	Congo	4.7	High	0%	0%	77%	20%	3%
Viet Nam	8.3	Very high	0%	0%	0%	0%	100%	Djibouti	4.7	High	0%	0%	10%	89%	1%
Myanmar	8.1	Very high	0%	0%	0%	0%	100%	Libya	4.7	High	0%	0%	77%	20%	3%
Mexico	7.9	Very high	0%	0%	0%	0%	100%	Mauritania	4.7	High	0%	0%	77%	20%	3%
Pakistan	7.9	Very high	0%	0%	0%	0%	100%	Vanuatu	4.7	High	0%	0%	47%	52%	1%
United States of America	7.8	Very high	0%	0%	0%	0%	100%	Togo	4.6	Medium	0%	0%	80%	17%	3%
Ecuador	7.5	Very high	0%	0%	0%	0%	100%	Trinidad & Tobago	4.6	Medium	0%	0%	50%	48%	2%
Thailand	7.5	Very high	0%	0%	0%	0%	100%	United Kingdom	4.5	Medium	0%	0%	77%	21%	2%
Dominican Republic	7.4	Very high	0%	0%	0%	0%	100%	Uzbekistan	4.5	Medium	0%	0%	86%	11%	3%
Peru	7.4	Very high	0%	0%	0%	10%	90%	Brunei Darussalam	4.4	Medium	0%	0%	85%	13%	3%
Madagascar	7.3	Very high	0%	0%	0%	0%	100%	Lebanon	4.4	Medium	0%	0%	84%	14%	2%
Colombia	7.2	Very high	0%	0%	0%	0%	100%	Slovenia	4.4	Medium	0%	0%	69%	30%	1%
Guatemala	7.2	Very high	0%	0%	0%	10%	90%	Zimbabwe	4.4	Medium	0%	0%	86%	12%	2%
Nicaragua	7.2	Very high	0%	0%	0%	0%	100%	Azerbaijan	4.3	Medium	0%	0%	86%	12%	2%
Egypt	7.1	Very high	0%	0%	0%	55%	45%	Romania	4.3	Medium	0%	0%	85%	12%	2%
El Salvador	7.1	Very high	0%	0%	0%	10%	90%	Burundi	4.2	Medium	0%	0%	84%	15%	2%
Honduras	7.1	Very high	0%	0%	0%	0%	100%	Jordan	4.2	Medium	0%	25%	65%	7%	3%
Mozambique	7.1	Very high	0%	0%	0%	10%	90%	Tajikistan	4.2	Medium	0%	10%	79%	10%	2%
Venezuela	7.1	Very high	0%	0%	0%	0%	100%	Antigua & Barbuda	4.1	Medium	0%	0%	87%	11%	1%
Iran	7	Very high	0%	0%	0%	70%	30%	Eritrea	4.1	Medium	0%	0%	88%	11%	1%
Papua New Guinea	7	Very high	0%	0%	0%	10%	90%	Israel	4.1	Medium	0%	0%	86%	12%	2%
Haiti	6.9	Very high	0%	0%	0%	10%	90%	Rwanda	4.1	Medium	0%	0%	85%	14%	1%
Korea Republic of	6.8	High	0%	0%	0%	82%	18%	Tonga	4.1	Medium	0%	0%	87%	12%	1%
Nigeria	6.8	High	0%	0%	0%	85%	15%	Georgia	4	Medium	0%	0%	87%	11%	1%
Chile	6.7	High	0%	0%	0%	86%	14%	Kazakhstan	4	Medium	0%	0%	89%	8%	2%
Costa Rica	6.7	High	0%	0%	0%	65%	35%	Montenegro	4	Medium	0%	0%	88%	12%	0%
Somalia	6.7	High	0%	0%	0%	71%	29%	Poland	4	Medium	0%	0%	89%	9%	2%
Malaysia	6.6	High	0%	0%	0%	63%	37%	Belgium	3.9	Medium	0%	0%	89%	10%	1%
Tanzania	6.6	High	0%	0%	0%	84%	16%	Bhutan	3.9	Medium	0%	0%	89%	11%	0%
Turkey	6.6	High	0%	0%	0%	85%	15%	Bulgaria	3.9	Medium	0%	0%	90%	8%	2%
Cambodia	6.5	High	0%	0%	0%	87%	13%	Cyprus	3.9	Medium	0%	0%	89%	10%	1%
Panama	6.5	High	0%	0%	0%	79%	21%	Armenia	3.8	Medium	0%	35%	57%	6%	2%
Senegal	6.4	High	0%	0%	0%	85%	15%	Kyrgyzstan	3.8	Medium	0%	10%	82%	7%	2%
Brazil	6.3	High	0%	0%	0%	91%	9%	Moldova Republic of	3.8	Medium	0%	0%	90%	8%	1%
Italy	6.3	High	0%	0%	0%	87%	13%	Palestine	3.8	Medium	0%	0%	91%	8%	2%
Cuba	6.1	High	0%	0%	0%	92%	8%	Paraguay	3.8	Medium	0%	10%	82%	7%	1%
Liberia	6.1	High	0%	0%	0%	91%	9%	Serbia	3.8	Medium	0%	0%	91%	7%	2%
Nepal	6.1	High	0%	0%	10%	83%	8%	Austria	3.7	Medium	0%	10%	82%	8%	1%
Tunisia	6.1	High	0%	0%	0%	91%	9%	Botswana	3.7	Medium	0%	10%	83%	6%	1%
Australia	6	High	0%	0%	0%	93%	7%	Namibia	3.7	Medium	0%	10%	82%	6%	1%
Canada	6	High	0%	0%	0%	94%	6%	North Macedonia	3.7	Medium	0%	10%	81%	8%	2%
Ghana	5.9	High	0%	0%	0%	92%	8%	Central African Republic	3.6	Medium	0%	10%	83%	6%	1%
Greece	5.9	High	0%	0%	0%	93%	7%	Kuwait	3.6	Medium	0%	10%	83%	6%	1%
Guinea	5.9	High	0%	0%	0%	93%	7%	Ukraine	3.6	Medium	0%	55%	38%	6%	2%
Jamaica	5.9	High	0%	0%	0%	94%	6%	Bosnia & Herzegovina	3.5	Medium	0%	10%	83%	7%	1%
Albania	5.8	High	0%	0%	0%	94%	6%	Comoros	3.5	Medium	0%	0%	99%	1%	0%
Algeria	5.8	High	0%	0%	0%	94%	6%	Dominica	3.5	Medium	0%	0%	93%	7%	0%
Congo DR	5.8	High	0%	0%	10%	84%	6%	Kiribati	3.5	Medium	0%	48%	46%	5%	1%
Iraq	5.8	High	0%	0%	10%	84%	6%	Turkmenistan	3.5	Medium	0%	78%	15%	4%	2%
Netherlands	5.7	High	0%	0%	50%	45%	5%	Hungary	3.4	Medium	0%	53%	40%	5%	1%
Russian Federation	5.7	High	0%	0%	0%	95%	5%	Slovakia	3.4	Medium	0%	10%	83%	6%	1%
Suriname	5.7	High	0%	0%	0%	94%	6%	Bahamas	3.3	Medium	0%	13%	81%	5%	1%
Afghanistan	5.6	High	0%	0%	54%	41%	5%	Equatorial Guinea	3.3	Medium	0%	45%	49%	5%	1%
Sri Lanka	5.6	High	0%	0%	0%	95%	5%	Samoa	3.3	Medium	0%	0%	94%	6%	0%
Korea DPR	5.5	High	0%	0%	0%	99%	1%	Uruguay	3.3	Medium	0%	0%	96%	4%	0%
Morocco	5.5	High	0%	0%	0%	95%	5%	Eswatini	3.2	Medium	0%	46%	49%	5%	0%
Spain	5.5	High	0%	0%	0%	95%	5%	Ireland	3.2	Medium	0%	0%	98%	2%	0%
Yemen	5.5	High	0%	0%	0%	95%	5%	Marshall Islands	3.1	Medium	0%	75%	20%	4%	1%
Cameroon	5.4	High	0%	0%	10%	85%	5%	Qatar	3.1	Medium	0%	79%	15%	4%	1%
France	5.4	High	0%	0%	0%	95%	5%	Liechtenstein	2.9	Medium	0%	79%	17%	4%	1%
Kenya	5.4	High	0%	0%	0%	97%	3%	Maldives	2.9	Medium	0%	82%	13%	4%	1%
Malawi	5.4	High	0%	0%	10%	85%	5%	Mongolia	2.9	Medium	0%	82%	13%	4%	1%
Timor-Leste	5.4	High	0%	0%	0%	97%	3%	Sweden	2.9	Medium	0%	48%	49%	4%	0%
Angola	5.3	High	0%	0%	28%	67%	5%	Switzerland	2.9	Medium	0%	63%	33%	4%	0%
Saudi Arabia	5.3	High	0%	0%	71%	25%	5%	Barbados	2.8	Medium	0%	10%	89%	2%	0%
Argentina	5.2	High	0%	0%	0%	97%	3%	Czech Republic	2.7	Low	0%	84%	12%	4%	1%
Benin	5.2	High	0%	0%	36%	60%	4%	Denmark	2.7	Low	0%	75%	22%	3%	0%
Fiji	5.2	High	0%	0%	0%	100%	0%	Palau	2.7	Low	0%	65%	33%	2%	0%
Oman	5.2	High	0%	0%	10%	87%	3%	Iceland	2.6	Low	0%	40%	59%	2%	0%
Sierra Leone	5.2	High	0%	0%	0%	97%	3%	Norway	2.6	Low	0%	65%	34%	1%	0%
Syria	5.2	High	0%	0%	73%	23%	4%	Lithuania	2.5	Low	0%	81%	16%	3%	0%
Gabon	5.1	High	0%	0%	10%	86%	4%	Saint Kitts and Nevis	2.5	Low	0%	85%	11%	3%	0%
Solomon Islands	5.1	High	0%	0%	0%	98%	2%	Seychelles	2.5	Low	0%	86%	11%	3%	1%
South Africa	5.1	High	0%	0%	53%	44%	4%	Micronesia	2.4	Low	0%	86%	11%	3%	0%
Uganda	5.1	High	0%	0%	60%	36%	4%	Belarus	2.3	Low	13%	76%	8%	3%	0%
Bolivia	5	High	0%	0%	20%	77%	4%	Cabo Verde	2.3	Low	0%	85%	13%	2%	0%
C"te d'Ivoire	5	High	0%	0%	48%	48%	4%	Finland	2.3	Low	0%	86%	12%	2%	0%
Lao PDR	5	High	0%	0%	36%	61%	4%	Lesotho	2.2	Low	13%	76%	8%	3%	0%
Mali	5	High	0%	0%	78%	18%	3%	Latvia	2.1	Low	0%	89%	9%	1%	0%
Sudan	5	High	0%	0%	53%	44%	3%	Saint Vincent & Grenadines	2.1	Low	0%	89%	11%	1%	0%
Zambia	5	High	0%	0%	76%	20%	4%	Singapore	1.9	Low	0%	92%	8%	0%	0%
Belize	4.9	High	0%	0%	0%	100%	0%	Saint Lucia	1.8	Low	10%	83%	7%	1%	0%
Croatia	4.9	High	0%	0%	1%	98%	1%	Estonia	1.5	Low	59%	36%	5%	0%	0%
Ethiopia	4.9	High	0%	0%	35%	62%	3%	Luxembourg	1.5	Low	81%	13%	4%	2%	0%
Gambia	4.9	High	0%	0%	10%	89%	1%	Tuvalu	1.5	Low	83%	11%	4%	2%	0%
Germany	4.9	High	0%	0%	16%	81%	3%	Grenada	1.4	Low	10%	89%	1%	0%	0%
Mauritius	4.9	High	0%	0%	65%	31%	4%	Malta	1.3	Low	84%	10%	4%	2%	0%
New Zealand	4.9	High	0%	0%	0%	100%	0%	Nauru	1.3	Low	85%	10%	4%	2%	0%
Portugal	4.9	High	0%	0%	10%	88%	2%	Bahrain	1.1	Very low	85%	11%	4%	1%	0%
Guinea-Bissau	4.8	High	0%	0%	10%	89%	2%	Sao Tome & Principe	1.1	Very low	79%	18%	2%	0%	0%
Guyana	4.8	High	0%	0%	10%	89%	1%								

Probability between 5 and 15% | Probability between 15 and 30% | Probability between 30 and 50% | Probability between 50 and 70% | Probability greater than 70%

Table 24. Probabilities of Natural hazard category scores under all tested combinations of weights – RCP8.5-SSP3 scenario in 2080, ordered from highest to lowest score.

INFORM Climate Change Risk Index Natural hazard category – RCP8.5-SSP3 2080	Natural	Class	Very Low	Low	Medium	High	Very High		Natural	Class	Very Low	Low	Medium	High	Very High
Philippines	9	Very high	0%	0%	0%	0%	100%	South Sudan	5.1	High	0%	0%	64%	32%	4%
Bangladesh	8.9	Very high	0%	0%	0%	0%	100%	United Arab Emirates	5.1	High	0%	0%	75%	21%	4%
Japan	8.9	Very high	0%	0%	0%	0%	100%	Congo	5	High	0%	0%	47%	49%	4%
India	8.7	Very high	0%	0%	0%	0%	100%	Guinea-Bissau	5	High	0%	0%	10%	88%	3%
Indonesia	8.7	Very high	0%	0%	0%	0%	100%	Lao PDR	5	High	0%	0%	10%	87%	3%
China	8.5	Very high	0%	0%	0%	0%	100%	Mauritius	5	High	0%	0%	55%	41%	4%
Myanmar	8.4	Very high	0%	0%	0%	0%	100%	Uzbekistan	5	High	0%	0%	84%	12%	4%
Viet Nam	8.4	Very high	0%	0%	0%	0%	100%	Burkina Faso	4.9	High	0%	0%	83%	14%	3%
Mexico	8.1	Very high	0%	0%	0%	0%	100%	Chad	4.9	High	0%	0%	79%	18%	3%
Pakistan	8.1	Very high	0%	0%	0%	0%	100%	Mauritania	4.9	High	0%	0%	78%	18%	4%
United States of America	7.9	Very high	0%	0%	0%	0%	100%	Slovenia	4.9	High	0%	0%	56%	40%	3%
Dominican Republic	7.7	Very high	0%	0%	0%	0%	100%	Israel	4.8	High	0%	0%	71%	26%	3%
Ecuador	7.7	Very high	0%	0%	0%	0%	100%	Lebanon	4.8	High	0%	0%	80%	17%	3%
Guatemala	7.6	Very high	0%	0%	0%	0%	100%	Niger	4.8	High	0%	0%	81%	16%	3%
Madagascar	7.6	Very high	0%	0%	0%	0%	100%	Romania	4.8	High	0%	0%	82%	15%	4%
Peru	7.6	Very high	0%	0%	0%	0%	100%	Tajikistan	4.8	High	0%	0%	82%	14%	3%
Thailand	7.6	Very high	0%	0%	0%	0%	100%	Togo	4.8	High	0%	0%	75%	22%	3%
Colombia	7.5	Very high	0%	0%	0%	0%	100%	Vanuatu	4.8	High	0%	0%	10%	89%	1%
Egypt	7.5	Very high	0%	0%	0%	10%	90%	Zimbabwe	4.8	High	0%	0%	82%	15%	3%
El Salvador	7.5	Very high	0%	0%	0%	0%	100%	Brunei Darussalam	4.7	High	0%	0%	78%	19%	3%
Mozambique	7.5	Very high	0%	0%	0%	0%	100%	Eritrea	4.6	Medium	0%	0%	79%	18%	3%
Honduras	7.4	Very high	0%	0%	0%	0%	100%	Kazakhstan	4.6	Medium	0%	0%	87%	10%	3%
Nicaragua	7.4	Very high	0%	0%	0%	0%	100%	Montenegro	4.6	Medium	0%	0%	78%	20%	3%
Venezuela	7.3	Very high	0%	0%	0%	0%	100%	Trinidad & Tobago	4.6	Medium	0%	0%	54%	44%	2%
Haiti	7.2	Very high	0%	0%	0%	0%	100%	United Kingdom	4.6	Medium	0%	0%	71%	26%	2%
Iran	7.2	Very high	0%	0%	0%	48%	52%	Azerbaijan	4.5	Medium	0%	0%	83%	15%	3%
Papua New Guinea	7.1	Very high	0%	0%	0%	10%	90%	Jordan	4.5	Medium	0%	10%	79%	8%	3%
Costa Rica	7	Very high	0%	0%	0%	10%	90%	Rwanda	4.5	Medium	0%	0%	77%	21%	2%
Malaysia	7	Very high	0%	0%	0%	10%	90%	Belgium	4.4	Medium	0%	0%	82%	16%	2%
Somalia	7	Very high	0%	0%	0%	10%	90%	Burundi	4.4	Medium	0%	0%	80%	19%	2%
Tanzania	7	Very high	0%	0%	0%	48%	52%	Georgia	4.4	Medium	0%	0%	83%	15%	3%
Chile	6.9	Very high	0%	0%	0%	82%	18%	Kyrgyzstan	4.4	Medium	0%	0%	87%	10%	3%
Nigeria	6.9	Very high	0%	0%	0%	84%	16%	Moldova Republic of	4.4	Medium	0%	0%	85%	13%	3%
Turkey	6.9	Very high	0%	0%	0%	77%	23%	Poland	4.4	Medium	0%	0%	85%	12%	3%
Panama	6.8	High	0%	0%	0%	10%	90%	Bulgaria	4.3	Medium	0%	0%	87%	10%	3%
Senegal	6.8	High	0%	0%	0%	75%	25%	Palestine	4.3	Medium	0%	0%	88%	9%	3%
Cambodia	6.7	High	0%	0%	0%	80%	20%	Serbia	4.3	Medium	0%	0%	88%	9%	3%
Italy	6.6	High	0%	0%	0%	80%	20%	North Macedonia	4.2	Medium	0%	0%	88%	9%	3%
Korea Republic of	6.6	High	0%	0%	0%	87%	13%	Armenia	4.1	Medium	0%	10%	80%	8%	2%
Brazil	6.5	High	0%	0%	0%	88%	12%	Austria	4.1	Medium	0%	0%	89%	9%	2%
Canada	6.4	High	0%	0%	0%	86%	14%	Bosnia & Herzegovina	4.1	Medium	0%	0%	88%	9%	2%
Tunisia	6.4	High	0%	0%	0%	88%	12%	Namibia	4.1	Medium	0%	10%	80%	8%	2%
Australia	6.3	High	0%	0%	0%	87%	13%	Tonga	4.1	Medium	0%	0%	86%	13%	1%
Cuba	6.3	High	0%	0%	0%	89%	11%	Botswana	4	Medium	0%	11%	80%	7%	2%
Liberia	6.3	High	0%	0%	0%	89%	11%	Kuwait	4	Medium	0%	10%	80%	9%	2%
Albania	6.2	High	0%	0%	0%	89%	11%	Paraguay	4	Medium	0%	10%	81%	8%	1%
Ghana	6.2	High	0%	0%	0%	89%	11%	Ukraine	4	Medium	0%	32%	59%	7%	3%
Greece	6.2	High	0%	0%	0%	90%	10%	Comoros	3.8	Medium	0%	0%	97%	3%	0%
Guinea	6.2	High	0%	0%	0%	89%	11%	Hungary	3.8	Medium	0%	52%	40%	6%	2%
Iraq	6.2	High	0%	0%	0%	91%	9%	Slovakia	3.8	Medium	0%	10%	81%	7%	2%
Jamaica	6.2	High	0%	0%	0%	91%	9%	Bhutan	3.7	Medium	0%	0%	91%	9%	0%
Nepal	6.2	High	0%	0%	0%	92%	8%	Central African Republic	3.7	Medium	0%	10%	82%	7%	1%
Suriname	6.2	High	0%	0%	0%	91%	9%	Kiribati	3.6	Medium	0%	43%	50%	5%	1%
Congo DR	6.1	High	0%	0%	0%	92%	8%	Qatar	3.6	Medium	0%	69%	24%	5%	2%
Algeria	6	High	0%	0%	0%	93%	7%	Turkmenistan	3.6	Medium	0%	76%	17%	5%	2%
Spain	6	High	0%	0%	0%	92%	8%	Dominica	3.5	Medium	0%	3%	90%	7%	0%
Yemen	6	High	0%	0%	0%	92%	8%	Eswatini	3.5	Medium	0%	10%	84%	6%	1%
Afghanistan	5.9	High	0%	0%	15%	80%	6%	Mongolia	3.5	Medium	0%	76%	18%	5%	2%
France	5.9	High	0%	0%	0%	93%	7%	Uruguay	3.5	Medium	0%	0%	94%	6%	0%
Malawi	5.9	High	0%	0%	0%	93%	7%	Bahamas	3.4	Medium	0%	10%	84%	6%	1%
Netherlands	5.9	High	0%	0%	10%	85%	6%	Equatorial Guinea	3.4	Medium	0%	10%	84%	6%	1%
Russian Federation	5.9	High	0%	0%	0%	94%	6%	Ireland	3.4	Medium	0%	0%	96%	4%	0%
Kenya	5.8	High	0%	0%	0%	94%	6%	Samoa	3.4	Medium	0%	0%	94%	6%	0%
Morocco	5.8	High	0%	0%	0%	93%	7%	Marshall Islands	3.2	Medium	0%	71%	23%	4%	1%
Timor-Leste	5.8	High	0%	0%	0%	96%	4%	Switzerland	3.2	Medium	0%	63%	31%	5%	1%
Korea DPR	5.7	High	0%	0%	0%	98%	2%	Czech Republic	3.1	Medium	0%	80%	15%	4%	2%
Sri Lanka	5.7	High	0%	0%	0%	94%	6%	Sweden	3.1	Medium	0%	10%	85%	5%	0%
Angola	5.6	High	0%	0%	10%	85%	5%	Liechtenstein	3	Medium	0%	69%	26%	4%	1%
Argentina	5.6	High	0%	0%	0%	94%	6%	Maldives	3	Medium	0%	81%	13%	4%	1%
Cameroon	5.6	High	0%	0%	10%	85%	6%	Denmark	2.9	Medium	0%	57%	38%	4%	0%
Benin	5.5	High	0%	0%	10%	85%	5%	Lithuania	2.9	Medium	0%	60%	36%	4%	0%
Bolivia	5.5	High	0%	0%	10%	85%	5%	Barbados	2.8	Medium	0%	10%	89%	2%	0%
Oman	5.5	High	0%	0%	10%	85%	5%	Latvia	2.8	Medium	0%	10%	88%	2%	0%
Sierra Leone	5.5	High	0%	0%	0%	96%	4%	Antigua & Barbuda	2.7	Low	0%	81%	15%	4%	1%
South Africa	5.5	High	0%	0%	31%	64%	5%	Lesotho	2.7	Low	0%	84%	11%	4%	1%
Fiji	5.4	High	0%	0%	0%	100%	0%	Palau	2.7	Low	0%	59%	39%	3%	0%
Gambia	5.4	High	0%	0%	0%	96%	4%	Belarus	2.6	Low	0%	85%	10%	3%	1%
Saudi Arabia	5.4	High	0%	0%	62%	33%	5%	Finland	2.6	Low	0%	72%	25%	3%	0%
Sudan	5.4	High	0%	0%	29%	66%	5%	Iceland	2.6	Low	0%	59%	39%	1%	0%
Syria	5.4	High	0%	0%	67%	29%	5%	Norway	2.6	Low	0%	61%	37%	2%	0%
Uganda	5.4	High	0%	0%	10%	85%	5%	Saint Kitts and Nevis	2.5	Low	0%	85%	11%	3%	1%
Belize	5.3	High	0%	0%	0%	99%	1%	Seychelles	2.5	Low	0%	85%	11%	3%	1%
C“te d'Ivoire	5.3	High	0%	0%	10%	86%	4%	Cabo Verde	2.4	Low	0%	82%	15%	2%	0%
Ethiopia	5.3	High	0%	0%	10%	86%	4%	Micronesia	2.4	Low	0%	85%	11%	3%	0%
Gabon	5.3	High	0%	0%	10%	86%	4%	Saint Vincent & Grenadines	2.1	Low	0%	89%	10%	1%	0%
Germany	5.3	High	0%	0%	10%	86%	4%	Bahrain	2	Low	78%	14%	5%	2%	1%
Mali	5.3	High	0%	0%	76%	20%	4%	Luxembourg	1.9	Low	77%	16%	5%	2%	0%
New Zealand	5.3	High	0%	0%	0%	98%	2%	Singapore	1.9	Low	0%	92%	8%	0%	0%
Solomon Islands	5.3	High	0%	0%	0%	98%	2%	Estonia	1.8	Low	0%	93%	7%	1%	0%
Zambia	5.3	High	0%	0%	57%	39%	4%	Saint Lucia	1.8	Low	10%	83%	7%	1%	0%
Croatia	5.2	High	0%	0%	0%	97%	3%	Tuvalu	1.5	Low	83%	11%	4%	2%	0%
Djibouti	5.2	High	0%	0%	0%	98%	2%	Grenada	1.4	Low	10%	89%	2%	0%	0%
Portugal	5.2	High	0%	0%	10%	86%	4%	Malta	1.4	Low	83%	12%	4%	2%	0%
Cyprus	5.1	High	0%	0%	10%	87%	4%	Nauru	1.3	Low	85%	10%	4%	2%	0%
Guyana	5.1	High	0%	0%	10%	88%	3%	Sao Tome & Principe	1.2	Very low	78%	19%	3%	0%	0%
Libya	5.1	High	0%	0%	69%	26%	4%								

Probability between 5 and 15% | Probability between 15 and 30% | Probability between 30 and 50% | Probability between 50 and 70% | Probability greater than 70%

7 Interpretation of the INFORM Climate Change Risk Index results

7.1 Climate-related impacts on exposed population

7.1.1 Population projections

The population projections in 2050 and 2080 for considered SSPs are shown in **Figure 13**, Annex 3 and Annex 20. By the middle of the century, world population is projected to increase from 7.3 billion in 2015 to the range between 9.8 billion (34% or 2.5 billion) under SSP3, and 8.3 billion (14% or 1 billion) under SSP1. By 2080, the range expands with the SSP3 reaching 11.4 billion (57% increase) and SSP1 falling to 7.7 billion (6.3% increase). SSP2 projections follow a medium path with 9 billion in 2050 (23% increase) and 9.2 billion in 2080 (26% increase). SSP trajectories are approximately similar to SSP1 in 2050 (15% increase or 1.1 billion), and slightly higher in 2080 (10% or 8 billion). By the middle of the century, the largest population increases are projected in Africa (95% or 1.1 billion) and Asia (27% or 1.2), and the smallest in Europe (-9% or -67 million) under SSP3. Americas population growth span between 12% (122 million) under SSP1 and 21% (213 million). Oceania and Europe show different growth patterns compared to other three continents with largest increase under SSP5 with 58% (22 million) and 13% (96 million) respectively. By 2080, the trajectories continue to grow in the same manner, except for Asia where the growth rates fall dramatically under SSP1 and SSP5 from 6.8% to -8.7% (300 million to -380 million) and 6.6% to -8.8 (289 million to -386 million).

Figure 13. Population projections in 2050 and 2080 based on four Shared Socioeconomic Pathways. The bars indicate the additional population to the baseline (GHSL 2015) for each scenario. SSPs include SSP1 (Sustainability - low challenges to mitigation and adaptation), SSP2 (Middle of the road - medium challenges to mitigation and adaptation), SSP3 (Regional rivalry - high challenges to mitigation and adaptation, SSP5 (Fossil fuel development - high challenges to mitigation with low challenges to adaptation).

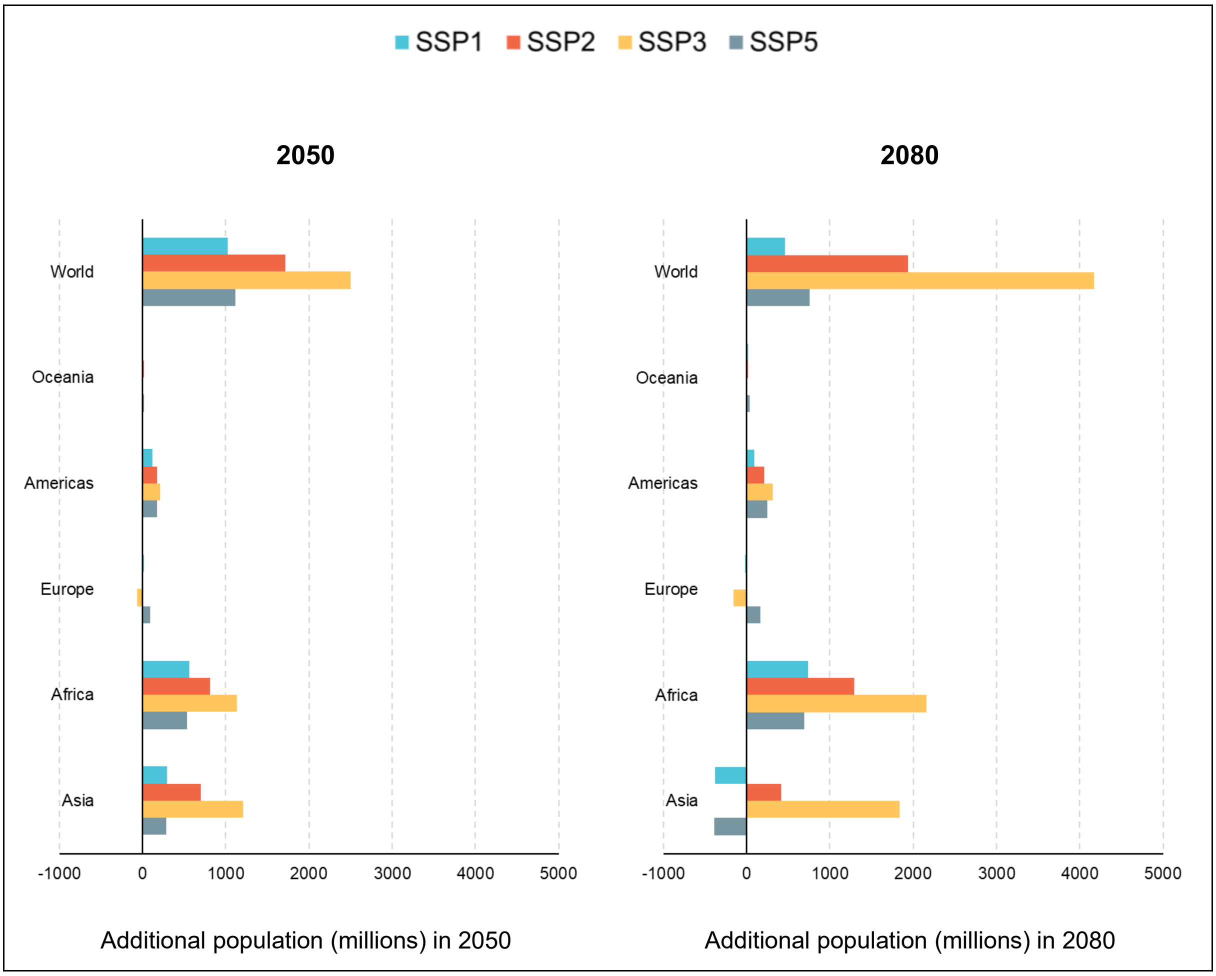

Source: Authors

7.1.2 River Flood

The river flood projections in 2050 and 2080 for considered RCP-SSP combinations are shown in **Figure 14** and Annex 4. By the middle of the century, global annual exposure to river floods is projected to increase from 206 million for the historical period to the range between 321 million (56% or 115 million) under RCP8.5-SSP3, and 261 million (27% or 56 million) under RCP4.5-SSP1. Exposure under SSP2 follow a medium path with 278 million (35% increase) and 300 million (45% increase) under RCP4.5 and RCP8.5 respectively. RCP8.5-SSP5 trajectories with 282 million exposed population (37% increase) are slightly higher than RCP4.5 combinations (RCP4.5-SSP1 and RCP4.5-SSP2), and lower than RCP8.5-SSP2. With no population growth, the exposure is projected to increase by 14% (29 million) and 22% (46 million) under moderate (RCP4.5) and high (RCP8.5) concentration pathways. This suggests that the population growth under SSPs has a considerably larger effect on the increase of global river flood exposure rather than climate change.

Regionally, Asia experiences the largest projected absolute exposed population to river floods in mid-century with the range between 186 million (29% or 42 million increase) and 235 million (63% or 91 million increase) under RCP4.5-SSP1 and RCP8.5-SSP3 respectively. Africa, however, faces the largest percent change (91%) under RCP8.5-SSP3. In Europe, the exposure to river floods is strictly related to population changes, where it falls drastically under RCP8.5-SSP3 (-10%) and increase by 17% under RCP8.5-SSP5.

Figure 14. The projected people exposed to river floods in 2050 and 2080 stratified by emissions and socioeconomic scenario combination. The bars indicate the projected additional people for each scenario relative to the baseline (ensemble mean of 1971-1999 historical flood hazard and GHSL 2015 population layer). SSPs include SSP1 (Sustainability - low challenges to mitigation and adaptation), SSP2 (Middle of the road - medium challenges to mitigation and adaptation), SSP3 (Regional rivalry - high challenges to mitigation and adaptation, SSP5 (Fossil fuel development - high challenges to mitigation with low challenges to adaptation). RCP=representative concentration pathways, SSP=shared socioeconomic pathways, GHSL=Global Human Settlement layer 2015.

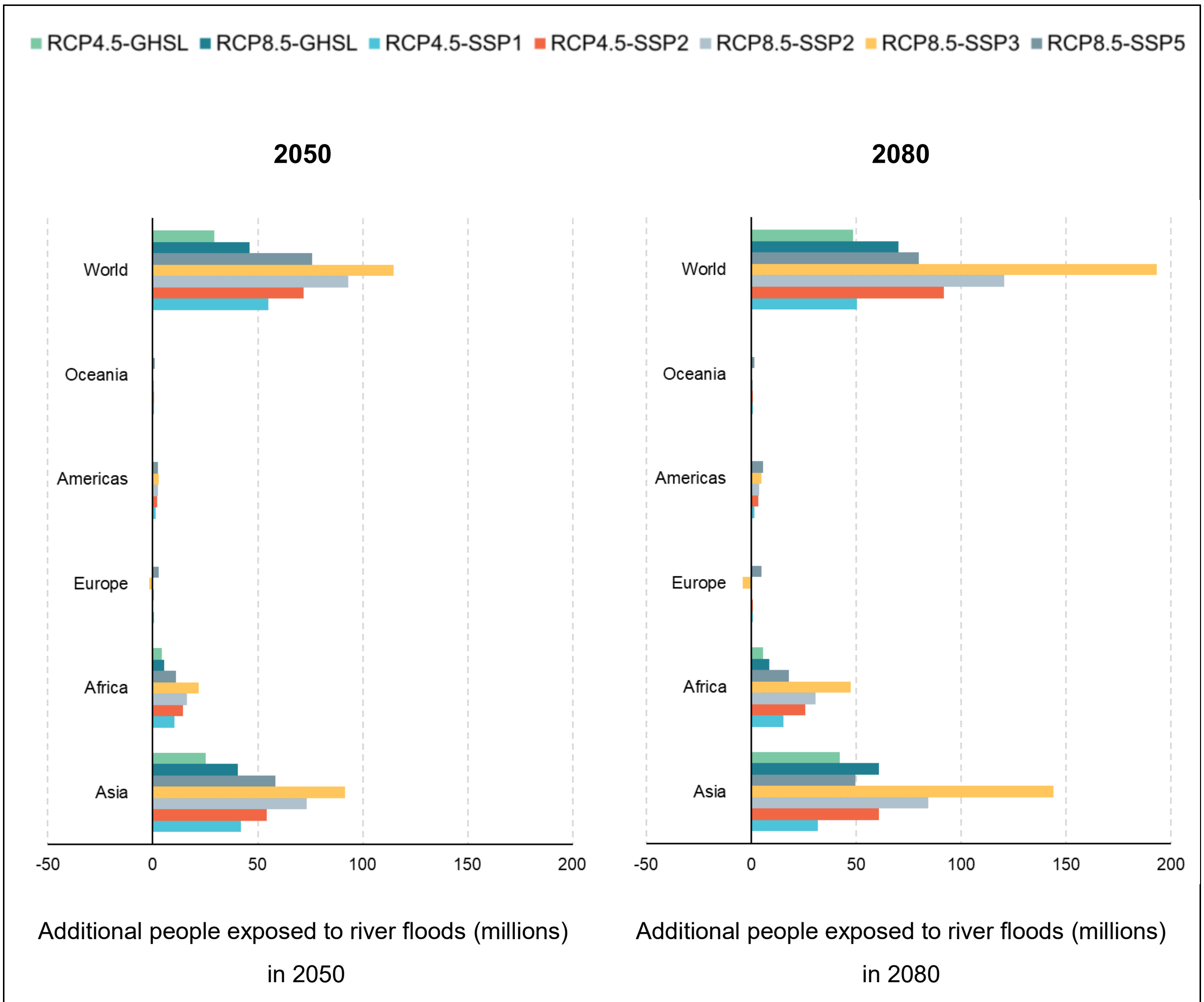

Source: Authors

By 2080, the global exposure range expands with the RCP8.5-SSP3 reaching 400 million (94% increase), and RCP4.5-SSP1 falling to 257 million (24% increase) - slightly lower than exposure in mid-century. Under constant population scenario, the exposure to river floods is projected to increase by 23% (48 million) and 34% (70 million) under moderate (RCP4.5) and high (RCP8.5) concentration pathways, suggesting relatively higher sensitivity to population changes rather than climate change under high emission scenario.

The regional trajectories continue to grow in the same manner as for the mid-century, except for Asia and Americas. In Asia the exposure growth rates fall under RCP4.5-SSP1 and RCP8.5-SSP5 from 29% to 22% (42 million to 32 million) and 40% to 34% (58 million to 49 million). In both cases, the exposure is lower than constant population scenarios, showing the extent the negative population growth in hazard prone areas counterbalances the climate change. In the case of Americas, the largest exposure growth occurs under RCP8.5-SSP5 (27% increase) in contrast to trajectories in 2050 where the largest changes are found under RCP8.5-SSP3 (14% vs 12%).

EM-DAT observations suggest similar regional flood exposure patterns for historical data (CRED, 2020). Accordingly, flood exposure is more frequent in Asia and Africa than other continents. In the period between 2000 and 2019, 1.5 billion people has been affected by floods in Asia (especially in China, India and Pakistan), accounted for 93% of global affected population. The projected results are comparable to other global impact studies (Farinosi et al., 2020; Arnell et al., 2019). Farinosi et al. (2020) and Arnell et al. (2019) find that the greatest increase in river flood frequency occurs is in Asia (especially south and south east Asia) and Africa, with the largest increase in exposure in Asia under SSP3 scenario. While Europe will face relatively small change with low forcings, and frequency could decrease depending on the population scenario.

7.1.3 Coastal Flood

The coastal flood projections in 2050 and 2080 for considered RCP-SSP combinations are shown in **Figure 15** and Annex 5. By the middle of the century, coastal flood exposure is globally projected to annually increase from 32 million for the historical period to the range between 74 million (131% or 41 million) under RCP8.5-SSP3, and 63 million (99% or 31 million) under RCP4.5-SSP1. Exposure under SSP2 follow a medium path with 67 million (111% increase) and 70 million (118% increase) under RCP4.5 and RCP8.5 respectively. RCP8.5-SSP5 trajectories with 66 million exposed population (107%) are slightly higher than RCP4.5-SSP1, and lower than RCP4.5-SSP2 and RCP8.5-SSP2. With no population growth, the exposure is projected to increase by 44% (14 million) and 49% (15 million) under moderate (RCP4.5) and high (RCP8.5) concentration pathways. Consistent with river floods, population growth under SSPs has a relatively larger effect on the increase of global coastal flood exposure rather than climate change.

The largest projected absolute exposed population to coastal floods in mid-century is found in Asia with the range between 49 million (88% or 23 million increase) and 59 million (125% or 33 million increase) under RCP4.5-SSP1 and RCP8.5-SSP3 respectively. Africa experiences the largest change (6.5 times more) under RCP8.5-SSP3. Contrary to river floods, exposure to coastal floods in Europe increases under all scenarios with the largest increase for RCP8.5-SSP5 (118% increase).

By 2080, the global exposure range expands between 117 million (267% increase - 85 million) under RCP8.5-SSP3, and 79 million (150% increase – 48 million) under RCP4.5-SSP1. Under constant population scenario, the exposure to coastal flood is projected to increase by 108% (34 million) and 133% (42 million) under moderate (RCP4.5) and high (RCP8.5) concentration pathways in 2080, suggesting a balanced impacts from climate and population changes at global scale. The projections under RCP8.5-SSP5 (59 million increase) and RCP4.5-SSP1 (48 million increase) are larger than those associated with "no population growth" scenarios under RCP8.5 (42 million increase) and RCP4.5 (34 million increase) respectively.

The regional trajectories continue to grow toward the end of the century in the same manner as for the mid-century. In Asia, the exposure growth rates under RCP4.5-SSP1 and RCP8.5-SSP5 are slightly higher than constant population scenarios which are not consistent with the total population changes. According to Merkens et al. (2016), SSP1 and SSP5 indicate larger population growth rates along the coasts by the end of century. Therefore, the population changes in the coastal zones tend to be greater than the total population changes in the country.

EM-DAT observations show that Asia is particularly affected by frequent storms, especially in the southern and south eastern regions, which account for 21% of the total number of storms and 79% of people affected by storms (CRED, 2020; UNISDR, 2015d). Recent global impact studies confirm that Asia, especially South Asia is projected to experience the largest change and population exposed to coastal flooding (Arnell et al., 2019; Kirezci et al., 2020). The estimates of the annual population exposed in the mid-21st century under RCP8.5-SSP3 and RCP8.5-SSP5 are comparable to those from (Marzi et al., 2021) calculated based on JRC LISFLOOD-FP (Vousdoukas et al., 2018) model (72 million and 70 million respectively).

Figure 15. The projected people exposed to coastal flood in 2050 and 2080 stratified by emissions and socioeconomic scenario combination. The bars indicate the projected additional people for each scenario relative to the baseline (ensemble mean of 1979–2014 historical coastal flood hazard and GHSL 2015 population layer). SSPs include SSP1 (Sustainability - low challenges to mitigation and adaptation), SSP2 (Middle of the road - medium challenges to mitigation and adaptation), SSP3 (Regional rivalry - high challenges to mitigation and adaptation, SSP5 (Fossil fuel development - high challenges to mitigation with low challenges to adaptation). RCP=representative concentration pathways, SSP=shared socioeconomic pathways, GHSL=Global Human Settlement layer 2015.

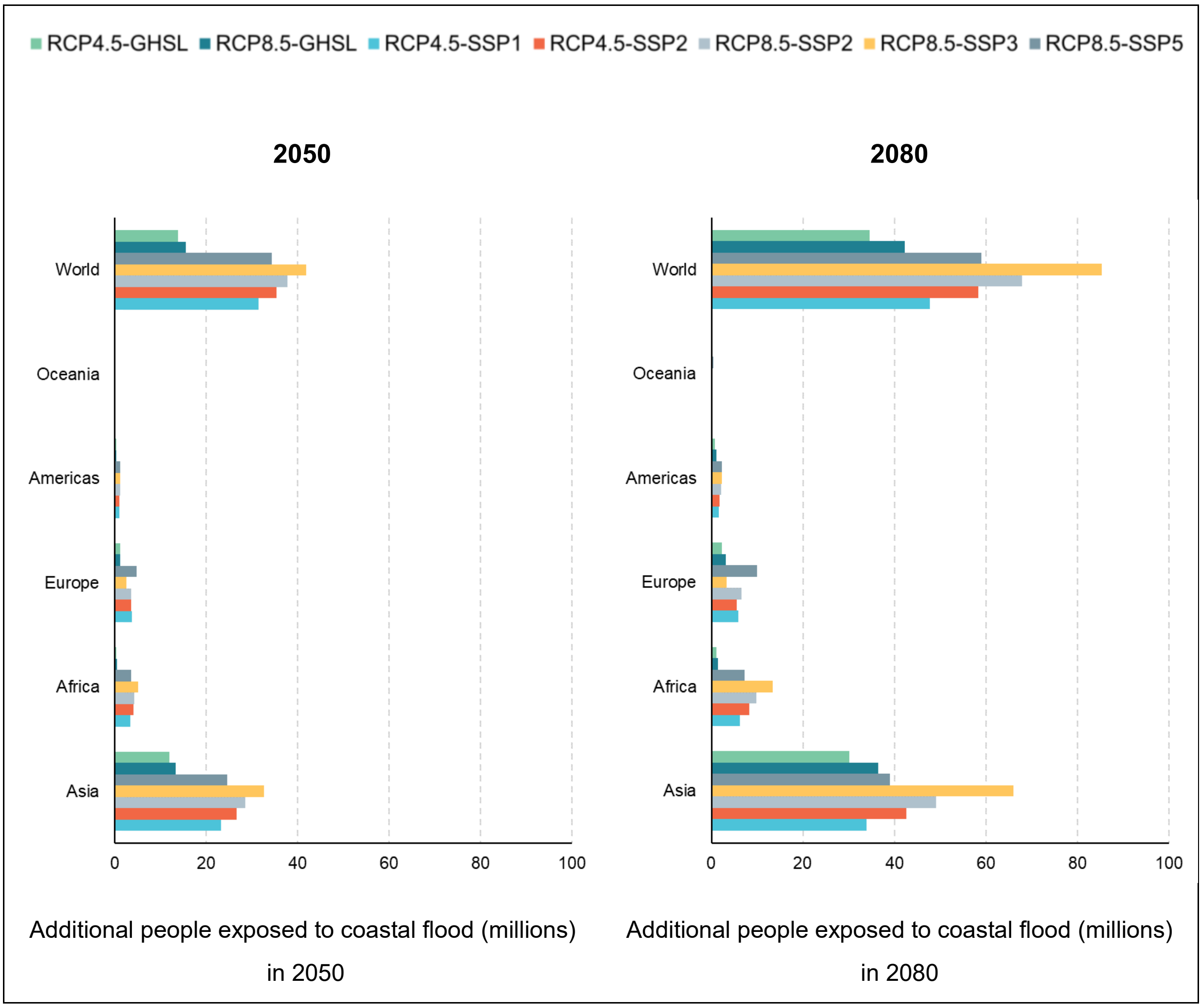

Source: Authors

7.1.4 Drought

Severe and extreme drought projections in 2050 and 2080 for considered RCP-SSP combinations are shown in **Figure 16** and Annex 6. Exposure to severe and extreme drought in the mid-21st century is globally projected to increase from 435 million for the historical period to the range between 1.6 billion (277% or 1.2 billion) under RCP8.5-SSP3, and 1.1 billion (173% or 753 million) under RCP4.5-SSP1. Exposure trajectories under SSP2 follow an intermediate path between upper and lower bounds with 1.2 billion (197% increase) and 1.5 billion (246% increase) under RCP4.5 and RCP8.5 respectively. RCP8.5-SSP5 trajectories with 1.4 billion exposed population (222%) are higher than RCP4.5-SSP1 and RCP4.5-SSP2, and lower than RCP8.5-SSP2. Considering no population growth, the exposure is projected to increase by 128% (556 million) and 168% (729 million) under moderate (RCP4.5) and high (RCP8.5) concentration pathways. In contrary to floods, climate change has a considerably larger effect on the increase of global drought exposure rather than population growth under SSPs by mid-century. Accordingly, the general patterns tend to remain similar due to the strong climate change signal, but the population differences between the scenarios tend to alter the intensity of the exposure.

Figure 16. The projected people exposed to drought in 2050 and 2080 stratified by emissions and socioeconomic scenario combination. The bars indicate the projected additional people for each scenario relative to the baseline (ensemble mean of 1976-2005 historical SPEI and GHSL 2015 population layer). SSPs include SSP1 (Sustainability - low challenges to mitigation and adaptation), SSP2 (Middle of the road - medium challenges to mitigation and adaptation), SSP3 (Regional rivalry - high challenges to mitigation and adaptation, SSP5 (Fossil fuel development - high challenges to mitigation with low challenges to adaptation). RCP=representative concentration pathways, SSP=shared socioeconomic pathways, GHSL=Global Human Settlement layer 2015.

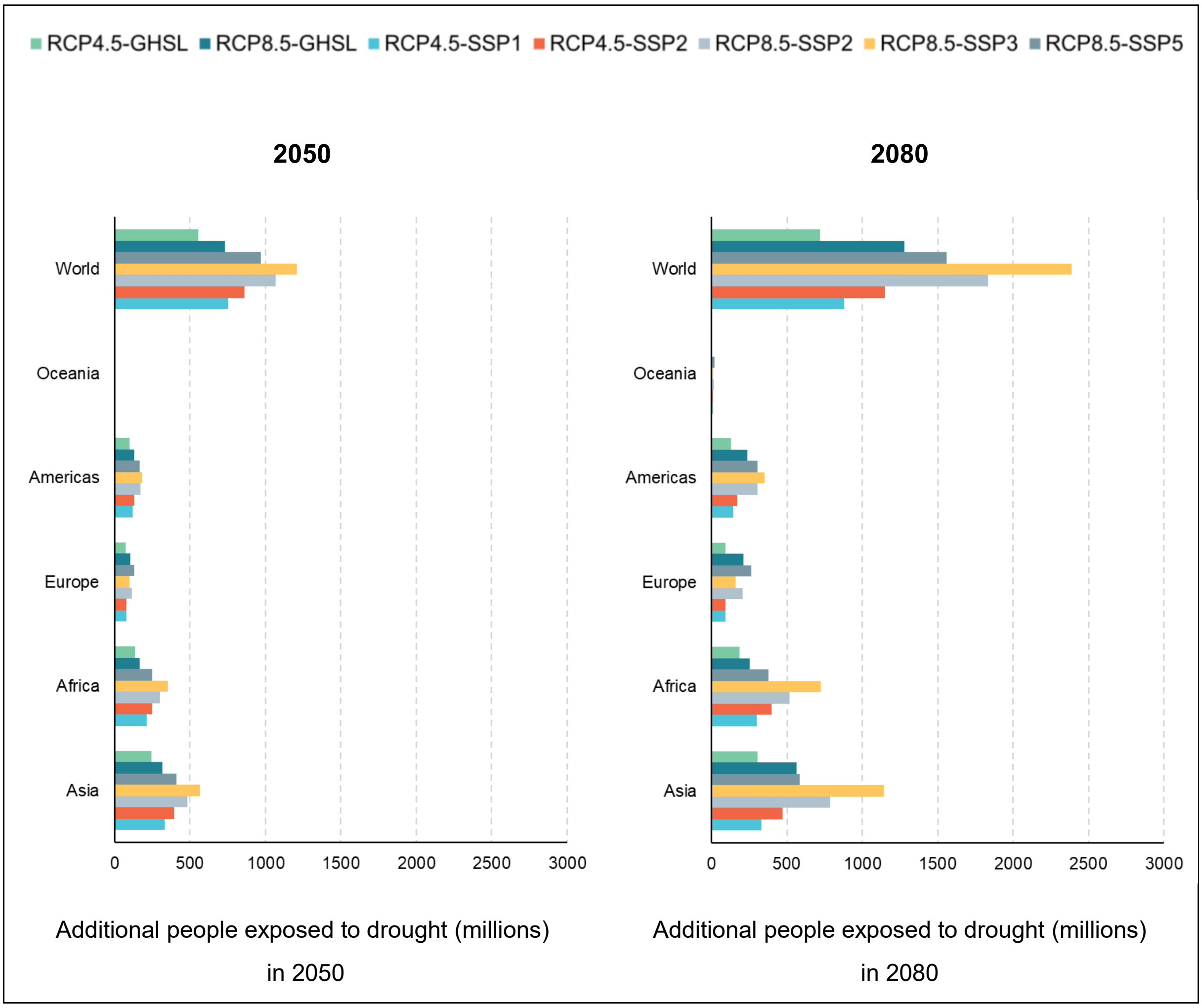

Source: Authors

The largest absolute exposed population to sever and extreme drought in mid-century is projected in Asia in a range between 588 million (131% or 334 million increase) and 822 million (224% or 568 million increase) under RCP4.5-SSP1 and RCP8.5-SSP3 respectively. The second and third largest absolute exposure is projected in Africa and Americas with the highest exposure under RCP8.5-SSP3 (429 million and 241 million respectively). The largest percent increases in population exposed are projected in Africa (485%) under RCP8.5-SSP3, and Oceania (496%) under RCP8.5-SSP5. Consistent with the population trends, Europe will experience largest exposure and changes under RCP8.5-SSP5 with 174 million exposed population (283% or 129 million increase)

By 2080, the global exposure range expands between 2.8 billion (549% increase) under RCP8.5-SSP3, and 1.3 billion (202% increase) under RCP4.5-SSP1. Under constant population scenario, drought exposure is projected to increase by 165% (719 million) and 294% (1.2 billion) under moderate (RCP4.5) and high (RCP8.5) concentration pathways in 2080, suggesting higher sensitivity to climate change rather than population changes at global scale by the end of century. The regional trajectories continue to grow toward the end of the century in the same manner as for the mid-century. In Europe, the projections fall below "no population growth" scenario (RCP8.5-GHSL) in the case of RCP8.5-SSP2 and RCP8.5-SSP3. In Asia, the exposure growth rates under RCP4.5-SSP1 and RCP8.5-SSP5 are almost equal to the corresponding constant population scenarios. The minor differences are likely caused by "High Migration" and "Fast urbanization" assumptions under SSP5 scenario (see Table 1).

EM-DAT historical observations reveal that more than one billion people were affected by droughts in the period 1995-2015 which was more than a quarter of all people affected by all types of weather-related disasters worldwide (UNISDR, 2015d). Historically, Africa has been affected by drought more than any other continent (about 40% of the global total between 2000 and 2019), especially in East Africa (CRED, 2020). Severe and extreme drought will increase in nearly every region with the largest increase primarily in the northern tropic latitude affecting Western Asia, Southern Europe, North Africa and Central America (Farinosi et al., 2020; Naumann et al., 2018; Spinoni et al., 2020). Our results for "no population growth" scenarios are in line with latest IPCC estimates where the frequency and intensity of an agricultural and ecological drought events will increase in the range between 200 to 300 percent under various warming levels (IPCC, 2021).

Droughts may last for years causing agricultural failures, loss of livestock, water shortages and outbreaks of epidemic diseases leading to sever humanitarian crisis in terms of hunger, poverty and displacement. In addition, at higher global warming levels, drought impacts will increasingly affect violent intrastate particularly in the most vulnerable regions (IPCC, 2022).

7.1.5 Epidemics

7.1.5.1 Malaria

Malaria projections in 2050 and 2080 for considered RCP-SSP combinations are shown in **Figure 17** and Annex 7. Malaria exposure in the mid-21st century is globally projected to increase in range between 92% (2.6 billion additional people) under RCP8.5-SSP3, and 51% (1.4 billion additional people) under RCP4.5-SSP1. Exposure trajectories under SSP2 follow an intermediate path between upper and lower bounds with 67% increase (1.9 billion additional people) and 73% increase (2.1 billion additional people) under RCP4.5 and RCP8.5 respectively. RCP8.5-SSP5 trajectories with 55% increase (1.5 billion additional people) are higher than RCP4.5-SSP1, and lower than RCP8.5-SSP2 and RCP4.5-SSP2. Under constant population assumption, the exposure is projected to increase by 30% (864 million) and 35% (1 billion) under moderate (RCP4.5) and high (RCP8.5) concentration pathways, suggesting slightly higher sensitivity to population growth rather than climate change.

The largest increase in Malaria exposure in mid-century is projected in Asia (667-1.2 million) and Africa (660-1.2 million) under RCP4.5-SSP1 and RCP8.5-SSP3 respectively. The exposure is more sensitive to climate change signal in Asia (528-617 million additional with no population growth) compared to Africa (228-252 million additional with no population growth). Europe as a current free of Malaria region will experience considerable increase in exposure in the range between 19 to 30 million, mainly driven by climate change. Oceania will experience second largest percentage change in exposure in the range between 78 to 101 under RCP4.5-SSP1 and RCP8.5-SSP2.

By 2080, the global increases in exposure range expands between 1.2 billion (43%) under RCP4.5-SSP1, and 3.9 billion (138%) under RCP8.5-SSP3. Under constant population scenario, malaria exposure is projected to increase by 992 million (34%) and 1.3 billion (45%) under moderate (RCP4.5) and high (RCP8.5) concentration pathways in 2080, suggesting population changes play larger role in defining malaria exposure at global scale by the end of century.

The regional trajectories continue to increase toward the end of the century in the same manner as for the mid-century. Africa will experience larger increase in exposure especially under SSP3 compared to Asia. In Europe, the projections under "no population growth" scenario showing higher sensitivity to amplified climate signals by the end of century. In Asia, the exposure growth rates under RCP8.5-SSP5 and RCP4.5-SSP1 are far lower than corresponding constant population scenarios. The exposure changes in Americas are fully consistent with population growth patterns among SSPs.

According to World Malaria Report 2021 (WHO, 2021b), global Malaria cases has increased from 227 million in 2019 to 241 million malaria cases in 2020, with the largest increase coming from Africa (228 million or 95% of total cases). Two percent of the total cases were found in South-East Asia, with India accounted for 83% of the cases in the region. Malaria cases in Eastern Mediterranean Region increases by 33% (1.7 million) between 2016 and 2020. In Americas, several countries have experienced substantial increase in Malaria cases in 2020 compared to 2019, including Haiti, Honduras, Nicaragua, Panama and Bolivia. According to IPCC (2022), malaria is projected to increase in some regions of Africa (highland areas), Asia, and South America (higher elevation). Climate change impacts on Malaria incidence can be exacerbated by sever and extreme droughts in those regions, which will experience substantial increases in frequency and intensity of extreme heat and droughts (see section 7.1.4).

Figure 17. The projected people exposed to malaria in 2050 and 2080 stratified by emissions and socioeconomic scenario combination. The bars indicate the projected additional people for each scenario relative to the baseline (ensemble mean of 1970-1999 historical period and GHSL 2015 population layer). SSPs include SSP1 (Sustainability - low challenges to mitigation and adaptation), SSP2 (Middle of the road - medium challenges to mitigation and adaptation), SSP3 (Regional rivalry - high challenges to mitigation and adaptation, SSP5 (Fossil fuel development - high challenges to mitigation with low challenges to adaptation). RCP=representative concentration pathways, SSP=shared socioeconomic pathways, GHSL=Global Human Settlement layer 2015.

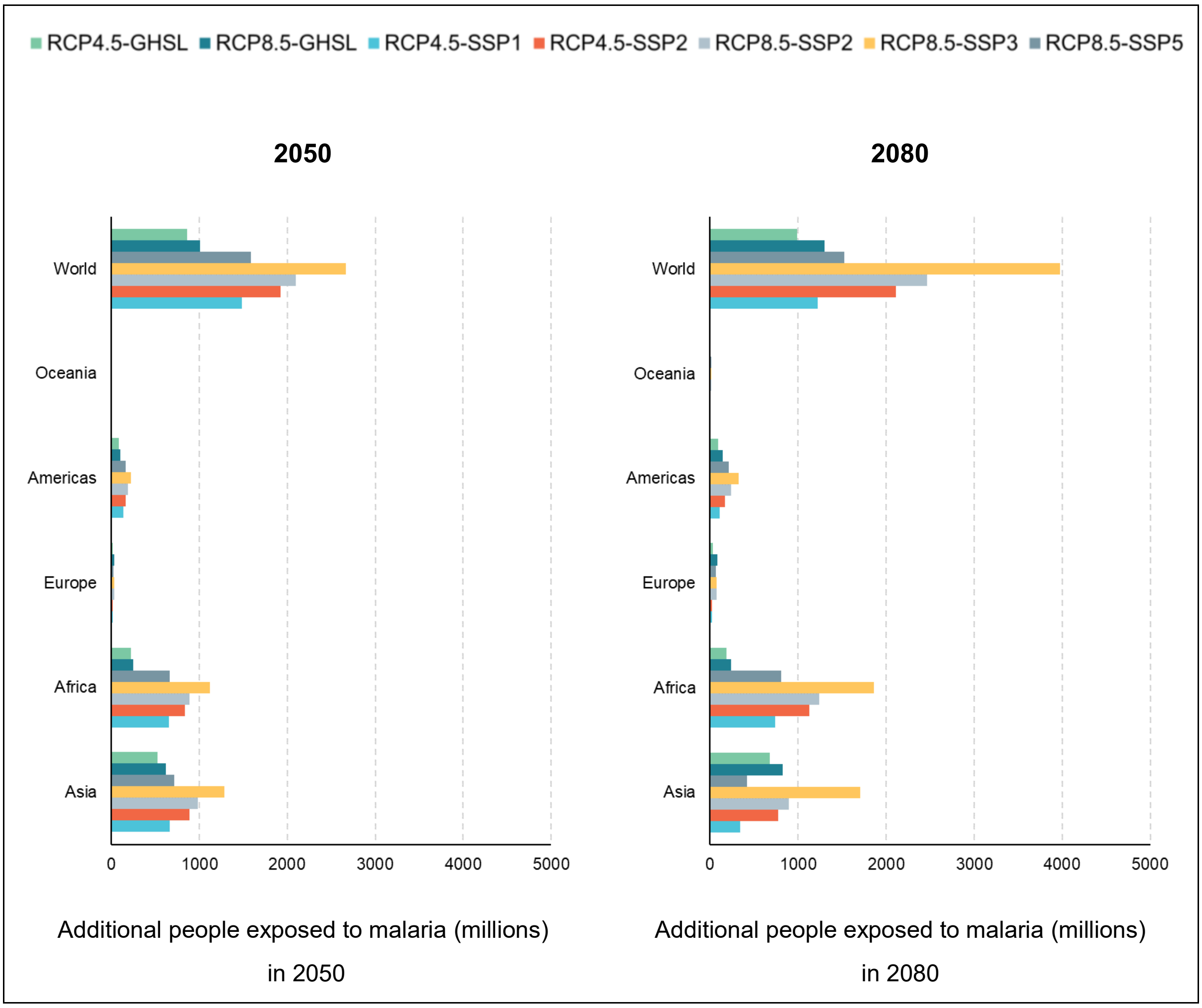

Source: Authors

7.1.5.2 Dengue

Dengue projections in 2050 and 2080 for considered RCP-SSP combinations are shown in **Figure 18** and Annex 8. Dengue exposure in the mid-21st century is globally projected to increase in range between 110% (3 billion additional people) under RCP8.5-SSP3, and 61% (1.6 billion additional people) under RCP8.5-SSP5. Exposure trajectories under SSP2 follow an intermediate path between upper and lower bounds with 86% increase (2.3 billion additional people) and 85% increase (2.3 billion additional people) under RCP4.5 and RCP8.5 respectively. RCP4.5-SSP1 trajectories with 64% increase (1.7 billion additional people) are higher than RCP8.5-SSP5, and lower than RCP8.5-SSP2 and RCP4.5-SSP2.

With no population growth, the exposure is projected to increase by one billion under both moderate (RCP4.5) and high (RCP8.5) concentration pathways. The optimal condition for dengue transmission is observed between 18·5°C and 33·0°C. Therefore, the projections decline at lower and higher temperatures, as for RCP8.5 in some regions. The results suggest larger dengue suitability under RCP4.5 thermal range, resulting higher exposure under RCP4.5-SSP1 and RCP4.5-SSP2 scenarios compared to other hazards.

Figure 18. The projected people exposed to dengue in 2050 and 2080 stratified by emissions and socioeconomic scenario combination. The bars indicate the projected additional people for each scenario relative to the baseline (ensemble mean of 1970-1999 historical period and GHSL 2015 population layer). SSPs include SSP1 (Sustainability - low challenges to mitigation and adaptation), SSP2 (Middle of the road - medium challenges to mitigation and adaptation), SSP3 (Regional rivalry - high challenges to mitigation and adaptation, SSP5 (Fossil fuel development - high challenges to mitigation with low challenges to adaptation). RCP=representative concentration pathways, SSP=shared socioeconomic pathways, GHSL=Global Human Settlement layer 2015.

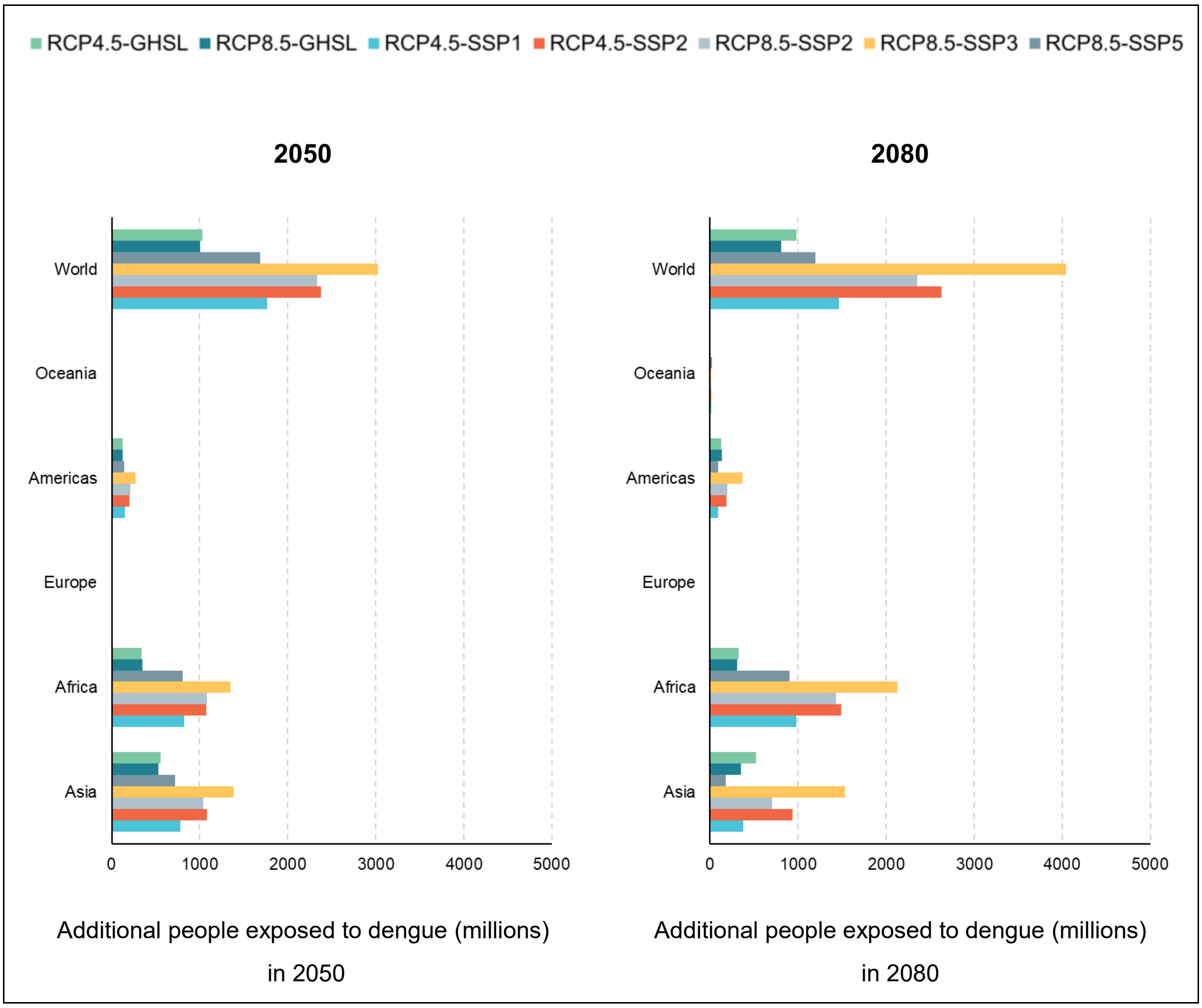

Source: Authors

The largest increase in Dengue exposure in mid-century is projected in Africa (806-1.3 million) and Asia (720-1.3 million) under RCP8.5-SSP5 and RCP8.5-SSP3 respectively. The exposure is more sensitive to climate change signal in Asia (526-558 million additional with no population growth) compared to Africa (334-346 million additional with no population growth). Europe remains a free of dengue region up to mid-century. Oceania will experience second largest percentage change in exposure in the range between 145 to 183 under RCP4.5-SSP1 and RCP8.5-SSP5. Dengue exposure in Americas will increase in the range between 146 million under RCP8.5-SSP5, and 275 million under RCP8.5-SSP3.

By 2080, the global increases in exposure range expands between 1.2 billion (44%) under RCP8.5-SSP5, and 4 billion (147%) under RCP8.5-SSP3. Under constant population scenario, Dengue exposure is projected to increase by 980 million (35%) and 805 million (29%) under moderate (RCP4.5) and high (RCP8.5) concentration pathways in 2080, suggesting population changes play larger role in defining dengue exposure at global scale by the end of century. The "no population growth" exposure results confirm larger dengue suitability under RCP4.5 thermal range in 2080.

The regional trajectories continue to increase toward the end of the century in the same manner as for the mid-century. Africa and Asia will experience the largest increase in exposure especially under SSP3. Europe will also experience dengue cases (60,000 cases) in 2080 under few scenarios especially under RCP8.5-SSP5. In Asia, the exposure growth rates under RCP8.5-SSP5 and RCP4.5-SSP1 are far lower than corresponding constant population scenarios. In Americas, the exposure under RCP8.5-SSP5 and RCP4.5-SSP1 are found lower than corresponding constant population scenarios, inconsistent with the regional population growth. Such inconsistency is mainly caused by low population growth (or decline) under those two scenarios in central and South America where the dengue suitability increases especially under RCP4.5 scenario.

According to WHO [31], number of dengue cases has increased drastically over the last two decades, from 505,430 cases to 5.2 million between 2000 and 2019. The cases have been found in 100 countries in African region, the Americas, the Eastern Mediterranean, South-East Asia and the Western Pacific, with Asia accounted for more than 70 percent of total cases (mainly in Bangladesh, Malaysia, Philippines and Vietnam). The projections used in this study are in line with current patters of dengue distribution. However, the risk may expand and shift to other regions due to higher thermal suitability and climate change (e.g. Europe). According to IPCC (2022), dengue exposure is projected to increase in Africa, Asia (East, South-East and South), Australia, South America, Mediterranean region of South Europe, and small Caribbean islands, and decline in North America.

7.2 Projected conflict risk

Average projected probability of conflict in 2050 and 2080 for considered SSPs are shown in **Figure 19** and Annex 9. The average conflict probability in the mid-21st century is globally projected to change in the range between 0.05 (41%) under SSP3, and -0.03 (-28%) for SSP5. Trajectories under SSP1 and SSP2 follow an intermediate path between upper and lower bounds with -24% and -6.5% increase respectively. In general, the average conflict probability increases only in the case of SSP3, and decreases elsewhere.

At regional scale, Africa and Asia experience the largest average conflict probability, 0.28 (53% increase) and 0.24 (18% increase) respectively under SSP3 scenario. Oceania has the smallest conflict probability (0.01) under all scenarios. The regional trajectories in 2050 are only in line with the global pattern in the case of Europe and Asia. Oceania experiences increasing average conflict probability under all scenarios with the largest increase under SSP3 and the smallest under SSP1. Americas and Africa follow the global trajectories except for SSP2 which increases compared to the baseline values. The largest increases are found in Africa and Americas, and smallest in Oceania under SSP3. Asia experiences the largest decrease in average conflict probability under SSP1, SSP2 and SSP5 scenarios.

By 2080, the global changes in average probability range expands between 0.07 (60%) under SSP3 and -0.06 (-49%) under SSP5. Trajectories under SSP1 and SSP2 remains between upper and lower bounds with -42% and -26% increase from the baseline respectively. In line with 2050 projections, the average conflict probability increases only in the case of SSP3, and decreases elsewhere. Consistent with mid-century projections, Africa and Asia experience the largest average conflict probability, 0.33 (80% increase from the baseline) and 0.26 (27% increase from the baseline) respectively under SSP3 scenario, and Oceania the smallest under all scenarios.

[31] https://www.who.int/news-room/fact-sheets/detail/dengue-and-severe-dengue

The regional trajectories in 2080 follow the global pattern except for Oceania where the average probability increases under SSP5 compared to the baseline values. In line with 2050 projections, the largest increases are found in Africa and Americas, and smallest in Oceania under SSP3. Asia experiences the largest decrease in average conflict probability under SSP1, SSP2 and SSP5 scenarios.

Results show that increases in socioeconomic development (GDP per capita and education) under SSP1, SSP2 and SSP5 leads to lower global conflict incidence with some regional differences, while larger populations especially under SSP3 result in higher rates of conflict. According to Riahi et al. (2017), with slow economic development, high inequalities and low investments in education and technologies, policies under SSP3 narrative shift toward national or regional security issues (e.g., energy and food insecurity), leading to resurgent nationalism and regional conflicts in the future. Hegre et al. (2016) found that the GDP per capita and social welfare improvements are essential to conflict reduction. Hence, the fossil-fuelled development narrative (SSP5) with the highest GDP per capita and lowest GINI would decrease substantially the risk of conflict in the future. The same can be applied to SSP1 (the second largest GDP per capita narrative) and SSP2 (intermediate GDP per capita growth) by the end of century (Riahi et al., 2017).

The results at regional scale are consistent with existing conflict clusters (Central Africa, the Middle East, and South Asia) with largest average conflict probability under all scenarios especially SSP3. Africa continues to see high average projected conflict probability in the future under all SSPs, mainly driven by sustained population growth.

Figure 19. The projected probability of civil conflict in 2050 and 2080 stratified by socioeconomic scenario combination. The bars indicate the change in projected probability of civil conflict for each scenario relative to the baseline (2020 – SSP5). SSPs include SSP1 (Sustainability - low challenges to mitigation and adaptation), SSP2 (Middle of the road - medium challenges to mitigation and adaptation), SSP3 (Regional rivalry - high challenges to mitigation and adaptation, SSP5 (Fossil fuel development - high challenges to mitigation with low challenges to adaptation). SSP=shared socioeconomic pathways.

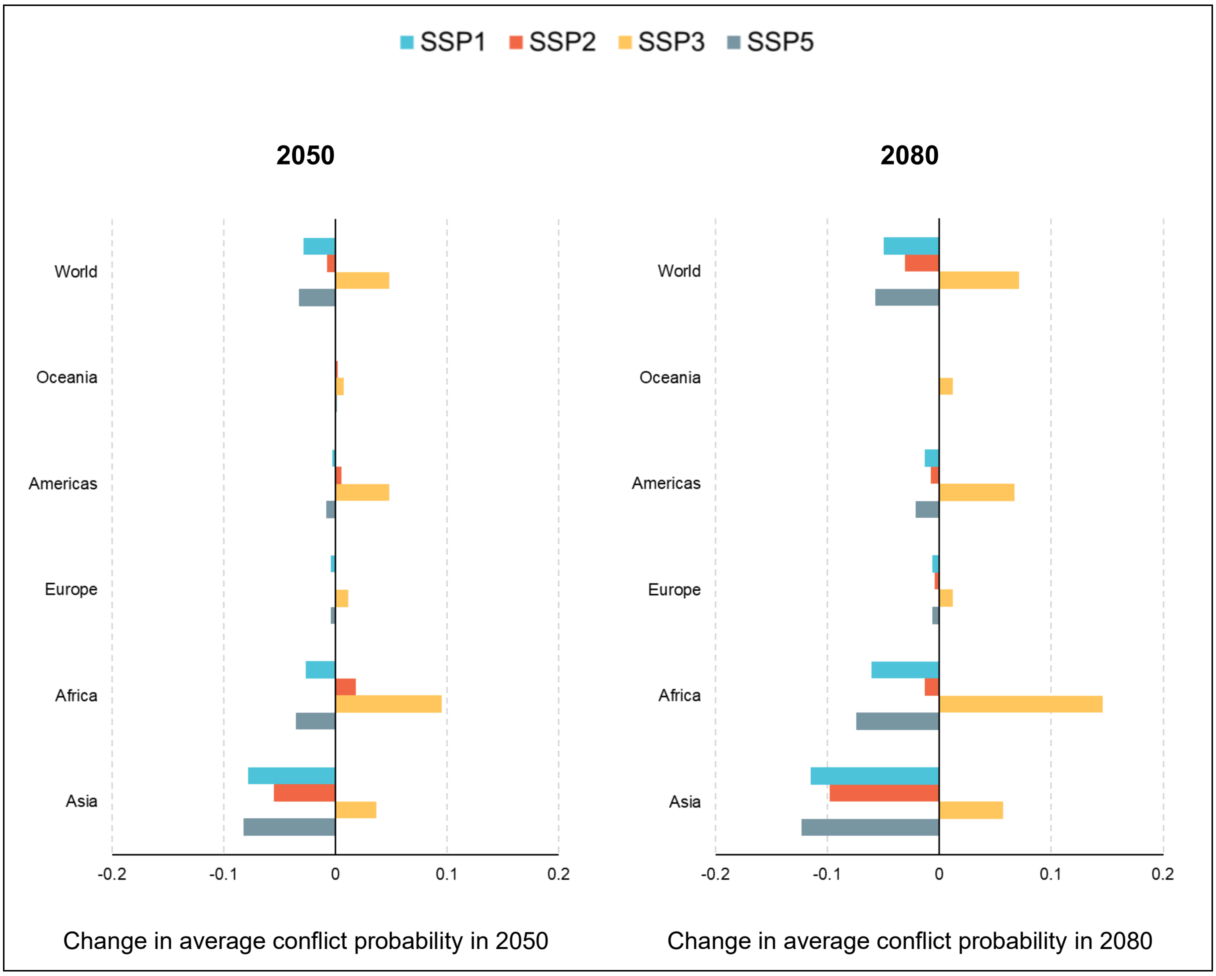

Source: Authors

7.3 INFORM Climate Change Risk Index

The exposed populations to each hazard presented and the conflict probability above (see Chapters 7.1 and 7.2) are used to calculate the risk, Hazard&Exposure, Natural hazard and Human hazard scores for baseline, 2050s and 2080s under various scenarios (see Chapter 4.3). In INFORM, exposed population is considered in terms of both total exposed population and exposed population relative to the total. We use risk classifications composed of a five threshold hierarchical scale to systematically identify risk in a consistent manner (Marin-Ferrer et al. 2017). Risk classes allow for the identification of the root causes of risk and therefore provide a greater ability to monitor, control and even manage risk. The format of results is aligned with the INFORM Risk Index (scale of 0-10, classifications from very low to very high risk).

7.3.1 Change in risk scores

Changes in risk, Hazard&Exposure, Natural hazard and Human hazard scores relative to the baseline under different scenarios in 2050s and 2080s are considered (Annex 10 to Annex 17). To illustrate the changes relative to the baseline scores, we use five classifications (large decrease to large increase) derived from hierarchical cluster analysis. Changes in Natural and human hazard scores are provided to better understand the root causes of changes in Hazard & Exposure and risk indices.

In our analysis of historical climate trends, the largest exposure to natural hazards occurs primarily in Asia and the Americas where total populations are currently greatest. The largest overall risk, however, occurs in Africa, Western and Southern Asia and Central America where vulnerabilities tend to be highest. The largest mid-century changes in Hazard & Exposure occur primarily in Southern Europe, northern and southern Africa, South America, and western and south-eastern Asia. The largest changes in overall risk are projected in parts of west and southern Africa, South America and Western Asia. Comparing the global and regional projected Hazard & Exposure between the baseline (current population and human hazard) and SSP scenarios illustrates that the general patterns tend to remain similar due to the strong climate change signal, but the projected population and conflict differences between the scenarios tend to alter the intensity of the Hazard & Exposure. In 2080s, the mid-century Hazard & Exposure pattern will be expanded to other regions including much of Europe, central Asia and North America with largest changes under RCP8.5. Nevertheless, the risk increases will be generally minimal due to high coping capacity (low vulnerability) in those areas.

Despite considerable changes in Hazard & Exposure levels, countries with currently high coping capacity levels with considerable amplified projected climate change hazards are able to counteract the adverse (e.g. United States). In contrast, countries with low coping capacity (high vulnerability) levels with large amplified climate change hazards show increased risk levels similar to the increment in amplified hazards (e.g. Angola). Somalia, Yemen and Afghanistan are the most vulnerable countries under all scenario combinations due to underperformances in both Hazard & Exposure and risk scores. In general, number of countries classified as having high and very high risk will increase especially under RCP8.5-SSP3 (36 countries in 2022, 52 and 55 in 2050 and 2080). The largest shifts the in risk classes between baseline and future occurs in high risk class under RCP8.5-SSP3 scenario (22 countries in 2022, 35 and 38 in 2050 and 2080 respectively).

7.3.2 Vulnerability gap

The change in vulnerability and lack of coping capacity (five classes, large decrease to large increase derived from hierarchal cluster analysis) due to climate, population and human hazard changes to maintain the current level of risk (see Chapter 4.4) provides an indication of the change in resilience required to overcome the effects of such changes (Annex 18 and Annex 19). While vulnerabilities associated with climate and population change, such as forced migration and food security are often linked, they are considered fixed at the current baseline values in this study. Countries with similar changes in hazard generally have widely varying levels of humanitarian impact. For instance, countries with low human development levels represent only 11% of the world population exposed to natural hazards between 1980 and 2000 but 53% of the total deaths in this period. High human development countries represent 15% of the exposed population but less than 2% of the deaths (UNDP, 2004). Since we alter only the exposure to natural hazards, the varying levels of disaster risk and resilience are not considered. We instead consider the current risk levels as a proxy to differentiate between high and low human development countries.

The results reveal that countries in Africa, South America and Western Asia tend to experience large increases in vulnerability gap in mid and late 21st century. Countries with Very Low current risk (mainly industrialized countries) are more resilient to climate change hazards and are therefore able to maintain a lower risk level. Similarly, in countries with Very High current risk levels (mainly non-industrialized countries), an increase in climate change hazard does not result in a risk class change and subsequent Vulnerability (lack of coping capacity) gap since the risk is already at its highest level. Therefore, a stable vulnerability gap in response to risk increase translates into different prevention, preparedness, and response measures depending on a country's socioeconomic structure and adaptive capacity, i.e. industrialised vs non-industrialized countries.

Relatively small number of countries such as Norway, Russia and Pakistan are projected to experience decrease in vulnerability gap under specific scenario combinations, suggesting that they would be able to keep current risk levels even with higher vulnerability and lack of coping capacity levels in the future. According to **Equation 4**, the vulnerability gap is a function of current risk of countries and changes in Hazard & Exposure scores. Therefore, small reduction in Hazard & Exposure scores results in decreases in vulnerability gap relative to the current risk levels.

7.4 Vulnerability gap from SDG and Sendai framework perspective

In order to explore the distinct contribution of vulnerability and coping capacity, we estimate the change in each dimension due to the change in Hazard & Exposure with risk is fixed at current levels for RCP8.5-SSP3 in 2050s (**Figure 20**). As many SDG and Sendai Framework indicators are included (or will be included) in the INFORM Risk Index[32] for assessing the vulnerability and lack of coping capacity dimension (Poljanšek et al., 2019b), we will be able to provide operational recommendations on where to allocate DRR and adaptation resources. The SDG and Sendai targets provide the frameworks necessary to monitor a country's progress towards reducing vulnerability and increasing capacity to the required level according to our results.

In investigating the distinct contribution of vulnerability and coping capacity, three different patterns can be identified among the countries with largest increases in vulnerability gap (combined vulnerability and lack of coping capacity) shown in Annex 18.

i) Countries like Turkmenistan which need larger reduction in lack of coping capacity compared to vulnerability to maintain the current risk. As INFORM Risk coping capacity dimension shows, Turkmenistan's low performance is mainly characterised by very low institutional capacity due to high corruption perception and weak government effectiveness. Based on Andrijevic et al. (2020) projections of the WGI government effectiveness and control of corruption components for 2050, Turkmenistan's performance under SSP3 scenario would remain relatively low. According to the United Nations Economic Commission for Europe (UNECE) review (UNECE, 2012), Turkmenistan is actively implementing development projects that consider coping capacity improvements into development plans, mostly driven by UNDP. In June 2018, Turkmenistan hosted the conference "Partnership for Development Financing at the Heart of the Great Silk Road" to discuss the issue of financing in relation to progress towards the SDG goals. Turkmenistan is working towards strengthening financial stability of the system and creation of favourable investment environment for development of non-hydrocarbon sectors of the economy (Service, 2019).

ii) Countries like Jordan, which require larger reduction in vulnerability compared to lack of coping capacity to maintain the current risk. Jordan's high vulnerability is largely driven by the high number of uprooted people according to INFORM Risk. Regional instability and the Syrian refugee crisis have resulted in multiple socioeconomic impacts in Jordan (UNCT, 2017). The poverty rate of Syrian refugees is very high, and there is evidence that poverty among refugees increased by several percentage points between 2013 and 2015 (EC, 2021d).

iii) Countries like Senegal which require large reduction in both vulnerability and lack of coping capacity levels to maintain the current risk. Senegal's underperformance in both dimensions is driven by underdevelopment and deprivation and low accessibility to health systems. Senegal is classified by the World Bank as a low-income country with the poverty rate at 35.4% in 2016, which is lower than the average for low-income countries worldwide. Poverty is linked to both macroeconomic volatility (commodity price spikes, the global financial crisis and epidemics) and idiosyncratic shocks (illnesses, deaths of family members, loss of assets and/or employment). A considerable share of the population is vulnerable to food insecurity and malnutrition, with over 15% of rural households and over 8% of urban. In addition, environmental and socioeconomic changes have intensified migration and displacement in Senegal. The main governance indicators reveal that the government effectiveness has also progressively declined (World Bank, 2018).

[32] The SDG indicators mainly correspond to the Vulnerability dimension of INFORM Risk Index, while the SFM indicators can contribute to Lack of Coping Capacity dimension.

Figure 20. Vulnerability and Lack of Coping Capacity Changes in mid-21st century required to maintain the current levels of risk.

a) Required changes in Vulnerability to Keep the Current Risk

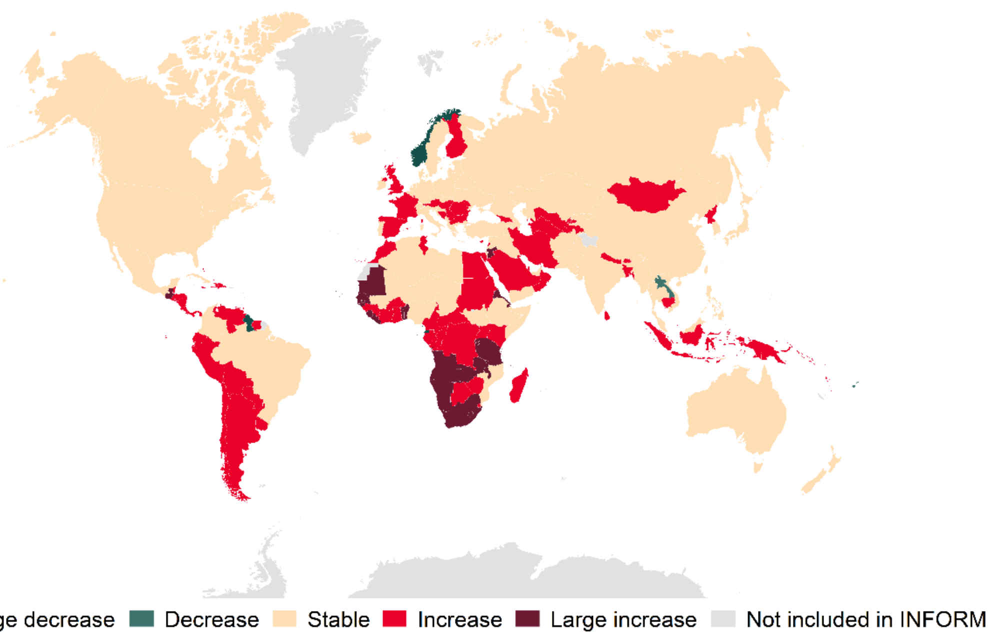

b) Required changes in lack of coping capacity to Keep the Current Risk

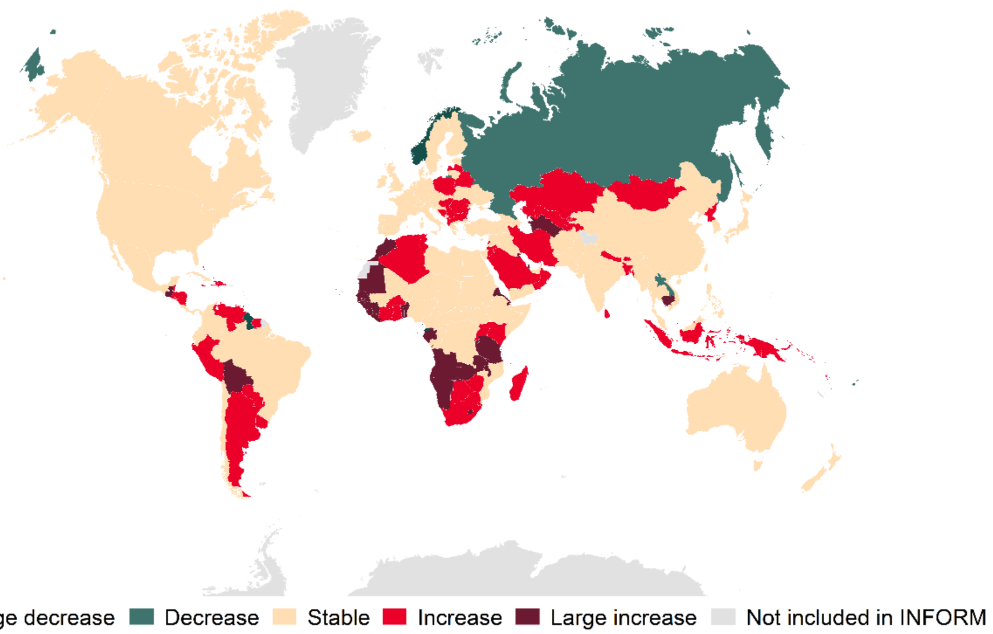

Source: Authors

7.5 Comparison of INFORM Climate Change Risk Index with ND-GAIN Country Index

INFORM Climate Change Risk index can be compared in a fair manner with ND-GAIN Country Index (University of Notre Dame, 2018). ND-GAIN Country Index measures a country's current vulnerability to climate disruptions in combination with its readiness to improve resilience (University of Notre Dame, 2018). ND-GAIN partitions vulnerability into exposure, sensitivity and adaptive capacity considering six life-supporting sectors. The exposure dimension includes projected impacts of climate-related hazards such as extreme sea level rise under RCP4.5 concentration pathway by mid-century.

In order to explore the similarities, we compute the Spearman and Pearson correlation coefficients (**Figure 21**). The Spearman's correlation coefficient is a nonparametric measure of statistical dependence between two ranked variables while Pearson's correlation coefficient is a measure of a linear relationship between the scores of the two variables. The correlations are strong and all statistically significant ($p < 0.001$), suggesting that the indices are statistically compatible. This result is expected as both models consider counterbalancing relationship between exposure, sensitivity (acceptability) and coping/adaptive capacity, with relatively similar components.

Figure 21. Comparison of INFORM Climate Change Risk (RCP4.5-SSP1 and RCP4.5-SSP2 in 2050) with ND-GAIN Country Index. For the sake of comparability, the ND-GAIN country scores are reverted and rescaled into range 0-10.

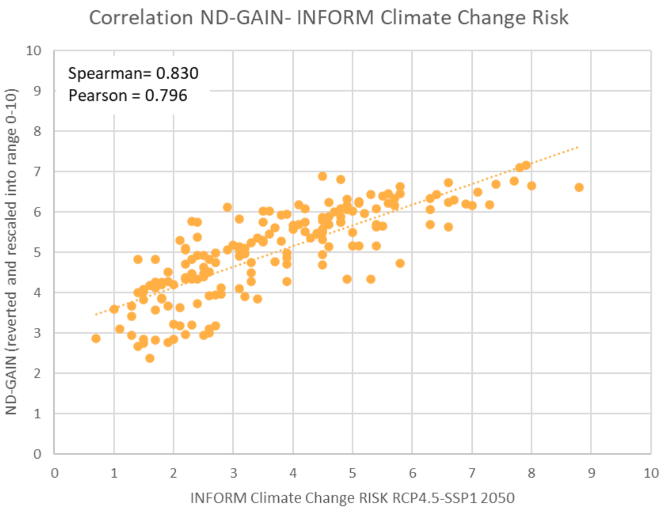

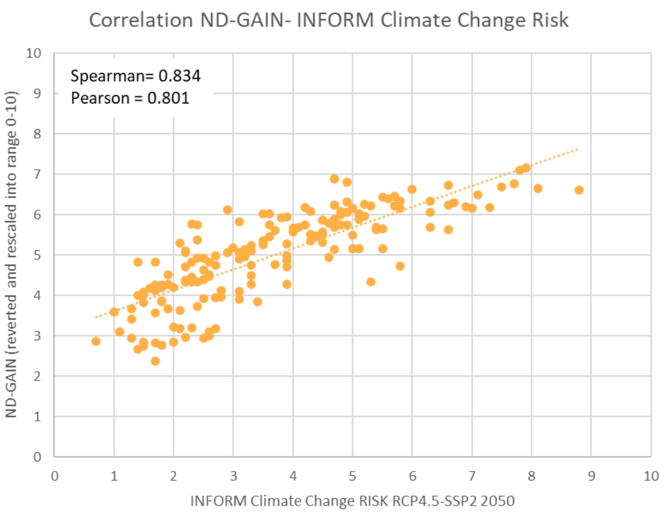

Source: Authors

8 INFORM Climate Change Tool

INFORM Climate Change tool provides insight into the results of the climate change risk analysis. The tool is designed to inform decision-making around the risk of climate-amplified hazards, as well as how increased risks could be offset by improved vulnerability and coping capacity. It helps the users to easily navigate within different scenario combinations and different points in time, exploring the potential changes in risk and Hazard&Exposure variables. The main features are Fact & Figures, Key Changes, Hazard Projections and Country profile.

8.1 Features

8.1.1 Fact & Figures

INFORM Climate Change Facts and Figures provide information on global distribution of countries by INFORM Risk classes, income group and regions under various RCP-SSP scenarios for baseline, 2050s and 2080s. The same approach is used for all three dimensions of INFORM Climate Change Risk Index: Hazard & Exposure, Vulnerability and Lack of Coping Capacity. Indices related to Vulnerability and Lack of coping capacity do not undergo any modifications and are directly adopted from INFORM Risk 2022 release. The thresholds used to map the dimensions are derived from hierarchal clustering model and are available in Annex 21 and Annex 22. The population count feature provides information on population estimates for various breakdowns (e.g. risk classes) as well as global distribution under various RCP-SSP scenarios.

Figure 22. INFORM Climate Change tool: Fact&Figures feature

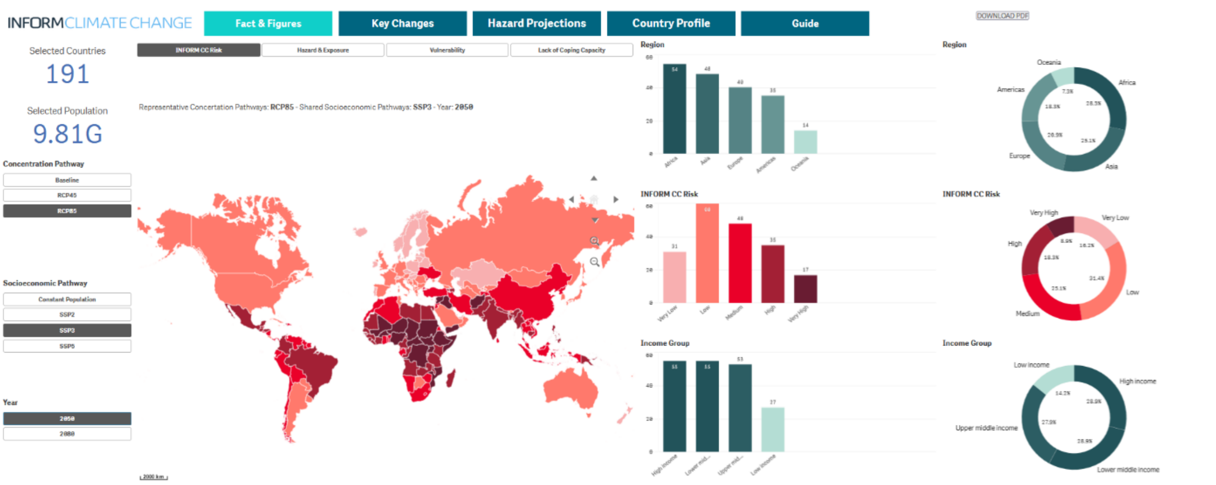

Source: Authors

8.1.2 Key changes

The key changes tab visualizes the variations in Risk, Hazard&Exposure, Natural Hazard, Human Hazard, Vulnerability gap and population density relative to the baseline under various RCP-SSP scenario combinations. The thresholds used to map the changes are based on hierarchal clustering model derived from the full range of changes for all scenario combinations and are available in Annex 23.

Figure 23. INFORM Climate Change tool: Key Changes feature

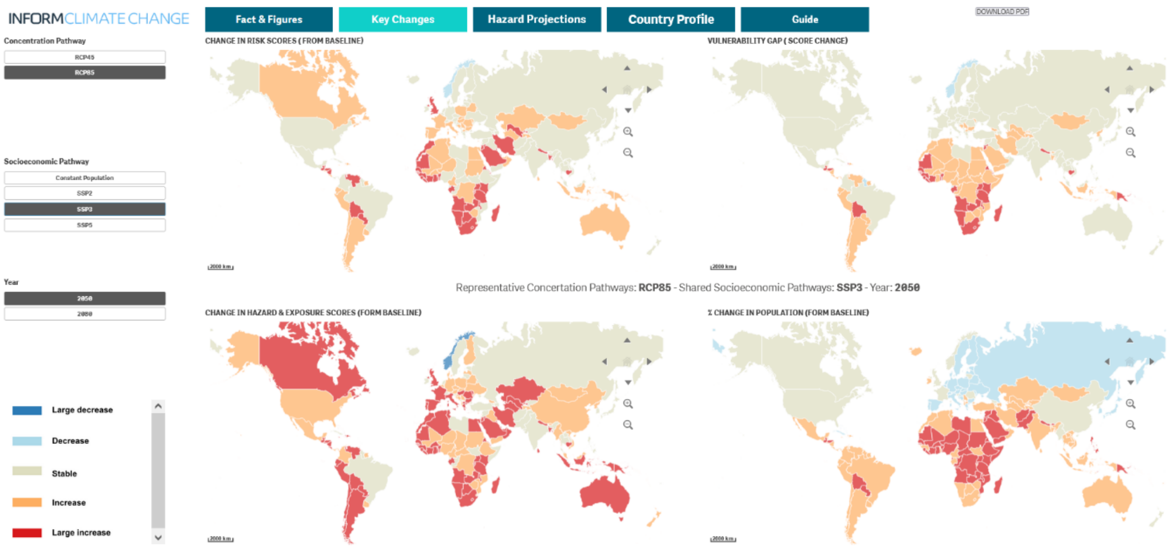

Source: Authors

8.1.3 Hazard projections

The Hazard Projection tab includes the projected scores of Hazard&Exposure dimension including climate-related, non-climate and non-modelled variables. The tab allow also comparison among different scenario combinations and/or different points in time for each hazard. The thresholds used to map the hazards are available in Annex 24. The thresholds are based on hierarchal clustering model derived from the worst-case scenario RCP8.5-SSP3 in 2050.

Figure 24. INFORM Climate Change tool: Hazard Projections feature

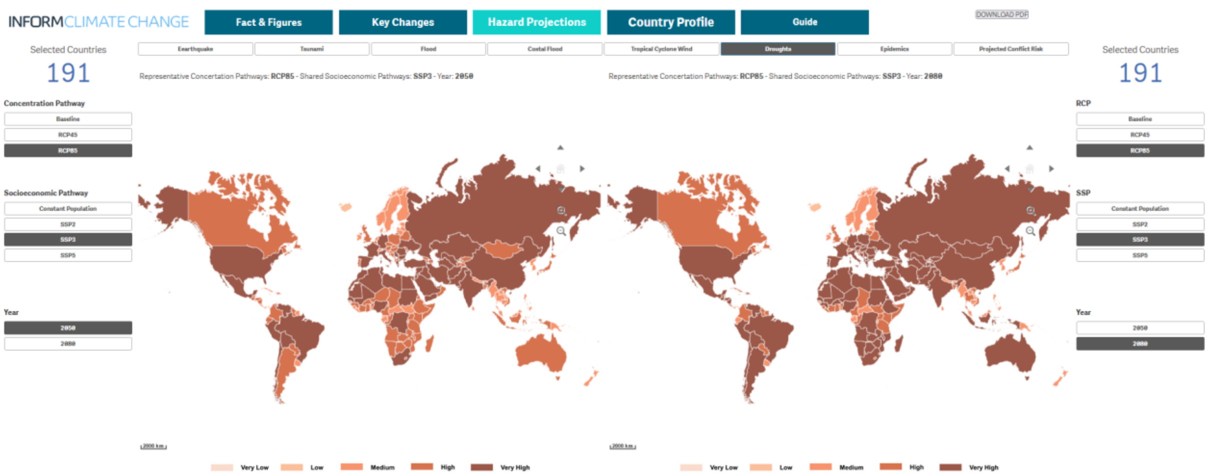

Source: Authors

8.1.4 Country profile

Country profiles feature contain more in-depth information on each country. In addition to the results in the global list, country risk profile show scores for each risk dimension and Hazard&Exposure component under various scenario combinations for baseline, 2050s and 2080s. Country risk profiles can be used to provide more in-depth information on risk in a particular country.

Figure 25. INFORM Climate Change tool: Country Profile feature

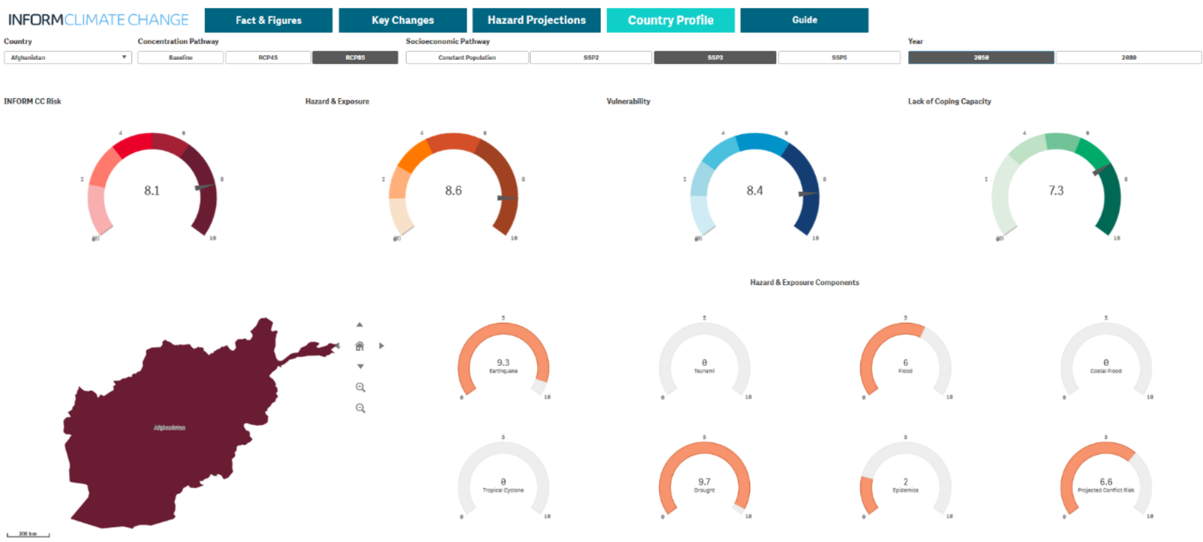

Source: Authors

8.1.5 Guide

The Guide feature provides brief explanation of the INFORM Climate Change Risk Index methodology, tool's features, Scenarios used, and definition of the concept such as Vulnerability gap, Change in risk and INFORM Climate Change Risk Index baseline, as well as sources of the hazard and exposure projections data.

9 Limitations

9.1 Methodological limitations

Composite indicator: The composite indicators are simplification of reality. The simple 'big picture' results which composite indicators show may invite politicians to draw simplistic policy conclusions. Composite indicators should be used in combination with the sub-indicators to draw sophisticated policy conclusions (UNFPA, 2015).

Precision: Uncertainty analysis revealed considerable variations in scores while exposed to methodological modifications. Therefore, scores presented with a high level of precision could be perceived to be more accurate than they are. To avoid such issue, the INFORM climate change Index results are clustered and all fall into one of five risk categories. These categories are generally robust and not influenced by methodological choices. The Index scores can provide further information about risk trends and help interpretation of the results. Be cautious interpreting values close to a category boundary (e.g. 3.4 vs. 3.6).

Representativeness: The usage of proxies limits the 'representativeness'. Certain phenomena that were addressed as important for the humanitarian risk assessment cannot be measured exactly in the way we want or adequate indicators are not available. In such situations, proxy measures are used which measure something that is close enough to reflect similar behaviour and can provide relative differences among the countries for ranking purposes. The proper representativeness of phenomena is limited to the presence of causes, consequences, measurable parts of the process or even accompanying processes. For example, the drought exposure is presented by the proportion of population living in the areas with sever and extreme SPEI values which is not able to cover potential economic impacts of droughts on livelihoods of targeted communities.

Risk assessment: The INFORM risk is calculated with a multiplicative equation where each of the dimensions are equally weighted (33% each). In this form INFORM's risk is more sensitive to Vulnerability and Lack of coping capacity, the internal forces of risk that can be most influenced by the DRR activities. IPCC considers vulnerability as a result of susceptibility to hazards and lack of coping and adaptive capacity while INFORM vulnerability reflects the susceptibility to hazards and has been combined with lack of coping capacity. Therefore, IPCC vulnerability components could be interchangeably assessed with the combined INFORM's vulnerability and lack of coping capacity. In this case, the combined vulnerability and lack of coping capacity and Hazard& Exposure dimensions can be equality weighted (50%) to better show the impacts of climate change amplified hazards. Nevertheless, for the sake of comparability with the original INFORM, and to better reflect the importance of DRR and CCA activities, we keep the original formula of the risk.

Vulnerability gap assessment: In countries with Very High current risk levels (mainly non-industrialized countries), an increase in climate change hazard does not result in considerable changes in risk and vulnerability gap since the risk is already at its highest level (upper bound of risk scores). Therefore, any conclusion on a low vulnerability gap in response to risk increase in such countries should be drawn with some caution.

9.2 Data limitations

Climate-related hazards: high divergence of forcing from the different RCPs occur mainly beyond mid-century. Extending to the end of the century should include a larger suite of climate change scenarios ranging from the RCP2.6 to RCP 8.5. With the larger suite climate change scenarios, other RCP-SSP combinations should be considered as well. In this study only two RCPs were used due to data availability reasons. Furthermore, other climate-related hazards with large humanitarian impacts such as heatwaves, urban flood and extreme winds should also be considered. Such hazards will be added in the future releases.

Transition between CMIP5 and CMIP6 climate models: Climate models play a major role in assessing the impact of climate change and developing adaption and mitigation strategies. IPCC sixth assessment report is based on the Coupled Model Intercomparison Project Phase 6 (CMIP6) of the World Climate Research Programme. These models have a wider range of climate sensitivity compared to CMIP5 climate models considered in previous IPCC assessment reports (IPCC, 2021). Nevertheless, projections by CMIP5 and CMIP6 models show significant changes in temperature and precipitation in the future (Bourdeau-Goulet and Hassanzadeh, 2021). The hazard projections based on the CMIP6 climate models will be incorporated in the INFORM Climate Change Risk as soon as the bias-corrected simulations' data are available.

Historical period ensembles: It should be noted that the year range of historical period and the RPs considered for the coastal flood and drought simulations are somewhat inconsistent with those for river flood and epidemics due to data availability reasons.

Differences in the gridded population datasets: In order to calculate the baseline and "constant population" exposure, hazard layers are overlayed with GHSL 2015 population density layer. Such choice has been made for the sake of comparability between the INFORM Climate Change Risk Index baseline and the original INFORM Risk Index. The future exposure is based on the population projections derived from SSP dataset. The baseline for SSPs goes back to the year 2000 and doesn't coincide with GHSL 2015. This may cause discrepancies in exposure results especially in the case of local analysis (e.g. floods) due to the different methodologies and input ancillary data used for generating each of the population datasets. Therefore, we suggest comparing projected country level results derived from "constant population" assumption separately from the SSPs. However, the results from the "constant population" scenario shows the sole impact of climate change without considering any socioeconomic development trends.

Small Island states: As a limitation, for very small countries (e.g., small Pacific Islands) drought is not computed due to their lack of representation in the driving CMIP5 models. The resolution of global climate models (GCMs) exceeds the size of countries (0.25°). Therefore, the exposure is binary for each land grid cell, i.e., either the total population is exposed, or no population is exposed. Since droughts typically affect large geographic areas, we assume no population exposed in those countries. The same challenge has been noted in several other studies using GCMs (e.g., Keener et al., 2012; Smirnov et al., 2016; The World Bank, 2016). To overcome this issue, Keener et al. (2012) suggests to downscale the global models by taking into consideration the regional and local phenomena influencing the regional climate system. Such methods will be applied in the future analysis of the INFORM Climate Change Risk Index.

10 Conclusion and way forward

Extreme weather and climate related events cause fatalities, injuries and displacement. Indicator-based assessment of risks and needs are used for humanitarian and development aid operations. These assessments are often based on historical observations or present-day hazard conditions. We have presented ways to extend the INFORM Risk Index already used by many actors across the multilateral system to understand the risk of humanitarian crises, to include future projections of climate change-altered hazards (floods, droughts and epidemics), exposed population and projected risk of conflict. To do so, we have used projections based on moderate and high-emissions (RCP4.5 and RCP8.5) and four Socioeconomic scenarios (SSP1, SSP2, SSP3 and SSP4) scenarios for mid and late 21st century. The projected risk is used to estimate changes in coping capacity and vulnerability required to compensate for the change in risk. This assessment exercise has been conducted in collaboration with major international organizations to stimulate reflection on how the extended index can be used to inform decision-making and operational choices.

This report describes the conceptual framework methodology for INFORM Climate Change as well as the results of the analysis. The results make explicit the trade-offs between evolving hazards and the investments in capacity and resilience building needed to compensate for the amplified hazards. The largest changes in overall risk are generally projected in parts of west and southern Africa, South America, Western Asia and Southern Europe. For countries initially classified as very low risk (for a major part developed nations), the increase in exposure to climate hazards may be countered by already high levels of coping capacity. In some cases, the dramatic increase in the exposure to natural hazards can only be compensated by sizeable reduction of vulnerability. In contrast, for countries already characterised by very high levels of risk, the increase in exposure to natural hazards requires substantial efforts to enhance coping capacities.

By adding climate and demographic projections, the INFORM Climate Change Risk Index offers snapshots of current and future conditions resulting from the "committed" climate change under different emission and socioeconomic scenarios. This knowledge can not only serve planning for humanitarian aid management, but also in drafting effective DRR and CCA strategies and plans (Hallegatte et al., 2020). The emphasis on required increase in coping capacity can inform decision making processes on adaptation options at local and national level (OECD, 2020). International partners (e.g. FCDO, IOM and IFRC) have recognized the benefits of such a tool in terms of horizon scanning and global humanitarian risk monitoring (IFRC, 2020). International partners (e.g. FCDO, IOM and IFRC) have recognized the benefits of such tool in terms of horizon scanning and global humanitarian risk monitoring (IFRC, 2020). Capturing the projections of climate, exposure and vulnerability in INFORM Climate Change Risk Index is key to invest in appropriate preparedness measures, according to FCDO. For UNDCO, climate change enhanced risk indices are able to explore long-term drivers of social inequalities. IOM's global preparedness effort benefits from INFORM's integration of climate and demographic projections as it provides an additional layer of information on the needs of individual mobile populations.

In parallel, online interactive tool was developed and implemented. INFORM Climate Change tool provides insight into the results of the climate change risk analysis. It helps the users to easily navigate within different scenario combinations and different points in time, exploring the potential changes in risk and Hazard&Exposure variables. The main features are Fact & Figures, Key Changes, Hazard Projections and Country profile. INFORM Climate Change tool can be found fully operational on INFORM central hub hosted by European Commission[33]. Furthermore, INFORM Climate Change brochure (Inter-Agency Standing Committee and the European Commission, 2022b) has been published to present the results of the analysis in the format to inform decision maker about the policy choices across climate mitigation and adaptation, disaster risk reduction, sustainable development and humanitarian assistance.

The results of our analysis show that increases in global risk are guaranteed in the future, however through policy choices we can still reduce the future risk through action on mitigation, adaptation and sustainable development. Quantitative analysis like INFORM Climate Change Risk Index can help us better understand the main drivers of future risk as well as follow our progress regarding adaptation efforts and disaster risk reduction. The Vulnerability gap measure can be updated annually using Vulnerability and Lack of Coping Capacity scores from the latest version of INFORM Risk Index, and used as a proxy to assess the efficacy of adaptation and risk reduction policies and practices.

Future research may focus on extending the INFORM Risk Index using available projections of various drivers of vulnerability and coping capacity such as social characteristics, migration, governance, urbanization,

33 https://drmkc.jrc.ec.europa.eu/inform-index/INFORM-Climate-Change/INFORM-Climate-Change-Tool

infrastructure, and health status under the SSPs. Furthermore, the hazard projections could be replaced with the ones based on the new generation of climate models (CMIP6 models) as soon as the bias-corrected simulations are available.

INFORM Climate Change Risk Index complements INFORM Risk Index and INFORM Severity in the INFORM Suite. INFORM initiative will focus now also on development of the INFORM Warning tool to provide information in systematic way on any indication of elevated risk, emerging crisis and crisis triggers needed for preparedness, early warning and early action phase.

References

Akoglu, H., 2018. User's guide to correlation coefficients. Turkish J. Emerg. Med. https://doi.org/10.1016/j.tjem.2018.08.001

Alfieri, L., Burek, P., Dutra, E., Krzeminski, B., Muraro, D., Thielen, J., Pappenberger, F., 2013. GloFAS – global ensemble streamflow forecasting and flood early warning. Hydrol. Earth Syst. Sci. 17, 1161–1175. https://doi.org/10.5194/hess-17-1161-2013

Alfieri, L., Dottori, F., Salamon, P., Wu, H., Feyen, L., 2020a. Global Modeling of Seasonal Mortality Rates From River Floods. Earth's Futur. 8. https://doi.org/10.1029/2020EF001541

Alfieri, L., Lorini, V., Hirpa, F.A., Harrigan, S., Zsoter, E., Prudhomme, C., Salamon, P., 2020b. A global streamflow reanalysis for 1980–2018. J. Hydrol. X 6, 100049. https://doi.org/10.1016/j.hydroa.2019.100049

Andrijevic, M., Crespo Cuaresma, J., Muttarak, R., Schleussner, C.F., 2020. Governance in socioeconomic pathways and its role for future adaptive capacity. Nat. Sustain. 3, 35–41. https://doi.org/10.1038/s41893-019-0405-0

Arnell, N.W., Lowe, J.A., Bernie, D., Nicholls, R.J., Brown, S., Challinor, A.J., Osborn, T.J., 2019. The global and regional impacts of climate change under representative concentration pathway forcings and shared socioeconomic pathway socioeconomic scenarios. Environ. Res. Lett. 14, 084046. https://doi.org/10.1088/1748-9326/AB35A6

Bakkensen, L.A., Fox-Lent, C., Read, L.K., Linkov, I., 2017. Validating Resilience and Vulnerability Indices in the Context of Natural Disasters. Risk Anal. 37, 982–1004. https://doi.org/10.1111/risa.12677

Beguería, S., Vicente-Serrano, S.M., Reig, F., Latorre, B., 2014. Standardized precipitation evapotranspiration index (SPEI) revisited: Parameter fitting, evapotranspiration models, tools, datasets and drought monitoring. Int. J. Climatol. 34, 3001–3023. https://doi.org/10.1002/joc.3887

Belles-Sampera, J., Merigó, J.M., Guillén, M., Santolino, M., 2014. Indicators for the characterization of discrete Choquet integrals. Inf. Sci. (Ny). 267, 201–216. https://doi.org/10.1016/J.INS.2014.01.047

Bendanillo, F.E., Yurong, R.R., Roble, N.D., Yee, J.C., Sotto, F.B., 2016. Species Composition, Abundance and Distribution of Seawater Bugs (Order Hemiptera: Class Insecta) in Badian, Cebu, Philippines. J. Aquat. Sci. Vol. 4, 2016, Pages 1-10 4, 1–10. https://doi.org/10.12691/JAS-4-1-1

Birkmann, J., Cardona, O.D., Carreño, M.L., Barbat, A.H., Pelling, M., Schneiderbauer, S., Kienberger, S., Keiler, M., Alexander, D., Zeil, P., Welle, T., 2013. Framing vulnerability, risk and societal responses: the MOVE framework. Nat. Hazards 67, 193–211. https://doi.org/10.1007/s11069-013-0558-5

Birkmann, J., Feldmeyer, D., McMillan, J.M., Solecki, W., Totin, E., Roberts, D., Trisos, C., Jamshed, A., Boyd, E., Wrathall, D., 2021. Regional clusters of vulnerability show the need for transboundary cooperation. Environ. Res. Lett. 16, 094052. https://doi.org/10.1088/1748-9326/AC1F43

Birkmann, J., Sauter, H., Jamshed, A., Sorg, L., Fleischhauer, M., Sandholz, S., Wannewitz, M., Greiving, S., Bueter, B., Schneider, M., Garschagen, M., 2020. Strengthening risk-informed decision-making: scenarios for human vulnerability and exposure to extreme events. Disaster Prev. Manag. An Int. J. 29, 663–679. https://doi.org/10.1108/DPM-05-2020-0147

Bose-O'Reilly, S., Daanen, H., Deering, K., Gerrett, N., Huynen, M.M.T.E., Lee, J., Karrasch, S., Matthies-Wiesler, F., Mertes, H., Schoierer, J., Shumake-Guillemot, J., van den Hazel, P., Frank van Loenhout, J.A., Nowak, D., 2021. COVID-19 and heat waves: New challenges for healthcare systems. Environ. Res. 198. https://doi.org/10.1016/J.ENVRES.2021.111153

Bourdeau-Goulet, S.C., Hassanzadeh, E., 2021. Comparisons Between CMIP5 and CMIP6 Models: Simulations of Climate Indices Influencing Food Security, Infrastructure Resilience, and Human Health in Canada. Earth's Futur. 9, e2021EF001995. https://doi.org/10.1029/2021EF001995

Bowlsby, D., Chenoweth, E., Hendrix, C., Moyer, J.D., 2020. The Future is a Moving Target: Predicting Political Instability. Br. J. Polit. Sci. 50, 1405–1417. https://doi.org/10.1017/S0007123418000443

Brown, S., Nicholls, R.J., Lowe, J.A., Hinkel, J., 2016. Spatial variations of sea-level rise and impacts: An application of DIVA. Clim. Change 134, 403–416. https://doi.org/10.1007/s10584-013-0925-y

Brzoska, M., 2018. Weather Extremes, Disasters, and Collective Violence: Conditions, Mechanisms, and Disaster-

Related Policies in Recent Research. Curr. Clim. Chang. Reports 2018 44 4, 320–329. https://doi.org/10.1007/S40641-018-0117-Y

Carrère, L., Lyard, F., 2003. Modeling the barotropic response of the global ocean to atmospheric wind and pressure forcing - comparisons with observations. Geophys. Res. Lett. 30. https://doi.org/10.1029/2002GL016473

Cederman, L.E., Weidmann, N.B., 2017. Predicting armed conflict: Time to adjust our expectations? Science (80- .). 355, 474–476. https://doi.org/10.1126/SCIENCE.AAL4483/ASSET/CA96934C-20A6-452A-AAD0-58E928FB5E81/ASSETS/GRAPHIC/355_474_FA-P2.JPEG

Chaji, A., Fukuyama, H., Khanjani Shiraz, R., 2018. Selecting a model for generating OWA operator weights in MAGDM problems by maximum entropy membership function. Comput. Ind. Eng. 124, 370–378. https://doi.org/10.1016/J.CIE.2018.07.040

Chenoweth, E., Ulfelder, J., 2015. Can Structural Conditions Explain the Onset of Nonviolent Uprisings?: http://dx.doi.org/10.1177/0022002715576574 61, 298–324. https://doi.org/10.1177/0022002715576574

Colón-González, F.J., Harris, I., Osborn, T.J., Bernardo, C.S.S., Peres, C.A., Hunter, P.R., Lake, I.R., 2018. Limiting global-mean temperature increase to 1.5-2 °C could reduce the incidence and spatial spread of dengue fever in Latin America. Proc. Natl. Acad. Sci. U. S. A. 115, 6243–6248. https://doi.org/10.1073/PNAS.1718945115

Colón-González, F.J., Sewe, M.O., Tompkins, A.M., Sjödin, H., Casallas, A., Rocklöv, J., Caminade, C., Lowe, R., 2021. Projecting the risk of mosquito-borne diseases in a warmer and more populated world: a multi-model, multi-scenario intercomparison modelling study. Lancet Planet. Heal. 5, e404–e414. https://doi.org/10.1016/S2542-5196(21)00132-7/ATTACHMENT/F6794FC7-A9E6-410F-B0FB-86D5C90BA907/MMC1.PDF

CRED, 2020. The human cost of disasters: an overview of the last 20 years (2000-2019). Brussels.

CRED, 2019. EM-DAT: The International Disaster Database [WWW Document]. Cent. Res. Epidemiol. Disasters. URL https://www.emdat.be/database

Crespo Cuaresma, J., 2017. Income projections for climate change research: A framework based on human capital dynamics. Glob. Environ. Chang. 42, 226–236. https://doi.org/10.1016/j.gloenvcha.2015.02.012

de Coninck, H., Revi, A., Babiker, M., Bertoldi, P., Buckeridge, M., Cartwright, A., Dong, W., Ford, J., Fuss, S., Hourcade, J.C., Ley, D., Mechler, R., Newman, P., Revokatova, A., Schultz, S., Steg, L., Sugiyama, T., 2018. Strengthening and Implementing the Global Response, in: Masson-Delmotte, V., Zhai, P., Pörtner, H.-O., Roberts, D., Skea, J., Shukla, P.R., Pirani, A., Moufouma-Okia, W., Péan, C., Pidcock, R., Connors, S., Matthews, J.B.R., Chen, Y., Zhou, X., Gomis, M.I., Lonnoy, E., Maycock, T., Tignor, M., Waterfield, T. (Eds.), Global Warming of 1.5°C. An IPCC Special Report on the Impacts of Global Warming of 1.5°C above Pre-Industrial Levels and Related Global Greenhouse Gas Emission Pathways, in the Context of Strengthening the Global Response to the Threat of Climate Change,. In Press.

de Graaf, I.E.M., van Beek, R.L.P.H., Gleeson, T., Moosdorf, N., Schmitz, O., Sutanudjaja, E.H., Bierkens, M.F.P., 2017. A global-scale two-layer transient groundwater model: Development and application to groundwater depletion. Adv. Water Resour. 102, 53–67. https://doi.org/10.1016/J.ADVWATRES.2017.01.011

De Groeve, T., Poljansek, K., Vernaccini, L., 2015. Index for Risk Management - INFORM. JRC Sci. Policy Reports - Eur. Comm. 96.

De Groeve, T., Poljansek, K., Vernaccini, L., 2014. Index for Risk Management - INFORM: Concept and Methodology. Luxembourg. https://doi.org/10.2788/78658

Dee, D.P., Uppala, S.M., Simmons, A.J., Berrisford, P., Poli, P., Kobayashi, S., Andrae, U., Balmaseda, M.A., Balsamo, G., Bauer, P., Bechtold, P., Beljaars, A.C.M., van de Berg, L., Bidlot, J., Bormann, N., Delsol, C., Dragani, R., Fuentes, M., Geer, A.J., Haimberger, L., Healy, S.B., Hersbach, H., Hólm, E. V., Isaksen, L., Kållberg, P., Köhler, M., Matricardi, M., Mcnally, A.P., Monge-Sanz, B.M., Morcrette, J.J., Park, B.K., Peubey, C., de Rosnay, P., Tavolato, C., Thépaut, J.N., Vitart, F., 2011. The ERA-Interim reanalysis: configuration and performance of the data assimilation system. Q. J. R. Meteorol. Soc. 137, 553–597. https://doi.org/10.1002/QJ.828

Dellink, R., Chateau, J., Lanzi, E., Magné, B., 2017. Long-term economic growth projections in the Shared Socioeconomic Pathways. Glob. Environ. Chang. 42, 200–214.

https://doi.org/10.1016/j.gloenvcha.2015.06.004

DiSera, L., Sjödin, H., Rocklöv, J., Tozan, Y., Súdre, B., Zeller, H., Muñoz, Á.G., 2020. The Mosquito, the Virus, the Climate: An Unforeseen Réunion in 2018. GeoHealth 4, e2020GH000253. https://doi.org/10.1029/2020GH000253

Dottori, F., Salamon, P., Bianchi, A., Alfieri, L., Hirpa, F.A., Feyen, L., 2016. Development and evaluation of a framework for global flood hazard mapping. Adv. Water Resour. 94, 87–102. https://doi.org/https://doi.org/10.1016/j.advwatres.2016.05.002

Droogers, P., Allen, R.G., 2002. Estimating reference evapotranspiration under inaccurate data conditions. Irrig. Drain. Syst. 16, 33–45. https://doi.org/10.1023/A:1015508322413

Dujmović, J., Cordeliers, L., 2006. A comparison of andness/orness indicators, in: Proceedings of the 11th Information Processing and Management of Uncertainty International Conference (IPMU 2006).

DWD, 2021. Climate predictions and climate projections. Offenbach am Main, Germany.

Ebi, K.L., Hallegatte, S., Kram, T., Arnell, N.W., Carter, T.R., Edmonds, J., Kriegler, E., Mathur, R., O'Neill, B.C., Riahi, K., Winkler, H., van Vuuren, D.P., Zwickel, T., 2014. A new scenario framework for climate change research: Background, process, and future directions. Clim. Change 122, 363–372. https://doi.org/10.1007/s10584-013-0912-3

EC, 2021a. Communication from the Commission to the the European Parliament and the Council on the EU's humanitarian action: new challenges, same principles. Brussels.

EC, 2021b. DG ECHO Guidance Note: Disaster Preparedness.

EC, 2021c. Forging a climate-resilient Europe - the new EU Strategy on Adaptation to Climate Change. Brussels.

EC, 2021d. European Civil Protection and Humanitarian Aid Operations: Jordan.

EC, 2020. Overview of natural and man-made disaster risks the European Union may face. Brussels.

EC, 2019a. COMMUNICATION FROM THE COMMISSION TO THE EUROPEAN PARLIAMENT, THE EUROPEAN COUNCIL, THE COUNCIL, THE EUROPEAN ECONOMIC AND SOCIAL COMMITTEE AND THE COMMITTEE OF THE REGIONS: The European Green Deal.

EC, 2019b. EDO Analytical Report: Drought in Europe.

EC, 2018. INDRIX – Inclusive Disaster Resilience Index [WWW Document]. Eur. Comm. URL http://indrix.samaritan-international.eu/project-results-documents/ (accessed 11.30.18).

EC, 2017. Drought Indicators [WWW Document]. Eur. Drought Obs. . URL https://edo.jrc.ec.europa.eu/edov2/php/index.php?id=1010 (accessed 2.16.21).

Eckstein, D., Künzel, V., Schäfer, L., 2021. GLOBAL CLIMATE RISK INDEX 2021: Who Suffers Most from Extreme Weather Events? Weather-Related Loss Events in 2019 and 2000-2019. Bonn, Germany.

ECLAC, 2015. Microseguros agropecuarios y gestión integral de riesgos en Centroamérica y la República 48 Dominicana: lineamientos estratégicos para su desarrollo y fortalecimiento. Mexico.

EEA, 2020. Monitoring and evaluation of national adaptation policies throughout the policy cycle.

EEA, 2017. Climate change adaptation and disaster risk reduction in Europe - Enhancing coherence of the knowledge base, policies and practices, 15/2017. European Environment Agency, Copenhagen (Denmark).

EEA, 2015. National monitoring, reporting and evaluation of climate change adaptation in Europe (No. 20/2015). European Environment Agency, Luxembourg. https://doi.org/10.2800/629559

Erkens, G., Sutanudjaja, E.H., 2015. Towards a global land subsidence map. Proc. Int. Assoc. Hydrol. Sci. 372, 83–87. https://doi.org/10.5194/PIAHS-372-83-2015

ESPON, 2011. ESPON CLIMATE-Climate Change and Territorial Effects on Regions and Local Economies. Luxembourg.

EU, 2008. Joint Statement by the Council and the Representatives of the Governments of the Member States meeting within the Council, the European Parliament and the European Commission.

Farinosi, F., Dosio, A., Calliari, E., Seliger, R., Alfieri, L., Naumann, G., 2020. "Will the Paris Agreement protect us from hydro-meteorological extremes?" Environ. Res. Lett. 15, 104037. https://doi.org/10.1088/1748-

9326/aba869

FEWS, N.E.T., 2018. Hunger-related mortality likely as IPC phase 4 outcomes and large-scale assistance needs persist. FEWS NET.

Fullér, R., 1996. OWA operators in decision making, in: Exploring the Limits of Support Systems. pp. 85–104.

Gao, J., 2017. Downscaling Global Spatial Population Projections from 1/8-degree to 1-km Grid Cells. NCAR Tech. Note NCAR/TN-537+STR. https://doi.org/10.5065/D60Z721H

Gleditsch, K.S., 2016. Transnational Dimensions of Civil War: http://dx.doi.org/10.1177/0022343307076637 44, 293–309. https://doi.org/10.1177/0022343307076637

Goldstone, J.A., Bates, R.H., Epstein, D.L., Gurr, T.R., Lustik, M.B., Marshall, M.G., Ulfelder, J., Woodward, M., 2010. A Global Model for Forecasting Political Instability. Am. J. Pol. Sci. 54, 190–208. https://doi.org/10.1111/J.1540-5907.2009.00426.X

Hallegatte, S., Rentschler, J., Rozenberg, J., 2020. Adaptation Principles. Adapt. Princ. https://doi.org/10.1596/34780

Hargreaves, G.H., 1994. Defining and using reference evapotranspiration. J. Irrig. Drain. Eng. 120, 1132–1139.

Hegre, H., Buhaug, H., Calvin, K. V, Nordkvelle, J., Waldhoff, S.T., Gilmore, E., 2016. Forecasting civil conflict along the shared socioeconomic pathways. Environ. Res. Lett. 11, 054002. https://doi.org/10.1088/1748-9326/11/5/054002

Hegre, H., Karlsen, J., Nygård, H.M., Strand, H., Urdal, H., 2013. Predicting Armed Conflict, 2010-2050. Int. Stud. Q. 57, 250–270. https://doi.org/10.1111/ISQU.12007/2/ISQU12007_F11.JPEG

Hegre, H., Nygård, H.M., Landsverk, P., 2021. Can We Predict Armed Conflict? How the First 9 Years of Published Forecasts Stand Up to Reality. Int. Stud. Q. 65, 660–668. https://doi.org/10.1093/ISQ/SQAA094

Hempel, S., Frieler, K., Warszawski, L., Schewe, J., Piontek, F., 2013. A trend-preserving bias correction – The ISI-MIP approach. Earth Syst. Dyn. 4, 219–236. https://doi.org/10.5194/ESD-4-219-2013

Heslin, A., 2020. Riots and resources: How food access affects collective violence: https://doi.org/10.1177/0022343319898227 58, 199–214. https://doi.org/10.1177/0022343319898227

HIIK, 2019. Conflict Barometer. Heidelberg, Germany.

Hoegh-Guldberg, O., Jacob, D., Taylor, M., Bindi, M., Brown, S., Camilloni, I., Diedhiou, A., Djalante, R., Ebi, K.L., Engelbrecht, F., J.Guiot, Hijioka, Y., Mehrotra, S., Payne, A., Seneviratne, S.I., Thomas, A., Warren, R., Zhou, G., 2018. Impacts of 1.5ºC Global Warming on Natural and Human Systems, in: Masson-Delmotte, V., Zhai, P., Pörtner, H.-O., Roberts, D., Skea, J., Shukla, P.R., Pirani, A., Moufouma-Okia, W., Péan, C., Pidcock, R., Connors, S., Matthews, J.B.R., Chen, Y., Zhou, X., Gomis, M.I., Lonnoy, E., Maycock, T., Tignor, M., Waterfield, T. (Eds.), Global Warming of 1.5°C. An IPCC Special Report on the Impacts of Global Warming of 1.5°C above Pre-Industrial Levels and Related Global Greenhouse Gas Emission Pathways, in the Context of Strengthening the Global Response to the Threat of Climate Change,. Intergovernmental Panel on Climate Change.

Hoshen, M.B., Morse, A.P., 2004. A weather-driven model of malaria transmission. Malar. J. 3, 1–14. https://doi.org/10.1186/1475-2875-3-32/FIGURES/7

IFRC, 2020. World Disasters Report 2020 - Come Heat or High Water. Geneva, Switzerland.

IFRC, 2013. A guide to mainstreaming guiding principles disaster risk reduction and climate change adaptation.

IIED, 2014. Tracking adaptation and measuring development (TAMD) | International Institute for Environment and Development [WWW Document]. Int. Inst. Environ. Dev. URL https://www.iied.org/tracking-adaptation-measuring-development-tamd (accessed 1.25.21).

Ilan, K., 2017. Linking disaster risk reduction, climate change, and the sustainable development goals. Disaster Prev. Manag. An Int. J. 26, 254–258. https://doi.org/10.1108/DPM-02-2017-0043

Inter-Agency Standing Committee and the European Commission, 2022a. INFORM REPORT 2022: Shared evidence for managing crises and disasters, EUR 31081 EN. Publications Office of the European Union, Luxembourg. https://doi.org/10.2760/08333, JRC129343

Inter-Agency Standing Committee and the European Commission, 2022b. INFORM Climate Change: Quantifying the impacts of climate and socio-economic trends on the risk of future humanitarian crises and disasters. Publications Office of the European Union, Luxembourg. https://doi.org/10.2760/383939

IPCC, 2022. Climate Change 2022: Impacts, Adaptation, and Vulnerability. Contribution of Working Group II to the Sixth Assessment Report of the Intergovernmental Panel on Climate Change. Cambridge University Press. https://doi.org/In Press

IPCC, 2021. Summary for Policymakers, in: Masson-Delmotte, V., Zhai, P., Pirani, A., Connors, S.L., Péan, C., Berger, S., Caud, N., Chen, Y., Goldfarb, L., Gomis, M.I., Huang, M., Leitzell, K., Lonnoy, E., Matthews, J.B.R., Maycock, T.K., Waterfield, T., Yelekçi, O., Yu, R., Zhou, B. (Eds.), Climate Change 2021: The Physical Science Basis. Contribution of Working Group I to the Sixth Assessment Report of the Intergovernmental Panel on Climate Change. In Press.

IPCC, 2019. IPCC Special Report on the Ocean and Cryosphere in a Changing Climate.

IPCC, 2014. II Glossary Annex - Climate Change 2014: Impacts, Adaptation and Vulnerability.

Jevrejeva, S., Grinsted, A., Moore, J.C., 2014. Upper limit for sea level projections by 2100. Environ. Res. Lett. 9. https://doi.org/10.1088/1748-9326/9/10/104008

Jiang, L., O'Neill, B.C., 2017. Global urbanization projections for the Shared Socioeconomic Pathways. Glob. Environ. Chang. 42, 193–199. https://doi.org/10.1016/j.gloenvcha.2015.03.008

Jin, L., Kalina, M., Qian, G., 2017. Discrete and continuous recursive forms of OWA operators. Fuzzy Sets Syst. 308, 106–122. https://doi.org/10.1016/J.FSS.2016.04.017

Jones, B., O'Neill, B.C., 2016. Spatially explicit global population scenarios consistent with the Shared Socioeconomic Pathways. Environ. Res. Lett. 11, 084003. https://doi.org/10.1088/1748-9326/11/8/084003

JRC, 2017. Global Conflict Risk Index [WWW Document]. Jt. Res. Cent. Eur. Comm. URL http://conflictrisk.jrc.ec.europa.eu/

Kabesiime, E., Owuor, C., Barihaihi, M., Kajumba, T., 2015. Monitoring and evaluating climate change adaptation and disaster risk reduction in Uganda: TAMD appraisal study.

KC, S., Lutz, W., 2017. The human core of the shared socioeconomic pathways: Population scenarios by age, sex and level of education for all countries to 2100. Glob. Environ. Chang. 42, 181–192. https://doi.org/10.1016/j.gloenvcha.2014.06.004

Keener, V.W., Marra, J.J., Finucane, M.L., Spooner, D., Smith, M.H. (Eds.), 2012. Climate Change and Pacific Islands: Indicators and Impacts. Report for The 2012 Pacific Islands Regional Climate Assessment. Island Press, Washington DC.

Kirezci, E., Young, I.R., Ranasinghe, R., Muis, S., Nicholls, R.J., Lincke, D., Hinkel, J., 2020. Projections of global-scale extreme sea levels and resulting episodic coastal flooding over the 21st Century. Sci. Rep. 10, 1–12. https://doi.org/10.1038/s41598-020-67736-6

Koren, O., Bagozzi, B.E., Benson, T.S., 2021. Food and water insecurity as causes of social unrest: Evidence from geolocated Twitter data: https://doi.org/10.1177/0022343320975091 58, 67–82. https://doi.org/10.1177/0022343320975091

Kriegler, E., Edmonds, J., Hallegatte, S., Ebi, K.L., Kram, T., Riahi, K., Winkler, H., van Vuuren, D.P., 2014. A new scenario framework for climate change research: The concept of shared climate policy assumptions. Clim. Change 122, 401–414. https://doi.org/10.1007/S10584-013-0971-5/FIGURES/2

Lafortune, G., Fuller, G., Moreno, J., Schmidt-Traub, G., Kroll, C., 2018. SDG Index and Dashboards Detailed Methodological paper. New York.

Lindley, S., Cook, P., Dennis, M., Gilchrist, A., 2019. Biodiversity, physical health and climate change: a synthesis of recent evidence, in: Marselle, M., Stadler, J., Korn, H., Irvine, K., Bonn, A. (Eds.), Biodiversity and Health in the Face of Climate Change. Springer Nature.

Liu-Helmersson, J., Quam, M., Wilder-Smith, A., Stenlund, H., Ebi, K., Massad, E., Rocklöv, J., 2016. Climate Change and Aedes Vectors: 21st Century Projections for Dengue Transmission in Europe. EBioMedicine 7, 267–277. https://doi.org/10.1016/J.EBIOM.2016.03.046

Liu-Helmersson, J., Rocklöv, J., Sewe, M., Brännström, Å., 2019. Climate change may enable Aedes aegypti infestation in major European cities by 2100. Environ. Res. 172, 693–699. https://doi.org/10.1016/J.ENVRES.2019.02.026

Liu, Y., Chen, J., 2021. Future global socioeconomic risk to droughts based on estimates of hazard, exposure, and vulnerability in a changing climate. Sci. Total Environ. 751, 142159. https://doi.org/10.1016/j.scitotenv.2020.142159

Mach, K.J., Planton, S., von Stechow, C., 2014. IPCC, 2014: Annex II: Glossary. Cli- mate Chang. 2014 Synth. Report. Contrib. Work. Groups I, II III to Fifth Assess. Rep. Intergov. Panel Clim. Chang.

Mahmood, R., Jia, S., Zhu, W., 2019. Analysis of climate variability, trends, and prediction in the most active parts of the Lake Chad basin, Africa. Sci. Reports 2019 91 9, 1–18. https://doi.org/10.1038/s41598-019-42811-9

Marin-Ferrer, M., Vernaccini, L., Poljansek, K., 2017. Index for Risk Management - INFORM. Concept and Methodology. Luxembourg.

Marzi, S., Mysiak, J., Essenfelder, A.H., Amadio, M., Giove, S., Fekete, A., 2019. Constructing a comprehensive disaster resilience index: The case of Italy. PLoS One 14. https://doi.org/10.1371/journal.pone.0221585

Marzi, S., Mysiak, J., Essenfelder, A.H., Pal, J.S., Vernaccini, L., Mistry, M.N., Alfieri, L., Poljansek, K., Marin-Ferrer, M., Vousdoukas, M., 2021. Assessing future vulnerability and risk of humanitarian crises using climate change and population projections within the INFORM framework. Glob. Environ. Chang. 71, 102393. https://doi.org/10.1016/J.GLOENVCHA.2021.102393

Marzi, S., Mysiak, J., Santato, S., 2018. Comparing adaptive capacity index across scales: The case of Italy. J. Environ. Manage. 223, 1023–1036. https://doi.org/10.1016/j.jenvman.2018.06.060

McMichael, C., Dasgupta, S., Ayeb-Karlsson, S., Kelman, I., 2020. A review of estimating population exposure to sea-level rise and the relevance for migration. Environ. Res. Lett. 15, 123005. https://doi.org/10.1088/1748-9326/ABB398

Merkens, J.-L., Reimann, L., Hinkel, J., Vafeidis, A.T., 2016. Gridded population projections for the coastal zone under the Shared Socioeconomic Pathways. Glob. Planet. Change 145, 57–66. https://doi.org/https://doi.org/10.1016/j.gloplacha.2016.08.009

Messina, L., Poljansek, K., Vernaccini, L., 2019. Usage of INFORM GRI in Humanitarian Aid and Development Assistance Initiatives, EUR 29894 EN. Luxembourg. https://doi.org/doi:10.2760/591043

Miola, A., Papadimitriou, E., Mandrici, A., McCormick, N., Gobron, N., 2015. INDEX FOR THE EU GLOBAL CLIMATE CHANGE ALLIANCE plus flagship Initiative. EUR 27480, Publications Office of the European Union. Luxebourg.

Mordecai, E.A., Caldwell, J.M., Grossman, M.K., Lippi, C.A., Johnson, L.R., Neira, M., Rohr, J.R., Ryan, S.J., Savage, V., Shocket, M.S., Sippy, R., Stewart Ibarra, A.M., Thomas, M.B., Villena, O., 2019. Thermal biology of mosquito-borne disease. Ecol. Lett. 22, 1690–1708. https://doi.org/10.1111/ELE.13335

Mordecai, E.A., Ryan, S.J., Caldwell, J.M., Shah, M.M., LaBeaud, A.D., 2020. Climate change could shift disease burden from malaria to arboviruses in Africa. Lancet Planet. Heal. 4, e416–e423. https://doi.org/10.1016/S2542-5196(20)30178-9

Muis, S., Verlaan, M., Winsemius, H.C., Aerts, J.C.J.H., Ward, P.J., 2016. A global reanalysis of storm surges and extreme sea levels. Nat. Commun. 7, 1–12. https://doi.org/10.1038/ncomms11969

Murnane, R.J., Daniell, J.E., Schäfer, A.M., Ward, P.J., Winsemius, H.C., Simpson, A., Tijssen, A., Toro, J., 2017. Future scenarios for earthquake and flood risk in Eastern Europe and Central Asia. Earth's Futur. 5, 693–714. https://doi.org/10.1002/2016EF000481

Mysiak, J., Torresan, S., Bosello, F., Mistry, M., Amadio, M., Marzi, S., Furlan, E., Sperotto, A., 2018. Climate risk index for Italy. Philos. Trans. R. Soc. A Math. Phys. Eng. Sci. 376. https://doi.org/10.1098/rsta.2017.0305

Nardo, M., Saisana, M., Saltelli, A., Tarantola, S., 2005. Tools for Composite Indicators Building (No. EUR 21869 EN).

Naumann, G., Alfieri, L., Wyser, K., Mentaschi, L., Betts, R.A., Carrao, H., Spinoni, J., Vogt, J., Feyen, L., 2018. Global Changes in Drought Conditions Under Different Levels of Warming. Geophys. Res. Lett. 45, 3285–3296. https://doi.org/10.1002/2017GL076521

NCCS, 2020. NASA Earth Exchange Global Daily Downscaled Projections (NEX-GDDP) [WWW Document]. NASA Cent. Clim. Simul. URL https://www.nccs.nasa.gov/services/data-collections/land-based-products/nex-gddp (accessed 6.9.20).

Norwegian Red Cross, 2019. Overlapping vulnerabilities: the impacts of climate change on humanitarian needs. Norwegian Red Cross, Oslo.

O'Neill, B.C., Carter, T.R., Ebi, K., Harrison, P.A., Kemp-Benedict, E., Kok, K., Kriegler, E., Preston, B.L., Riahi, K., Sillmann, J., van Ruijven, B.J., van Vuuren, D., Carlisle, D., Conde, C., Fuglestvedt, J., Green, C., Hasegawa, T., Leininger, J., Monteith, S., Pichs-Madruga, R., 2020. Achievements and needs for the climate change scenario framework. Nat. Clim. Chang. 10, 1074–1084. https://doi.org/10.1038/s41558-020-00952-0

O'Neill, B.C., Carter, T.R., Ebi, K.L., Edmonds, J., Hallegatte, S., Kemp-Benedict, E., Kriegler, E., Mearns, L., Moss, R., Riahi, K., van Ruijven, B., van Vuuren, D., 2012. Meeting Report of the Workshop on The Nature and Use of New Socioeconomic Pathways for Climate Change Research, Boulder, CO, November 2-4, 2011.

O'Neill, B.C., Kriegler, E., Ebi, K.L., Kemp-Benedict, E., Riahi, K., Rothman, D.S., van Ruijven, B.J., van Vuuren, D.P., Birkmann, J., Kok, K., Levy, M., Solecki, W., 2017. The roads ahead: Narratives for shared socioeconomic pathways describing world futures in the 21st century. Glob. Environ. Chang. 42, 169–180. https://doi.org/10.1016/j.gloenvcha.2015.01.004

O'Neill, B.C., Kriegler, E., Riahi, K., Ebi, K.L., Hallegatte, S., Carter, T.R., Mathur, R., van Vuuren, D.P., 2014. A new scenario framework for climate change research: the concept of shared socioeconomic pathways. Clim. Change 122, 387–400. https://doi.org/10.1007/s10584-013-0905-2

OCHA, 2014. Saving Lives Today and Tomorrow: Managing the Risk of Humanitarian Crises.

OECD, 2020. Common Ground Between the Paris Agreement and the Sendai Framework. https://doi.org/https://doi.org/https://doi.org/10.1787/3edc8d09-en

OECD, 2008. Handbook on constructing composite indicators. OECD Publ.

Outten, S., Sobolowski, S., 2021. Extreme wind projections over Europe from the Euro-CORDEX regional climate models. Weather Clim. Extrem. 33, 100363. https://doi.org/10.1016/J.WACE.2021.100363

Pappenberger, F., Dutra, E., Wetterhall, F., Cloke, H.L., 2012. Deriving global flood hazard maps of fluvial floods through a physical model cascade. Hydrol. Earth Syst. Sci. 16, 4143–4156. https://doi.org/10.5194/hess-16-4143-2012

Paruolo, P., Saisana, M., Saltelli, A., 2012. Ratings and rankings: voodoo or science? J. R. Stat. Soc. 176, 609–634. https://doi.org/First published10.1111/j.1467-985X.2012.01059.x

Pesaresi, M., Ehrlich, D., Ferri, S., Florczyk, A., Freire, S., Halkia, M., Julea, A., Kemper, T., Soille, P., Syrris, V., 2016. Operating procedure for the production of the Global Human Settlement Layer from Landsat data of the epochs 1975, 1990, 2000, and 2014.

Pinar, M., Cruciani, C., Giove, S., Sostero, M., 2014. Constructing the FEEM sustainability index: A Choquet integral application. Ecol. Indic. 39, 189–202. https://doi.org/10.1016/J.ECOLIND.2013.12.012

Poljansek, K., Casajus Valles, A., Marin Ferrer, M., Artes Vivancos, T., Boca, R., Bonadonna, C., Branco, A., Campanharo, W., De Jager, A., De Rigo, D., Dottori, F., Durrant Houston, T., Estreguil, C., Ferrari, D., Frischknecht, C., Galbusera, L., Garcia Puerta, B., Giannopoulos, G., Girgin, S., Gowland, R., Grecchi, R., Hernandez Ceballos, M.A., Iurlaro, G., Kambourakis, G., Karlos, V., Krausmann, E., Larcher, M., Lequarre, A.S., Liberta`, G., Loughlin, S.C., Maianti, P., Mangione, D., Marques, A., Menoni, S., Montero Prieto, M., Naumann, G., Jacome Felix Oom, D., Pfieffer, H., Robuchon, M., Necci, A., Salamon, P., San-Miguel-Ayanz, J., Angiorgi, M., Raposo De, M., Do, N.E.S., De Sotto Mayor, M.L., Theocharidou, M., Trueba Alonso, C., Theodoridis, G., Tsionis, G., Vogt, J., Wood, M., 2021. Recommendations for National Risk Assessment for Disaster Risk Management in EU: Where Science and Policy Meet, Version 1, EUR 30596 EN. Publications Office of the European Union, Luxembourg. https://doi.org/10.2760/80545, JRC123585

Poljanšek, K., Casajus Valles, A., Marín Ferrer, M., De Jager, A., Dottori, F., Galbusera, L., García Puerta, B., Giannopoulos, G., Girgin, S., Angel Hernandez Ceballos, M., Iurlaro, G., Karlos, V., Krausmann, E., Larcher, M., Sophie Lequarre, A., Marianthi, T., Montero Prieto, M., Naumann, G., Necci, A., Salamon, P., Sangiorgi, M., Luísa Sousa, M., Trueba Alonso, C., Tsionis, G., Vogt, J. V, 2019a. Recommendations for National Risk Assessment for Disaster Risk Management in EU. EUR 29557 EN, Publications Office of the European Union. https://doi.org/10.2760/084707

Poljansek, K., Disperati, P., Vernaccini, L., Nika, A., Marzi, S., Essenfelder, A.H., 2020. INFORM Severity Index, EUR 30400 EN, JRC122162 ed, Publications Office of the European Union. Luxembourg. https://doi.org/10.2760/94802

Poljanšek, K., Ferrer, M., Vernaccini, L., Marzi, S., Messina, L., 2019b. Review of the Sendai Framework Monitor and Sustainable Development Goals indicators for inclusion in the INFORM Global Risk Index of the Sendai Framework Monitor and Sustainable Development Goals indicators for inclusion in the, in: INFORM Global Risk Index. https://doi.org/10.2760/54937

Poljansek, K., Ferrer, M.M., Groeve, T. De, Clark, I., 2017. Science for disaster risk management 2017: knowing better and losing less. Publ. Off. Eur. Union EUR 28034 EN. https://doi.org/10.2788/842809, JRC102482

Poljanšek, K., Marin-Ferrer, M., Vernaccini, L., Messina, L., 2018. Incorporating epidemics risk in the INFORM Global Risk Index, EUR 29603 EN, JRC114652 ed. Publications Office of the European Union, Luxembourg. https://doi.org/10.2760/647382

Puth, M.T., Neuhäuser, M., Ruxton, G.D., 2015. Effective use of Spearman's and Kendall's correlation coefficients for association between two measured traits. Anim. Behav. 102, 77–84. https://doi.org/10.1016/J.ANBEHAV.2015.01.010

RESIN, 2018. European Climate Risk Typology [WWW Document]. Eur. Comm. URL http://european-crt.org/map.html (accessed 12.3.18).

Riahi, K., van Vuuren, D.P., Kriegler, E., Edmonds, J., O'Neill, B.C., Fujimori, S., Bauer, N., Calvin, K., Dellink, R., Fricko, O., Lutz, W., Popp, A., Cuaresma, J.C., KC, S., Leimbach, M., Jiang, L., Kram, T., Rao, S., Emmerling, J., Ebi, K., Hasegawa, T., Havlik, P., Humpenöder, F., Da Silva, L.A., Smith, S., Stehfest, E., Bosetti, V., Eom, J., Gernaat, D., Masui, T., Rogelj, J., Strefler, J., Drouet, L., Krey, V., Luderer, G., Harmsen, M., Takahashi, K., Baumstark, L., Doelman, J.C., Kainuma, M., Klimont, Z., Marangoni, G., Lotze-Campen, H., Obersteiner, M., Tabeau, A., Tavoni, M., 2017. The Shared Socioeconomic Pathways and their energy, land use, and greenhouse gas emissions implications: An overview. Glob. Environ. Chang. 42, 153–168. https://doi.org/10.1016/j.gloenvcha.2016.05.009

Rojas, O., 2018. Agricultural extreme drought assessment at global level using the FAO-Agricultural Stress Index System (ASIS). Weather Clim. Extrem. https://doi.org/10.1016/j.wace.2018.09.001

Rudari, R., Silvestro, F., Campo, L., Rebora, N., Boni, G., Herold, C., 2015. Improvement of the global flood model for the GAR 2015. United Nations Office for Disaster Risk Reduction (UNISDR), Centro Internazionale in Monitoraggio Ambientale (CIMA), UNEP GRID-Arendal (GRID-Arendal), Geneva, Switzerland.

Ryan-Mosley, T., 2019. We are Finally Getting Better at Predicting Organized Conflict. MIT Technol. Rev. 122.

Ryan, S.J., Carlson, C.J., Mordecai, E.A., Johnson, L.R., 2019. Global expansion and redistribution of Aedes-borne virus transmission risk with climate change. PLoS Negl. Trop. Dis. 13, e0007213. https://doi.org/10.1371/JOURNAL.PNTD.0007213

Ryan, S.J., Lippi, C.A., Zermoglio, F., 2020. Shifting transmission risk for malaria in Africa with climate change: A framework for planning and intervention. Malar. J. 19, 1–14. https://doi.org/10.1186/S12936-020-03224-6/FIGURES/7

Saisana, M., Saltelli, A., 2008. Uncertainty and Sensitivity Analysis of the 2008 Environmental Performance Index. European Communities, Luxembourg. https://doi.org/10.2788/91982

Saito, T., Kubota, T., 2020. Tsunami Modeling for the Deep Sea and Inside Focal Areas. https://doi.org/10.1146/annurev-earth-071719-054845 48, 121–145. https://doi.org/10.1146/ANNUREV-EARTH-071719-054845

Service, T.S.P., 2019. Voluntary National Review of Turkmenistan.

Smirnov, O., Zhang, M., Xiao, T., Orbell, J., Lobben, A., Gordon, J., 2016. The relative importance of climate change and population growth for exposure to future extreme droughts. Clim. Change 138, 41–53. https://doi.org/10.1007/s10584-016-1716-z

Spinoni, J., Barbosa, P., Bucchignani, E., Cassano, J., Cavazos, T., Christensen, J.H., Christensen, O.B., Coppola, E., Evans, J., Geyer, B., Giorgi, F., Hadjinicolaou, P., Jacob, D., Katzfey, J., Koenigk, T., Laprise, R., Lennard, C.J., Kurnaz, M.L., Li, D., Llopart, M., McCormick, N., Naumann, G., Nikulin, G., Ozturk, T., Panitz, H.-J., Rocha, R.P. da, Rockel, B., Solman, S.A., Syktus, J., Tangang, F., Teichmann, C., Vautard, R., Vogt, J. V., Winger, K., Zittis, G., Dosio, A., 2020. Future Global Meteorological Drought Hot Spots: A Study Based on CORDEX Data. J.

Clim. 33, 3635–3661. https://doi.org/10.1175/JCLI-D-19-0084.1

Spinoni, J., Barbosa, P., De Jager, A., McCormick, N., Naumann, G., Vogt, J. V., Magni, D., Masante, D., Mazzeschi, M., 2019. A new global database of meteorological drought events from 1951 to 2016. J. Hydrol. Reg. Stud. 22, 100593. https://doi.org/10.1016/J.EJRH.2019.100593

Sutanudjaja, E.H., Van Beek, R., Wanders, N., Wada, Y., Bosmans, J.H.C., Drost, N., Van Der Ent, R.J., De Graaf, I.E.M., Hoch, J.M., De Jong, K., Karssenberg, D., López López, P., Peßenteiner, S., Schmitz, O., Straatsma, M.W., Vannametee, E., Wisser, D., Bierkens, M.F.P., 2018. PCR-GLOBWB 2: A 5 arcmin global hydrological and water resources model. Geosci. Model Dev. 11, 2429–2453. https://doi.org/10.5194/GMD-11-2429-2018

Svoboda, M., Fuchs, B.A., 2016. Handbook of Drought Indicators and Indices. Integrated Drought Management Programme, Integrated Drought Management Tools and Guidelines Series 2. WMO and GWP.

Tate, E., 2012. Social vulnerability indices: a comparative assessment using uncertainty and sensitivity analysis. Nat. Hazards 63, 325–347. https://doi.org/10.1007/s11069-012-0152-2

Tavares, A.O., Barros, J.L., Freire, P., Santos, P.P., Perdiz, L., Fortunato, A.B., 2021. A coastal flooding database from 1980 to 2018 for the continental Portuguese coastal zone. Appl. Geogr. 135, 102534. https://doi.org/10.1016/J.APGEOG.2021.102534

The World Bank, 2016. Climate change and Disaster Management: Pacific Possible Background Paper No.6. Washington DC.

Tompkins, A.M., Ermert, V., 2013. A regional-scale, high resolution dynamical malaria model that accounts for population density, climate and surface hydrology. Malar. J. 12, 1–24. https://doi.org/10.1186/1475-2875-12-65/FIGURES/13

Törnros, T., Menzel, L., 2014. Addressing drought conditions under current and future climates in the Jordan River region. Hydrol. Earth Syst. Sci. 18, 305–318. https://doi.org/10.5194/hess-18-305-2014

UK Centre for Ecology and Hydrology, 2020. SPEI [WWW Document]. URL https://eip.ceh.ac.uk/apps/droughts/spei.html (accessed 12.6.20).

UN, 2016. Too important to fail-addressing the humanitarian financing gap, High-Level Panel on Humanitarian Financing Report to the Secretary-General.

UN, 2015. Transforming our World: The 2030 Agenda for Sustainable Development. A/RES/70/1.

UNCT, 2017. The United Nations Country Team Common Country Assessment of Hashemite Kingdom of Jordan.

UNDP, 2004. Reducing Disaster Risk, A Challenge for Development. United Nations Development Programme, New York, USA.

UNDRR, 2019. Global Assessment Report on Disaster Risk Reduction. Geneva, Switzerland.

UNECE, 2012. Turkmenistan Environmental Performance Reviews.

UNFCCC, 2020. As Climate Impacts Increase, UN Agencies Step Up Cooperation on Disaster Risk Reduction | UNFCCC [WWW Document].

UNFPA, 2015. Maternal Mortality in Humanitarian Crises and in Fragile Settings.

UNHCR, 2021. Climate change and disaster displacement [WWW Document]. URL https://www.unhcr.org/climate-change-and-disasters.html (accessed 3.13.22).

UNISDR, 2015a. Sendai Framework for Disaster Risk Reduction 2015-2030.

UNISDR, 2015b. Indicators for Measuring the Integration of Disaster Risk Reduction in UN Programming.

UNISDR, 2015c. Making Development Sustainable: The Future of Disaster Risk Management. Global Assessment Report on Disaster Risk Reduction. Geneva.

UNISDR, 2015d. The Human Cost of Weather-Related Disasters 1995-2015.

UNISDR, 2007. Hyogo Framework for Action 2005-2015.

University of Notre Dame, 2018. ND - GAIN: Notre Dame Global Adaptation Initiative [WWW Document]. Notre Dame Glob. Adapt. Initiat. URL https://gain.nd.edu/our-work/country-index/methodology/ (accessed 11.30.18).

Vafeidis, A.T., Nicholls, R.J., McFadden, L., Tol, R.S.J., Hinkel, J., Spencer, T., Grashoff, P.S., Boot, G., Klein, R.J.T., 2008. A New Global Coastal Database for Impact and Vulnerability Analysis to Sea-Level Rise. J. Coast. Res. 244, 917–924. https://doi.org/10.2112/06-0725.1

Vafeidis, A.T., Schuerch, M., Wolff, C., Spencer, T., Merkens, J.L., Hinkel, J., Lincke, D., Brown, S., Nicholls, R.J., 2019. Water-level attenuation in global-scale assessments of exposure to coastal flooding: A sensitivity analysis. Nat. Hazards Earth Syst. Sci. 19, 973–984. https://doi.org/10.5194/NHESS-19-973-2019

van Vuuren, D.P., Kriegler, E., O'Neill, B.C., Ebi, K.L., Riahi, K., Carter, T.R., Edmonds, J., Hallegatte, S., Kram, T., Mathur, R., Winkler, H., 2014. A new scenario framework for Climate Change Research: Scenario matrix architecture. Clim. Change 122, 373–386. https://doi.org/10.1007/s10584-013-0906-1

van Vuuren, D.P., Riahi, K., Calvin, K., Dellink, R., Emmerling, J., Fujimori, S., KC, S., Kriegler, E., O'Neill, B., 2017. The Shared Socio-economic Pathways: Trajectories for human development and global environmental change. Glob. Environ. Chang. https://doi.org/10.1016/j.gloenvcha.2016.10.009

Vicente-Serrano, S.M., Beguería, S., López-Moreno, J.I., 2010. A Multiscalar Drought Index Sensitive to Global Warming: The Standardized Precipitation Evapotranspiration Index. J. Clim. 23, 1696–1718. https://doi.org/10.1175/2009JCLI2909.1

Vousdoukas, M.I., Mentaschi, L., Hinkel, J., Ward, P.J., Mongelli, I., Ciscar, J.C., Feyen, L., 2020. Economic motivation for raising coastal flood defenses in Europe. Nat. Commun. 11, 1–11. https://doi.org/10.1038/s41467-020-15665-3

Vousdoukas, M.I., Mentaschi, L., Voukouvalas, E., Verlaan, M., Jevrejeva, S., Jackson, L.P., Feyen, L., 2018. Global probabilistic projections of extreme sea levels show intensification of coastal flood hazard. Nat. Commun. 9, 2360. https://doi.org/10.1038/s41467-018-04692-w

Wald, D.J., Quitoriano, V., Heaton, T.H., Kanamori, H., 1999. Relationships between Peak Ground Acceleration, Peak Ground Velocity, and Modified Mercalli Intensity in California: https://doi.org/10.1193/1.1586058 15, 557–564. https://doi.org/10.1193/1.1586058

Walton, D., van Aalst, M.K., 2020. Climate-related extreme weather events and COVID-19. A first look at the number of people affected by intersecting disasters. IFRC, Geneva.

Wang, M.W., Stanley, J.C., 1970. Differential Weighting: A Review of Methods and Empirical Studies. Rev. Educ. Res. 40, 663–705. https://doi.org/10.3102/00346543040005663

Ward, P.J., Jongman, B., Weiland, F.S., Bouwman, A., Van Beek, R., Bierkens, M.F.P., Ligtvoet, W., Winsemius, H.C., 2013. Assessing flood risk at the global scale: Model setup, results, and sensitivity. Environ. Res. Lett. 8, 044019. https://doi.org/10.1088/1748-9326/8/4/044019

Ward, P.J., Winsemius, H.C., Kuzma, S., Bierkens, M.F., Bouwman, A., De Moel, H., Loaiza, A.D., Eilander, D., Englhardt, J., Erkens, G., Gebremedhin, E.T., 2020. Aqueduct Floods Methodology. World Resour. Inst. 1–28.

Watts, N., Amann, M., Arnell, N., Al., E., 2019. The 2019 report of The Lancet Countdown on health and climate change: ensuring that the health of a child born today is not defined by a changing climate. Lancet 394, 1836–78. https://doi.org/10.1016/S0140-6736(19)32596-6

Weedon, G.P., Balsamo, G., Bellouin, N., Gomes, S., Best, M.J., Viterbo, P., 2014. The WFDEI meteorological forcing data set: WATCH Forcing Data methodology applied to ERA-Interim reanalysis data. Water Resour. Res. 50, 7505–7514. https://doi.org/10.1002/2014WR015638

Weedon, G.P., Gomes, S., Viterbo, P., Shuttleworth, W.J., Blyth, E., ÖSterle, H., Adam, J.C., Bellouin, N., Boucher, O., Best, M., 2011. Creation of the WATCH Forcing Data and Its Use to Assess Global and Regional Reference Crop Evaporation over Land during the Twentieth Century. J. Hydrometeorol. 12, 823–848. https://doi.org/10.1175/2011JHM1369.1

Welle, T., Birkmann, J., 2015. The World Risk Index – An Approach to Assess Risk and Vulnerability on a Global Scale. J. Extrem. Events 02, 1550003. https://doi.org/10.1142/S2345737615500037

WHO, 2021a. World health statistics 2021: monitoring health for the SDGs, sustainable development goals. Geneva.

WHO, 2021b. World malaria report. Geneva.

WHO, 2019. World malaria report. Geneva.

WHO, 2018. COP24 special report: health and climate change. Geneva.

Wijenayake, V., 2019. Integration of SDGs, the Sendai Framework, DRR, and NDCs for Effective Development Planning. Asia-Pacific Network for Global Change Research.

Winsemius, H.C., Van Beek, L.P.H., Jongman, B., Ward, P.J., Bouwman, A., 2013. A framework for global river flood risk assessments. Hydrol. Earth Syst. Sci. 17, 1871–1892. https://doi.org/10.5194/hess-17-1871-2013

WMO, 2021. Updated 30-year reference period reflects changing climate [WWW Document]. URL https://public.wmo.int/en/media/news/updated-30-year-reference-period-reflects-changing-climate (accessed 3.13.22).

World Bank, 2018. Systematic Country Diagnostic of Senegal.

World Bank, 2013. World Development Report 2014 : Risk and Opportunity — Managing Risk for Development.

Yager, R., 1988. On ordered weighted averaging aggregation operators in multicriteria decisionmaking. IEEE Trans. Syst. Man. Cybern. 18, 183–190.

Yager, R.R., 1988. On ordered weighted averaging aggregation operators in multi-criteria decision making. IEEE Trans. Syst. Man Cybern. 18, 183–190.

Yamazaki, D., Kanae, S., Kim, H., Oki, T., 2011. A physically based description of floodplain inundation dynamics in a global river routing model. Water Resour. Res. 47. https://doi.org/10.1029/2010WR009726

Zabeo, A., 2011. A decision support system for the assessment and management of surface waters. Ca'Foscari University of Venice.

List of boxes

List of tables

List of figures

Annexes

Annex 1. Correlation matrix - INFORM Climate Change Risk Baseline. Element i,j equals to the Pearson's correlation coefficient between the i th row and the j th column variable.

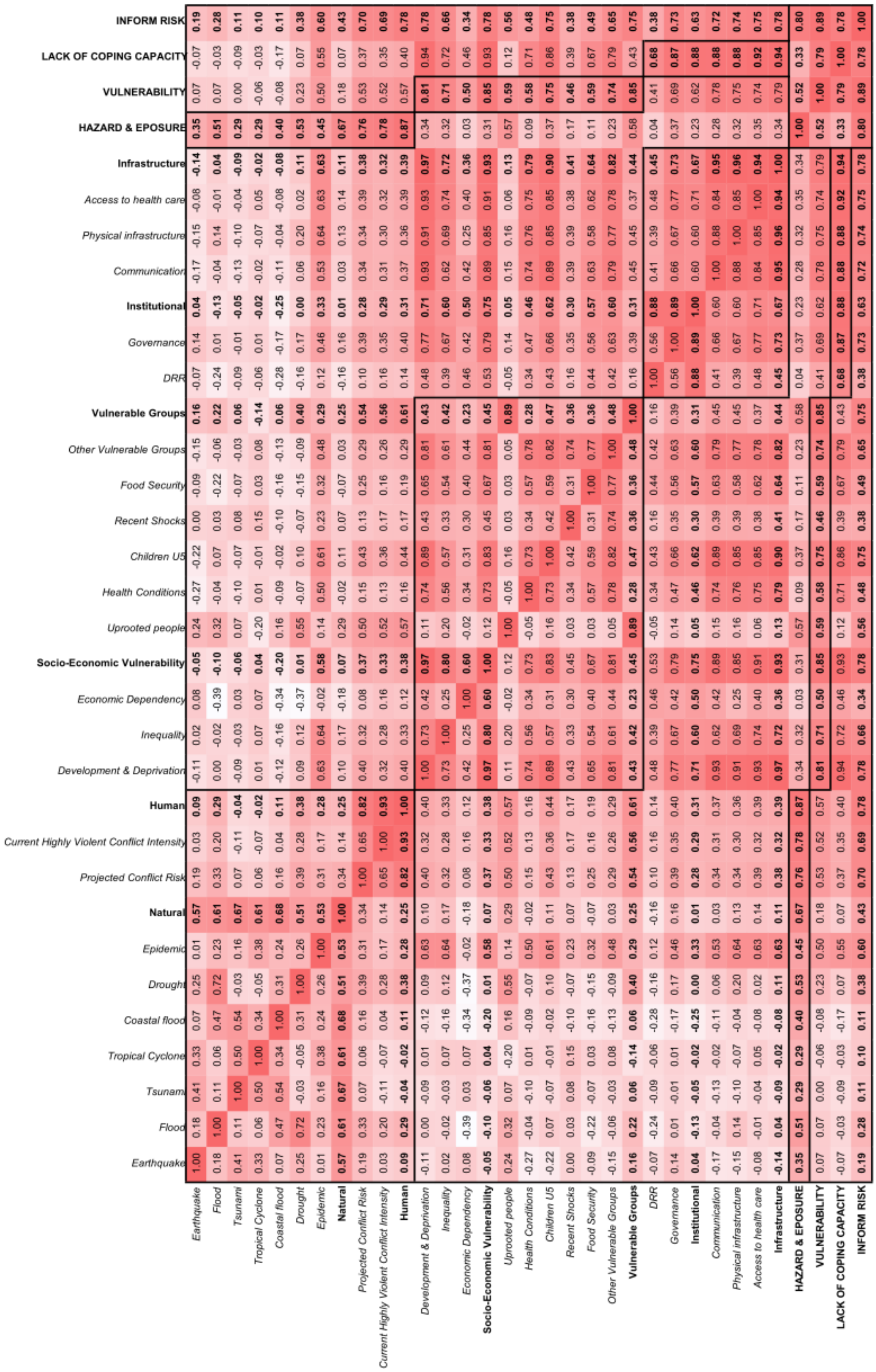

Annex 2. Comparison between INFORM Risk 2022 and INFORM Climate Change Risk Baseline – risk, risk class, Hazard&Exposure, Natural and Human components.

Version		INFORM Risk 2022					INFORM Climate Change Risk Baseline					
COUNTRY	**ISO3**	**RISK**	**RISK CLASS**	**HAZARD & EXPOSURE**	**Natural**	**Human**	**RISK**	**RISK CLASS**	**HAZARD & EXPOSURE**	**Natural**	**Human**	**Shifts**
Afghanistan	AFG	8.2	Very High	8.9	6.7	10	8	Very High	8.4	4.5	10	No
Albania	ALB	2.8	Low	3.8	6.3	0.1	2.6	Low	3	5.2	0.1	No
Algeria	DZA	4	Medium	5.1	4.9	5.3	3.9	Medium	4.8	4.4	5.2	No
Angola	AGO	4.8	Medium	3	3.2	2.8	4.5	Medium	2.6	3.6	1.5	No
Antigua and Barbuda	ATG	2.1	Low	2	3.7	0	2	Low	1.6	3	0	No
Argentina	ARG	2.9	Low	2.6	4	0.9	2.9	Low	2.6	4.4	0.3	No
Armenia	ARM	5.4	High	8.4	4.4	10	5.3	High	8.1	2.9	10	No
Australia	AUS	2.3	Low	2.7	4.8	0	2.4	Low	3	5.1	0.1	No
Austria	AUT	1.7	Very Low	1.3	2.5	0	1.9	Very Low	1.7	3.1	0.1	No
Azerbaijan	AZE	5.9	High	8.5	4.8	10	5.8	High	8.2	3.3	10	No
Bahamas	BHS	2.2	Low	1.8	3.3	0	1.9	Very Low	1.2	2.3	0	Yes
Bahrain	BHR	1.2	Very Low	0.5	0.9	0.1	1.1	Very Low	0.4	0.6	0.1	No
Bangladesh	BGD	5.7	High	6.9	8.2	5	5.5	High	6.3	8.3	2.8	No
Barbados	BRB	2	Low	2.1	3.8	0	1.8	Very Low	1.6	2.9	0	Yes
Belarus	BLR	1.8	Very Low	1.8	2	1.6	1.4	Very Low	0.9	1.7	0.1	No
Belgium	BEL	1.7	Very Low	1.2	1.8	0.5	1.9	Very Low	1.8	3.3	0.1	No
Belize	BLZ	3.9	Medium	3.1	5.4	0	3.3	Low	2	3.6	0	Yes
Benin	BEN	4.5	Medium	2.7	2.9	2.4	4.1	Medium	2	3.2	0.6	No
Bhutan	BTN	3.1	Low	1.9	3.5	0	3.2	Low	2	3.5	0.1	No
Bolivia	BOL	4.2	Medium	3.8	4.7	2.8	3.5	Medium	2.1	3.8	0.1	No
Bosnia and Herzegovina	BIH	3.5	Medium	2.5	4	0.8	3.1	Low	1.7	3	0.1	Yes
Botswana	BWA	3.1	Low	1.7	2.8	0.4	2.9	Low	1.5	2.8	0.1	No
Brazil	BRA	4.9	Medium	7.2	4	9	5	High	7.7	5.6	9	Yes
Brunei Darussalam	BRN	1.7	Very Low	1.4	2.7	0	1.9	Very Low	1.9	3.4	0	No
Bulgaria	BGR	2.5	Low	2.2	3.5	0.6	2.2	Low	1.6	2.9	0.1	No
Burkina Faso	BFA	6.4	High	5.5	3.5	7	6.4	High	5.4	3.3	7	No
Burundi	BDI	5.9	High	4.7	3.6	5.7	5.1	High	3	3.3	2.7	No
Cabo Verde	CPV	2.2	Low	0.9	1.7	0.1	1.9	Very Low	0.6	1	0.1	Yes
Cambodia	KHM	4.6	Medium	3.9	5.8	1.3	4.6	Medium	3.9	5.3	2.1	No
Cameroon	CMR	6.1	High	5.6	3.7	7	6.2	High	5.8	4.3	7	No
Canada	CAN	2.4	Low	2.5	4.3	0.1	2.5	Low	3	5.1	0.1	No
Central African Republic	CAF	7.8	Very High	6.2	3.2	8	7.7	Very High	6	2.8	8	No
Chad	TCD	7.9	Very High	7.3	4.1	9	7.8	Very High	7.1	3.3	9	No
Chile	CHL	3.6	Medium	4.5	6.2	2.1	3.3	Low	3.6	5.9	0.2	Yes
China	CHN	4.1	Medium	6.4	7.5	4.9	3.9	Medium	5.8	8.3	1.2	No
Colombia	COL	5.4	High	6.9	6.7	7	5.4	High	6.8	6.6	7	No
Comoros	COM	3.8	Medium	1.5	2.7	0.1	3.8	Medium	1.5	2.5	0.3	No
Congo	COG	5.4	High	3.1	3.9	2.2	5.2	High	2.8	4.5	0.6	No
Congo DR	COD	7.6	Very High	7.4	4.6	9	7.6	Very High	7.3	4.3	9	No

Costa Rica	CRI	3.2	Low	3.6	6	0.1	3.2	Low	3.5	5.9	0.1	No
Côte d'Ivoire	CIV	5.4	High	4	3.9	4	4.7	Medium	2.7	3.9	1.3	Yes
Croatia	HRV	2.3	Low	2.8	4.8	0.1	2.2	Low	2.5	4.4	0.1	No
Cuba	CUB	2.4	Low	3.7	5.6	1.2	2.4	Low	3.5	5.9	0.1	No
Cyprus	CYP	2.9	Low	2.4	4.3	0	2.6	Low	1.8	3.3	0.1	No
Czech Republic	CZE	1.1	Very Low	0.9	1.7	0	1.2	Very Low	1.2	2.1	0.1	No
Denmark	DNK	1.1	Very Low	0.6	1.2	0	1.4	Very Low	1.2	2.2	0.1	No
Djibouti	DJI	5.2	High	3.8	5.5	1.6	4.4	Medium	2.3	3.7	0.6	Yes
Dominica	DMA	3	Low	2.8	4.9	0	2.6	Low	1.9	3.5	0	No
Dominican Republic	DOM	4.3	Medium	4.5	6.7	1.3	4.2	Medium	4.2	6.8	0.1	No
Ecuador	ECU	4.5	Medium	4.6	6.9	1.1	4.4	Medium	4.4	7	0.1	No
Egypt	EGY	4.7	Medium	6.1	4.9	7	4.8	Medium	6.3	5.4	7	No
El Salvador	SLV	4.6	Medium	4.9	6.6	2.5	4.3	Medium	3.9	6.3	0.4	No
Equatorial Guinea	GNQ	3.7	Medium	2	2.9	1.1	3.8	Medium	2.1	3.8	0.1	No
Eritrea	ERI	5.8	High	5.3	3.5	6.7	4	Medium	1.8	2.7	0.9	Yes
Estonia	EST	0.8	Very Low	0.5	0.9	0	1	Very Low	0.8	1.4	0.1	No
Eswatini	SWZ	3.6	Medium	1.9	2.5	1.3	3.3	Low	1.5	2.8	0.1	Yes
Ethiopia	ETH	6.8	Very High	7.3	4.4	9	6.8	Very High	7.2	3.9	9	No
Fiji	FJI	2.8	Low	2.2	3.9	0	3.2	Low	3.2	5.4	0.1	No
Finland	FIN	0.9	Very Low	0.3	0.5	0	1.3	Very Low	0.9	1.6	0.1	No
France	FRA	2.2	Low	2.1	3.4	0.6	2.4	Low	2.7	4.6	0.2	No
Gabon	GAB	3.6	Medium	2.2	2.6	1.8	3.7	Medium	2.3	4.1	0.1	No
Gambia	GMB	3.9	Medium	2	3.1	0.8	3.6	Medium	1.7	3	0.1	No
Georgia	GEO	3.7	Medium	3.6	4.4	2.7	3.1	Low	2	3.5	0.3	Yes
Germany	DEU	1.9	Very Low	1.4	2.6	0.1	2.4	Low	2.6	4.4	0.2	Yes
Ghana	GHA	4.3	Medium	3.6	3.8	3.3	4	Medium	3	4.9	0.4	No
Greece	GRC	2.8	Low	3.5	5.9	0.1	2.7	Low	3	5.1	0.1	No
Grenada	GRD	1.9	Very Low	0.9	1.7	0	1.7	Very Low	0.7	1.3	0	No
Guatemala	GTM	5.3	High	4.8	6.6	2.3	5.1	High	4.3	6.2	1.8	No
Guinea	GIN	4.6	Medium	3.1	3.9	2.2	4.4	Medium	2.7	4.4	0.6	No
Guinea-Bissau	GNB	4.4	Medium	2.1	2.7	1.4	4.1	Medium	1.6	2.8	0.2	No
Guyana	GUY	3.9	Medium	2.2	3.9	0.1	4.3	Medium	3	5.1	0.1	No
Haiti	HTI	6.2	High	5.8	7	4.3	5.5	High	4	6.3	0.6	No
Honduras	HND	5.3	High	4.5	6.5	1.5	4.9	Medium	3.6	5.9	0.2	Yes
Hungary	HUN	1.8	Very Low	1.9	3.5	0	1.5	Very Low	1.2	2.2	0.1	No
Iceland	ISL	1.3	Very Low	1.2	2.2	0	1.3	Very Low	1.4	2.7	0	No
India	IND	5.2	High	6.8	7.7	5.7	5.5	High	7.8	8.4	7	No
Indonesia	IDN	4.6	Medium	6.7	7.7	5.4	4.4	Medium	6.1	8.4	1.9	No
Iran	IRN	4.7	Medium	5.6	6.7	4.3	4.3	Medium	4.1	5.9	1.8	No
Iraq	IRQ	6.6	Very High	7.7	5.6	9	6.6	Very High	7.5	5	9	No
Ireland	IRL	1.5	Very Low	1.2	2.2	0	1.7	Very Low	1.6	2.9	0	No
Israel	ISR	2.4	Low	3.9	4.7	3.1	2.6	Low	4.9	3.3	6.2	No
Italy	ITA	2.4	Low	2.9	5	0.1	2.5	Low	3.3	5.6	0.1	No
Jamaica	JAM	3.1	Low	3.2	5.4	0.1	3	Low	3	5.1	0.1	No
Japan	JPN	2.2	Low	5.3	8.1	0	2.3	Low	6.2	8.9	0.2	No
Jordan	JOR	4.4	Medium	3.3	4.1	2.3	3.5	Medium	1.6	2.8	0.2	No

Kazakhstan	KAZ	1.8	Very Low	2.3	4	0.1	1.6	Very Low	1.7	3	0.1	No
Kenya	KEN	5.7	High	5.3	5.1	5.4	4.6	Medium	2.8	4.6	0.4	Yes
Kiribati	KIR	3.8	Medium	2.1	3.8	0	3	Low	1	2	0	Yes
Korea DPR	PRK	5	High	4	5.3	2.3	4.6	Medium	3.1	5.2	0.2	Yes
Korea Republic of	KOR	1.9	Very Low	3.5	5.9	0	2.1	Low	4.2	6.8	0.1	Yes
Kuwait	KWT	1.8	Very Low	1.2	1.6	0.8	1.7	Very Low	0.9	1.6	0.1	No
Kyrgyzstan	KGZ	3.3	Low	3.7	5	2.2	2.7	Low	1.9	3.4	0.1	No
Lao PDR	LAO	4.1	Medium	3.4	5	1.3	4	Medium	3.2	5.3	0.4	No
Latvia	LVA	1.4	Very Low	1.1	2.1	0	1.3	Very Low	0.8	1.5	0.1	No
Lebanon	LBN	4.9	Medium	4.4	5.2	3.6	3.9	Medium	2.3	4	0.3	No
Lesotho	LSO	4.1	Medium	1.7	2.6	0.8	3	Low	0.7	1.2	0.2	Yes
Liberia	LBR	5.4	High	3.2	4	2.2	5.3	High	3	4.8	0.7	No
Libya	LBY	6.2	High	8.2	3.7	10	6.2	High	8.2	3.4	10	No
Liechtenstein	LIE	0.8	Very Low	0.7	1.3	0	1.1	Very Low	1.5	2.8	0	No
Lithuania	LTU	1.2	Very Low	0.8	1.6	0	1.4	Very Low	1.2	2.1	0.1	No
Luxembourg	LUX	0.9	Very Low	0.4	0.8	0	1.1	Very Low	0.6	1.2	0	No
Madagascar	MDG	5.1	High	3.9	6.2	0.6	5.2	High	4	6.4	0.4	No
Malawi	MWI	4.7	Medium	2.9	4.6	0.8	4.5	Medium	2.5	4.2	0.5	No
Malaysia	MYS	3.1	Low	3.1	4.9	0.7	3.4	Low	4.3	6.1	1.8	No
Maldives	MDV	2.3	Low	1.8	3.1	0.2	2.1	Low	1.3	2.4	0	No
Mali	MLI	7	Very High	7.3	4.2	9	6.9	Very High	7.1	3.4	9	No
Malta	MLT	1.9	Very Low	1.3	2.5	0	1.5	Very Low	0.7	1.3	0	No
Marshall Islands	MHL	3.6	Medium	2	3.6	0	3.1	Low	1.2	2.2	0	Yes
Mauritania	MRT	5.1	High	3.6	5.4	1.3	4.6	Medium	2.5	3.9	0.8	Yes
Mauritius	MUS	1.9	Very Low	2	3.7	0	2.1	Low	2.6	4.5	0.1	Yes
Mexico	MEX	4.9	Medium	6.9	6.7	7	5	High	7.2	7.3	7	Yes
Micronesia	FSM	3.6	Medium	2.3	4.2	0	2.9	Low	1.2	2.3	0	Yes
Moldova Republic of	MDA	2.8	Low	2.7	4	1.1	2.3	Low	1.5	2.7	0.1	No
Mongolia	MNG	2.6	Low	1.6	2.9	0.1	2.4	Low	1.3	2.4	0.1	No
Montenegro	MNE	2.3	Low	2.5	4.2	0.4	2.2	Low	2.2	3.9	0.1	No
Morocco	MAR	3.7	Medium	3.4	4.6	2	3.6	Medium	2.9	4.4	1.1	No
Mozambique	MOZ	7.2	Very High	7.8	5.9	9	7.2	Very High	7.8	6	9	No
Myanmar	MMR	6.3	High	7.4	7.8	7	6.2	High	7.3	7.6	7	No
Namibia	NAM	3.9	Medium	2.5	4.5	0	3.2	Low	1.4	2.6	0.1	Yes
Nauru	NRU	3.2	Low	1.6	2.9	0	2.4	Low	0.7	1.3	0	No
Nepal	NPL	5	High	5	5.7	4.3	4.5	Medium	3.7	5.5	1.3	Yes
Netherlands	NLD	1.3	Very Low	1	2	0	2	Low	3.3	5.5	0.1	Yes
New Zealand	NZL	1.6	Very Low	2.5	4.5	0	1.6	Very Low	2.3	4.2	0	No
Nicaragua	NIC	4.7	Medium	4.8	6.6	2.3	4.3	Medium	3.7	6	0.5	No
Niger	NER	7.4	Very High	7.3	4.4	9	7.3	Very High	7.1	3.5	9	No
Nigeria	NGA	6.5	Very High	7.3	4.1	9	6.6	Very High	7.7	5.7	9	No
North Macedonia	MKD	2.3	Low	2.1	3.7	0.1	2.1	Low	1.5	2.8	0.1	No
Norway	NOR	1	Very Low	0.3	0.6	0	1.9	Very Low	2.2	3.9	0.1	No
Oman	OMN	2.5	Low	2.9	5	0.1	2.4	Low	2.5	4.3	0.3	No
Pakistan	PAK	5.9	High	6.8	7.4	6.2	6	High	6.9	7	6.8	No
Palau	PLW	2.8	Low	1.7	3.2	0	2.5	Low	1.2	2.3	0	No

Palestine	PSE	4.5	Medium	3.5	3.3	3.7	3.4	Low	1.5	2.8	0	Yes
Panama	PAN	3.8	Medium	3.7	6.2	0	3.8	Medium	3.5	5.8	0.2	No
Papua New Guinea	PNG	5.9	High	5	6.7	2.7	5.4	High	3.9	6.3	0.4	No
Paraguay	PRY	2.9	Low	1.9	2.6	1.1	2.7	Low	1.5	2.7	0.2	No
Peru	PER	4.8	Medium	5.1	7.1	2	4.5	Medium	4.2	6.5	0.9	No
Philippines	PHL	5.3	High	7.8	8.4	7	5.3	High	7.9	8.6	7	No
Poland	POL	1.6	Very Low	1.3	2.4	0.1	1.7	Very Low	1.8	3.2	0.1	No
Portugal	PRT	1.6	Very Low	1.8	3.3	0	1.7	Very Low	2.3	4	0.1	No
Qatar	QAT	1.5	Very Low	0.9	1.7	0	1.2	Very Low	0.5	0.9	0.1	No
Romania	ROU	2.4	Low	2.6	4	1	2.1	Low	1.8	3.2	0.1	No
Russian Federation	RUS	3.5	Medium	5.5	5.7	5.2	3.3	Low	4.8	5	4.5	Yes
Rwanda	RWA	4.5	Medium	3	3.6	2.3	4.7	Medium	3.5	2.9	4.1	No
Saint Kitts and Nevis	KNA	1.9	Very Low	1.5	2.8	0	1.9	Very Low	1.3	2.5	0	No
Saint Lucia	LCA	2.2	Low	1.4	2.6	0	1.9	Very Low	0.9	1.8	0	Yes
Saint Vincent and the Grenadines	VCT	2.6	Low	1.4	2.7	0	2.4	Low	1.2	2.2	0	No
Samoa	WSM	3.1	Low	2	3.6	0	3	Low	1.8	3.3	0	No
Sao Tome and Principe	STP	2.5	Low	0.7	1.3	0	1.9	Very Low	0.3	0.6	0	Yes
Saudi Arabia	SAU	2.7	Low	3.9	3.1	4.7	2.1	Low	1.9	3.3	0.2	No
Senegal	SEN	4.3	Medium	2.8	4.5	0.6	4.5	Medium	3.3	4.8	1.5	No
Serbia	SRB	3	Low	3.1	4.4	1.6	2.4	Low	1.6	2.9	0.1	No
Seychelles	SYC	1.8	Very Low	1.5	2.8	0	1.8	Very Low	1.6	2.9	0	No
Sierra Leone	SLE	5.2	High	3.5	4	3	4.7	Medium	2.7	4.2	0.9	Yes
Singapore	SGP	0.5	Very Low	0.5	0.9	0	0.6	Very Low	0.8	1.5	0.1	No
Slovakia	SVK	1.5	Very Low	1.5	2.8	0	1.5	Very Low	1.5	2.7	0.1	No
Slovenia	SVN	1.2	Very Low	1.9	3.4	0	1.3	Very Low	2.3	4	0.1	No
Solomon Islands	SLB	4.5	Medium	3.6	5.9	0.4	4.1	Medium	2.6	4.6	0.1	No
Somalia	SOM	8.8	Very High	8.9	6.9	10	8.8	Very High	8.7	6	10	No
South Africa	ZAF	4.5	Medium	4.9	5	4.8	3.7	Medium	2.7	4	1.1	No
South Sudan	SSD	8.4	Very High	7.2	4	9	8.5	Very High	7.3	4.4	9	No
Spain	ESP	2.1	Low	2.3	4	0.1	2.2	Low	2.7	4.4	0.5	No
Sri Lanka	LKA	3.6	Medium	3.9	5.2	2.2	3.4	Low	3.2	5.1	0.7	Yes
Sudan	SDN	6.4	High	5.7	4.1	7	6.4	High	5.7	4	7	No
Suriname	SUR	3.3	Low	2.5	4	0.7	3.5	Medium	2.9	5	0.1	Yes
Sweden	SWE	1.4	Very Low	0.6	1.1	0	1.8	Very Low	1.4	2.5	0.1	No
Switzerland	CHE	1.4	Very Low	1.2	2.3	0	1.5	Very Low	1.5	2.7	0.1	No
Syria	SYR	7.1	Very High	8.7	5.7	10	7	Very High	8.3	3.9	10	No
Tajikistan	TJK	4.4	Medium	5	5.8	4.1	3.4	Low	2.4	3.7	0.9	Yes
Tanzania	TZA	5.3	High	4.3	5.2	3.3	4.9	Medium	3.3	5.2	0.9	Yes
Thailand	THA	3.8	Medium	4.6	6.1	2.7	4.1	Medium	6	6.9	5	No
Timor-Leste	TLS	4.3	Medium	2.7	4.6	0.2	4.5	Medium	3	5.1	0.1	No
Togo	TGO	4.8	Medium	2.9	3.1	2.6	4.1	Medium	1.8	3.1	0.2	No
Tonga	TON	3.5	Medium	3	5.2	0	3.2	Low	2.3	4.1	0	Yes
Trinidad and Tobago	TTO	2.6	Low	1.8	3.2	0.1	2.7	Low	1.9	3.4	0.1	No
Tunisia	TUN	3.3	Low	3.7	4.4	2.9	3	Low	2.9	5	0.1	No
Turkey	TUR	4.9	Medium	7.9	6.1	9	4.9	Medium	7.8	5.8	9	No

Turkmenistan	TKM	2.4	Low	2.2	3.7	0.4	1.9	Very Low	1.1	2	0.1	Yes
Tuvalu	TUV	3.4	Low	1.6	2.9	0	2.7	Low	0.8	1.6	0	No
Uganda	UGA	6	High	4.6	4.5	4.7	6.2	High	5.1	3.7	6.2	No
Ukraine	UKR	4.5	Medium	5.4	3.2	7	4.5	Medium	5.2	2.6	7	No
United Arab Emirates	ARE	1.7	Very Low	2.3	4.2	0	1.6	Very Low	2.1	3.8	0.1	No
United Kingdom	GBR	1.9	Very Low	2.1	2.4	1.8	2	Low	2.4	3.8	0.7	Yes
United States of America	USA	3.4	Low	6.2	6.6	5.7	3.1	Low	4.9	7.5	0.4	No
Uruguay	URY	1.8	Very Low	0.9	1.7	0.1	2.1	Low	1.4	2.4	0.2	Yes
Uzbekistan	UZB	3.1	Low	3.9	5.2	2.3	2.5	Low	2.1	3.4	0.6	No
Vanuatu	VUT	4.4	Medium	3.3	5.6	0	3.9	Medium	2.3	4.2	0	No
Venezuela	VEN	4.7	Medium	5.2	6.2	4	4.2	Medium	3.9	6.2	0.4	No
Viet Nam	VNM	3.7	Medium	5.6	7.4	2.9	3.7	Medium	5.3	7.9	0.6	No
Yemen	YEM	8.2	Very High	8.4	4.3	10	8.1	Very High	8.3	4	10	No
Zambia	ZMB	4.2	Medium	2.2	3.6	0.6	4.2	Medium	2.1	3.5	0.4	No
Zimbabwe	ZWE	5.1	High	3.7	4.8	2.3	4.4	Medium	2.4	3.9	0.5	Yes

Annex 3. 2015 GHSL and projected populations, percent change and additional people for the SSPs with respect to 2015 GHSL for each continent in millions.

SCENARIO	YEAR		ASIA	AFRICA	EUROPE	AMERICAS	OCEANIA	WORLD
BASELINE (GHSL)	2015	Pop_abs	4362.00	1184.52	736.08	986.55	38.47	7307.62
SSP1	2050	Pop_abs	4662.53	1750.46	755.87	1109.30	52.97	8331.13
		%change	6.89	47.78	2.69	12.44	37.70	14.01
		Add.Pop	300.53	565.94	19.79	122.75	14.50	1023.51
	2080	Pop_abs	3981.67	1926.62	717.69	1084.21	59.13	7769.33
		%change	-8.72	62.65	-2.50	9.90	53.72	6.32
		Add.Pop	-380.33	742.11	-18.39	97.66	20.66	461.71
SSP2	2050	Pop_abs	5060.58	1996.87	748.38	1165.69	53.89	9025.42
		%change	16.02	68.58	1.67	18.16	40.09	23.51
		Add.Pop	698.59	812.35	12.30	179.14	15.42	1717.80
	2080	Pop_abs	4779.33	2481.32	725.53	1195.36	61.71	9243.24
		%change	9.57	109.48	-1.43	21.17	60.41	26.49
		Add.Pop	417.33	1296.81	-10.56	208.81	23.24	1935.62
SSP3	2050	Pop_abs	5573.19	2317.13	669.08	1199.80	47.39	9806.58
		%change	27.77	95.62	-9.10	21.62	23.19	34.20
		Add.Pop	1211.19	1132.61	-67.00	213.25	8.92	2498.96
	2080	Pop_abs	6200.33	3348.27	583.27	1298.36	48.62	11478.83
		%change	42.14	182.67	-20.76	31.61	26.39	57.08
		Add.Pop	1838.33	2163.75	-152.81	311.80	10.15	4171.22
SSP5	2050	Pop_abs	4651.69	1724.19	832.41	1159.33	61.08	8428.70
		%change	6.64	45.56	13.09	17.51	58.79	15.34
		Add.Pop	289.69	539.67	96.33	172.78	22.62	1121.09
	2080	Pop_abs	3975.78	1873.38	899.10	1235.93	78.84	8063.02
		%change	-8.85	58.16	22.15	25.28	104.94	10.34
		Add.Pop	-386.22	688.86	163.01	249.38	40.37	755.41

Annex 4. Baseline and projected exposed population to river flood, percent change and additional exposed people for the SSPs with respect to the baseline for each continent in millions.

SCENARIO	YEAR		ASIA	AFRICA	EUROPE	AMERICAS	OCEANIA	WORLD
BASELINE	2015	Pop_abs	144.04	23.83	16.76	20.47	1.26	206.36
RCP4.5-SSP1	2050	Pop_abs	186.11	34.02	17.43	21.70	1.96	261.22
		%change	29.21	42.74	4.01	6.04	54.85	26.59
		Add.Pop	42.07	10.19	0.67	1.24	0.69	54.86
	2080	Pop_abs	176.01	39.11	17.70	21.94	2.20	256.96
		%change	22.20	64.12	5.64	7.18	74.17	24.52
		Add.Pop	31.97	15.28	0.94	1.47	0.94	50.61
RCP4.5-SSP2	2050	Pop_abs	198.31	38.34	16.99	22.66	1.95	278.25
		%change	37.68	60.88	1.41	10.71	54.49	34.84
		Add.Pop	54.27	14.51	0.24	2.19	0.69	71.90
	2080	Pop_abs	205.04	49.62	17.59	23.84	2.23	298.32
		%change	42.35	108.22	4.95	16.48	76.07	44.56
		Add.Pop	61.01	25.79	0.83	3.37	0.96	91.96
RCP8.5-SSP2	2050	Pop_abs	217.40	40.02	17.34	22.90	1.93	299.59
		%change	50.94	67.93	3.48	11.91	52.41	45.18
		Add.Pop	73.37	16.19	0.58	2.44	0.66	93.24
	2080	Pop_abs	228.53	54.56	17.01	24.48	2.20	326.78
		%change	58.66	128.95	1.51	19.60	74.01	58.36
		Add.Pop	84.49	30.73	0.25	4.01	0.94	120.42
RCP8.5-SSP3	2050	Pop_abs	235.46	45.61	15.12	23.29	1.61	321.09
		%change	63.48	91.38	-9.79	13.78	27.69	55.60
		Add.Pop	91.43	21.78	-1.64	2.82	0.35	114.73
	2080	Pop_abs	288.20	71.42	12.84	25.52	1.58	399.56
		%change	100.09	199.69	-23.40	24.71	24.70	93.63
		Add.Pop	144.17	47.59	-3.92	5.06	0.31	193.20
RCP8.5-SSP5	2050	Pop_abs	202.56	34.99	19.60	23.03	2.26	282.44
		%change	40.63	46.83	16.94	12.51	79.00	36.87
		Add.Pop	58.53	11.16	2.84	2.56	1.00	76.08
	2080	Pop_abs	193.67	41.98	21.71	26.03	2.95	286.34
		%change	34.46	76.17	29.54	27.17	133.38	38.76
		Add.Pop	49.63	18.15	4.95	5.56	1.69	79.98
RCP4.5-GHSL	2050	Pop_abs	169.40	28.20	16.35	20.50	1.35	235.79
		%change	17.61	18.32	-2.46	0.15	6.81	14.26
		Add.Pop	25.37	4.37	-0.41	0.03	0.09	29.44
	2080	Pop_abs	186.15	29.43	17.23	20.80	1.32	254.93
		%change	29.24	23.48	2.82	1.62	4.68	23.54
		Add.Pop	42.12	5.60	0.47	0.33	0.06	48.57
RCP8.5-GHSL	2050	Pop_abs	184.52	29.29	16.78	20.61	1.33	252.54
		%change	28.11	22.91	0.16	0.72	5.33	22.38
		Add.Pop	40.48	5.46	0.03	0.15	0.07	46.18
	2080	Pop_abs	205.03	32.49	16.78	21.05	1.34	276.70
		%change	42.34	36.33	0.15	2.86	6.17	34.09
		Add.Pop	60.99	8.66	0.03	0.59	0.08	70.34

Annex 5. Baseline and projected exposed population to coastal flood, percent change and additional exposed people for the SSPs with respect to the baseline for each continent in millions.

SCENARIO	YEAR		ASIA	AFRICA	EUROPE	AMERICAS	OCEANIA	WORLD
BASELINE	2015	Pop_abs	26.23	0.95	4.06	0.56	0.02	31.81
RCP4.5-SSP1	2050	Pop_abs	49.44	4.45	7.78	1.56	0.08	63.32
		%change	88.51	369.74	91.51	181.54	271.91	99.02
		add	23.21	3.50	3.72	1.01	0.06	31.50
	2080	Pop_abs	60.08	7.20	9.96	2.10	0.17	79.50
		%change	129.07	659.57	145.10	278.16	647.80	149.90
		add	33.85	6.25	5.89	1.55	0.15	47.69
RCP4.5-SSP2	2050	Pop_abs	52.87	5.03	7.61	1.65	0.09	67.25
		%change	101.60	431.12	87.24	197.01	280.25	111.37
		add	26.64	4.09	3.54	1.09	0.06	35.43
	2080	Pop_abs	68.87	9.19	9.66	2.30	0.18	90.20
		%change	162.62	869.66	137.88	313.83	675.99	183.53
		add	42.65	8.24	5.60	1.74	0.15	58.39
RCP8.5-SSP2	2050	Pop_abs	54.74	5.32	7.75	1.71	0.09	69.61
		%change	108.72	461.10	90.85	208.16	301.45	118.81
		add	28.51	4.37	3.69	1.16	0.07	37.80
	2080	Pop_abs	75.36	10.73	10.57	2.72	0.28	99.66
		%change	187.36	1032.11	160.27	389.04	1141.23	213.26
		add	49.13	9.78	6.51	2.16	0.26	67.85
RCP8.5-SSP3	2050	Pop_abs	58.95	6.15	6.69	1.76	0.08	73.63
		%change	124.80	548.60	64.70	216.49	254.79	131.44
		add	32.73	5.20	2.63	1.20	0.06	41.82
	2080	Pop_abs	92.21	14.33	7.43	2.89	0.21	117.07
		%change	251.59	1412.03	82.93	420.90	811.66	267.98
		add	65.98	13.38	3.37	2.34	0.19	85.25
RCP8.5-SSP5	2050	Pop_abs	50.84	4.60	8.87	1.72	0.10	66.12
		%change	93.86	384.97	118.23	208.69	351.16	107.83
		add	24.61	3.65	4.80	1.16	0.08	34.30
	2080	Pop_abs	65.24	8.16	14.13	2.86	0.37	90.77
		%change	148.76	761.62	247.89	415.40	1530.59	185.32
		add	39.01	7.22	10.07	2.31	0.35	58.96
RCP4.5-GHSL	2050	Pop_abs	38.19	1.38	5.23	0.92	0.04	45.76
		%change	45.63	45.66	28.67	65.62	85.19	43.84
		add	11.97	0.43	1.16	0.36	0.02	13.95
	2080	Pop_abs	56.37	2.12	6.43	1.35	0.07	66.35
		%change	114.96	123.91	58.24	142.61	222.27	108.54
		add	30.15	1.17	2.37	0.79	0.05	34.53
RCP8.5-GHSL	2050	Pop_abs	39.58	1.44	5.34	0.96	0.04	47.36
		%change	50.93	51.50	31.48	72.55	95.25	48.87
		add	13.36	0.49	1.28	0.40	0.02	15.55
	2080	Pop_abs	62.71	2.44	7.14	1.63	0.11	74.03
		%change	139.12	158.01	75.65	193.24	386.69	132.70
		add	36.48	1.50	3.07	1.07	0.09	42.22

Annex 6. Baseline and projected exposed population to drought, percent change and additional exposed people for the SSPs with respect to the baseline for each continent in millions.

SCENARIO	YEAR		ASIA	AFRICA	EUROPE	AMERICAS	OCEANIA	WORLD
BASELINE	2015	Pop_abs	254.08	73.22	45.62	60.42	1.73	435.07
RCP4.5-SSP1	2050	Pop_abs	587.81	287.69	123.21	182.94	7.09	1188.75
		%change	131.35	292.91	170.08	202.77	308.92	173.23
		add	333.74	214.47	77.59	122.52	5.36	753.67
	2080	Pop_abs	587.70	372.48	137.64	206.83	10.74	1315.40
		%change	131.31	408.72	201.72	242.31	519.01	202.34
		add	333.62	299.26	92.02	146.41	9.00	880.33
RCP4.5-SSP2	2050	Pop_abs	648.89	324.43	122.36	193.42	7.09	1296.19
		%change	155.39	343.08	168.22	220.12	308.61	197.92
		add	394.81	251.21	76.74	133.00	5.35	861.11
	2080	Pop_abs	727.25	473.21	139.29	231.86	10.86	1582.48
		%change	186.23	546.28	205.33	283.73	526.25	263.73
		add	473.17	399.99	93.67	171.44	9.13	1147.40
RCP8.5-SSP2	2050	Pop_abs	735.01	372.30	158.55	230.94	8.67	1505.46
		%change	189.29	408.46	247.54	282.22	399.78	246.03
		add	480.93	299.08	112.93	170.52	6.94	1070.39
	2080	Pop_abs	1042.75	592.51	252.83	365.25	16.40	2269.74
		%change	310.41	709.21	454.21	504.50	845.34	421.69
		add	788.68	519.29	207.21	304.83	14.67	1834.67
RCP8.5-SSP3	2050	Pop_abs	822.33	428.81	143.48	240.74	7.14	1642.50
		%change	223.66	485.64	214.51	298.43	311.67	277.52
		add	568.26	355.59	97.86	180.32	5.41	1207.43
	2080	Pop_abs	1396.81	799.27	206.36	411.62	10.86	2824.92
		%change	449.76	991.60	352.35	581.23	526.02	549.30
		add	1142.74	726.05	160.74	351.19	9.13	2389.85
RCP8.5-SSP5	2050	Pop_abs	666.56	324.71	174.90	226.90	10.34	1403.41
		%change	162.35	343.47	283.39	275.52	496.07	222.57
		add	412.49	251.49	129.28	166.47	8.61	968.34
	2080	Pop_abs	840.01	452.19	311.67	365.13	23.04	1992.05
		%change	230.61	517.58	583.19	504.30	1228.23	357.87
		add	585.93	378.97	266.05	304.71	21.31	1556.97
RCP4.5-GHSL	2050	Pop_abs	497.66	210.51	116.89	161.87	4.45	991.38
		%change	95.87	187.51	156.23	167.89	156.44	127.86
		add	243.58	137.29	71.27	101.44	2.71	556.30
	2080	Pop_abs	557.80	259.84	140.07	190.58	5.83	1154.12
		%change	119.54	254.88	207.03	215.41	235.92	165.27
		add	303.73	186.62	94.45	130.15	4.09	719.04
RCP8.5-GHSL	2050	Pop_abs	572.05	241.88	152.74	191.86	5.45	1163.99
		%change	125.15	230.35	234.81	217.54	214.05	167.54
		add	317.97	168.66	107.12	131.44	3.71	728.91
	2080	Pop_abs	819.85	329.19	256.81	297.88	8.70	1712.42
		%change	222.68	349.59	462.94	392.99	401.23	293.59
		add	565.77	255.97	211.19	237.45	6.96	1277.35

Annex 7. Baseline and projected exposed population to Malaria, percent change and additional exposed people for the SSPs with respect to the baseline for each continent in millions.

SCENARIO	YEAR		ASIA	AFRICA	EUROPE	AMERICAS	OCEANIA	WORLD
BASELINE	2015	Pop_abs	1963.21	545.44	0.06	366.53	9.05	2884.30
RCP4.5-SSP1	2050	Pop_abs	2629.95	1205.55	19.06	501.04	16.13	4371.73
		%change	33.96	121.03	-	36.70	78.20	51.57
		add	666.74	660.12	19.00	134.50	7.08	1487.43
	2080	Pop_abs	2303.73	1288.19	25.37	477.51	16.38	4111.17
		%change	17.34	136.18	-	30.28	80.92	42.54
		add	340.51	742.75	25.30	110.98	7.33	1226.87
RCP4.5-SSP2	2050	Pop_abs	2854.82	1386.79	19.51	532.27	17.36	4810.76
		%change	45.42	154.25	-	45.22	91.78	66.79
		add	891.61	841.36	19.45	165.74	8.31	1926.46
	2080	Pop_abs	2741.92	1672.80	27.65	538.28	18.89	4999.54
		%change	39.66	206.69	-	46.86	108.71	73.34
		add	778.71	1127.37	27.58	171.75	9.84	2115.24
RCP8.5-SSP2	2050	Pop_abs	2949.19	1430.58	31.08	555.73	18.19	4984.78
		%change	50.22	162.28	-	51.62	100.95	72.82
		add	985.98	885.15	31.02	189.20	9.14	2100.48
	2080	Pop_abs	2856.59	1788.17	72.85	607.77	21.57	5346.94
		%change	45.51	227.84	-	65.81	138.30	85.38
		add	893.37	1242.73	72.78	241.23	12.52	2462.64
RCP8.5-SSP3	2050	Pop_abs	3248.05	1666.31	30.34	587.37	18.16	5550.24
		%change	65.45	205.50	-	60.25	100.59	92.43
		add	1284.84	1120.88	30.28	220.84	9.11	2665.94
	2080	Pop_abs	3667.86	2406.65	71.71	691.73	21.43	6859.38
		%change	86.83	341.23	-	88.72	136.77	137.82
		add	1704.65	1861.21	71.65	325.20	12.38	3975.08
RCP8.5-SSP5	2050	Pop_abs	2680.28	1209.09	29.37	533.96	17.71	4470.40
		%change	36.52	121.67	-	45.68	95.59	54.99
		add	717.06	663.65	29.30	167.43	8.65	1586.10
	2080	Pop_abs	2383.23	1357.36	65.64	581.05	21.74	4409.02
		%change	21.39	148.86	-	58.52	140.19	52.86
		add	420.02	811.93	65.57	214.51	12.69	1524.72
RCP4.5-GHSL	2050	Pop_abs	2488.95	773.17	20.96	453.36	12.15	3748.59
		%change	26.78	41.75	-	23.69	34.21	29.97
		add	525.74	227.73	20.90	86.83	3.10	864.29
	2080	Pop_abs	2640.97	733.86	33.34	455.83	11.89	3875.88
		%change	34.52	34.55	-	24.36	31.35	34.38
		add	677.75	188.43	33.28	89.29	2.84	991.59
RCP8.5-GHSL	2050	Pop_abs	2581.18	797.38	33.01	473.01	12.73	3897.30
		%change	31.48	46.19	-	29.05	40.60	35.12
		add	617.96	251.94	32.95	106.48	3.68	1013.00
	2080	Pop_abs	2788.25	787.35	85.33	511.44	13.54	4185.91
		%change	42.02	44.35	-	39.53	49.57	45.13
		add	825.04	241.92	85.27	144.90	4.49	1301.61

Annex 8. Baseline and projected exposed population to Dengue, percent change and additional exposed people for the SSPs with respect to the baseline for each continent in millions

SCENARIO	YEAR		ASIA	AFRICA	EUROPE	AMERICAS	OCEANIA	WORLD
BASELINE	2015	Pop_abs	1822.90	576.18	0.00	346.08	8.47	2753.63
RCP4.5-SSP1	2050	Pop_abs	2600.44	1404.62	0.00	495.05	20.79	4520.90
		%change	42.65	143.78	-	43.04	145.40	64.18
		add	777.54	828.45	0.00	148.96	12.32	1767.27
	2080	Pop_abs	2204.28	1553.62	0.00	437.03	22.62	4217.54
		%change	20.92	169.64	-	26.28	167.04	53.16
		add	381.38	977.44	0.00	90.94	14.15	1463.91
RCP4.5-SSP2	2050	Pop_abs	2904.93	1654.46	0.00	548.12	22.15	5129.66
		%change	59.36	187.14	-	58.38	161.46	86.29
		add	1082.03	1078.28	0.00	202.04	13.68	2376.03
	2080	Pop_abs	2760.00	2067.57	0.00	534.79	25.45	5387.81
		%change	51.41	258.84	-	54.53	200.41	95.66
		add	937.10	1491.39	0.00	188.71	16.98	2634.18
RCP8.5-SSP2	2050	Pop_abs	2859.69	1655.25	0.00	553.64	22.58	5091.16
		%change	56.88	187.28	-	59.97	166.62	84.89
		add	1036.79	1079.07	0.00	207.55	14.11	2337.53
	2080	Pop_abs	2525.95	2007.99	0.04	544.89	27.51	5106.38
		%change	38.57	248.50	-	57.45	224.77	85.44
		add	703.05	1431.81	0.04	198.81	19.04	2352.75
RCP8.5-SSP3	2050	Pop_abs	3206.05	1929.15	0.00	621.14	21.62	5777.96
		%change	75.88	234.82	-	79.48	155.19	109.83
		add	1383.15	1352.97	0.00	275.06	13.15	3024.32
	2080	Pop_abs	3353.17	2704.63	0.03	714.20	25.11	6797.14
		%change	83.95	369.41	-	106.37	196.43	146.84
		add	1530.27	2128.45	0.03	368.12	16.64	4043.51
RCP8.5-SSP5	2050	Pop_abs	2542.92	1383.12	0.00	492.20	23.95	4442.19
		%change	39.50	140.05	-	42.22	182.70	61.32
		add	720.02	806.94	0.00	146.12	15.48	1688.56
	2080	Pop_abs	2002.30	1478.84	0.06	441.29	31.81	3954.30
		%change	9.84	156.66	-	27.51	275.57	43.60
		add	179.39	902.66	0.06	95.21	23.34	1200.67
RCP4.5-GHSL	2050	Pop_abs	2380.99	920.76	0.00	470.71	15.41	3787.87
		%change	30.62	59.80	-	36.01	81.88	37.56
		add	558.09	344.58	0.00	124.63	6.94	1034.24
	2080	Pop_abs	2346.99	900.71	0.00	470.52	15.66	3733.87
		%change	28.75	56.32	-	35.96	84.91	35.60
		add	524.09	324.53	0.00	124.43	7.19	980.24
RCP8.5-GHSL	2050	Pop_abs	2349.74	922.54	0.00	475.22	15.70	3763.20
		%change	28.90	60.11	-	37.31	85.39	36.66
		add	526.84	346.36	0.00	129.14	7.23	1009.57
	2080	Pop_abs	2176.93	885.97	0.05	478.99	16.86	3558.80
		%change	19.42	53.77	-	38.40	98.99	29.24
		add	354.03	309.80	0.05	132.91	8.38	805.17

Annex 9. Baseline and projected average probability of civil conflict for each continent, and future changes for each SSP relative to the baseline (2020 – SSP5)

SCENARIO	YEAR		ASIA	AFRICA	EUROPE	AMERICAS	OCEANIA	WORLD
BASELINE	2015	Prob	0.21	0.18	0.03	0.05	0.01	0.12
SSP1	2050	Prob	0.13	0.15	0.02	0.05	0.01	0.09
		%change	-37.96	-14.78	-15.79	-5.12	5.74	-24.21
		abs diff	-0.08	-0.03	0.00	0.00	0.00	-0.03
	2080	Prob	0.09	0.12	0.02	0.04	0.01	0.07
		%change	-55.84	-33.45	-24.67	-26.75	-6.49	-42.28
		abs diff	-0.12	-0.06	-0.01	-0.01	0.00	-0.05
SSP2	2050	Prob	0.15	0.20	0.03	0.05	0.01	0.11
		%change	-26.72	9.99	-0.67	10.83	34.23	-6.50
		abs diff	-0.06	0.02	0.00	0.01	0.00	-0.01
	2080	Prob	0.11	0.17	0.02	0.04	0.01	0.09
		%change	-47.58	-7.43	-16.52	-15.20	-0.32	-26.07
		abs diff	-0.10	-0.01	0.00	-0.01	0.00	-0.03
SSP3	2050	Prob	0.24	0.28	0.04	0.10	0.01	0.17
		%change	17.67	52.71	43.49	98.64	133.31	40.65
		abs diff	0.04	0.10	0.01	0.05	0.01	0.05
	2080	Prob	0.26	0.33	0.04	0.12	0.02	0.19
		%change	27.51	80.60	46.18	136.74	205.16	60.36
		abs diff	0.06	0.15	0.01	0.07	0.01	0.07
SSP5	2050	Prob	0.12	0.15	0.02	0.04	0.01	0.08
		%change	-39.85	-19.45	-16.03	-16.37	16.81	-27.90
		abs diff	-0.08	-0.04	0.00	-0.01	0.00	-0.03
	2080	Prob	0.08	0.11	0.02	0.03	0.01	0.06
		%change	-59.97	-40.99	-25.20	-43.37	6.52	-48.61
		abs diff	-0.12	-0.07	-0.01	-0.02	0.00	-0.06

Annex 10. Baseline Hazard & Exposure of INFORM Climate Change Risk index and absolute changes projected for the mid-21st century under concentration and development scenarios indicated in the panel title

INFORM CC Hazard & Exposure Index – Baseline

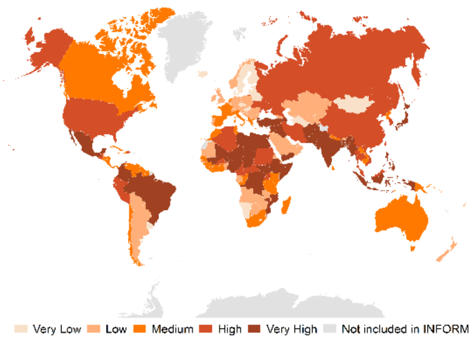

Hazard & Exposure Changes – RCP45 – GHSL 2015

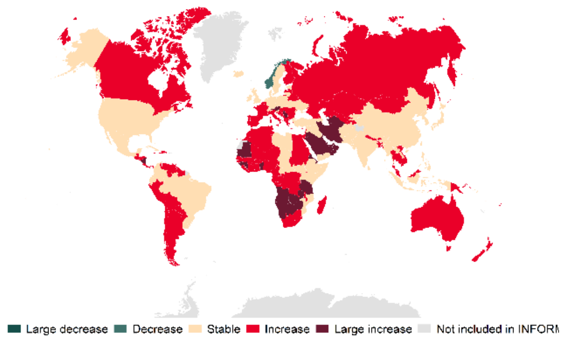

Hazard & Exposure Changes – RCP45 – SSP1

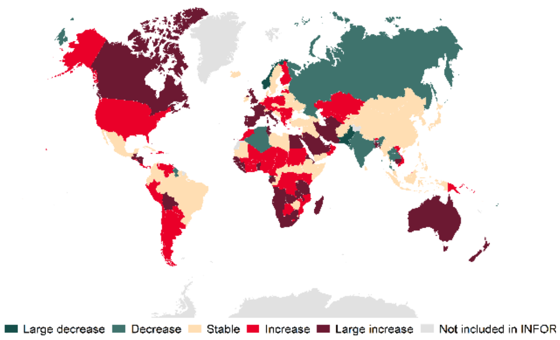

Hazard & Exposure Changes – RCP45 – SSP2

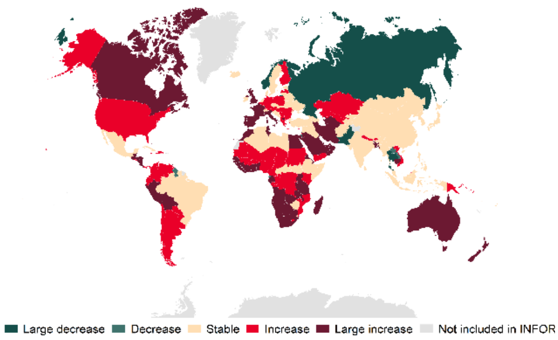

Hazard & Exposure Changes – RCP85 – GHSL 2015

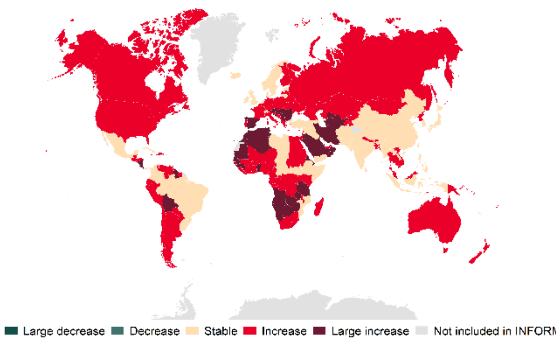

Hazard & Exposure Changes – RCP85 – SSP2

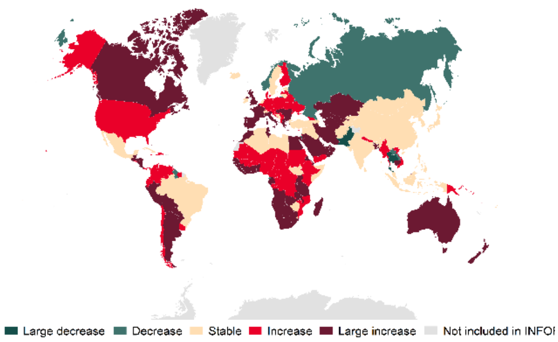

Hazard & Exposure Changes – RCP85 – SSP3

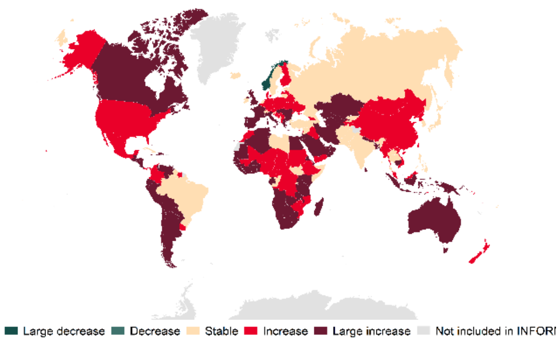

Hazard & Exposure Changes – RCP85 – SSP5

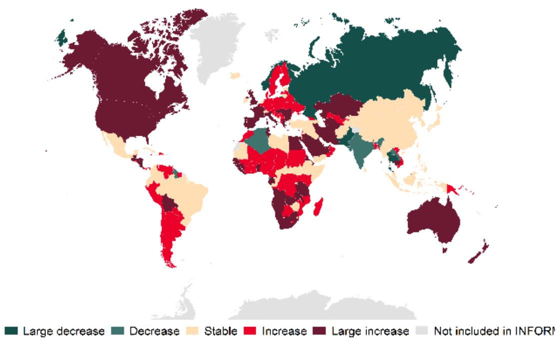

Annex 11. Baseline Hazard & Exposure of INFORM Climate Change Risk index and absolute changes projected for 2080s under concentration and development scenarios indicated in the panel title.

INFORM CC Hazard & Exposure Index – Baseline

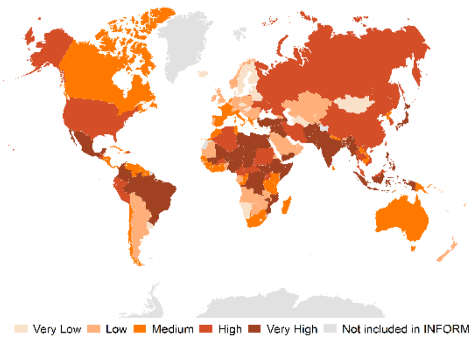

Hazard & Exposure Changes – RCP45 – GHSL 2015

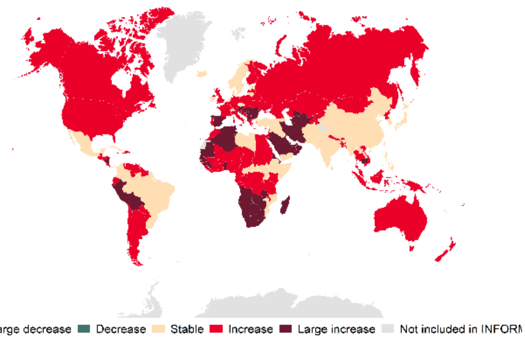

Hazard & Exposure Changes – RCP45 – SSP1

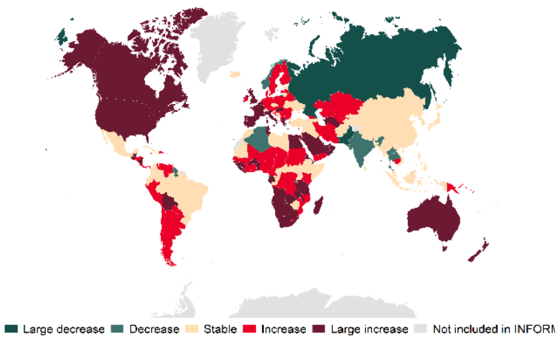

Hazard & Exposure Changes – RCP45 – SSP2

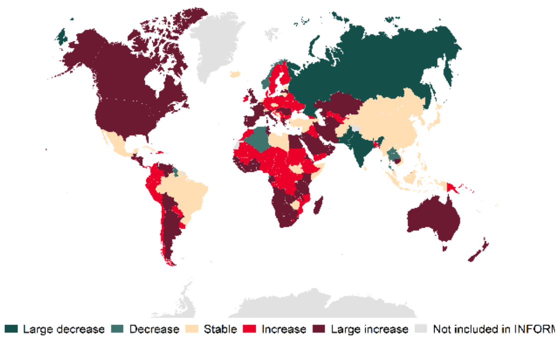

Hazard & Exposure Changes – RCP85 – GHSL 2015

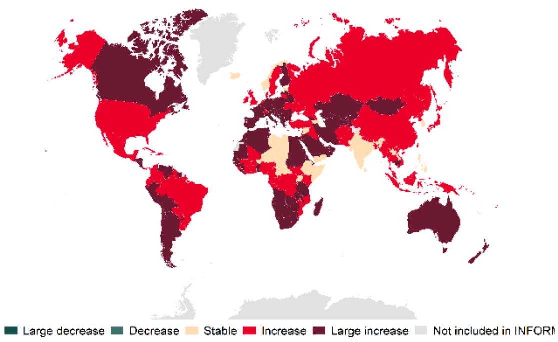

Hazard & Exposure Changes – RCP85 – SSP2

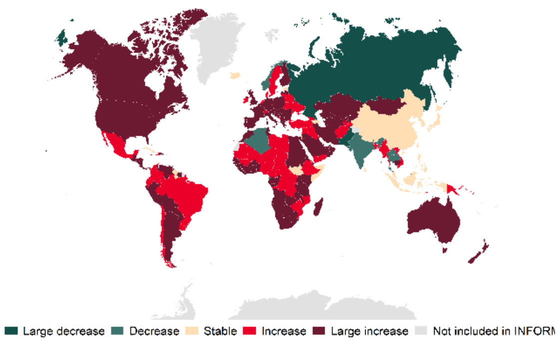

Hazard & Exposure Changes – RCP85 – SSP3

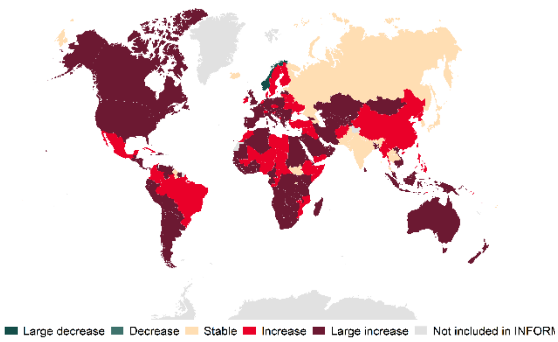

Hazard & Exposure Changes – RCP85 – SSP5

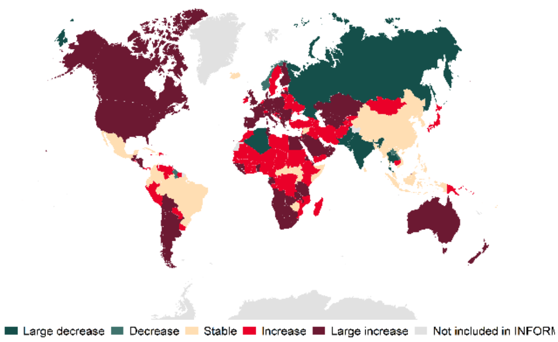

Annex 12. Baseline Natural hazard of INFORM Climate Change Risk Index and absolute changes projected for 2050s under concentration and development scenarios indicated in the panel title.

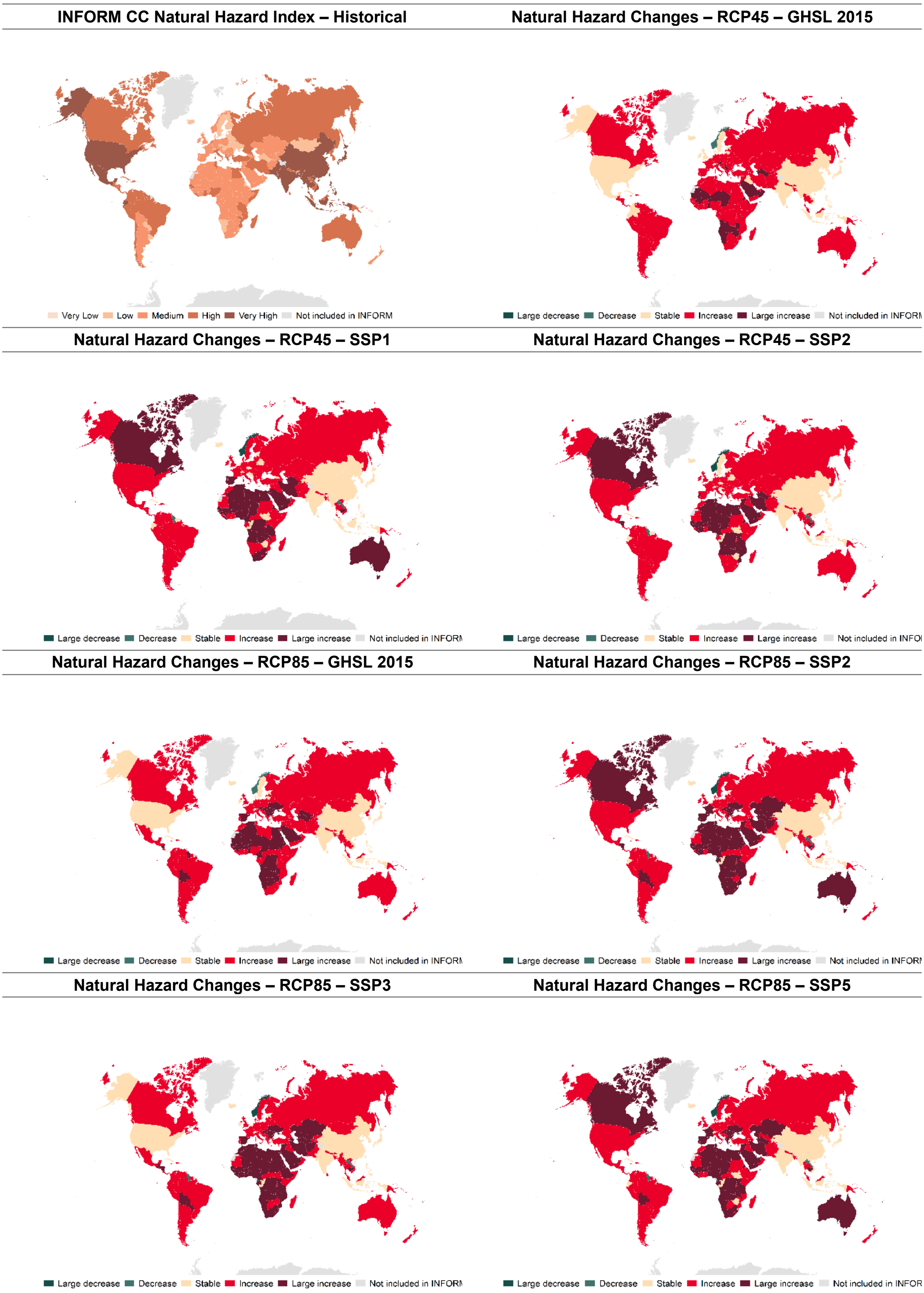

Annex 13. Baseline Natural hazard of INFORM Climate Change Risk Index and absolute changes projected for 2080s under concentration and development scenarios indicated in the panel title.

INFORM CC Hazard & Exposure Index – Baseline	Natural Hazard Changes – RCP45 – GHSL 2015

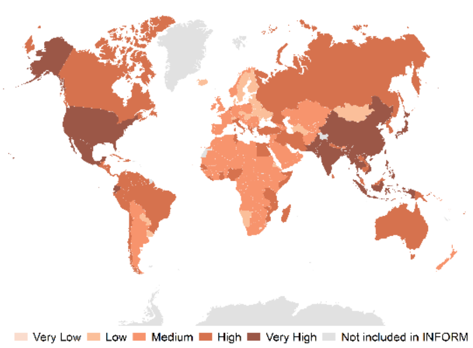

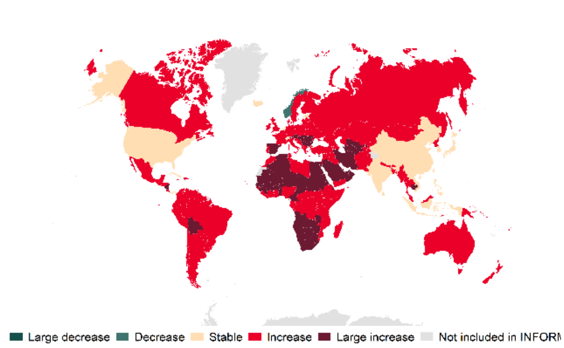

Natural Hazard Changes – RCP45 – SSP1	Natural Hazard Changes – RCP45 – SSP2

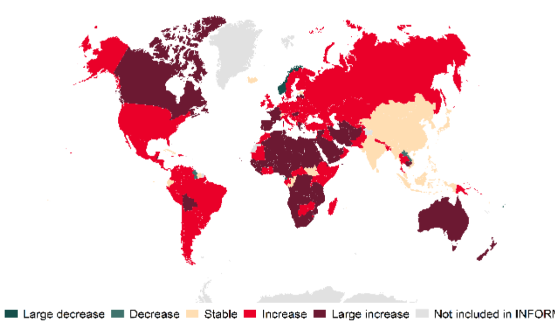

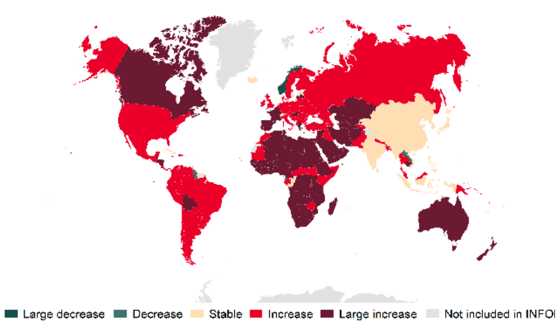

Natural Hazard Changes – RCP85 – GHSL 2015	Natural Hazard Changes – RCP85 – SSP2

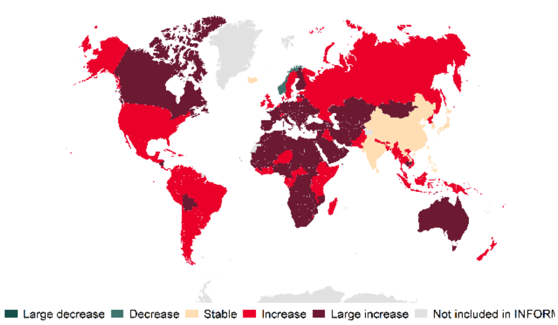

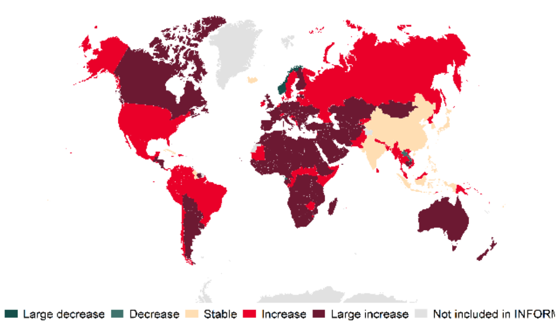

Natural Hazard Changes – RCP85 – SSP3	Natural Hazard Changes – RCP85 – SSP5

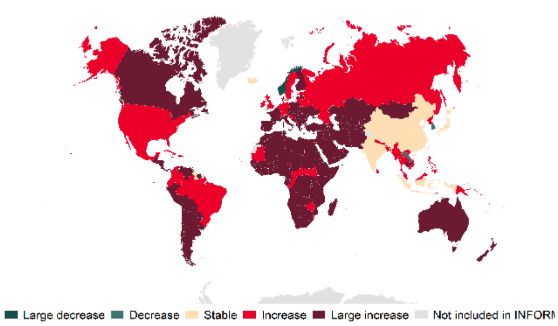

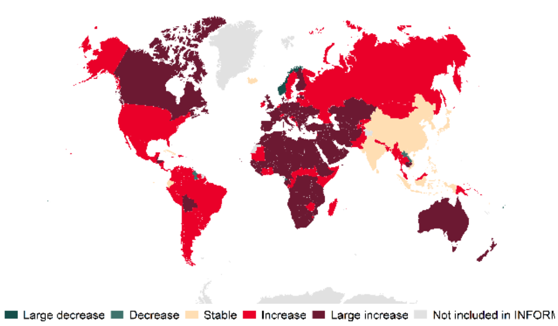

Annex 14. Baseline Human hazard of INFORM Climate Change Risk Index and absolute changes projected for 2050 under SSPs indicated in the panel title.

INFORM CC Human Hazard Index – Baseline	Human Hazard Changes – SSP1
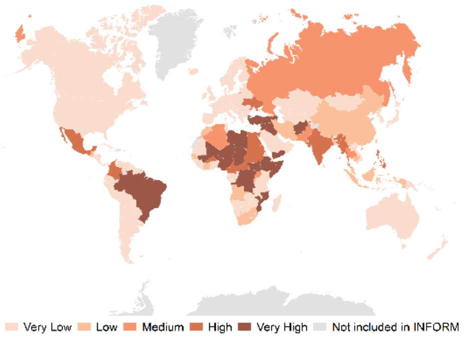	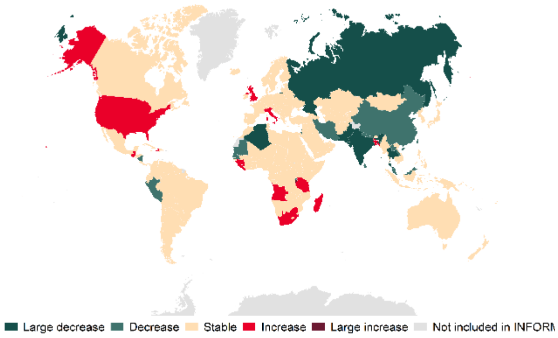
Human Hazard Changes – SSP2	**Human Hazard Changes – SSP3**
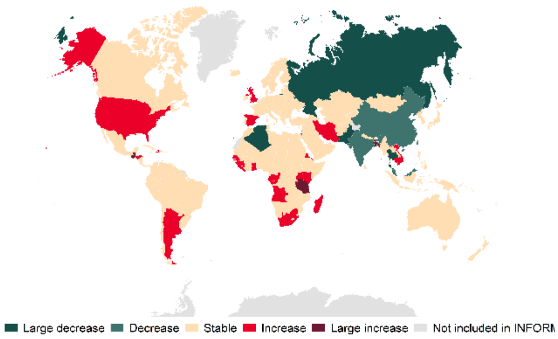	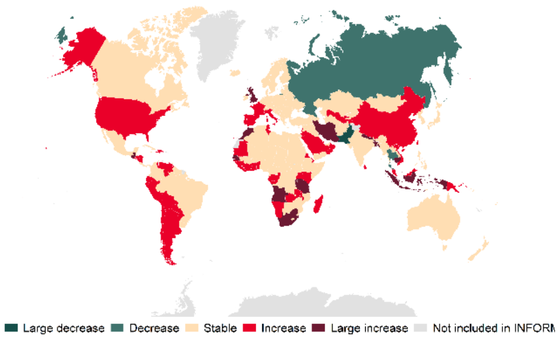

Human Hazard Changes – SSP5

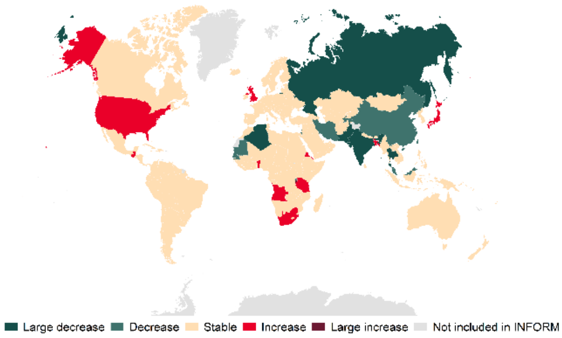

Annex 15. Baseline Human hazard of INFORM Climate Change Risk Index and absolute changes projected for 2080 under SSPs indicated in the panel title.

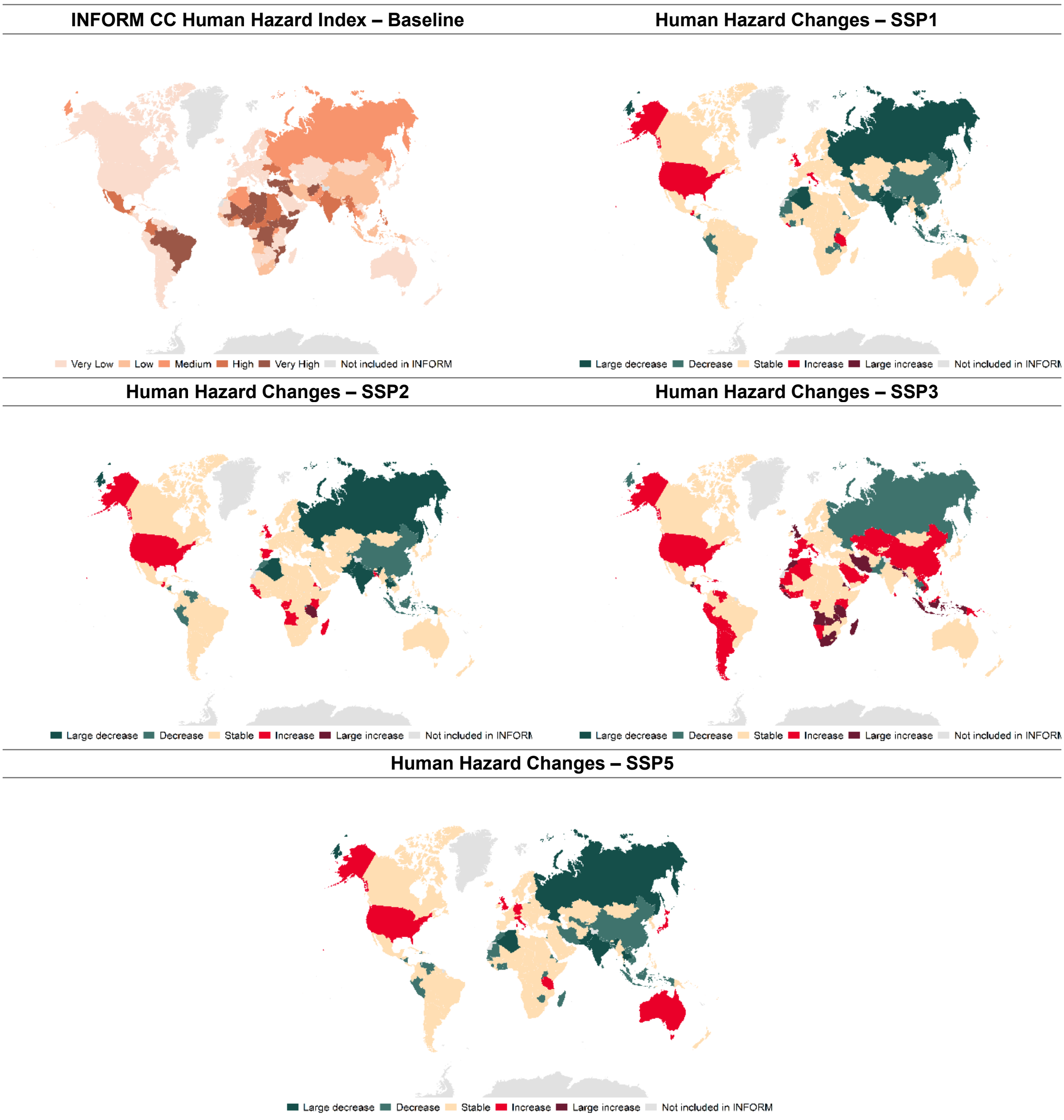

Annex 16. INFORM Climate Change Risk Index baseline and absolute changes projected for the mid-21st century under various concentration and development scenarios indicated in the panel title

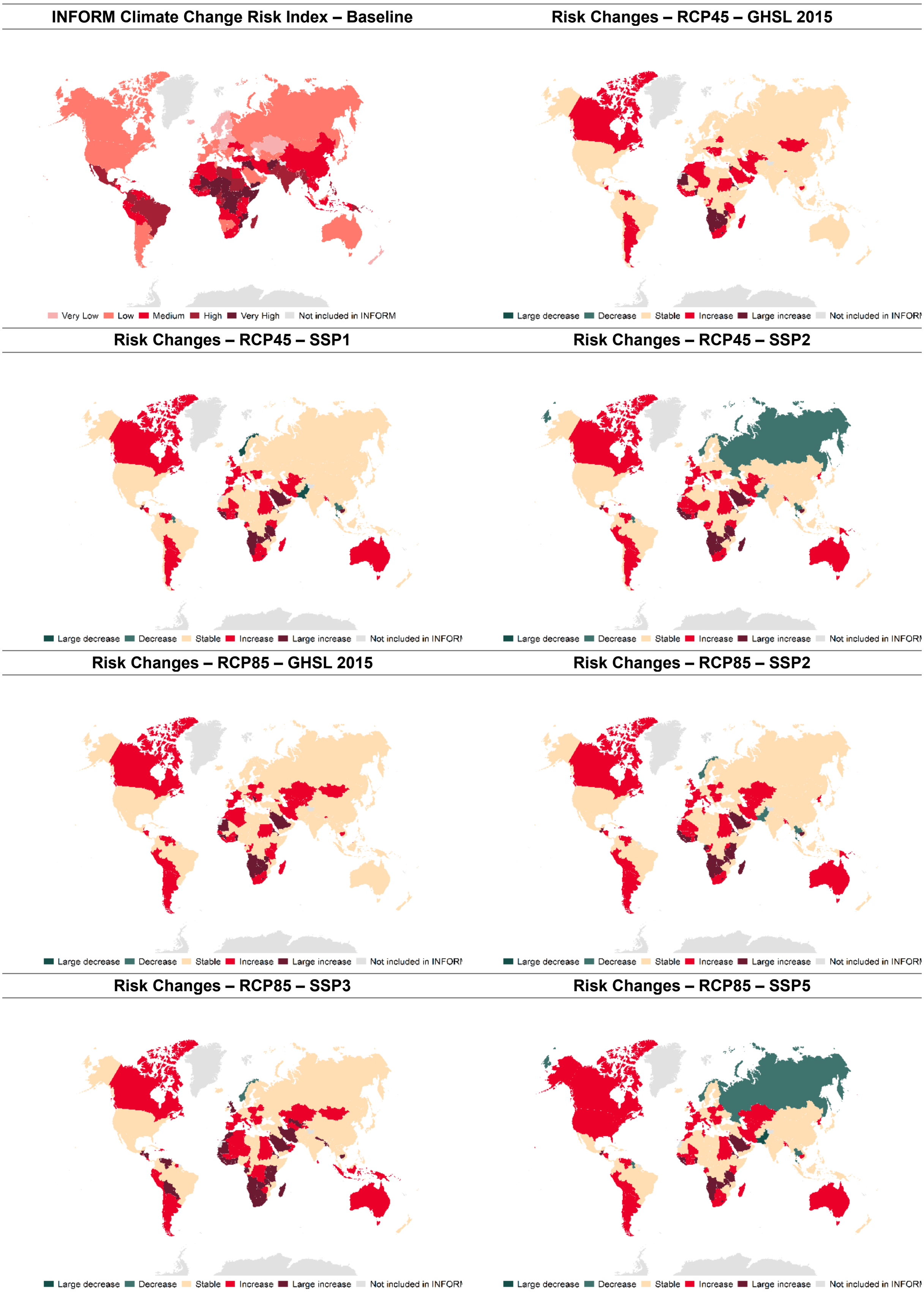

Annex 17. INFORM Climate Change Risk Index baseline and absolute changes projected for 2080s under various concentration and development scenarios indicated in the panel title.

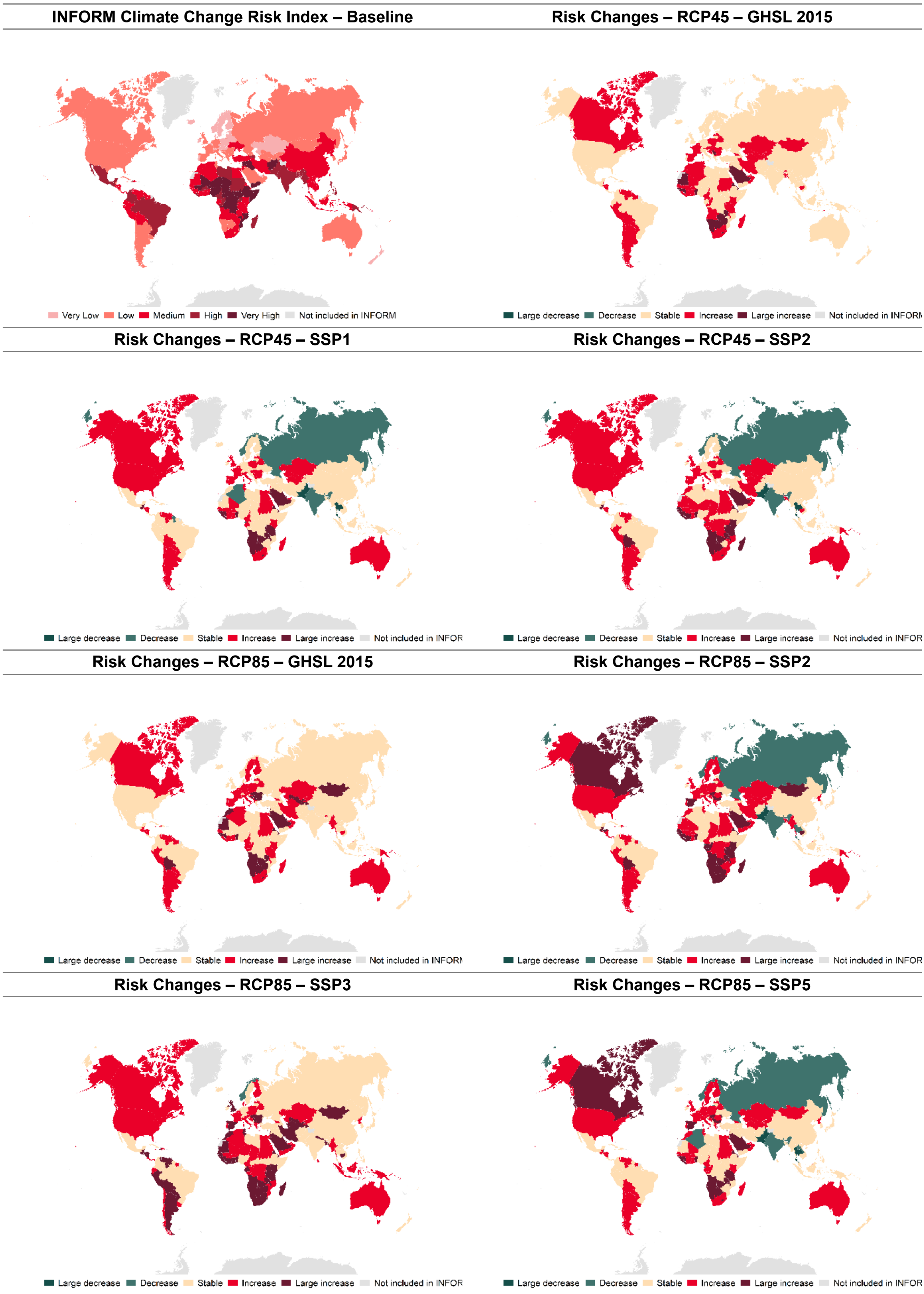

Annex 18. Vulnerability gap scores in the mid-21st century for various concentration and development scenarios indicated in the panel title.

Vulnerability Gap – RCP45 – GHSL 2015	Vulnerability Gap – RCP45 – SSP1
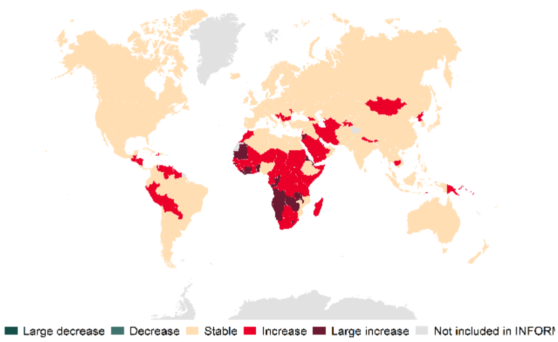	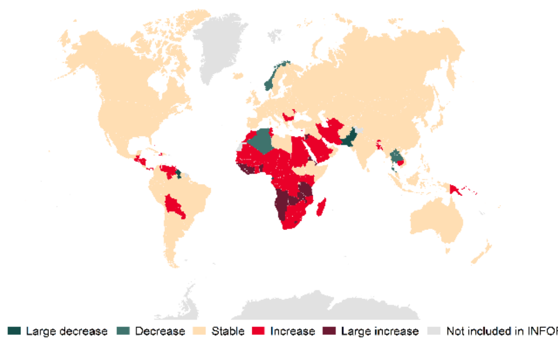
Vulnerability Gap – RCP45 – SSP2	**Vulnerability Gap – RCP85 – GHSL 2015**
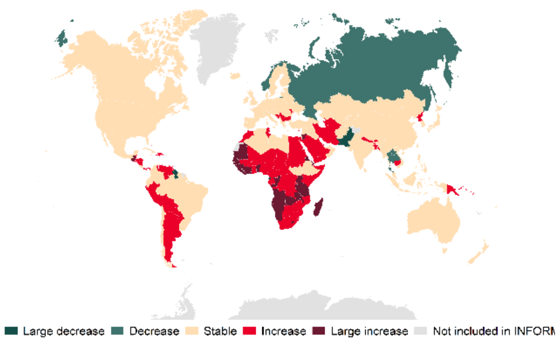	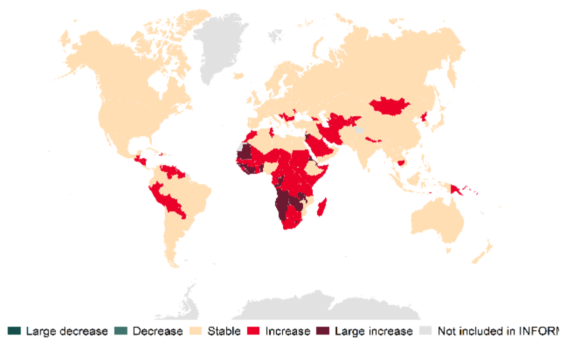
Vulnerability Gap – RCP85 – SSP2	**Vulnerability Gap – RCP85 – SSP3**
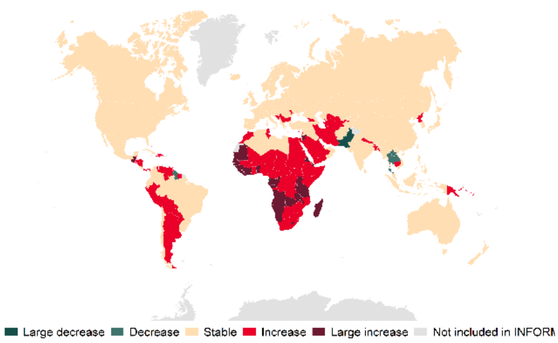	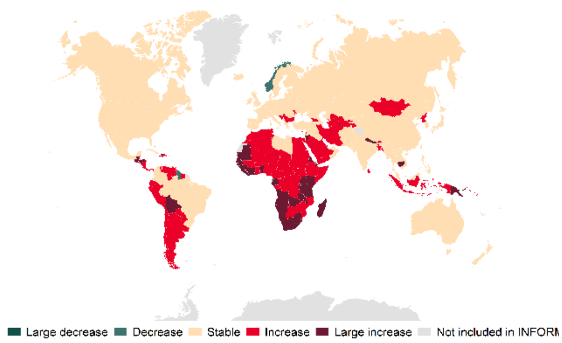

Vulnerability Gap – RCP85 – SSP5

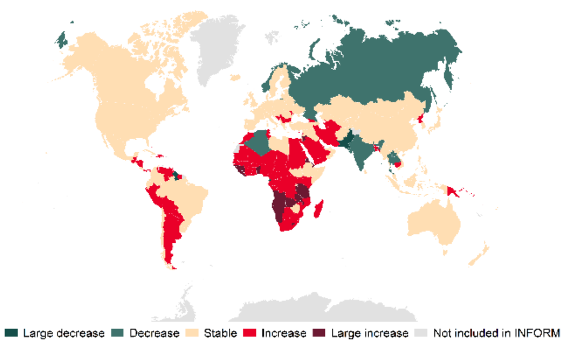

Annex 19. Vulnerability gap scores in 2080s for various concentration and development scenarios indicated in the panel title.

Vulnerability Gap – RCP45 – GHSL 2015	Vulnerability Gap – RCP45 – SSP1

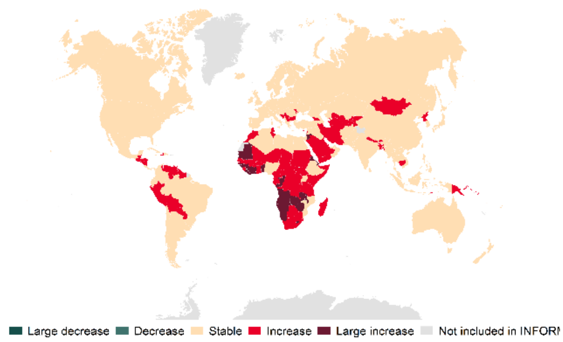

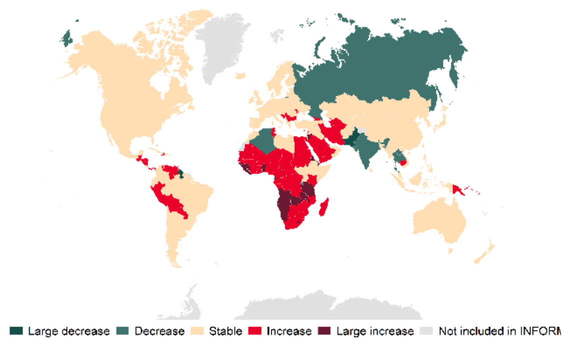

Vulnerability Gap – RCP45 – SSP2	Vulnerability Gap – RCP85 – GHSL 2015

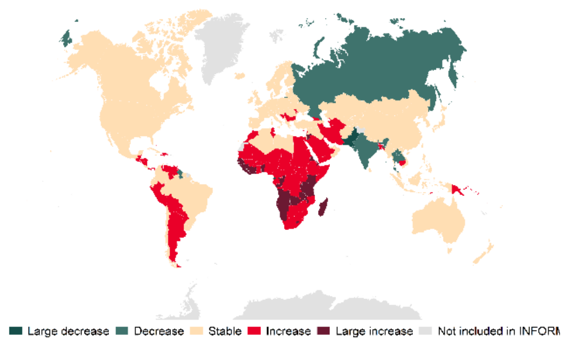

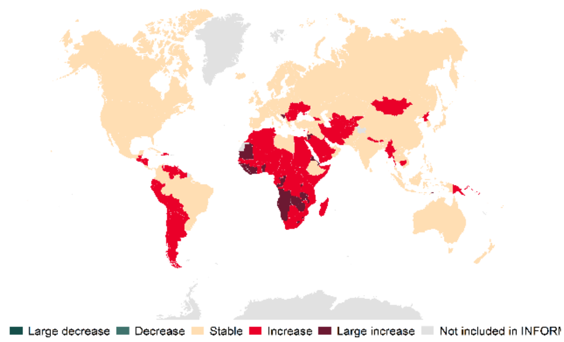

Vulnerability Gap – RCP85 – SSP2	Vulnerability Gap – RCP85 – SSP3

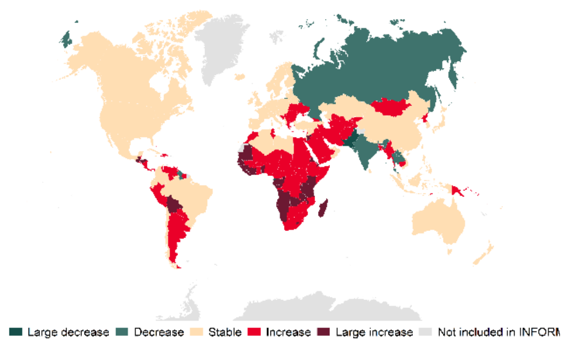

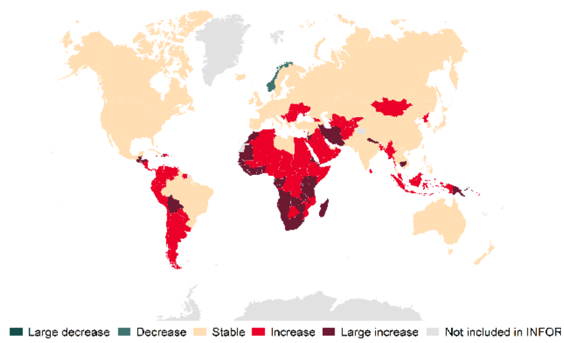

Vulnerability Gap – RCP85 – SSP5

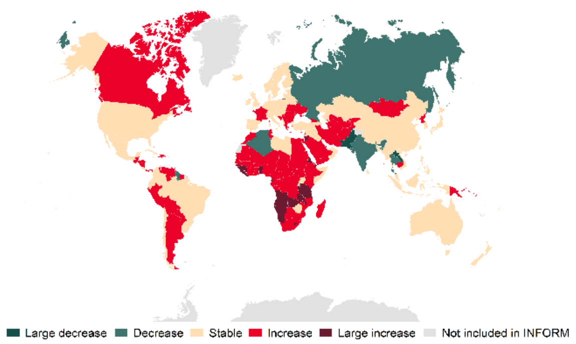

Annex 20. Percentage of change in population in 2050 and 2080 under considered SSPs relative to 2015.

SSP1 - 2050	SSP1 - 2080

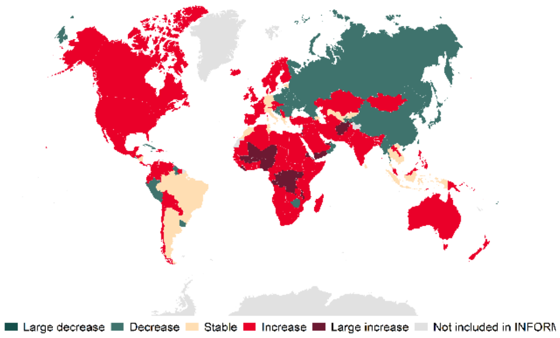

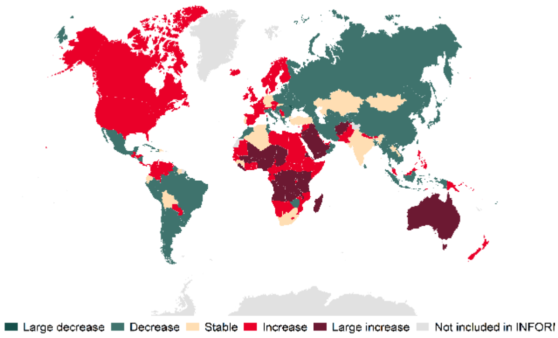

SSP2 - 2050	SSP2 - 2080

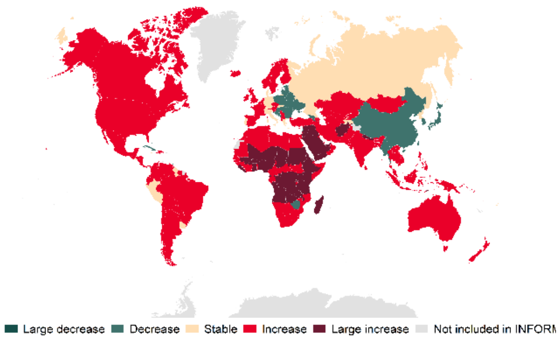

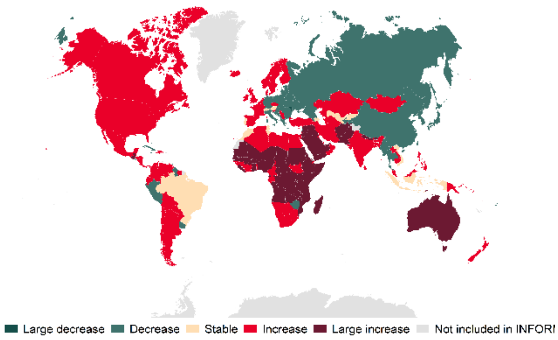

SSP3 - 2050	SSP3 - 2080

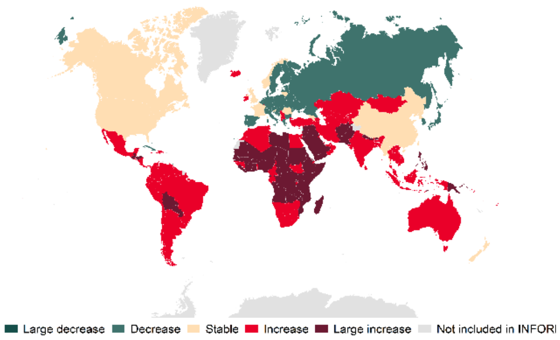

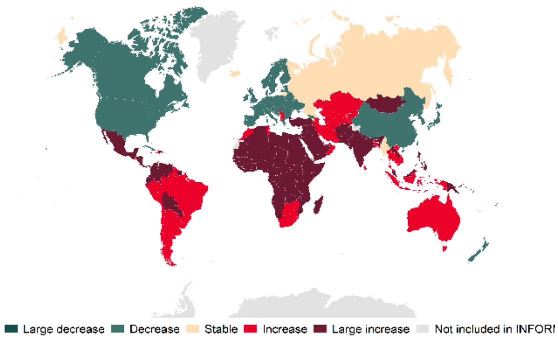

SSP5 - 2050	SSP5 - 2080

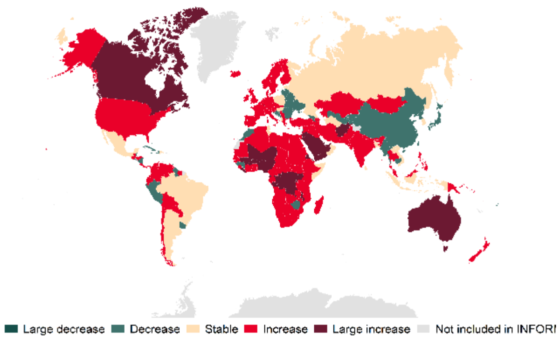

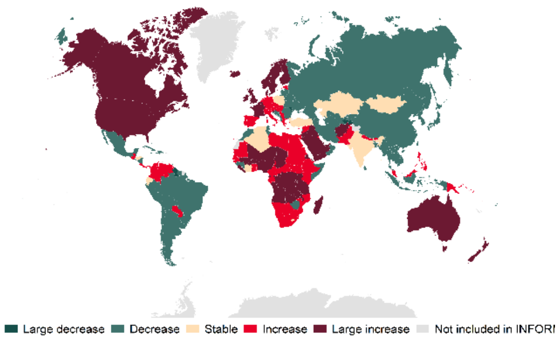

Annex 21. Thresholds used for INFORM Climate Change Risk Index dimensions

Index	Very Low	Low	Medium	High	Very High
Risk					
Min	0.0	2.0	3.5	5.0	6.5
Max	1.9	3.4	4.9	6.4	10.0
Hazard&Exposure					
Min	0.0	1.5	2.7	4.1	6.1
Max	1.4	2.6	4	6	10.0
Vulnerability					
Min	0.0	2.0	3.3	4.8	6.4
Max	1.9	3.2	4.7	6.3	10.0
Lack of Coping Capacity					
Min	0.0	3.2	4.7	6.0	7.4
Max	3.1	4.6	5.9	7.3	10.0

Annex 22. Thresholds used for Hazard&Exposure categories

Index	Very Low	Low	Medium	High	Very High
Natural					
Min	0.0	1.3	2.8	4.7	6.9
Max	1.2	2.7	4.6	6.8	10.0
Human					
Min	0.0	1.0	3.1	7	9.0
Max	0.9	3.0	6.9	8	10.0

Annex 23. Thresholds used for Key changes (Risk, Hazard&Exposure, Natural, Human, Vulnerability Gap and Population)

Index	Large decrease	Decrease	Stable	Increase	Large increase
Risk difference					
Min	-0.5	-0.29	-0.19	0.12	0.31
Max	-0.3	-0.2	0.1	0.3	1.2
Hazard&Exposure difference					
Min	-1.4	-0.69	-0.2	0.21	0.6
Max	-0.7	-0.21	0.2	0.59	2.8
Natural Hazard difference					
Min	-1.3	-0.79	-0.19	0.31	0.91
Max	-0.8	-0.2	0.3	0.9	2.7
Human Hazard difference					
Min	-5.5	-1.69	-0.29	0.21	1.61
Max	-1.7	-0.3	0.2	1.6	4.8
Vulnerability gap					
Min	-7.9	-3.49	-1.19	1.51	6.1
Max	-3.5	-1.2	1.5	6.0	22.804
Population					
Min	-97	-59.9	-4.9	5.1	60.1
Max	-60	-5	5	60	529

Annex 24. Thresholds used for Hazard projections

Index	Very Low	Low	Medium	High	Very High
Earthquake					
Min	0.0	1.5	4	6.4	8.5
Max	1.4	3.9	6.3	8.4	10.0
Flood					
Min	0.0	1.2	3.4	5.1	7.1
Max	1.1	3.3	5	7	10.0
Tsunami					
Min	0.0	1.4	4.4	5.9	7.5
Max	1.3	4.3	5.8	7.4	10.0
Cyclone wind					
Min	0.0	1.5	4.2	6.5	8.3
Max	1.4	4.1	6.2	8.2	10.0
Coastal flood					
Min	0.0	1.5	3.9	5.5	7.3
Max	1.4	3.8	5.4	7.2	10.0
Drought					
Min	0.0	2.2	4.2	7.0	8.5
Max	2.1	4.1	6.9	8.4	10.0
Epidemics					
Min	0.0	1.3	3.2	5.2	8.2
Max	1.2	3.1	5.1	8.1	10.0
Projected conflict					
Min	0.0	1.2	3.4	6.2	8.5
Max	1.1	3.3	6.1	8.4	10.0

The European Commission's science and knowledge service

Joint Research Centre

JRC Mission

As the science and knowledge service of the European Commission, the Joint Research Centre's mission is to support EU policies with independent evidence throughout the whole policy cycle.

EU Science Hub
ec.europa.eu/jrc

@EU_ScienceHub

EU Science Hub - Joint Research Centre

EU Science, Research and Innovation

EU Science Hub

Publications Office
of the European Union